



PHD

Three-dimensional physical model studies of air injection: In-situ combustion and downhole catalytic upgrading using horizontal wells

Al-Saghr, Abdulbaset Mohammed

Award date:
1998

Awarding institution:
University of Bath

[Link to publication](#)

Alternative formats

If you require this document in an alternative format, please contact:
openaccess@bath.ac.uk

General rights

Copyright and moral rights for the publications made accessible in the public portal are retained by the authors and/or other copyright owners and it is a condition of accessing publications that users recognise and abide by the legal requirements associated with these rights.

- Users may download and print one copy of any publication from the public portal for the purpose of private study or research.
- You may not further distribute the material or use it for any profit-making activity or commercial gain
- You may freely distribute the URL identifying the publication in the public portal ?

Take down policy

If you believe that this document breaches copyright please contact us providing details, and we will remove access to the work immediately and investigate your claim.

**THREE-DIMENSIONAL PHYSICAL MODEL STUDIES OF
AIR INJECTION: IN-SITU COMBUSTION AND
DOWNHOLE CATALYTIC UPGRADING
USING HORIZONTAL WELLS**

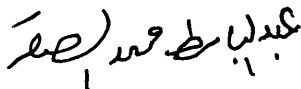
ABDULBASET MOHAMMED AL-SAGHR

Submitted for the degree of Doctor of Philosophy of the University of Bath

**Department of Chemical Engineering
University of Bath
Bath BA2 7AY, UK**

October 1998

Attention is drawn to the fact that copyright of this thesis rests with its author. This copy of the thesis has been supplied on condition that any one who consults it is understood to recognise that its copyright rests with its author and no quotation from this thesis and no information derived from it may be published without the prior written consent from the author



UMI Number: U602169

All rights reserved

INFORMATION TO ALL USERS

The quality of this reproduction is dependent upon the quality of the copy submitted.

In the unlikely event that the author did not send a complete manuscript and there are missing pages, these will be noted. Also, if material had to be removed, a note will indicate the deletion.



UMI U602169

Published by ProQuest LLC 2014. Copyright in the Dissertation held by the Author.
Microform Edition © ProQuest LLC.

All rights reserved. This work is protected against
unauthorized copying under Title 17, United States Code.



ProQuest LLC
789 East Eisenhower Parkway
P.O. Box 1346
Ann Arbor, MI 48106-1346

UNIVERSITY OF BATH LIBRARY		
75	07 DEC 1998	

DEDICATED TO

MY PARENTS

MY WIFE

MY FAMILY MEMBERS

MY FRINDS

AKNOWLEDGMENT

I would like to express my deepest gratitude to my supervisor, Professor Malcolm Greaves, who being most generous with his time, providing valuable guidance and encouragement throughout the project.

Gratitude is also extended to Dr. Richard Rathbone who reviewed the first year project report for his useful discussion.

I would like also to express my appreciation and my thanks to the technicians team in the Department of Chemical Engineering for their help with the maintenance and modification of the rig.

I wish to thank British Petroleum “Sunbury Research Center” and Petroleum Recovery Institute-Calgary for analysing oil samples.

I wish to express my appreciation to National Oil Company of Libya and Zueitina Oil Company for their financial support.

Finally, I would highly appreciated my family for their continued support, help, encouragement and prayers.

ABSTRACT

The effect of the horizontal producer well design, arranged in line drive, on the *In-Situ* combustion process performance, has been tested in 3-D combustion experiments.

Extensive measurements of temperature profiles in the sandpack was carried out.

This study has extended the understanding of the ISC-horizontal wells process by investigating the influence of fluid entry points along the horizontal producer well on the combustion behaviour. Two different horizontal producer well designs were used in two sets of experiments, one using a low hole perforation density producer (Design 1) and the second, using a high hole perforation density producer (Design 2). Medium heavy Clair crude oil (19.8 ° API) and light Forties Mix 1 crude oil (30.8 °API) were used in the experiments to take account of the different mobilities of the oils.

Horizontal well Design 2 was found to increase the rate of desaturation of the oil layer in the downstream region (ahead of the combustion front). This result in a reduced fuel availability ahead of the combustion front, causing the combustion front to die.

For the medium heavy Clair oil, a high hole perforation density along the horizontal producer well resulted in a higher oxygen content in the produced gas but this did not affect combustion front propagation. However, for the light forties Mix 1 oil, the combustion front could not be sustained in a HTO mode and early oxygen breakthrough occurred.

A new horizontal well design has been developed to mimic the behaviour in a heavy oil reservoir under *in-situ* combustion process conditions but in a light oil reservoir. This employed a co-aligned horizontal well with a sliding inner tube, which enable continues sleeve-back to be achieved.

The results showed that a stable, sustained combustion was achieved with the light oil when the sleeve-back design was used, even when the horizontal producer well had a high hole perforation density.

Study have made to investigate the feasibility of *in-situ* upgrading using a downhole catalytic bed placed along the horizontal producer well.

Two sets of experiments were performed using heavy Wolf Lake crude oil (10.95 °API) in both dry and wet combustion modes. In each set, one experiment was performed without the catalytic bed.

Results obtained show that a substantial reduction in sulphuer and heavy metals in the produced oil from the catalytic runs. The API gravity of the produced oil was 7 to 10 points higher than the original crude oil.

TABLE OF CONTENTS

	ACKNOWLEDGEMENT.....	I
	ABSTRACT.....	II
	TABLE OF CONTENTS.....	IV
	NOMENCLATURE.....	XIII
CHAPTER 1	INTRODUCTION.....	1
CHAPTER 2	LITERATURE REVIEW.....	7
	Historical Back Ground.....	7
2.0	Basic Principles of In-Situ Combustion.....	9
2.1	Methods of In-Situ Combustion.....	9
2.1.1	Dry Forward Combustion.....	10
2.1.2	Wet Forward Combustion.....	14
2.1.3	Reverse In-Situ Combustion.....	16
2.1.4	Other In-Situ Combustion Variations	18
2.2	Reaction Kinetics of In-Situ Combustion.....	20
2.2.1	Low Temperature Oxidation Reactions (LTO).....	23
2.2.2	Medium Temperature Oxidation Reactions (MTO).....	26
2.2.3	High Temperature Oxidation Reactions (HTO).....	28
2.3	Parameters Affecting In-Situ Combustion Performance.....	30
2.3.1	Effect of Matrix Surface Area.....	30
2.3.2	Effect of Pressure.....	33
2.3.3	Effect of Water Air Ratio.....	35
2.3.4	Effect of Oxygen Enrichment.....	37
2.4	In-Situ Combustion with Light Crude Oil.....	39
2.5	Three-Dimensional Scaled Model Studies.....	42
2.6	Scaled In-Situ Combustion Experiments.....	44
2.7	Thermal Recovery Methods Using Horizontal Wells.....	49

TABLE OF CONTENTS

2.7.1	Steam Assisted Gravity Drainage Process (SAGD).....	49
2.7.2	Heated Annulus Steam Drive Process (HASD).....	51
2.7.3	Combustion Override Split-production Horizontal Well Process (COSH)	52
2.7.4	Vapour Extraction Process (VAPEX).....	53
2.7.5	Pressure Controlled Gravity Drainage Process (PCGD).....	53
2.8	Laboratory Studies with Horizontal Wells.....	55
2.8.1	In-Situ Combustion Using Horizontal Wells.....	56
2.8.2	Horizontal Wells in Direct Line Drive Configuration.....	57
2.9	Heavy Oil Upgrading Technology.....	60
2.9.1	Upgrading Methods.....	61
CHAPTER 3	EQUIPMENT AND EXPERIMENTAL PROCEDURE.....	73
3.1	Equipment.....	74
3.1.1	Combustion Cell.....	74
3.1.2	Gas Injection Unit.....	75
3.1.3	Water Injection Unit.....	75
3.1.4	Fluid Production Unit.....	76
3.1.5	Gas Analysis Unit.....	77
3.1.6	Temperature Control Equipment.....	78
3.1.7	Data Acquisition Unit.....	79
3.1.8	Ignitor.....	79
3.2	Design of Horizontal Producer Wells.....	80
3.2.1	Low Hole Perforation Density Horizontal Producer Well (Design 1).....	81
3.2.2	High Hole Perforation Density Horizontal Producer Well (Design 2).....	81
3.2.3	Sleeved-back Horizontal Producer Well (Design 3).....	81
3.2.4	Calibration of the Sleeve-back Tubing.....	84
3.3	Experimental Procedure.....	85
3.3.1	Preparation of Sandpack for In-Situ Combustion Experiments.....	85
3.3.2	Preparation of Sandpack for In-Situ Upgrading Experiments.....	86
3.3.3	Normal Operating Procedure.....	88
3.3.4	Operating Procedure of Sleeve-back Well Assembly.....	90
3.3.5	Normal Shut Down Procedure.....	92

TABLE OF CONTENTS

3.3.6	Experimental Plan.....	92
CHAPTER 4	EXPERIMENTAL RESULTS AND DISCUSSION.....	116
PART I	Experiments with Conventional Horizontal Producer Well.....	116
4.1	Main Combustion Parameters.....	117
4.1.1	Produced Gas Composition.....	117
4.1.2	Apparent Atomic H/C and Carbon Molar Ratios.....	118
4.1.3	Oxygen Utilisation.....	120
4.1.4	Air Requirement.....	123
4.1.5	Fuel Consumption.....	123
4.1.6	Oil and Water Production.....	125
4.1.7	Combustion Front Velocity.....	131
4.1.8	Temperature Contours.....	132
4.1.9	Post-mortem Analysis.....	175
PART II	Experiments with Modified Horizontal Producer Well.....	198
4.2	Experimental Results of Run 966.....	198
4.2.1	Produced Gas Composition.....	198
4.2.2	Combustion Behaviour.....	200
4.2.3	Oil and Water Production.....	201
4.2.4	Temperature Contours.....	203
4.2.5	Post-mortem Analysis.....	216
CHAPTER 5	DOWNHOLE CATALYTIC UPGRADING.....	218
5.1	Main Combustion Parameters.....	219
5.1.1	Produced Gas Composition.....	219
5.1.2	Apparent H/C and Carbon Molar Ratios.....	222
5.1.3	Oxygen Utilisation.....	223
5.1.4	Fuel Consumption and Air Requirement.....	223
5.1.5	Oil and Water Production.....	224
5.2	Analysis of Produced Liquids.....	226
5.2.1	Oil Density.....	227
5.2.2	Oil Viscosity.....	232
5.2.3	Boiling Range Distribution.....	234

TABLE OF CONTENTS

5.2.4	Elemental Analysis.....	234
5.2.5	Compositional Analysis.....	236
5.2.6	Gas Chromatograph Analysis.....	238
5.3	Temperature Contours.....	239
5.4	Post-mortem Analysis.....	292
CHAPTER 6	CONCLUSIONS AND RECOMMENDATIONS.....	298
	REFERENCES.....	305
APPENDIX A	Equipment Specifications and Manufacturer.....	317
APPENDIX B	Technical Information Sheet of Buckland Silica Sand.....	319
APPENDIX C	Metal Analysis of Co Mo Catalyst.....	320
APPENDIX D	Properties of Produced Oil and Water for Upgrading Experiments.....	321
APPENDIX E	SIMDIS Analysis.....	324
APPENDIX F	Combustion Parameters Calculation.....	326
APPENDIX G	Material Balance.....	329
APPENDIX H	COSHH.....	332

TABLES

No		PAGE
2.1	Commercial ISC Projects	39
3.1	Horizontal Producer Wells used in Previous Studies.....	95
3.2	Specification of Design 1 and 2 Horizontal Producer Wells.....	95
3.3	Specification of Design 3 Horizontal Producer Well.....	96
3.4	Specification of Horizontal Injection Well.....	96
3.5	Sandpack Properties for In-Situ Combustion Runs.....	97
3.6	Sandpack Properties for Run 966.....	98
3.7	Sandpack Properties for In-Situ Upgrading Runs.....	99
3.8	Operating Conditions for In-Situ Combustion Runs.....	99
3.9	Operating Conditions for Run 966.....	100
3.10	Operating Conditions for In-Situ Upgrading Runs.....	100
4.1	Effect of Hole Perforation Density on Produced Gas Composition.....	117
4.2	Combustion Performance.....	120
4.3	Effect of Hole Perforation Density on Fluid Saturation in Sandpack.....	126
4.4	Effect of Hole Perforation Density on Production Rate.....	127
4.5	Oil Recovery.....	130
4.6	Physical Properties of Produced Liquids.....	131
4.7	Production Performance and Sweep Efficiency.....	174
4.8	Produced Gas Composition for Runs 963,964 and 966.....	199
4.9	Combustion Performance of Run 966.....	201
4.10	Production Performance of Run 966.....	202
4.11	Oil Recovery of Run 966.....	203
5.1	Produced Gas Composition.....	219
5.2	Combustion Performance.....	222
5.3	Production Performance and Sweep Efficiency.....	225
5.4	Oil Recovery.....	225
5.5	Experimental Conditions and Upgrading achieved in Previous Works.....	228
5.6	Density and Viscosity of Produced Oil During Stabilised Period.....	229
5.7	SARA Analysis.....	238

FIGURES

No		PAGE
2.1	Schematic diagram of dry forward In-Situ Combustion process.....	13
2.2	Wet forward combustion: temperature and saturation profiles.....	15
2.3	Reverse combustion: temperature and saturation profiles.....	17
2.4	The concept of Steam-Assisted Gravity Drainage (SAGD).....	50
2.5	The concept of Heated Annulus Steam Drive (HASD).....	51
2.6	The concept of Combustion Override Split-production Horizontal well (COSH)	52
2.7	The concept of Pressure Controlled Gravity Drainage (PCGD).....	54
2.8A	The concept of Toe-to-Heel Air Injection (THAI).....	59
2.8B	Production mode of Toe-to-Heel Air Injection (THAI).....	59
2.9A	Injection mode of 'Burn and Turn' In-Situ Catalytic Upgrading.....	68
2.9B	Production mode of 'Burn and Turn' In-Situ Catalytic Upgrading.....	68
2.10	Diagram of In-Situ Catalytic Upgrading using downhole injection.....	69
2.11	Diagram of a combustion assisted In-Situ Catalytic Upgrading.....	71
2.12	Mechanism of horizontal well gravel packing.....	72
2.13	Diagram of Toe-to-Heel Air Injection process with downhole catalytic bed....	72
3.1	Flow diagram of 3-D combustion model.....	101
3.2	Combustion cell assembly.....	102
3.3	Thermocouple positions.....	103
3.4	Cell dimensions and location of well ports.....	104
3.5	Photograph of the control panel.....	105
3.6	Photograph of gas chromatograph.....	105
3.7	Photograph of gas analysers and Wet Test Meter.....	106
3.8	Arrangement of combustion cell inside aluminum insulation box.....	107
3.9	Photograph of insulation aluminum box.....	108
3.10	Photograph of computer workstation.....	108
3.11	Well arrangement and ignitor position inside 3-D cell.....	109
3.12	Design 1 horizontal producer well.....	110
3.13	Design 2 horizontal producer well.....	110
3.14	Design 3 co-aligned horizontal producer well assembly.....	111
3.15A	Operating regime for Design 3 horizontal producer well assembly.....	112
3.15B	Arrangement of perforations for Design 3 horizontal producer well.....	112
3.16A	Mechanism of adjusting sleeve-back of Design 3 horizontal producer well....	113
3.16B	Dimensions of screw-bracket assembly for Design 3 horizontal producer.....	113
3.17	Design 3 well assembly as installed on the 3-D combustion cell.....	114
3.18	Horizontal injection well.....	115
4.1	Produced gas composition for Run 961.....	139
4.2	Produced gas composition for Run 962.....	139
4.3	Produced gas composition for Run 963.....	140
4.4	Produced gas composition for Run 964.....	140
4.5	Apparent H/C and molar (CO/CO+CO ₂) ratios for Run 961.....	141
4.6	Apparent H/C and molar (CO/CO+CO ₂) ratios for Run 962.....	141
4.7	Apparent H/C and molar (CO/CO+CO ₂) ratios for Run 963.....	142
4.8	Apparent H/C and molar (CO/CO+CO ₂) ratios for Run 964.....	142

TABLE OF CONTENTS

4.9	Oxygen utilisation and Air-Fuel Requirement for Run 961.....	143
4.10	Oxygen utilisation and Air-Fuel Requirement for Run 962.....	143
4.11	Oxygen utilisation and Air-Fuel Requirement for Run 963.....	144
4.12	Oxygen utilisation and Air-Fuel Requirement for Run 964.....	144
4.13	Carbon combustion rate for Run 961.....	145
4.14	Carbon combustion rate for Run 962.....	145
4.15	Carbon combustion rate for Run 963.....	146
4.16	Carbon combustion rate for Run 964.....	146
4.17	Oil and water production rate for Run 961.....	147
4.18	Oil and water production rate for Run 962.....	147
4.19	Cumulative production for Run 961.....	148
4.20	Cumulative production for Run 962.....	148
4.21	Oil and water recovery for Run 961.....	149
4.22	Oil and water recovery for Run 962.....	149
4.23	Oil and water production rate for Run 963.....	150
4.24	Oil and water production rate for Run 964.....	150
4.25	Cumulative production for Run 963.....	151
4.26	Cumulative production for Run 964.....	151
4.27	Oil and water recovery for Run 963.....	152
4.28	Oil and water recovery for Run 964.....	152
4.29	Temperature contours for Run 961 at ignition.....	153
4.30	Temperature contours for Run 961 at 120 minutes.....	154
4.31	Temperature contours for Run 961 at 240 minutes.....	155
4.32	Temperature contours for Run 961 at 360 minutes.....	156
4.33	Temperature contours for Run 961 at 480 minutes.....	157
4.34	Temperature contours for Run 961 at 600 minutes.....	158
4.35	Temperature contours for Run 962 at ignition.....	159
4.36	Temperature contours for Run 962 at 120 minutes.....	160
4.37	Temperature contours for Run 962 at 240 minutes.....	161
4.38	Temperature contours for Run 962 at 360 minutes.....	162
4.39	Temperature contours for Run 962 at 480 minutes.....	163
4.40	Temperature contours for Run 962 at 600 minutes.....	164
4.41	Temperature contours for Run 963 at ignition.....	165
4.42	Temperature contours for Run 963 at 120 minutes.....	166
4.43	Temperature contours for Run 963 at 240 minutes.....	167
4.44	Temperature contours for Run 963 at 360 minutes.....	168
4.45	Temperature contours for Run 963 at 500 minutes.....	169
4.46	Temperature contours for Run 964 at ignition.....	170
4.47	Temperature contours for Run 964 at 60 minutes.....	171
4.48	Temperature contours for Run 964 at 120 minutes.....	172
4.49	Temperature contours for Run 964 at 180 minutes.....	173
4.50	Post-mortem photographs for Run 961 at 60 and 90mm from inlet.....	177
4.51	Post-mortem photographs for Run 961 at 140 and 170mm from inlet.....	178
4.52	Post-mortem photographs for Run 961 at 200 and 230mm from inlet.....	180
4.53	Post-mortem photographs for Run 961 at 270 and 300mm from inlet.....	182
4.54	Post-mortem photographs for Run 962 at 60 and 90mm from inlet.....	184
4.55	Post-mortem photographs for Run 962 at 110 and 140mm from inlet.....	185
4.56	Post-mortem photographs for Run 962 at 170 and 220mm from inlet.....	187
4.57	Post-mortem photographs for Run 963 at 60 and 90mm from inlet.....	190

TABLE OF CONTENTS

4.58	Post-mortem photographs for Run 963 at 130 and 170mm from inlet.....	191
4.59	Post-mortem photographs for Run 963 at 200 and 240mm from inlet.....	193
4.60	Post-mortem photographs for Run 964 at ignitor,70 and 140mm from inlet.....	196
4.61	Produced gas composition for Run 966.....	205
4.62	Apparent H/C and molar CO/CO+CO ₂ ratios for Run 966.....	205
4.63	Oxygen utilisation and Air-Fuel Requirement for Run 966.....	206
4.64	Carbon combustion rate for upstream well section of Run 966.....	206
4.65	Carbon combustion rate for downstream well section of Run 966.....	207
4.66	Oil and water production rate for Run 966.....	207
4.67	Cumulative production for Run 966.....	208
4.68	Oil and water recovery for Run 966.....	208
4.69	Oil and water recovery for upstream well section of Run 966.....	209
4.70	Oil and water recovery for downstream well section of Run 966.....	209
4.71	Temperature measured by central thermocouple for Run 966.....	210
4.72	Temperature contours for Run 966 at ignition.....	211
4.73	Temperature contours for Run 966 at 120 minutes.....	212
4.74	Temperature contours for Run 966 at 240 minutes.....	213
4.75	Temperature contours for Run 966 at 431 minutes.....	214
4.76	Temperature contours for Run 962 at 600 minutes.....	215
4.77	Post-mortem sketches for Run 966.....	217
5.1	Produced gas composition for Run 971.....	245
5.2	Produced gas composition for Run 975.....	245
5.3	Produced gas composition for Run 972.....	246
5.4	Produced gas composition for Run 976.....	246
5.5	Apparent H/C and molar (CO/CO+CO ₂) ratios for Run 971.....	247
5.6	Apparent H/C and molar (CO/CO+CO ₂) ratios for Run 975.....	247
5.7	Apparent H/C and molar (CO/CO+CO ₂) ratios for Run 972.....	248
5.8	Apparent H/C and molar (CO/CO+CO ₂) ratios for Run 976.....	248
5.9	Oxygen utilisation and Air-Fuel Requirement for Run 971.....	249
5.10	Oxygen utilisation and Air-Fuel Requirement for Run 975.....	249
5.11	Oxygen utilisation and Air-Fuel Requirement for Run 972.....	250
5.12	Oxygen utilisation and Air-Fuel Requirement for Run 976.....	250
5.13	Oil and water production rate for Run 971.....	251
5.14	Oil and water production rate for Run 975.....	251
5.15	Cumulative production for Run 971.....	252
5.16	Cumulative production for Run 975.....	252
5.17	Oil and water recovery for Run 971.....	253
5.18	Oil and water recovery for Run 975.....	253
5.19	Oil and water production rate for Run 972.....	254
5.20	Oil and water production rate for Run 976.....	254
5.21	Cumulative production for Run 972.....	255
5.22	Cumulative production for Run 976.....	255
5.23	Oil and water recovery for Run 972.....	256
5.24	Oil and water recovery for Run 976.....	256
5.25	Density and API gravity for Run 971.....	257
5.26	Density and API gravity for Run 975.....	257
5.27	Density and API gravity for Run 972.....	258
5.28	Density and API gravity for Run 976.....	258
5.29	Viscosity of produced oil for Run 971.....	259

TABLE OF CONTENTS

5.30	Viscosity of produced oil for Run 975.....	259
5.31	Viscosity of produced oil for Run 972.....	260
5.32	Viscosity of produced oil for Run 976.....	260
5.33	pH of produced water for Run 971.....	261
5.34	pH of produced water for Run 975.....	261
5.35	pH of produced water for Run 972.....	262
5.36	pH of produced water for Run 976.....	262
5.37	Simulated boiling range distribution for Wolf Lake crude oil.....	263
5.38	Simulated boiling range distribution for produced oil (Run 976).....	263
5.39	Analysis of metal and sulphur content for crude and produced oil.....	264
5.40	GC analysis for Wolf Lake crude oil.....	265
5.41	GC analysis for produced oil from Run 976.....	266
5.42	Temperature contours for Run 971 at ignition.....	267
5.43	Temperature contours for Run 971 at 120 minutes.....	268
5.44	Temperature contours for Run 971 at 240 minutes.....	269
5.45	Temperature contours for Run 971 at 360 minutes.....	270
5.46	Temperature contours for Run 971 at 480 minutes.....	271
5.47	Temperature contours for Run 971 at 600 minutes.....	272
5.48	Temperature contours for Run 971 at 720 minutes.....	273
5.49	Temperature contours for Run 975 at ignition.....	274
5.50	Temperature contours for Run 975 at 120 minutes.....	275
5.51	Temperature contours for Run 975 at 300 minutes.....	276
5.52	Temperature contours for Run 975 at 480 minutes.....	277
5.53	Temperature contours for Run 975 at 600 minutes.....	278
5.54	Temperature contours for Run 975 at 720 minutes.....	279
5.55	Temperature contours for Run 972 at ignition.....	280
5.56	Temperature contours for Run 972 at 120 minutes.....	281
5.57	Temperature contours for Run 972 at 180 minutes.....	282
5.58	Temperature contours for Run 972 at 240 minutes.....	283
5.59	Temperature contours for Run 972 at 300 minutes.....	284
5.60	Temperature contours for Run 972 at 330 minutes.....	285
5.61	Temperature contours for Run 976 at ignition.....	286
5.62	Temperature contours for Run 976 at 120 minutes.....	287
5.63	Temperature contours for Run 976 at 180 minutes.....	288
5.64	Temperature contours for Run 976 at 240 minutes.....	289
5.65	Temperature contours for Run 976 at 300 minutes.....	290
5.66	Temperature contours for Run 976 at 318 minutes.....	291
5.67	Post-mortem photographs for Run 971 at inlet, injector and ignitor.....	294
5.68	Post-mortem sketches for Run 971 at 60,100,170 and 230mm.....	296
5.69	Post-mortem sketch for Run 975 at 150mm.....	297
5.70	Post-mortem sketch for Run 972 at 230mm.....	297
5.71	Post-mortem sketch for Run 976 at 230mm.....	297

NOMENCLATURE

SYMBOL	DEFINATION
API	American Petroleum Institute
ARC	Accelerated Rate Calorimetry
COFCAW	Combination of forward combustion and water flooding
COSH	Combustion Override Split-production Horizontal well
DDP	Double Displacement Process
DSC	Differential Scanning Calorimetry
EOR	Enhance Oil Recovery
GC	Gas Chromatograph
HASD	Heated Annuls Steam Drive
HIHP	Horizontal Injector Horizontal Producer
HDC	Hydrocracking
HDS	Hydrodesulphurisation
HDM	Hydrodemetalisation
HTO	High Temperature Oxidation
IOR	Improved Oil Recovery
ISC	In-Situ Combustion
LTO	Low Temperature Oxidation
MTO	Medium Temperature Oxidation
OOIP	Original Oil in Place
OWIP	Original Water in Place
PCGD	Pressure Controlled Gravity Drainage
SAGD	Steam-Assisted Gravity Drainage
THAI	Toe-to Heel Air Injection
TGA	Thermogravimetric Analysis
VAPEX	Vapour Extraction
VIVP	Vertical Injector Vertical Producer
WAR	Water Air Ratio
WTM	Wet Test Meter

Symbol	Definition	Dimensions
AFR	Air to fuel ratio	$L^3 L^{-3}$
AOR	Air to oil ratio	$L^3 L^{-3}$
C_f	Instantaneous concentration of fuel	
CO	Carbon monoxide	
CO ₂	Carbon dioxide	
Co Mo	Cobalt Molybdenum	
D	Distance	L
E	Activation Energy	$L t^2$
g	Acceleration of gravity	$L t^{-2}$
g_c	Dimensional constant	$m L t^{-2}$
h	Thickness	L
H/C	Hydrogen to carbon ratio of fuel	
k	Absolute permeability	L^2
K	Reaction rate constant	t^{-1}
k_h	Horizontal permeability	L^2
k_v	Vertical permeability	L^2
l	Length	L
m	Molar ratio (CO/CO+CO ₂)	
P	Pressure	$m L^{-1} t^{-2}$
P _{O₂}	Partial pressure of oxygen	$m L^{-1} t^{-2}$
R	Universal gas constant	$L^2 T^{-2} T^{-1}$
S _{gi}	Initial gas saturation	Fraction
S _{oi}	Initial oil saturation	Fraction
S _{or}	Residual oil saturation	Fraction
S _{wi}	Initial water saturation	Fraction
S _{wr}	Residual water saturation	Fraction
T	Absolute temperature	T
t	Time	t

Greek

ρ	Fluid density	m L^{-3}
μ	Fluid viscosity	$\text{m L}^{-1}\text{t}^{-1}$
\emptyset	Matrix porosity	Fraction
α	Thermal diffustivity	$\text{L}^2 \text{t}^{-1}$

Subscripts

F	Field Scale
i	Reaction Regime
M	Model Scale
m	Reaction order with respect to oxygen
n	Reaction order with respect to fuel concentration

CHAPTER ONE

INTRODUCTION

INTRODUCTION

Petroleum plays a large role in providing the day-to-day energy needed to sustain economic development and quality of life. Its importance, as a major source of energy, is due to two main reasons: Firstly, renewable resources, such as, solar and wind energy require further development to solve technical and practical problems before they can compete reasonably with oil. Secondly, nuclear energy needs further technical progress to overcome serious environmental and safety concerns. Therefore, oil and gas will remain by far, the main source of energy for the foreseeable future. The increase demand for oil and the decline in the discovery of new reserves has forced the petroleum industry to improve methods to increase the ultimate recovery from existing reservoirs. However, developing new recovery methods that may extract 100 % of the oil in place has been the target of the petroleum industry for years.

Oil recovery methods can be divided into three main categories: primary, secondary, and tertiary methods; the latter is commonly known as “enhanced recovery” or EOR.

In the natural flow period (i.e. primary recovery), oil will flow into the well bore by the effect of natural reservoir energy, which is caused by gas expansion, and water influx. In this method, the overall yield, 5 to 20% of original oil in place (OOIP) depends on the crude type and the geological structure of the reservoir.

Once the natural reservoir energy effect has ceased, another driving force needs to be applied to produce additional oil. Thus, gas or water may be injected into the reservoir to maintain the pressure and to displace the oil. These techniques are known as secondary recovery methods (also known as conventional methods of EOR).

However, when the oil viscosity is very high and the mobility ratio is unfavourable, the efficiency of these methods can be very low. Generally, secondary recovery methods provide the means to recover a further 10 to 20% of the oil in place.

On average, two-third of the reserves remains unrecoverable using the current primary and secondary recovery methods. Therefore, new recovery methods need to be developed to improve the maximum recovery.

Improved oil recovery (IOR) is the application of technologies which involves the use of thermal, gases, chemical means, horizontal drilling and indeed, any other techniques to extract the remaining oil in the reservoir after the use of conventional primary and secondary recovery methods (*Egbogah*, 1994).

Horizontal and multi-lateral wells are being introduced in ever-increasing numbers to achieve further gains in reservoir productivity. Two hundred horizontal wells were drilled a decade ago. Now, one company has reported drilling more than 2,100 horizontal wells in North America. Advances have also been achieved in the depths drilled, reaching 8,761m and lengths now reaching 11,000m. Multi-lateral wells, with four or more sidetracks, are not uncommon now and offer further optimisation gains.

Recently, a new technique to control gas and water production rates by varying the fluid entry points along the well length has been successfully tested.

Horizontal wells are now being used in EOR projects, especially in thermal oil recovery. They provide flexibility in developing well patterns for enhancing the sweep efficiency of thermal oil recovery.

At present, thermal recovery methods, mainly steam injection, are the most successful EOR methods in use today. Approximately 80 % of all tertiary oil produced worldwide is by thermal methods (*Ahner et al*,1994). The idea of thermal methods is to raise the reservoir temperature, which leads to a substantial reduction in oil viscosity, which, in turn, enhances the oil mobility. These methods have mainly been used to recover heavy crudes and tar sands which are immobile at the initial reservoir temperature.

There are two main methods of thermal recovery, namely; hot fluid injection and *in-situ* combustion (ISC). The former method has found most success in bitumen and tar sands, whereas *in-situ* combustion (ISC) is finding increasing consideration for conventional lighter oil reservoirs.

ISC is an important enhanced recovery method which has been extensively studied during the past 30 years. Although many successful field projects have been reported, considerable development may be required before *in-situ* combustion can be extensively applied on a commercial basis.

ISC has been investigated in the laboratory using both one-dimensional combustion tube tests and three-dimensional scaled model experiments. Although combustion tube tests have provided much useful information on combustion parameters, they do not provide detailed information about sweep efficiency or actual transport of fluids within the porous media into the producing well. These valuable data can only be obtained by 3-D tests, which simulating the actual 3-D flow regime occurs under real reservoir conditions.

In-situ combustion involves the injection of compressed air or oxygen into an oil reservoir through injection wells to create and propagate a high temperature zone (combustion front) through the oil-bearing zone. The fuel necessary to sustain this front, coke, is a product of chemical reactions taking place at the combustion front during distillation and thermal cracking of the crude oil ahead of the combustion front. The availability of this fuel, has been considered the most complicated problem in the process especially in light oil reservoirs.

Fuel availability for combustion, has been discussed in detail by a number of investigators, some of them related the problem to the reservoir rock properties (i.e. mineralogy and rock texture), others, relate it to the reservoir fluid properties (i.e. crude type, composition and saturation), some of them attribute the problem to the displacement mechanisms that occur ahead of the combustion front.

The direct -line drive configuration using a horizontal producer well provides valuable means to improve the performance of ISC in heavy and light oil reservoirs.

In addition to improving the sweep efficiency of the process, it provides the means of controlling the flow along the well length.

As the combustion front advances along the horizontal production well, the production well may be used to control the rate at which desaturation occurs ahead of the combustion front. This is very important because it will effect fuel deposition and combustion performance.

There is steady and inevitable decline in the production of light, premium crude oil, and hence the world's supply of crude oil is inexorably moving towards poor quality, heavy oil reserves. The challenge will be to improve the quality of heavy oil to achieve market value and environmental concerns. Upgrading of heavy oil is to remove the heaviest, least desirable fractions while leaving behind an oil that has been greatly reduced in its metal, nitrogen, sulphur, and Conradson carbon content.

Previously, upgrading of heavy crudes is achieved by conventional surface upgrading techniques. However, there have been some reported *in-situ* upgrading attempts. The common feature between them is the presence of a heat source, hydrogen, and a catalyst agent. Moreover, deliberate use of conventional catalysts has also been proposed.

This involve placing of catalyst near the production end so produced fluids will pass through the catalytic bed, resulting in upgrading of the oil.

In this study, a semi-scaled three-dimensional physical model was used to study the effect of the horizontal producer well on the combustion performance using the 'Toe-to-Heel' Air Injection Process (THAI). The process was also used to investigate the

feasibility of *in-situ* upgrading when a catalytic bed is placed along the horizontal producer well.

The thesis structure is arranged so that Chapter Two includes specific *in-situ* combustion process mechanisms and a literature review of reaction kinetics, experimental studies, horizontal well technology and heavy oil upgrading technology. Chapter Three describes the experimental system and well designs, including details of the experimental procedure. Chapter Four is divided into two parts. Part One presents the result and discussion of experiments conducted with conventional horizontal producer wells, whilst Part Two presents results of the experiment performed with a sleeved-back horizontal producer well. Chapter Five presents the results and discussion of Downhole Catalytic Upgrading experiments and finally, the conclusions and recommendations for future work are presented in Chapter Six.

CHAPTER TWO

LITERATURE REVIEW

Historical back ground

The first application of air injection as a gas-drive is dated back to 1911 near Marietta, Ohio. This development was introduced by I. L. Dunn, O.C. Dunn and H.E. Smith and led to the method being referred to as the Smith-Dunn or Marietta process. In the first application, 4248m³ of air was compressed daily and injected into one well at a pressure of 2.7 bar, the oil being driven to near-by surrounding wells (*Uren, L.C., 1939*).

An underground combustion was accidentally started. Oil production was increased and heating in the reservoir was noted, but neither was attributed to a subsurface fire. The produced gas contained 10 to 15 % CO₂ (*Schumacher, 1980*). The first field experiments of *in-situ* combustion (ISC) were conducted in the former Soviet Union in the late 1930s. Since 1948, significant progress has been made through laboratory investigations and pilot tests. Mobil and Sinclair oil companies carried out tests in 1952. Mobil's work concentrated on tar sands, while Sinclair targeted the unrecoverable light oils that were left in the reservoir after a waterflood (*Moss and White, 1983*).

During the period 1950-65, a considerable laboratory work was performed, especially by Mobil and Gulf oil companies. In 1962, the first field test of simultaneous air/water injection was conducted in the Loco field of Southern Oklahoma. The process is known as a combination thermal drive (CTD). In 1967, Amoco, Exxon and Shell published papers on a modified process of *in-situ* combustion called "Combination of Forward Combustion and Water Flood" (COFCAW). This was a major breakthrough for ISC. During 1965-75, mature projects experienced many operational difficulties and problems. Since 1975, interest in *in-situ* combustion has been ebbing because of the previous

problems associated with it (*Farouq Ali*,1994), but there is now renewed interest in air injection for application in light, medium and heavy oil reservoirs.

So far, more than 160 *in-situ* combustion pilot tests of various types have been reported (*Turta*,1994). Although, there are more than sixteen active commercial projects world-wide, wider acceptance of the process is anticipated, as previous problems are now understood and great gains have been made in new proven technologies. Air injection now embraces all previous viscosity oxidation in an oil reservoir.

Recently *Turta et al* (1998), has proposed classification of air injection processes into four different processes. They are classified on the process basis of their spontaneous ignition potential and gas miscibility at reservoir conditions.

1. Immiscible air flooding (IAF) with intensive oxidation (HTO)
2. Immiscible air flooding (IAF) without intensive oxidation (LTO)
3. Miscible air flooding (MAF) with intensive oxidation (HTO)
4. Miscible air flooding (MAF) without intensive oxidation (LTO)

According to this classification, classic *in-situ* combustion is an immiscible air flooding process dominated by high temperature oxidation(HTO) and can be applied in light, medium and heavy oil reservoir, when the reservoir and oil characteristic are beneficial. Failure to apply the process correctly in the past, i.e. in good candidate reservoirs, has been one of the biggest factors mitigating against success. The renewed interest now, is driven either because air is seen as a cheap, available source of gas and /or the thermal and oil recovery efficiency, and also potential for heavy oil upgrading, is beginning to be recognised as very major benefits of the air injection process.

2.0 Basic Principles of In-Situ Combustion

In-situ combustion is a thermal recovery process in which air, oxygen, or oxygen-enriched air is injected into the reservoir in order to burn part of the oil (coke) to improve the flow of the unburned part. This coke is a product of chemical reactions between the injected air or oxygen, and the reservoir oil. These chemical reactions are triggered by an ignition device or spontaneous ignition when the injected oxygen contacts the oil near the well bore. This raises temperature in the zone surrounding the well to a significantly high temperature, so that continuous air injection causes a high temperature wave (combustion front) to propagate through the reservoir. Usually the temperature reached at the combustion front is much greater than the saturation temperature of water, in most cases between 400 to 600°C (*Burger et al*,1985). The heat generated in the combustion zone is responsible for distillation and vaporisation processes. The lighter fractions of the crude oil are transferred downstream and condense in the cooler zones forming an oil bank, whereas the heavier fractions remains behind and are converted to a semi solid residue or coke.

2.1 Methods of In-Situ Combustion

There are two basic methods of ISC namely: forward and reverse combustion. The classification refers to the direction of the combustion front movement; either towards the production well or towards the injection well. The direction of the front movement depends on the place at which ignition takes place. If the vicinity of the injection well is raised to a sufficiently high temperature, ignition will occur and the combustion front will move towards the production well (forward combustion). In contrast, if the vicinity

of the production well heated, this zone will ignite and the combustion front will move towards the injection well (i.e. against the injected gas), this is known as reverse combustion. The commonly used one is the forward combustion; which can be conducted in “Dry” or “Wet” modes.

2.1.1 Dry forward combustion

The oxidant is injected through an injection well and the reservoir oil in the surrounding of well bore is ignited, either, spontaneously or by ignition device (e.g. gas burner or electrical heater). After the permeability to gas develops, the combustion front moves radially away from the injection well and governed principally by the type and amount of fuel burned, the air injection rate, and the oxygen content of the injected air. As the combustion front moves away from the injection well, several distinct zones develop and a number of different but related mechanisms are being taken place. A schematic diagram of the classical process is shown in Figure 2.1.

Tadema (1959), described seven such zones:

1.The burnt zone: combustion has already taken place leaves behind a hot, clean sand that can be used to heat the injected air before the gas reaches the combustion zone, thus, a small part of the combustion energy is recovered; the remaining heat is lost to the surrounding formation. It is believed that the percentage of unburned fuel in this zone depends on the temperature of the combustion front. The temperature decreases up stream.

2.The combustion zone: Oxygen is consumed by the combustion reactions of the residual hydrocarbon and the coke, producing water and combustion gases. All water and light fractions are vaporised, and move downstream. The rate of the advancing combustion front depends essentially on the amount of fuel deposited. Temperature reached in this zone depends on the reservoir's rock and fluid properties; maximum temperatures of 300 - 800° C have been observed (*White and Moss,1983*). This thermal energy, transfers to the formation above, below, and ahead of the combustion front by convection in the reservoir fluids and by conduction through the formation rock.

3.The vaporisation zone (coke formation zone):

Immediately ahead of the combustion front the temperature is high enough to vaporise the lighter hydrocarbons and water to form a substantial steam plateau . Any oil that has not been displaced or vaporised is thermally cracked to produce a coke on the sand grains. This coke constitutes the principal fuel for the process. These cracking reactions may occur in the presence of oxygen, if the oxygen has not been completely consumed in the combustion zone.

4.The condensation zone: As the steam plateau moves forward and contacts the cooler sand, the steam loses heat rapidly to the formation and condenses, thus, reducing the viscosity, increasing the mobility and improving the oil displacement. The lighter hydrocarbons may be dissolved in the crude, thus enhancing its mobility. This effect plays very important role in oil displacement (*Poettman et al, 1976*).

5.The water bank : A high water saturation zone is formed by the condensed steam and the connate water. Most of the displaced oil and combustion gases from the upstream

zones accumulates in the water bank; the displacement mechanism is by water; temperature is lower than the condensation temperature of water.

6.The oil bank: A head of the water bank, high oil saturation zone is formed. The oil saturation in this zone depends on the efficiency of the steam displacement process (*Islam et al*,1989). The physical and chemical properties of the accumulated oil are different from the virgin oils. The mobility will depend on the temperature and the light fractions dissolved in the oil.

7.The virgin formation: This zone represents the initial reservoir conditions, and is unaffected except by the cold combustion gases.

In addition to the high thermal efficiency of *in-situ* combustion, five driving mechanisms can be observed, namely: water drive, gas drive, steam drive, miscible drive and solvent drive.

- Water drive: the oil zone is subjected to water drive, this water is that initially in place and the water produced by combustion reactions.
- Gas drive: A very effective gas drive forms during ISC; where the combustion gases (CO_2 , and CO), and inert gases transfer heat to the oil and displace it downstream.
- Steam drive: Due to the high temperature generated during the process, the water initially present in the formation, and water produced by combustion reactions are vaporised to form a steam zone. The large amount of latent heat released by condensing this steam imparts substantial energy to the oil in and ahead of the steam zone.

- Miscible drive: Carbon dioxide results from the combustion reactions, is partially dissolves in the oil and reduces the viscosity. The solubility of CO_2 increases as the reservoir pressure increases.
- Solvent drive: The lighter hydrocarbons produced during distillation, dissolve in the crude, thus reducing its viscosity and enhancing oil displacement.

Clearly, no other oil recovery process can displace fluids by this combination of driving mechanisms. In dry forward combustion most of the heat generated remains behind the combustion front (i.e. in the burnt zone) because of the poor heat carrying capacity of air, thus only 20 % of the generated heat will transfer down stream. This provided the need to use wet combustion to recover most of this stored heat.

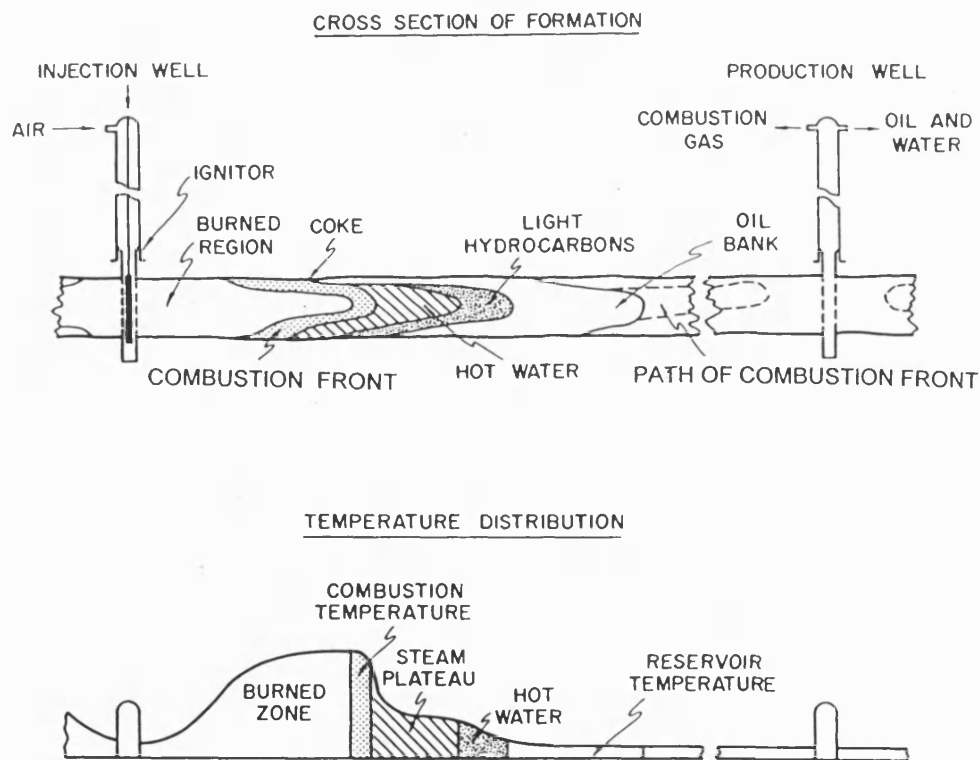


Figure 2.1 Schematic diagram of dry in-situ combustion process (*Nelson et al, 1963*)

2.1.2 Wet forward combustion

During dry forward *in-situ* combustion process a substantial amount of heat energy is left behind the combustion front and eventually lost to the adjacent formation. As a result, the thermal efficiency is reduced. In order to recover the heat left, and consequently improve the thermal efficiency of forward combustion, water is injected simultaneously or alternately with air to scavenge the heat energy from the burned sand. Thus, better heat distribution and less air requirement can be achieved. As the process proceeds, several zones develop as shown in Figure 2.2.

Zone 1: This zone has already been swept by the combustion front and contains little or no hydrocarbon. The cooling effect of the water reduces the temperature to lower than the boiling point of water, therefore the pores contain a liquid water saturation, whereas, the reminder of the space is occupied by the injected air.

Zone 2: Water is in the vapour phase in this zone, and the pores are saturated with a mixture of injected air and steam. The vaporised water is at the boundary between zones 1 and 2.

Zone 3: The combustion zone. Oxygen is consumed in the combustion of the hydrocarbons and of the deposited coke formed in the downstream part of the zone.

Zone 4: The vaporisation- condensation zone. The temperature is close to the vaporisation of water. Condensation of steam and water takes place and some oil light fractions are vaporised and carried downstream.

Zone 5: Water and oil zone. All the water condenses and forms a water bank preceded by an oil bank. Further downstream, the formation gradually regains its initial conditions.

The advantages of wet combustion over dry combustion may be summarised in the following points:

- The injected water results in better displacement efficiency.
- The large steam zone formed during the process results in higher sweep efficiency.
- Heat is transferred more effectively from the hot matrix upstream to the downstream zones.
- Less fuel is needed at the combustion front; and less air is therefore required. Faster propagation of the combustion front results.
- Wet combustion yields higher oil recovery.
- Wet combustion is expected to be less destructive to producing wells than other combustion process.

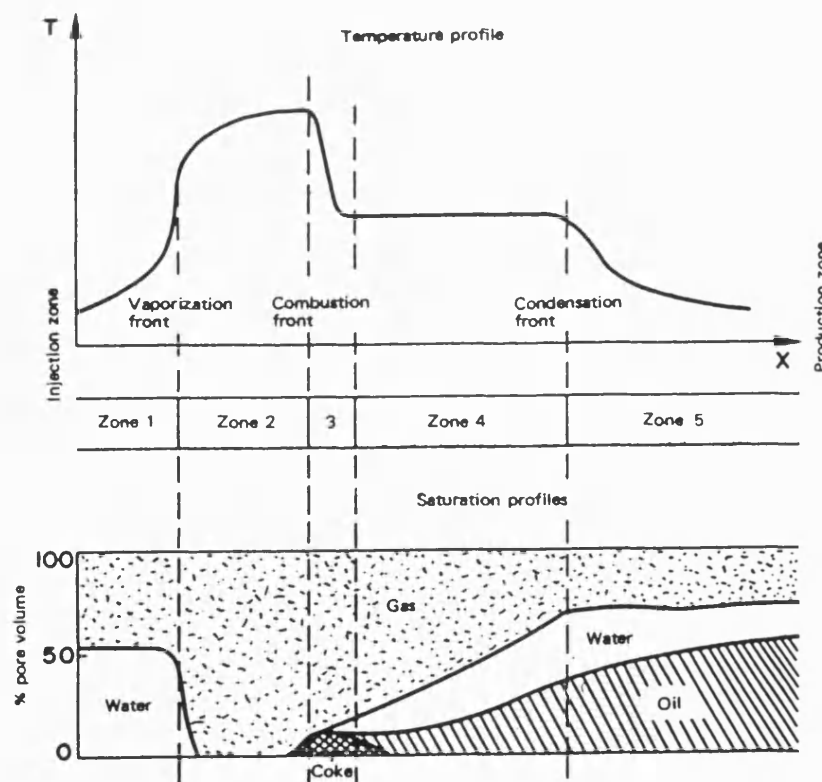


Figure 2.2 Wet forward combustion: temperature and saturation profiles. (Burger *et al*, 1985)

2.1.3 Reverse in-situ combustion

This process was developed as a method of recovering extremely heavy crude oil.

Reverse combustion is started as a forward combustion process by injecting air through wells that will eventually become producing wells. After the combustion front moves a short distance from the injection well, air injection is switched to adjacent wells.

Continued injection of air from adjacent wells forces oil to flow towards the previously ignited wells while the combustion front moves in the opposite direction. This traversing of the combustion front can result in a highly upgraded oil.

Burger et al (1985) have identified the various zones starting upstream and moving downstream, as shown in Figure 2.3 :

Zone 1. The injected air forces the crude oil toward the production wells, while the formation remains in the initial conditions. If the reservoir temperature is high enough and the oil is easily oxidisable, low temperature oxidation reactions could take place.

Zone 2. The temperature in this zone increases by conduction from the hot zone downstream and by the oxidation reactions, which assist in vaporisation of water, distillation of the light oil fractions, and cracking of some of the hydrocarbons. The gaseous and liquid fractions are carried downstream while some compounds form a carbon deposit or coke.

Zone 3. In this zone, the temperature reaches its peak. The oxidation reactions consume all oxygen which is not used in the previous zones.

Zone 4. In this zone the unburned coke remains behind on the porous medium and all the gaseous or liquid components flow downstream. The temperature decreases as the combustion front gets further away. In fact, reverse combustion has never been applied

to commercial oil production because of its poor sweep efficiency and process control difficulty (Moss and White, 1983). Drawbacks of the process may be summarised in the following points:

- Only the lighter fractions burn, leaving a heavy residue on the sand grains. This increases the air requirement which, in turn, increase the overall cost of the project.
- The strong tendency for spontaneous ignition increases the possibility of converting the process to forward combustion, i.e. the process is inherently unstable. However, there is still interest in this form of the process for heavy oil.
- Damage to the producing well completion can occur on ignition.

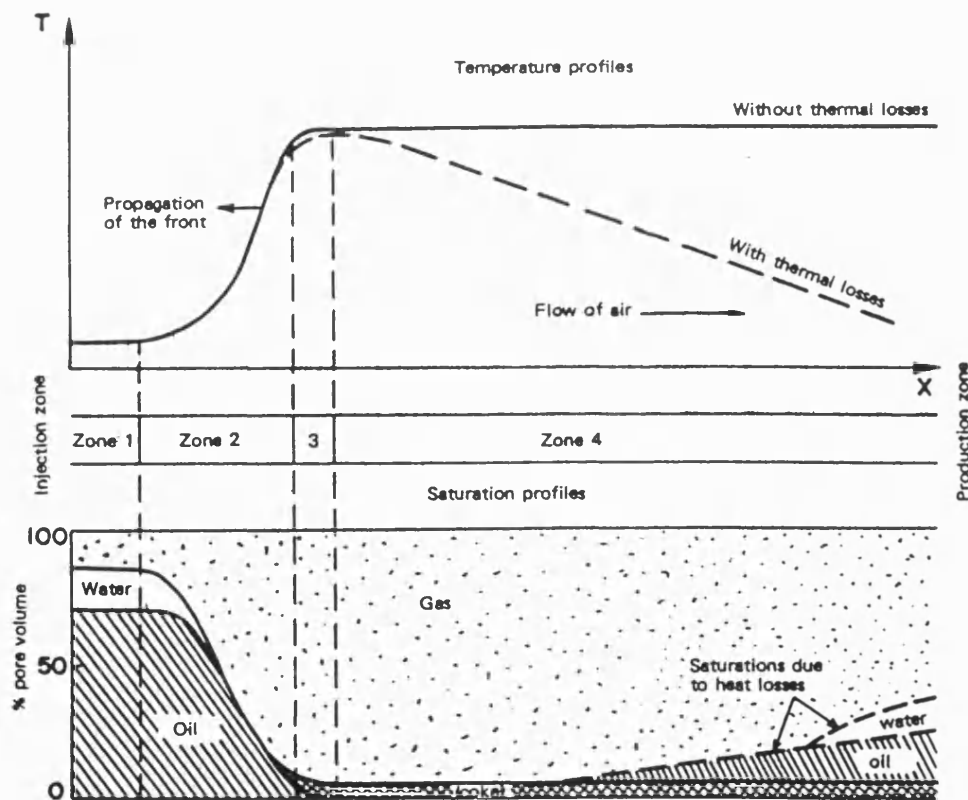


Figure 2.3 Reverse combustion: temperature and saturation profiles (Burger *et al*, 1985)

2.1.4 Other in-situ combustion variations

Enriched air injection, is a modification of the standard ISC process with the potential to overcome a number of the latter's drawbacks. Starting in the early 1980s, tests were undertaken to demonstrate these potential advantages compared to the conventional process. The use of oxygen instead of air has economic advantages, especially for high injection pressure operations. The advantages of oxygen enrichment may be summarised in the following points (*Shahani et al*, 1994):

- Faster oil production.
- Lower injection pressure.
- Greater well spacing.
- Increased carbon dioxide partial pressure.
- Lower volumes of injected and produced gases.
- Purer produced gas.

Although these benefits have been demonstrated in the laboratory, and successfully applied in field tests, the process is still at the developmental stage.

Nzekwu et al (1990) reported a combined cyclic steam stimulation followed by *in-situ* combustion in a pilot on the Cold Lake lease. The cyclic steam process recovers only 15 to 20 % of the oil in place. To improve recovery, *in-situ* combustion has been developed as a follow-up process. The combination of these processes takes advantage of the early production response of cyclic steam stimulation and the potential of high recovery and thermal efficiency of the combustion process. They reported that the frontal velocities (1.5 to 3.0 m/d) are more than 50 times the rates recently reported for other *in-situ* combustion processes.

Turta (1994) reported the first field testing of a combined *in-situ* combustion and foam injection in Karajanbas field. Foaming surfactant solutions were injected in 3 combustion wells arranged in line drive over 5 months period of testing. He reported that the oil production increased 2.4 fold, while water cut decreased by 20-25%.

Fassihi and *Merjerrison* (1994) reported a pressure cycling *in-situ* combustion at the Morgan field in Canada. The process consisted of two stages; namely: the injection period and the production period. The air injection period started with a low rate into the central injectors while the producers were open for production. When an unsteady flow was observed (due to gas slugging and sand production), the producers were shut-in. When a significant drop in production rate was observed, the air injection rate was increased to 28Msm³/D. Once the designed pressure level was achieved, air injection was terminated and the production period was started by reopen the producers. Production was continued until the rate dropped below its economic limit or when air had to be injected to sustain combustion in the reservoir.

Fassihi and *Gillham* (1994) reported the first project to combine air injection with the Double Displacement Process (DDP) in the West Hackberry field, Louisiana.

DDP is defined as the gas displacement of a water invaded oil column. The two displacement mechanisms are: oil displacement by gravity drainage and water displacement by the oil/gas movement down structure. When *in-situ* combustion is combined with DDP, the oil bank formed may increase the thickness of the oil column created by gravity drainage.

2.2 Reaction Kinetics of In-Situ Combustion

The main aim of studying the kinetics of ISC is to understand the complex nature of the process. Also, reaction kinetic data is very helpful in determining the conditions required to achieve ignition and sustain combustion. Although extensive work had been carried out for this purpose, a complete understanding of the complex physical and chemical changes taking place within the combustion zone is yet to be achieved.

In-situ combustion is a complex process involving three-phase fluid flow with heat, mass, momentum transfer, and oxidation reactions. The oxidation of crude oil in a porous medium can be initiated whenever oxygen comes into contact with oil at different temperatures. Many of the published studies indicate that oxidation of hydrocarbons may involve both complex homogenous and heterogeneous reactions that vary in importance, depending on temperature.

Tadema (1959) studied the reaction kinetics by the differential thermal analysis method (DTA). He reported two different combustion reactions, one at about 270 °C and one at 400 °C. Analysis of produced gases showed that oxygen was taken up near 270 °C.

A small fraction of oxygen was consumed to form CO and CO₂, while, the majority of oxygen reacted with hydrogen to form water. A coke-like residue was also found near this peak location. At the high temperature peak of 400 °C, mainly CO₂ and CO were formed, little water was produced and no hydrocarbon residue was found.

He concluded that during the first reaction, near 270 °C, mainly hydrogen is burned off, leaving a coke-like residue. This residue can only burn near 400 °C to produce CO₂ and CO. He also reported that the atomic hydrogen/carbon ratio of burned fuel decreased with temperature.

Weijdem (1968) identified three successive stages in the oxidation of oil, (1) at low temperature oxygen is taken up in the oil molecules, presumably without any particular degradation of these molecules, (2) at increased temperature oxidative cracking occurs accompanied by the production of CO_2 and H_2O , which leaves coke residue; (3) at still higher temperatures the coke, which consists of partially pure carbon, is burnt.

Bousaid and *Ramey* (1968) have found that the oxidation rate of crude oil in porous media depends on the carbon concentration, combustion temperature and oxygen partial pressure. The specific reaction rate constants are related to combustion temperature by the Arrhenius equation. They also found that the activation energy decreased as a result of the addition of clay and it was not sensitive to the gravity of the crude oil.

Burger and *Sahuquet* (1972) studied the kinetics of oxidation reactions involved in *in-situ* combustion. They considered the complete and incomplete combustion reaction of hydrocarbons to CO_2 and CO occurring at about 200°C , as low temperature oxidation reactions. They described the oxidation reactions of the crude oil and derived the most important processes by taking into account the formation bonds between one carbon atom and oxygen.

Bea (1977) used DTA & TGA techniques to study the oxidation of crude oils. He reported two temperature peaks, the first peak started below 205°C , indicating the onset of low temperature oxidation reactions. A second peak appeared around 370°C , and when the temperature reached 482°C the reaction was completed.

It is believed that the reaction mechanism between fuel (coke) and oxygen is a heterogeneous flow reaction and the oxidant gas must pass through the burning zone to

make the combustion front move. Within the burning zone, four known transport processes occur (*Fassihi et al*,1980):

1. Oxygen diffuses from the bulk gas stream to the fuel interface.
2. Oxygen then adsorbs and reacts with the fuel.
3. Combustion products, CO₂, CO, and water are adsorbed.
4. These products transfer into the bulk gas stream.

If any of these steps is inherently much slower than the remaining ones then it will be the rate determining step.

Hughes et al (1987) investigated the effect of oxygen partial pressure and sand surface area on the overall activation energy of the process as well as on the peak temperature.

They found that an increase in oxygen partial pressure and specific surface area of the porous media caused a decrease in both the activation energy and the peak temperature.

Greaves et al (1988) studied the combustion kinetics of Maya crude oil and found that they are dependent on fuel concentration, oxygen partial pressure and combustion peak temperature.

Hughes et al (1995) reported that the nature of reactions involved in *in-situ* combustion is significantly governed by the type of porous media.

Burger et al (1972), and *Fassihi et al* (1984), have established via elevated gas analysis, that the overall oxidation mechanism of crude oils in porous media may be represented by grouping them into three classes :

1. Low temperature oxidation reactions (LTO) which are heterogeneous (gas-liquid) and produce little or no carbon oxides.

2. Medium temperature oxidation reactions (MTO) fuel formation reactions which are homogeneous (gas) and involve the products of distillation and pyrolysis.
3. High temperature oxidation reactions (HTO) fuel combustion reactions which are heterogeneous (gas-solid), in which oxygen reacts with the fuel formed during MTO.

It is important to recognise that the hydrocarbon fuel is different for the three reactions.

For the LTO it is the unreacted crude oil, for the MTO it is the oxygenated oil and for the HTO it is the products of pyrolysis and oxidation. (*Shallcross et al*,1991).

2.2.1 Low Temperature Oxidation (LTO)

Low temperature oxidation reactions are exothermic heterogeneous reactions which take place between the gas and liquid phases at temperatures less than that required for complete combustion ($< 300^{\circ}\text{C}$). It is characterised by the absence or low level of carbon oxides in the effluent gas and yields water and oxygenated hydrocarbons such as carboxylic acids, aldehydes, ketones, alcohols and hydroperoxides.

The resulting oil can have higher viscosity, lower volatility, and lower gravity than the virgin oil (*Alexander* 1962, *Babu* 1984 and *Fassihi* 1986). LTO reactions may occur in the vaporisation, condensation, water and virgin zones.

Many papers have been published about LTO reactions, *Alexander et al* (1962) investigated the effect of LTO on fuel formation. They reported that if crude oil is subjected to prolonged LTO reactions, the fuel content is increased especially in light oil reservoirs; it appears that oxygen is partially consumed at the combustion front. As a consequence, oil ahead of the front is subjected to some LTO, particularly when the temperature exceeds (93-121 $^{\circ}\text{C}$). They concluded that LTO reactions have a pronounced

effect on fuel deposition and composition. *Poettmann et al* (1967) have demonstrated that if the crude oil is subjected to low temperature oxidation then fuel content is increased as much as 100 per cent over what it is if no LTO occurs. Also, they established that fuel content is a function of the reservoir rock and oil properties.

In a combustion tube study carried out by *Dabbous and Fulton* (1971), reaction rates were measured for two types of crude, 19.9 and 27.1 °API. Their results indicated a higher oxidation rate under similar reaction conditions for the higher API gravity crude. Light crudes appear to be more susceptible to LTO.

Adegbesan et al (1987), studied the kinetic of LTO reactions of Athabasca bitumen. The studies were carried out in a temperature range of 60 to 149 °C and at an oxygen partial pressure of 7.3 to 324 psi. The bitumen used was free of water and minerals.

They concluded that the overall rates of the oxygen consumption by LTO reactions are relatively small when compared with rates characteristic of high temperature oxidation. Also they found that total pressure had no influence on the LTO reactions and they depended on oxygen partial pressure.

Moore et al (1986), studied the kinetics of thermal cracking and low-temperature oxidation of Athabasca bitumen during dry, wet and superwet combustion. They concluded that during superwet combustion, LTO is the most likely mechanism for fuel deposition; whereas thermal cracking reactions can account for fuel deposition during dry and normal wet combustion. Also they concluded that LTO reactions will promote fuel lay down during dry and normal wet combustion. Their results indicated that thermal cracking alone may not be sufficient to deposit fuel and low-temperature oxidation

reactions are also important. Thus, LTO reactions should be considered when designing *in-situ* combustion.

Fassihi et al (1986), studied the LTO of four oils ranging from 10.1° to 31.1 API, they concluded that LTO increased both oil viscosity and density. For the 31.1°API oil, these increases were minor and should have insignificant effects on process performance. For the heavier oils (10.1, 10.4, and 17.3°API), relatively minor extents of oxidation resulted in more than a six fold increase in viscosity. They reported that LTO significantly increased the asphaltene content of the oxidised oil . They found the oxidation of carbon to CO and CO₂ has a higher activation energy than the LTO reactions.

Sibbald et al (1988) used a differential moving-frame descriptive model to analyse data from stabilised combustion processes produced in combustion tube experiments. Their results indicated that a substantial proportion of oxygen consumption occurred below the 300 °C level. This result is an important finding in showing that LTO reactions may occur as a normal part of the process of stabilised combustion front propagation.

Islam (1989) reported that LTO may result from incomplete oxygen consumption in the combustion zone, or air channeling into down stream zones, or a tilted combustion front surface.

Fassihi et al (1990) also attributed LTO reactions to oxygen channeling, which results from both reservoir heterogeneity and insufficient combustion rate. They reported that LTO tends to be more pronounced when oxygen is injected into the reservoir.

Belgrave (1990), has shown that LTO is an important fuel forming step in *in-situ* combustion, especially for heavy oil recovery.

Yannimaras et al (1997) have tested the oxidation characteristics of North Sea Maureen oil with air in the presence of reservoir rock and brine by using an accelerating rate calorimeter (ARC).

They reported that there is a minimum air flow rate below which temperature will remain in the low temperature oxidation mode. Similar results have been reported by *Showalter* (1963).

2.2.2 Medium Temperature Oxidation (MTO) (Fuel deposition)

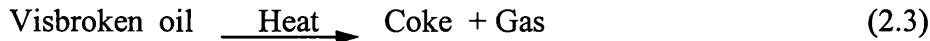
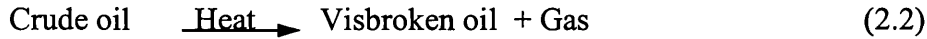
At temperatures above 300°C, the residual oil cracks into volatile fractions and a nonvolatile heavy residue consisting of coke, which constitutes the primary fuel for combustion. Both cracking reactions produce hydrogen gas and some light hydrocarbons in the gas phase. In an oxygenated environment, a portion of these hydrocarbons is oxidised; hence medium temperature oxidation occurs. It is assumed that the pyrolysis of crude oils take place by chain reactions (*Abu-Khamsin*, 1988).

These reactions include the breaking of C-C bonds, H-C bonds, polymerisation, condensation and alkylation. As a result, the reaction kinetics of this cracking can be extremely complex. Also, it is almost impossible to describe the mechanism precisely, even for a pure component because it not only produces solid like coke but also upgrades the remaining oil which affects the vaporisation behaviour of crude oil (*Lin et al*, 1984).

The reaction may be represented as:



There is an assumption that crude oil does not crack directly into coke and gas, but it goes through an intermediate step of visbreaking, then cracking into coke.



Alexander et al (1962) have observed that the amount of fuel deposited increases with an increase in oil saturation, oil viscosity and atomic hydrogen-carbon ratio, but decreases with an increase in API gravity.

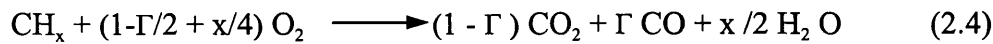
The amount of fuel deposited, is very important factor in *in-situ* combustion project design because the maximum oil recovery is the difference between the initial oil-in-place and the amount of fuel deposited. A high fuel concentration will reduce the combustion front velocity and increase air requirements, which increase the overall cost of the project. On the other hand, if the fuel concentration is too low, heat generated may be insufficient to propagate a self-sustaining combustion (*Mamora, 1994*).

Wu and Fulton (1971) identified that thermal cracking occurs in both the cracking zone and the evaporation zone, while coke is produced in the cracking zone. Therefore, the mechanism of fuel deposition is controlled by two important factors; the kinetics of the cracking reaction and the evaporation of crude oil components (i.e. displacement processes). These processes, determine the amount of fuel that will be deposited and how much fuel will be consumed. The displacement processes are hot water drive, gas drive, vaporisation, miscible displacement, fluid and gravity drainage (*Fassihi et al, 1984*).

Because the light oils contain more volatile components and are vaporised to a larger extent, vaporisation and miscible gas displacement processes play a more important role in light oil reservoirs .

2.2.3 High Temperature Oxidation (HTO) (Fuel combustion)

High temperature oxidation reactions are the main source of heat for the *in-situ* combustion process. They are a heterogeneous reaction occurring between the oxygen in the gas phase and the coke at temperatures above 343°C. These reactions produce carbon monoxide, carbon dioxide and water. HTO reactions can be represents by the following equation: (*Burger et al*,1985)



Where,

x = Atomic hydrogen/carbon ratio of the fuel

Γ = Molar ratio $\text{CO}/(\text{CO}+\text{CO}_2)$

The combustion rate (R_c) of crude oil in a porous medium was expressed by (*Wilson et al* 1963, *Bousaid and Ramey*,1968, *Burger and Sahuget*,1972 and *Fassihi et al*,1984) as follows:

$$R_{ci} = K_i \text{PO}_2^{\text{mi}} \text{C}_f^{\text{ni}} \quad (2.5)$$

Where,

C_f = instantaneous concentration of fuel

K = reaction constant

P_{O_2} = partial pressure of oxygen

m = reaction order with respect of oxygen

n = reaction order with respect of fuel concentration

i = reaction regime

The reaction rate is often assumed to be first order with respect to fuel for each reaction concentration, (i.e. $n = 1$) (*Fassihi et al*,1989).

The reaction constant (K), is normally expressed as a function of temperature, T , by the Arrhenius equation:

$$K = A_r \exp (-E/RT) \quad (2.6)$$

Where,

A_r = Arrhenius constant

E = activation energy

R = universal gas constant

T = absolute temperature

The effectiveness of HTO depends on the rate of heat generated by combustion and the efficiency of heat utilisation which depends on reservoir fluid distribution and the thermal properties of the reservoir rock and the adjacent formation.

One of the earlier studies to investigate the combustion reaction was done by *Bousaid* and *Ramey* in 1968. A total of 48 runs were made wherein a stationary thin layer of coke on unconsolidated sand was burned isothermally in a combustion cell. Individual runs were made at various temperature levels to permit determination of the effect of temperature upon the reaction.

They concluded that the carbon burning rate of crude oil in a porous medium was found to be dependent on carbon concentration, combustion temperature and oxygen partial pressure. They found that activation energy decreased significantly with the addition of clay to their sand matrix and it appeared to be insensitive to the oils used. Their results showed first order reaction rates in both oxygen partial pressure and carbon concentration.

Dabbous and Fulton (1974) observed that the combustion reaction is first-order with respect to oxygen partial pressure and second-order with respect to carbon concentration.

Greaves et al (1988), found that the combustion kinetics are dependent on fuel concentration, oxygen partial pressure and combustion peak temperature. The reaction rates for carbon concentration were found to be first order. For dry combustion, the oxygen partial pressure was found to have an approximate first order reaction rate, while for wet combustion, the value was less than half, due to the limiting factor of oxygen diffusion.

2.3 Parameters Affecting In-Situ Combustion Performance

2.3.1 Effect of matrix surface area:

Many oil reservoir formations are known to contain substantial amounts of fines including considerable amounts of clay minerals. Because of the large surface area involved and the high reactivity of such surfaces, the response of the formations to various recovery processes may be dominated by reactions at the clay surface (*Wilbur et al*,1980).

For *in-situ* combustion process, the specific surface area of the porous media is one of the most important factors to achieve smoothly advanced combustion front. Many studies have been carried out on the effect of surface area and associated materials on the ISC performance. The main conclusion is that surface area and fine solid materials may significantly influence combustion kinetics and fuel deposition.

Poettman et al (1967) studied the effect of the specific area of the reservoir rock. They concluded that a larger specific area results in an increased fuel deposition especially when clay particles were added to the matrix.

Bousaid and Ramey (1968) presented kinetic data from an isothermal combustion reactor in which a 13.9 °API crude oil was combusted at temperatures ranging from 266 to 671 °C. They observed a decrease in activation energy from 61,887 to about 48,394 Joules/gram mole when the porous media contained 20 % wt clay.

Hardy et al (1972) have reported that combustion could not be sustained when clean sand was used instead of the actual reservoir rock. They attributed that to the lower fuel adsorption on the sand surface.

Fassihi et al (1980) performed combustion tube tests on different crude oils in sandpacks containing clay. They reported that the average front temperature for the sandpack containing clay was about 510 °C, whereas in the clay-free sandpack the average temperature was 343 °C. They concluded that clay particles and fine sands enhance deposition of more fuel because of the adsorption characteristic on a higher surface area.

Vossoughi et al 1982, investigated the effects of surface area on *in-situ* combustion using thermogravimetric analysis (TGA). The experiments were done in the absence of clay by using silica sand with variable specific surface area. They concluded that for low specific

surface area experiments ($1120 \text{ cm}^2/\text{gr}$), the oil content immediately ahead of the front reduced below its original level, while the opposite affect occurred for high specific surface area experiments ($3330 \text{ cm}^2/\text{gr}$). Their results show a minimum specific surface area is required for any particular crude oil in order to establish a self-sustained combustion front in clean unconsolidated sandpacks.

In another study, *Vossoughi et al* (1984) investigated the effect of clay on dry ISC process. Sand mixtures of varying clay content were saturated with crude oil and water. They found that more fuel was deposited as the clay content of the mixture was increased, as a result the combustion peak temperature increased. They reported a significant reduction in the activation energy resulting from the addition of clay. This phenomenon may be contributed to the composition of the clay minerals mostly consisting of silica and alumina which are classified as solid acid catalysts. Their catalytic activities are related to their acid site density and strength. Activation energy decreases with an increase in the acidity.

Greaves et al (1987) investigated ISC behaviour in dry and wet modes using three different crude oils (36.6, 32.4, and 22.1 °API). They found that with light crude oils, it was not possible to sustain a stable combustion front using a clean silica sand, without first incorporating a clay additive, or other combustion surface promoter. It has also been found that clay content in the range 5 to 10 % wt did not significantly effect the level of oxygen utilisation.

Shallcross et al (1991), performed experiments to study the effects of various additives on the oxidation kinetics of Californian and Venezuelan oils. They concluded that the presence of iron, tin, and aluminum enhanced fuel deposition for Huntington beach oil

(density = 943 kg /m³). In contrast, the presence of copper, nickel, and cadmium had little or no effect. They found the presence of a ketal did not reduce the amount of fuel deposited by the Venezuelan oil (density = 996 kg /m³).

Mamora and Brigham (1993) have reported results similar to that observed by *Fassihi et al* (1980). They attributed higher combustion temperature associated with the use of clay or fine sands to the reduction in permeability, which increase residual oil saturation and hence fuel concentration resulting in higher combustion temperature.

2.3.2 Effect of pressure:

Commercial applications of ISC were mainly in heavy oil reservoirs, which are characterised by low initial pressure. The effect of pressure on the process performance have been studied by number of investigators. *Wilson et al* (1963), conducted combustion tube tests to study the effect of pressure on forward and reverse combustion. They used five types of crude at pressures ranging from 1 to 69 bar. In forward combustion, they found that increasing the pressure increases peak temperature, decreases combustion front velocities, but did not affect oil recovery. In reverse combustion, they found that increasing the pressure resulted in decreasing peak temperatures and oil recovery and increases the rate of advance.

Bae (1977) observed that the effect of pressure is oil dependent, but in general, increase in pressure causes the low temperature heat generation to increase.

Prasad and Slater (1986) conducted combustion tube runs at pressures up to 207 bar.

They found some benefits not observed at low pressure. Immiscible displacement of oil by carbon dioxide was found to be an important mechanism for both dry and normal wet combustion accompanied by an associated increase in oil production rate.

This was caused by gas at its high partial pressure, dissolving in the oil, swelling it and also reducing its viscosity.

Adegbesan et al (1987) have studied the effect of pressure on LTO reaction kinetics. The pressure applied in the study ranged from 22 to 44 bar. They concluded that the total pressure had no influence on LTO reaction but the reaction rates were found to depend on oxygen partial pressure.

Morre et al (1990) studied the effect of pressure on Athabasca oil cores in combustion tube runs by using enriched-air (95 % O₂). They found that increasing the operating pressure caused a significant rise in the oxygen and fuel requirements. They observed that the pressure effect with air is not effective to the same extent as for oxygen.

Tiffin and Yannimaras (1997) investigated the effect of pressure on the combustion behaviour of two light crudes. Experiments were conducted at pressure ranging from 6.9 to 37.2 Mpa using automated high pressure combustion tube. They concluded that the air/fuel ratio was relatively constant with pressure, while fuel deposition and air requirements increased slightly with pressure. They also reported the need for a high injection rate to operate the runs under high pressure. In the field, this can be a very limiting factor for sustaining HTO, or a propagating combustion front pattern; if the oxygen flux declines in the reservoir (limited air compression capacity) the process will drop into a LTO mode. However, a high temperature front (< 300 ° C) can still propagated.

Kisler and Shallcross (1997) have studied the oxidation kinetics of a light Australian crude oil by using Effluent Gas Analysis technique (EGA). They reported that high

pressures increased oxygen consumption throughout the oxidation and pyrolysis reactions.

2.3.3 Effect of water air ratio (WAR):

Injecting a small amount of water with the air can greatly enhance the forward combustion process. This is because the water becomes partially, or fully, evaporated upon contact with the burned zone and the steam generated displaces even more oil very effectively, resulting in a speeding-up of oil production. The term “wet combustion” is used to describe any process that involves the injection of air and water, either continuously, in a slug fashion, or cyclically. Wet combustion, optimal wet combustion, super wet combustion, and quenched combustion have all been used to describe the various WAR’s used in a combustion drive.

One of the first extensive studies of wet combustion was that conducted by *Dietz and Weijdem* (1968). According to the water injection rate, they classified the process into “normal wet” and “partially quenched”.

Normal wet combustion:

If water is injected at a low rate, the injected water will evaporate to superheated steam upon contact with the burnt zone before it reaches the combustion zone. The evaporation front should not overrun the combustion front and the coke deposit is completely burned. The steam flows through the combustion zone and behaves as inert gas then condenses downstream of the combustion zone as soon as the flue gas temperature decreases below the dewpoint temperature.

Partially quenched combustion

At moderate water injection rate, the vaporisation front velocity may be high enough to travel immediately behind the combustion front, hence, the residence time of coke in the combustion zone may not be sufficient for its complete combustion to be achieved.

Therefore, the combustion zone is quenched and some of the coke is left unburned (also known as incomplete combustion).

Due to the moderate thermal level of the process (250-300°C), it is obvious that the process is maintained by low temperature oxidation reactions and not by the high temperature oxidation reactions (*Burger et al*, 1973).

Parrish and *Criag* (1969) have described a Combination of Forward Combustion and Water flooding process. The COFCAW process involve the injection of air and water simultaneously (or alternately) after a small heat bank is initiated by dry forward combustion.

In their study, they used nine different crude oils with API gravity ranged from 18 to 40. They observed significant reduction in air requirement and fuel consumption in wet combustion experiments. They attributed that to the reduced residence time of gases and time for fuel deposition.

Burger and *Sahuguet* (1975) who conducted a study on wet combustion, they found that the combustion front velocity was higher in wet combustion than in dry. The velocity increased as the water air ratio was increased. When water was injected along with air, the fuel content also decreased as a result of more efficient sweep in the steam zone,

reduce the oil residual (S_{or}), thus the combustion front velocity and oil recovery increased.

Moore et al (1986), studied the effect of water injection on oil recovery for Athabasca bitumen. They concluded that, the fuel consumption and air requirement decreased with increasing WAR. The normal wet tests also provided higher recovery than the dry runs.

Greaves et al (1987) carried out combustion tube tests to study dry and wet combustion using three different crude oils ranging from 36.6 to 22.1 API. They concluded that a considerable reduction in air requirement occurred with wet combustion. Changing the mode of combustion from dry to wet greatly reduced the amount of fuel burned and at WAR of 3.75 the fuel consumption was only 31 % of that required for dry combustion.

Venkatesan et al (1990) studied wet combustion of heavy oil in detail. They found that increasing WAR leads to increase the size of the steam zone, which resulted in decreasing of oil saturation downstream, thus, reducing the amount of fuel burnt.

2.3.4 Effect of oxygen enrichment:

A great deal of attention has been directed for using oxygen enrichment since 1980 as many of its potential advantages have been recognised. *Moss and Cady* (1982) reported combustion tube results using oxygen concentrations up to 95%. They concluded that the peak temperature and oxygen utilisation were found to be similar for both oxygen and air. The apparent fuel lay down was 20 to 10 % higher over air dry and wet combustion.

Hansel et al (1984), conducted combustion tube experiments by using oxygen enrichment to evaluate the combustion characteristics of light oil. They used low initial oil saturation under different percentage of oxygen enrichment (21 to 95 % O_2) at constant gas influx.

They concluded that combustion with 40 to 95 % oxygen was vigorous, whereas combustion with air and 30% oxygen was unsatisfactory. Also they reported that front velocity increased and faster production was obtained with oxygen enrichment. The H/C ratio, peak temperature, oxygen utilisation and CO/CO₂ ratio were found to be the same under both oxygen enrichment and air.

Hughes et al (1990) reported that an increase of partial pressure of oxygen give better use of the fuel laid down in the combustion process and related to the virtual completion of LTO reaction at 377 °C with high concentration of oxygen (30-40 %). They also added that increasing oxygen concentration also produced a decrease in the activation energy for the high temperature oxidation reaction.

Petit (1997) studied the effect of total pressure, oxygen partial pressure and oxygen flux on the combustion kinetics of two crude oils having API gravities of 25.7 and 16°. He reported that at constant oxygen flux and increased oxygen partial pressure, there was a less than a proportional increase in combustion front velocity. At low pressure (10 bar), he observed that fuel availability and the air requirement at the front are slightly affected by the oxygen partial pressure. For 16 °API crude oil, he reported a slight increase in fuel availability and air requirements with oxygen enrichment. The opposite effect was observed for the lightest oil.

At high pressures (70-100 bar), there was no affect on the combustion of the heaviest oil, but there was a reduction of approximately 40 % in the oxygen requirement at front for the lightest oil.

2.4 In-Situ Combustion with Light Crude Oil

In-situ combustion has been mainly applied to heavy and medium oil reservoirs to reduce viscosity; thus it was thought that the process was only applicable to low-gravity oils.

However, *in situ* combustion has shown to be technically feasible in light oil reservoirs and a review of the *in-situ* combustion literature shows that several technically successful field operations have involved light oils up to 40 ° API (Table 2.1).

Table 2.1 Commercial ISC Projects Involving light oil Reservoirs (Tzanco *et al*, 1990)

Location	Year started	Gravity (API)	Viscosity (mPa.s)	Temperature (° C)	Pressure (MPa)
Pontotoc, S. Okla.	1952	18.5	7413	16	0.39
Sloss, Nebraska	1963	38.8	0.8	93	21.77
May-Libby, Louisiana	1966	40	3	57	10.73
Baneni, Romania	1977	31.7	2	42	14
Ochiuri Sud, Romania	1977	31.1	6	25	3
Posesti, Romania	1977	31.1	6.4	25	4
Moreni, Romania	1980	29.3	4	45	11
Countess B, Alta.	1983	28	8	32	9.6
Demjen East, Hungary	1986	39	6.2	38	N/A

The main concern with light oils is the lack of fuel to ensure that the process is self-sustaining. Generally, when air is introduced to an oil bearing zone, exothermal reactions take place between the oxygen and the oil. These oxidation reactions resulting in heat generation and production of carbon oxides. The heat is transferred ahead of the

combustion front by the generated flue gases CO_2 , CO , N_2 and the vaporised light fractions, resulted in desaturating the reservoir rock downstream.

In a light oil reservoir, the more volatile components are vaporised to a large extent, ahead of the front, displacing more oil ahead of the front. As a result, the residual oil saturation ahead of the front may be reduced to a low value which is not sufficient to sustain combustion.

In fact, the philosophy behind the application of ISC in light oil reservoirs is different from its application in heavy and medium oil reservoirs. In heavy oil reservoirs, the low oil mobility contributes to its high viscosity, whereas in light oil reservoirs, the low oil mobility is not a result of its viscosity, but is primarily due to low oil permeability, which is directly related to the oil saturation in the reservoir. However, the mechanisms that contribute to good recovery of low gravity crude may also enhance oil recovery when ISC is applied to light oil reservoirs.

Garon and Wygal (1974) have conducted combustion tube experiments with a very light crude oil having API gravity of 48° and viscosity of 1.8 mPa.s. The experiments were performed in dry and wet combustion modes at three pressure levels: atmospheric, 7 Mpa and 14 Mpa. They reported successful propagation of combustion front in the wet mode at pressure 14 Mpa. On contrast, neither dry combustion at 14 MPa nor wet and dry at lower pressures could be sustained.

Tzanco et al (1990) performed 15 combustion tube tests using reconstituted cores from the countess B and D reservoirs and crudes (27.5 to 30°API). In their tests, a definite transition in the oxidation kinetics was observed at 260 to 270°C . The transition was primarily from liquid phase oxygen addition reactions to combustion type reactions.

They concluded that countess B oil does not appear to be burning a coke-like fuel but it appears to be burning an oxidised asphaltene fraction.

Shallcross (1995) presented experiments to study the oxidation kinetics of light Australian crude oil. The experiments showed that the catalytic effect of the metals on light crude oils was more pronounced than for heavier crudes. He added that sodium, copper and iron promoted the fuel formation and combustion reaction.

In their tests with light oils, *Tiffin* and *Yannimaras* (1995), they concluded that ISC can be applied in light oil reservoirs at high pressure. The main discovery was that at high reservoir temperature and pressure ($> 100^{\circ}\text{C}$ and >400 psi) a light oil will autoignite. Thus, ISC is overall stable, because it will reignite downstream when the fuel is high enough. Furthermore, reservoir sands tend to improve the process performance in light oil reservoirs compared to outcrop sand stone.

Turta et al (1998) stated that the generation of a high peak temperature was realised in reservoirs containing oil with a viscosity of 2-6 mPa.s, but the values of these peak temperatures were lower than those for heavy oil reservoirs.

In some cases, the normal development and propagation of an ISC front was not achieved due to the following reasons:

1. Low reservoir temperature
2. Insufficient amount of fuel
3. Unfavourable reservoir properties.

Erickson et al (1993) described a new air injection process applied in Williston Basin projects, which were characterised by low porosity, low permeability reservoirs containing very light oils. They introduced the process termed high pressure air injection

(HPAI), which they claimed was equivalent to the classic ISC process. Although no high temperature were measured in the producers or in the observation wells, the CO₂ concentration in the produced gases seems to suggest the generation of a true ISC front, which according to Turta's classification (1998), combines miscible air flooding with intensive high temperature oxidation (HTO-MAF).

2.5 Three-Dimensional Scaled Model Studies

Most of the experimental flow studies of *in-situ* combustion have been performed under one-dimensional flow condition, i.e. in combustion tubes. These experiments are conducted to examine the feasibility of the process under specific reservoir conditions. They are used to determine air/oxygen and fuel requirements, as well as to validate numerical simulators.

In fact, results from such one-dimensional flow experiments are only approximately true because they do not simulate the multi-dimensional processes occurring in the real reservoir. Such effects as gas fingering, gas override and gas by-passing are largely absent.

For example, combustion tube experiments showed that the process was not feasible in the Williston Basin reservoir due to insufficient fuel deposition, but the actual field application proved that the process performed very well. This clearly shows that combustion tube experiments alone are not sufficient in simulating the field process (Turta *et al*,1998).

In addition, combustion tube experiments cannot provide any useful information regarding sweep efficiency and overall process stability. This valuable information can

only be obtained in the laboratory by 3-D experiments. Results from 3-D model experiments may be used in conjunction with data from combustion tube tests to predict the process performance in the field. Moreover, the results can be used to validate numerical simulators.

The first 3-D ISC scaled model experiments were reported by *Binder et al* (1967). Dry and wet fire flooding experiments were performed. The scaling criteria were tested in two cylindrical models differing in volume by a factor of 325. They reported that recovery levels of 60-70 % were achieved from a relatively thick, homogeneous bed at spacing-thickness ratio of 3; whereas for the experiments of a spacing-thickness ratio of 7, recovery was in the range of 30-50 % at about the same flux rate. They also reported an increase in air requirements by about 50 % for the heterogeneous bed.

Garon et al (1982) have investigated *in-situ* combustion of tar sand reservoirs in 3-D physical model to determine the relative performance of three different types of reservoir heterogeneities. They found that the preheating phase with the bottom water zone had a pronounced effect on fire-flooding performance. They also reported that a short steam preheating phase did not provide sufficient oil saturation in the communicating bottom water zone to ensure formation of a closed combustion front. The results from this investigation demonstrated the usefulness of 3-D modeling of the process to provide the basic understanding of the mechanisms of *in-situ* combustion in heterogeneous reservoirs.

Garon et al (1984) reported results from 3-D *in-situ* combustion scaled model experiments. They studied the effect of oxygen versus air injection, water-oxygen ratios, and crude oil parameters on sweep efficiency of the process. They reported that the

volumes of reservoir burned prior to combustion channeling were comparable for oxygen and air injection.

Also they found that the volumes of the reservoir swept by steam ahead of the combustion front increased with water injection. They reported that *in-situ* combustion in a reservoir with a medium gravity oil resulted in better sweep as compared to a heavy oil reservoir. The results indicated that wet combustion required less oxygen or air and increased the oil recovery and production rate.

Greaves et al (1991,1993 and 1996) have conducted extensive 3-D semi-scaled model studies to investigate the performance of the *in-situ* combustion process using vertical and horizontal wells in homogeneous and heterogeneous porous media. These experiments have confirmed the usefulness of 3-D combustion cell model to provide quantitative and qualitative evaluation of sweep efficiency over wide range of operating conditions.

2.6 Scaled In-Situ Combustion Experiments

Physical models of a particular recovery process, as applied to an oil-bearing porous media, can be partially scaled or unscaled. Scaled physical models have the advantage of simulating most of the physical phenomena associated with a particular process. A scaled model is designed on the basis of the principle of similarity, which is characterised by the same ratios of dimensions, forces, velocities and concentration differences, as those occurring in the prototype.

The need for scaling when conducting ISC experiments is of great importance to understand the significance of the results obtained and to translate them to actual field

practice. In fact, the complexity of the experimental conditions associated with 3-D scaled *in-situ* combustion experiments has limited the number of investigations.

The first detailed study in this subject was made by *Binder et al* (1967). Their criteria are based upon a simplified version of combustion, which considers single gas component flow (allowing the presence of a second phase) and conductive heat transport. Their scaling criteria are presented below, representing dimensionless length, time, velocity, balance of viscous and gravitational forces and vertical to horizontal permeability ratio.

$$l/h, \alpha t/l^2, v t/l\phi, \mu_g v/K_v K_{rg} \Delta\rho, K_v/K_h \quad (2.7)$$

where

l = length of the reservoir model

h = thickness of the reservoir model

α = thermal diffusivity

t = time

v = superficial velocity

ϕ = porosity of reservoir

μ_g = gas viscosity

K_v = vertical permeability

K_h = horizontal permeability

K_{rg} = gas relative permeability

$\Delta\rho$ = change in fluid density

They showed that their model results were in fair agreement with the results of three major field tests conducted at that time.

Garon et al (1974) reported results of *in-situ* combustion experiments conducted in 3-D scaled model. The scaled model inter-well distance was 0.81m, with a scaling factor between model and field of 120. This resulted in thin oil layer dimension in the model (0.16m). The experimental time of one hour corresponded to 1.64 years for the field.

The scaling method employed in this study has been discussed by *Binder et al* (1967) for *in-situ* combustion, *Pujob and Boberg* (1972) for steam flooding and by *Kimber and Farouq Ali* (1987).

The scaling factor used in this study is 250, which allows a model thickness of 0.1 meter with an inter-well distance of 0.4 meter. Those dimensions corresponding to a field prototype having a thickness of 25 meters and a well spacing of 100 meters.

It is necessary to maintain geometric similarity between the physical model and the field.

This requires that:

$$[L/D]_M = [L/D]_F \quad (2.8)$$

Where L is the well spacing, D is the bed or oil layer thickness and the subscripts M and F refer to the model and the field prototype respectively.

Diffusion

To scale diffusion of heat and mass, the characteristic flux in model must be increased in direct proportion to the geometric scale factor. This requires that:

$$[L U]_M = [L U]_F \quad (2.9)$$

Where L and u are characteristic length and fluxes respectively. Gravity effects can be scaled only through a corresponding increasing the model vertical permeability:

$$[L K]_M = [L K]_F \quad (2.10)$$

Where k is the permeability.

Scaling of flow

Because of the well configuration used, the pressure controlled draw-down action of the horizontal producer well is a very important factor in controlling the flow behaviour.

The pressure draw-down is a force acting against the buoyancy forces causing gravity override where adequate vertical permeability is present. The degree of gravity override would be correctable by the ratio of gravity forces to horizontal viscous forces, which may be expressed as:

$$\frac{L g \Delta \rho}{\Delta P g_c} = \frac{A k \rho g \Delta \rho}{\mu w_i g_c} \quad (2.11)$$

In this expression, $(\Delta P/L)$ represents the increase pressure gradient, $(g \Delta \rho / g_c)$ represents the buoyancy force gradient between two fluids having a density difference $\Delta \rho$ and g_c is the dimensional constant, (w_i / A) is the mass injection rate. ρ and K / μ are the density and mobility of the injected fluid respectively.

The draw-down force can be expressed by $\rho g \Delta z$, where ρ is the fluid density, g is the gravitational constant, and Δz is the vertical distance.

The draw-down force can be added to the right hand side of Equation 2.11, which may be expressed as:

$$\frac{L g \Delta \rho}{\Delta P g_c} = \frac{A k \rho g \Delta \rho}{\mu w_i g_c} + \rho g \Delta z \quad (2.12)$$

Thus, 'Toe to Heel' displacement using horizontal well line drive, provides gravity-assistance to the combustion front, by controlling gas override tendency.

Scaling of pressure

Yannimaras and Tiffin, (1995) who undertook a series of *in-situ* combustion experiments operating at pressures between 69 bar and 372 bar. They found that, on increasing the experimental pressure, the air requirement (m^3/m^3 of matrix) increased, therefore a greater injection flux had to be used.

$$\left[\frac{P_F}{P_M} \right] = \left[\frac{Q_F}{Q_M} \right] \quad (2.13)$$

$$\left[\frac{P}{Q} \right]_M = \left[\frac{P}{Q} \right]_F \quad (2.14)$$

Where Q is the air flux and P is the operating pressure.

For lower pressures, a similar set of experiments need to be performed to further clarify the effect of pressure on the air requirement and hence the flux.

Some phenomena remain un-scaled between the model and the field such as capillary pressure, relative permeability, combustion zone kinetics, and well bore effect.

Pujol and Boberg (1972) have found that the capillary effect may not be very significant for medium and heavy oils in high permeability sands. The reaction kinetics are not scaled because the residence time in the model is much smaller and simulation studies by *Lin et al* (1984) have shown that results were insensitive to the kinetics of combustion reaction.

2.7 Thermal Recovery Methods Using Horizontal Wells

The introduction of horizontal wells has been responsible for tremendous advances in oil field development, especially advanced EOR processes. Horizontal and multi-lateral wells are being introduced in ever-increasing numbers to achieve further gains in reservoir productivity. Two hundred horizontal wells were drilled a decade ago. Now, one company has reported drilling more than 2,100 horizontal wells in North America (Koen,1992). Advances have also been achieved in the depths drilled, reaching 8,761m (Blikar *et al*,1994).

The success of horizontal well technology is due mainly to the advantages horizontal wells offer such as productivity enhancement, recovery improvement, coning reduction and sand problem attenuation. As injectors, horizontal wells can enhance injection rates, thus providing larger producing capacity with high production rates. Horizontal well technology has created new possibilities in the application of conventional thermal recovery processes (Joshi, 1991). The implementation of thermal recovery processes using horizontal wells can be effected in five major process variations:

1. Steam assisted gravity drainage (SAGD)
2. Heated annulus steam drive (HASD)
3. Combustion override split- production horizontal well (COSH)
4. Pressure controlled gravity drainage (PCGD)
5. Vapour extraction (VAPEX)

2.7.1 Steam-Assisted Gravity Drainage (SAGD)

In this process (SAGD), the injector(s) and the producer are usually kept close together for easy communication between them as shown in Figure 2.4. Steam is injected from

either a horizontal well, or one or more vertical wells completed above the horizontal producer. A steam saturated zone is developed with a temperature approaching that of the injected steam. As the latent heat of the steam is transferred by thermal conduction into the surrounding matrix, steam is condensed. The condensed water and heated oil drains by gravity forces into the horizontal production well.

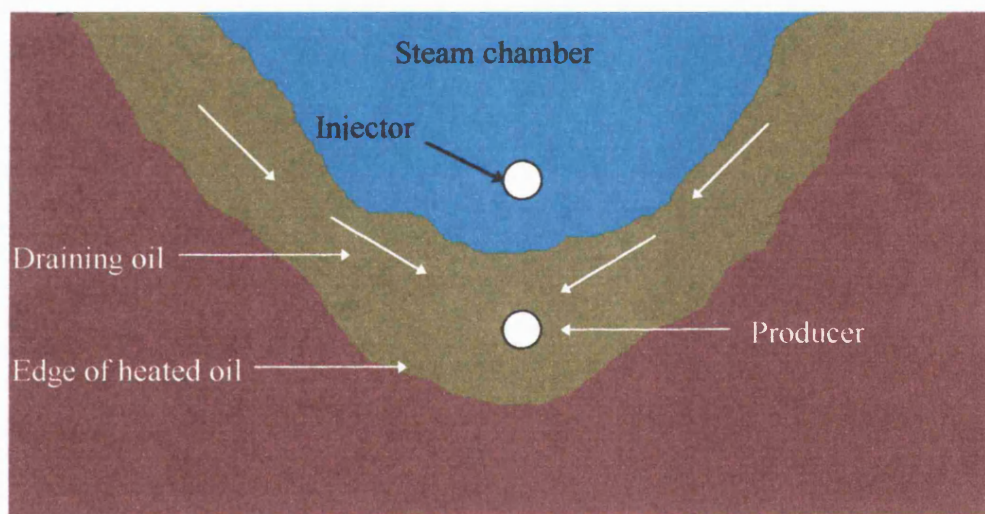


Figure 2.4 The concept of Steam Assisted Gravity Drainage process (SAGD)
(Butler *et al*, 1981)

2.7.2 Heated Annulus Steam Drive Process (HASD)

This process consists of a horizontal, cased, unperforated pipe running between a vertical steam injection well and a vertical production well as presented in Figure 2.5.

The process is started by circulating steam through the injection tubing and condensate is produced via the casing. Over a period of time, a heated region is formed around the horizontal pipe and hence, oil mobility is increased. Thereafter, steam injection is switched to the vertical injection well, while production is initiated at the vertical production well. As a consequence, fluids move along the annular region towards the producer.

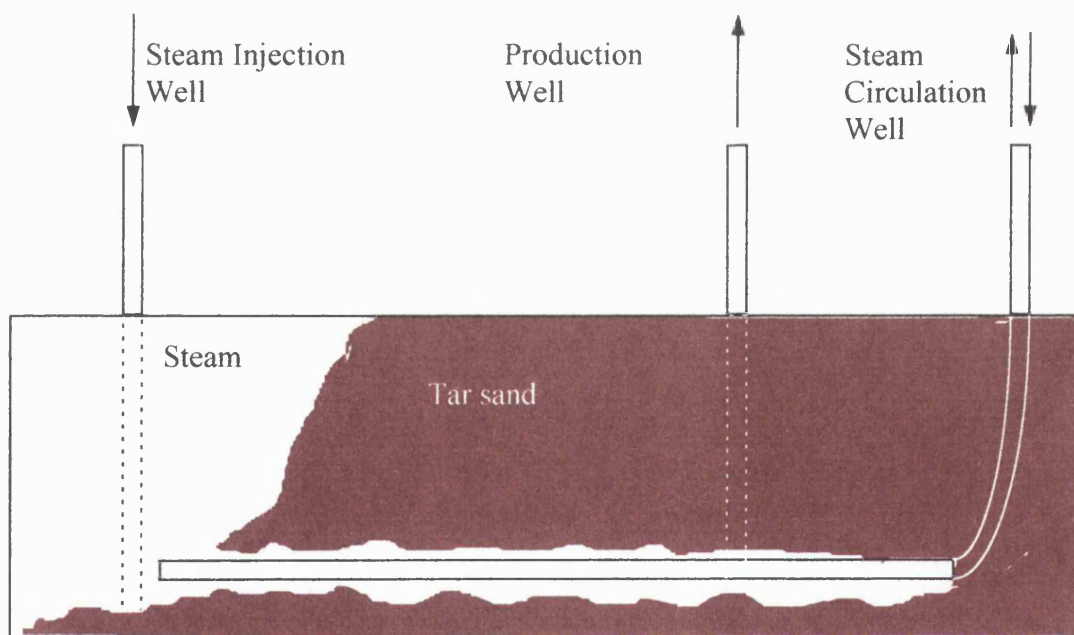


Figure 2.5 The concept of Heated Annulus Steam Drive process (HASD)
(Sufi et al, 1990)

2.7.3 Combustion Override Split-production Horizontal well (COSH)

The COSH process was conceived to combine the high recovery potential of gravity drainage with the energy efficiency of the *in-situ* combustion process. It minimises problems associated with combustion operations such as gas production, oxygen breakthrough, combustion damage and sand production, (Kisman and Lau, 1993).

The process involves rows of vertical injection wells completed in the top part of the reservoir and cooled by water circulation to minimise thermal stress to downhole equipment. Flank gas production wells, which are initially completed near the top, are used to produce the generated combustion gases (see Figure 2.6).

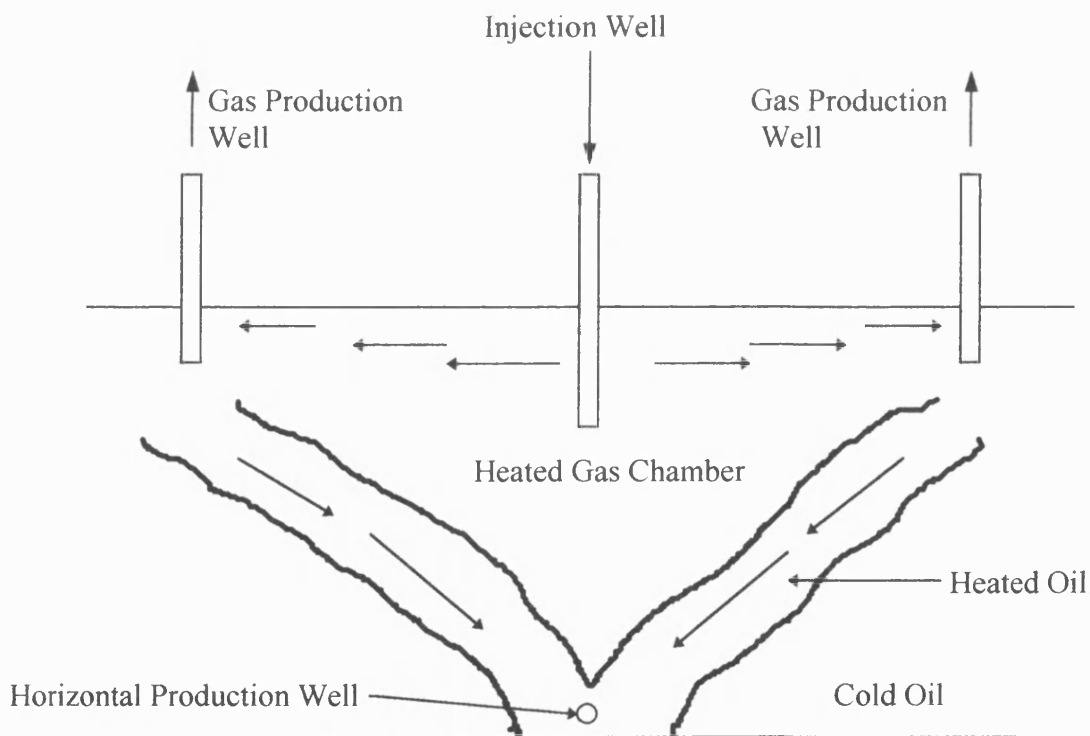


Figure 2.6 The concept of Combustion Override Split-production Horizontal well process (COSH) (Kisman et al, 1993)

A horizontal production well is placed near the bottom of the produced formation under the vertical injection wells. As combustion is developed around the injectors, a hot gas chamber is formed in the vicinity of each injector, which is similar to the steam chamber in SAGD process. Most of the generated gases are produced via the gas production wells, while heated oil and water are drained by gravity into the horizontal production well. There have been no applications of this process so far.

2.7.4 Vapour Extraction Process (VAPEX)

The VAPEX process is an evolution of the SAGD concept in which the injected steam is replaced by a low boiling hydrocarbon solvent and hot water (*Butler and Mokrys, 1991*). The function of the solvent is to dilute the oil and distribute the heat laterally away from the injector. The function of the hot water is to warm the reservoir to maintain vaporisation of the injected solvent. Following hot water/solvent injection, a vapour chamber is developed between the injector and the producer. The hydrocarbon vapour dissolves in the bitumen or heavy oil and reduces the viscosity, and the diluted oil drains to a horizontal production well. Production rates are directly related to the concentration of the solvent used, which is very expensive and cannot be completely recovered.

2.7.5 Pressure Controlled Gravity Drainage (PCGD)

In this process, two horizontal production wells are used with one vertical injection well (*Sawhney et al, 1997*). Toes of both horizontal wells are directed towards the injection well as shown in Figure 2.7 this configuration is similar to 'Toe to Heel' *in-situ* combustion process proposed by *Greaves* (1991) and now referred to as THAI (Toe to

Heel Air Injection). A horizontal injection well perforated at selective intervals can be used instead of number of vertical injectors. Injected Steam rises to the top of the formation and heated oil starts to drain to the toes of the horizontal wells. As the steam chamber moves towards the heel (toe to heel) it contacts cold oil and creates a steam chamber similar to the steam chamber initially developed near the toe.

Numerical simulation of a 500m long horizontal well showed that PCGD is superior to SAGD.

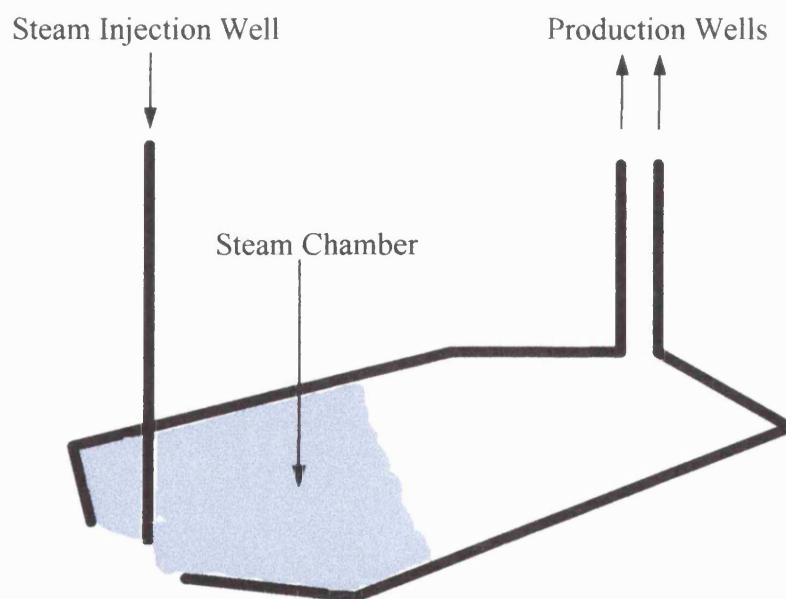


Figure 2.7 The concept of Pressure Controlled Gravity Drainage process (PCGD)
(Sawhney *et al*,1997)

2.8 Laboratory Studies with Horizontal Wells

Several investigations have been conducted to evaluate the performance of horizontal wells in different IOR methods. *Joshi* (1988) performed low pressure steam-assisted gravity drainage (SAGD) experiments. He suggested that production rates are two to five times greater than unstimulated vertical well production due to the large reservoir contact area.

Islam et al (1989) reported a new recovery method for heavy-oil reservoirs containing bottom water zone by using horizontal wells. The method involves electromagnetic heating of the production wells with gravity stabilised gas or water injection. They found that recoveries as high as 77 % OOIP may be obtained, even if the thickness of the water and oil zones were equal.

Ahner and sufi (1990), have studied the gravity drainage behaviour of steam flooding in a heavy oil reservoir using horizontal wells at several injection rates and various configurations. They observed that, the steam rose to the top of the model and swept it from the top down (gravity drainage) even with communication between injector and producer. More efficient sweeping is achieved when the well spacing was decreased by horizontal well.

Bagci et al (1992,1993) found that in cyclic operations, the use of a horizontal well increased the recovery by 30-50 %. In a line drive configuration, the recovery using two horizontal wells was 70 % higher than the corresponding vertical well configuration.

McGee et al (1996) have reported on field test results of electrical horizontal well project in the Lloydminster heavy oil area. In this project, two deviated vertical wells and one

horizontal well where connected electrically and heated. Although a significant production response was achieved, on going operations were not achieved because of equipment failure and sand production.

McLntyre et al (1996) have reported use of a tubing set-up in a number of horizontal production wells operated by Husky Oil Operations Ltd. The technique allows one to change tubing inflow location with the use of a wireline. Field production data has proven that the technique is effective in controlling gas and water production rates. This suggests that it might be possible to control fluid inflow along the well length by simply changing the fluid entry points.

2.8.1 In-Situ Combustion Using Horizontal Wells

Few details have been published regarding the implementation of horizontal wells in conjunction with *in-situ* combustion both in laboratory research and in field testing. The first comprehensive study on the application of ISC/horizontal wells was carried out by *Greaves et al* (1991). They demonstrated that higher sweep efficiency was achieved with both single and dual- horizontal producers. Moreover, the gas override phenomenon was greatly reduced and the vertical sweep efficiency of the combustion front considerably improved compared to the single vertical producer.

In another study, *Greaves et al* (1993) proved that sweep efficiency and oil recovery were substantially increased when using horizontal producer wells. They showed that the volumetric sweep efficiency increased from 59 % for the vertical wells case to 70 % for the horizontal wells case. *Kisman and Lau* (1993) have performed experiments which employed horizontal wells in conventional patterns. This resulted in lower sweep

efficiencies and oil recovery comparing with the line drive configuration used by *Greaves et al* (1993).

Battrum field is one of the oldest fields in which *in-situ* combustion has been used since 1964. Two horizontal producing wells were drilled in 1992 and 1993 in order to improve the horizontal displacement. According to *Ames et al* (1994), the productivity of one well is ten times that of nearby vertical wells.

2.8.2 Horizontal wells in direct line drive configuration

The well configuration in a reservoir can have a significant effect on the recovery process behaviour, which in turn, determines both the technical and economical success of the project.

This is especially true for any IOR process, particularly those involving gas injection, which require strategic placement of producers and injectors in order to reduce the effect of mobility variations between the injected gas and the displaced oil. Although the displacement efficiency of *in-situ* combustion is not in question, efficient control of the process is required to deplete the reservoir in a stable and cost effective way. This can be achieved, by distributing the producers and injectors in optimum pattern among the reservoir area. Direct line drive is an attractive pattern, which can be used to optimise the process.

Using a horizontal producer well, to effect a 'Toe to Heel' displacement, provides direct drainage of the oil along the path of the horizontal well, eliminates the need for steaming or pre-heating (see Figure 2.8 a and b). Gravity drainage is one of the driving mechanisms involved in this configuration, and there is also a pressure drop along the

length of the horizontal well (i.e. from the toe to the heel), which acts along the centre of the reservoir. This pressure gradient provides the draw-down action, which is an additional drive mechanism. The draw-down effect provides gravity assisted to the inflow of heated fluids ahead of the combustion front into the exposed section of the horizontal well. This is restricted, in the ideal case, to heavy viscous oil reservoirs where the oil mobility in the downstream cold zones is very limited, or zero. There will be some heat exchange provided by the hot produced fluids flowing through the horizontal well production string, which will raise the temperature of the cold region, causing some drainage. The draw-down effect provides simultaneous drainage of the mobilised oil and combustion gases into the horizontal producer well, which results in a faster production response. It also preserves the quality of the thermally cracked oil if the mobilised oil was upgraded. Most importantly, it provides instantaneous production of the combustion gases by virtue of the downwards flow gradient towards the horizontal producer, which reduces or eliminates gas override. In addition, the horizontal producer is traversed by the combustion front (Figure 2.8 a), thus providing unique flexibility for efficient control of the front pattern to maximise sweep efficiency, which theoretically can approach 100%. Also, this configuration allows the horizontal well to be used to optimise the process performance by adjusting inflow of fluids ahead of the combustion front.

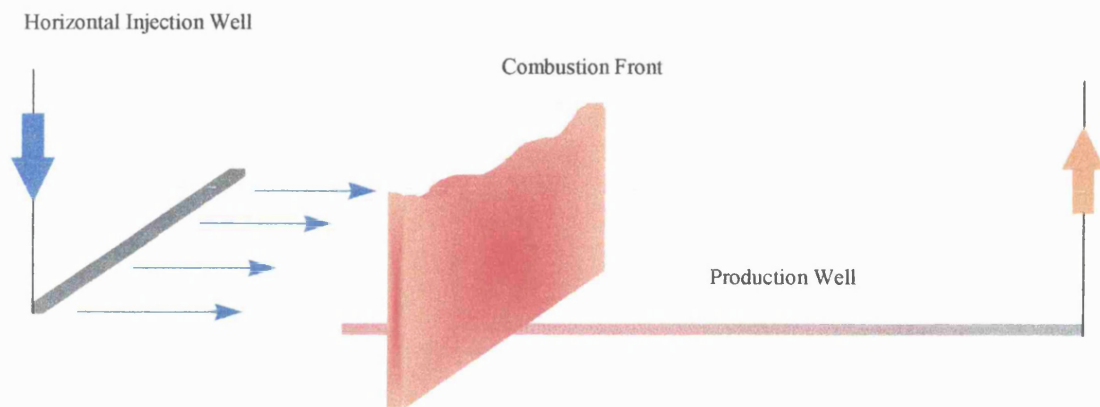


Figure 2.8A The concept of Toe to Heel Air Injection process (THAI)

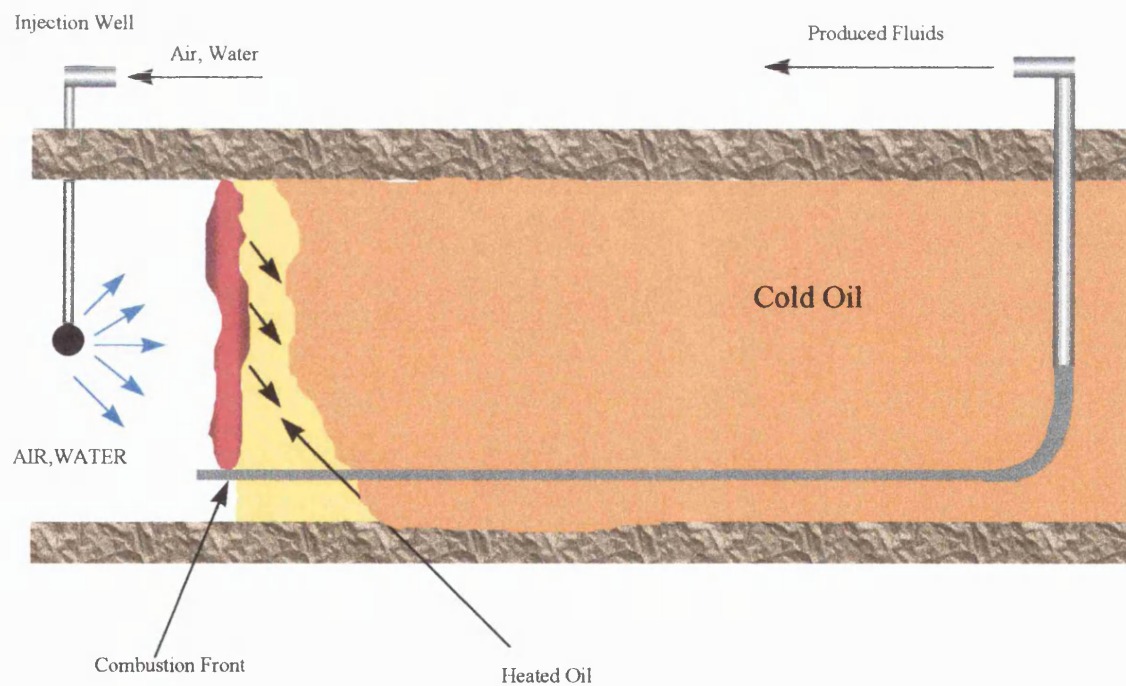


Figure 2.8B Production mode of Toe to Heel Air Injection process (THAI)

2.9 Heavy Oil Upgrading Technology

Large reserves of heavy oil remain unexploited world wide because of its low market value and problems of processing and transportation. On the other hand, there is a steady and inevitable decline in the production of light, premium crude oil. Hence, countries with significant heavy oil resources are likely to emerge as a significant oil producers in the next century. However, the biggest challenge will be to improve the quality of heavy oil in order to achieve both market penetration as well as meeting environmental concerns. On a practical level, most of existing refineries are only designed to process conventional light crudes and have limited capability to handle any significant amounts of heavier crudes.

Heavy crudes are usually characterised by low API gravity, high density, viscosity, and boiling point as well as containing high amounts of sulphur, nitrogen, vanadium, nickel, and asphaltenes. Their hydrogen to carbon ratios are undesirably low. The objective of the upgrading process is to remove the heaviest, least desirable fractions while leaving behind an oil that has been greatly reduced in its metal, nitrogen, sulphur, and Conradson carbon content.

There are various ways of upgrading heavy crude oil and bitumens. The choice of process, or a combination of techniques may depending on the type of crude oil and also particular refinery logistics. Upgrading methods range from simple visbreaking, which lowers oil viscosity, primarily to increase its pumpability, to sophisticated chemical processes capable of converting heavy crude into high quality synthetic lighter crude oil.

2.9.1 Upgrading Methods

There are two basic methods for heavy oil upgrading: carbon removal and hydrogen addition.

Carbon Removal (Coking)

Carbon removal basically removes the heavy asphaltene fraction of the heavy oil, thereby increasing the hydrogen carbon ratio of the liquid fraction. Carbon removal processes can be catalytic or non-catalytic. Non catalytic processes include physical separation, thermal cracking, gasification, and combustion. Physical separation and thermal cracking processes produce a high carbon residue stream (coke), which is usually used as fuel in combustion processes. Gasification and combustion processes convert the residue feed to either gas or energy. Catalytic carbon removal processes uses a catalyst to absorb the coke onto its surface, which is then removed via combustion in the treating vessel.

The main carbon removal processes are Delayed Coking, Fluid Coking, and Flexicoking. Coking is the most widely used method for heavy crude upgrading, but the major drawback of this process is that a considerable portion of the feed is transformed to solid coke residue and gas, instead of more valuable liquid products. Furthermore, the quality of the coke is usually poor because of the presence of heavy metal impurities.

Hydrogen Addition (Hydrocracking)

This is a catalytic process, in which the feedstock is reacted in the presence of hydrogen. The H/C ratio is increased as more hydrogen atoms are attached to cracked chains of carbon-hydrogen molecules. Hydrocracking processes provide the greatest liquid yields for a given feed but the high hydrogen consumption associated with these processes is

one of the main drawbacks. Because of the high pressures and the processing reactor equipment is very expensive, the hydrogen addition processes are classified into Fixed bed and Expanded bed types.

In currently operating commercial plants, upgrading is achieved by either coking followed by separate hydrotreating or low conversion hydrocracking and coking followed by separate hydrotreating. More recently, high conversion hydrocracking processes with integrated hydrotreating have been selected for new projects because of the higher liquid obtainable yields, and also because of the better quality products, and greatly reduced residue.

To achieve high conversion effectively and economically, optimal conditions of temperature, hydrogen partial pressure, and catalyst must be chosen. The temperature is generally as high as is practical to maximise reaction rates, minimise reactor volume and suppress coking of the catalyst. The pressure chosen is generally as low as possible to minimise the capital and operating cost. This pressure must favour high conversion reactions. The catalyst chosen must accelerate the reactions and therefore allow operation at a pressure that is lower than would otherwise be required (*Padamsey et al, 1990*).

Hydrodesulphurisation (HDS) is the conventional means for the removal of sulphur compounds from crude oil. It is essentially the reaction of hydrogen with the predominantly hydrocarbon feedstock in the presence of a catalyst to produce a desulphurised hydrocarbon product and hydrogen sulphide. In addition, some hydrocracking reactions will occur, where the hydrocarbon chains are broken into smaller molecules. Heavy metals are deposited on the catalyst surfaces.

The operating conditions for HDS are: pressure 25-100 bar, temperature, 340-420°C. The most severe conditions are necessary with a residue feedstock.

The catalyst should exhibit long term stability (i.e. no loss of surface area with time, or during regeneration) and minimum sensitivity to poisons such as carbon, vanadium and nickel. The main catalyst, which meets these requirements, is molybdenum disulphide supported on alumina and promoted with either cobalt or nickel; the so-called Co Mo or Ni Mo catalyst.

It is well known that catalyst activity generally decreases with time and hence in some desulphurisation processes, fresh catalyst is continually added in order to maintain constant catalyst activity. This high rate of catalyst replacement would result in high catalyst operating cost, therefore, regeneration of the used catalyst is necessary to minimise the operating cost.

One method of regeneration is to use a steam/air mixture to remove deposits from the catalyst surface, thus restoring their activity (*Goodman et al*,1970).

Specially designed vessels (Reactors) are used for upgrading processes or other oil processing methods. Various types of reactors are employed such as fixed bed, co-current and counter moving bed, ebullated bed and slurry reactors.

Generally, the reactor contains the catalyst and the feedstock flow through the catalyst in the presence of hydrogen at specific temperature. A series of reactors may be used for high quality products.

Previously, upgrading of heavy crudes is achieved by conventional surface upgrading techniques. However, thermal processing of crude oil can result in a degree of upgrading,

and there have been some reported *in-situ* upgrading attempts. The common feature between them is the presence of a heat source, hydrogen, and a catalytic agent.

The latter may exist in the reservoir rock itself, or in the oil in the form of minerals.

Magnie (1980) reported the injection of hydrogen in the presence of a heat source into the oil zone. Injected hydrogen dissolved in the oil, causing an expansion in the oil and rise in its temperature, thus reducing oil viscosity. During the process, hydrogen may upgrade oil, using minerals in the reservoir as catalyst to assist in the hydrogenation reaction.

Dean et al (1982) have reported a hydrogenation process which involves terminating a forward combustion process and injecting hydrogen into the burned-out zone. A fluid is injected into the former production well to drive the oil to the heated-hydrogen-rich zone, thus effecting hydrogenation prior to production.

Ware et al (1987) have reported the injection of heated solvent and hydrogen into a heavy crude or shale deposit via a production well. The well is then shut-in for soaking, and upgraded oil produced from the same well.

Hoffman (1989) reported a similar process in which liquid-phase hydrogen precursors are injected during a steam flood. This results in asphaltene removal and hydrogenation, and upgraded oil is produced.

The drawback of these processes was mainly due to: (*Moore et al*,1996)

1. Poor contacting between oil, hydrogen, and catalyst
2. Limited supplies of heat
3. Catalyst type

Moore *et al* (1996) called for a more deliberate use of catalyst, those which have proved to be effective for conventional surface upgrading, to be used to improve *in-situ* upgrading. They summarised the requirements for *in-situ* upgrading as:

1. Provision for a downhole bed of catalyst
2. Mobilisation of oil and flue gases over the catalyst

Hydrogen required for the process may be generated by any of the four generic reactions, which are considered as being responsible for hydrogen generation during *in-situ* combustion process.

(1) Thermal cracking which produces methane, ethane, propane, as well as hydrogen, carbon monoxide, carbon dioxide and hydrogen sulphide.

(2) Aquathermolysis (steam/oil reactions) over the temperature range 200-300°C produces CO₂, CH₄, H₂ and H₂S. The total quantities of gases produced by aquathermolysis are less than 1-% wt for their oil.

3-Coke gasification, which include either of the reactions:

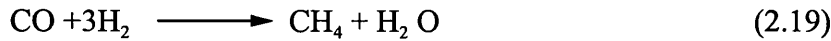


4-Water-gas shift reaction (WGS):



It is possible that other reactions may occur, i.e. methanation reactions:(Davies *et al*,1984)





In a one dimensional flow regime, coke gasification, as described by Equation 2.15, is not likely to occur during dry combustion (*Hajdo et al*,1985). Because coke is actually present in a narrow zone ahead of the front, it therefore has little opportunity for contact with steam or water. This ideal flow regime only exists in a combustion tube where the flow is one dimensional and the porous media is, absolutely, homogeneous.

In three dimensional flow situations, as in the field or in 3-D combustion cells, it is possible to find some hydrocarbon residues left behind the combustion front due to over-riding, by-passing and fingering. The hydrocarbon residue left behind is actually incompletely burned coke, it may be subject to gasification if contacted by steam due to water injection, thus hydrogen may be generated.

Hajdo et al (1985) have summarised the superiority of three dimensional flow in hydrogen generation during *in-situ* combustion in the following points:

1. Coke gasification can occur behind the combustion front.
2. The generated hydrogen can channel through/around an active front to a producer.
3. Sustained hydrogen generation and production can occur during a period of water injection without the continued injection of air.

A unique detailed study of *in-situ* upgrading, which utilised the *in-situ* combustion process is a one-dimensional combustion tube study was conducted by *Moore et al* 1996. They used a combustion tube to carry out dry-forward combustion experiments using

a Middle-Eastern crude oil of 15 ° API gravity. In one experiment, they packed the last three zones of the tube, at the production end, with a mixture of sand and catalyst using a 50/50 volume ratio. The catalyst used was fresh alumina-supported nickel molybdenum. The catalyst zone temperature was kept constant at 325 ° C (by external heaters) to ensure sufficient catalyst activity. Another experiment was conducted without catalyst, but using the same operating parameters.

They reported a 50 % sulphur removal and an 8 point API gravity increase in the oil produced from the catalytic run. The heated catalyst efficiently converts CO to additional H₂, i.e. by the water-gas shift reaction. High API gravity oil was produced, but the API gravity is decreased as the combustion front propagates toward the production end. This suggests that the catalyst activity was decreasing with time, although temperature of the catalyst zone was kept constant. This was due to coke deposition on the catalyst surface. *Moore et al* (1996) have proposed placing of a catalyst bed near the production end by using conventional gravel packing techniques, so that heated oil and hot gases, generated by combustion reactions, are passed over the catalyst bed, and consequently, hydrogenation takes place to produce upgraded oil.

They proposed three different processes for *in-situ* upgrading:

1. “Burn and Turn” In-Situ Catalytic Upgrading:

This process is carried out in two stages. Firstly, a dry or wet combustion is initiated in the vicinity of the catalyst bed, and allowed to propagate away for some distance to raise the reservoir temperature. In the second stage, combustion is terminated and the injection well is switched to production, forcing reservoir fluids and combustion gases to pass over

the heated catalyst. Both stages are repeated in order to maintain the heated catalyst and to remove coke deposits. The process is illustrated in Figure 2.9A and B.

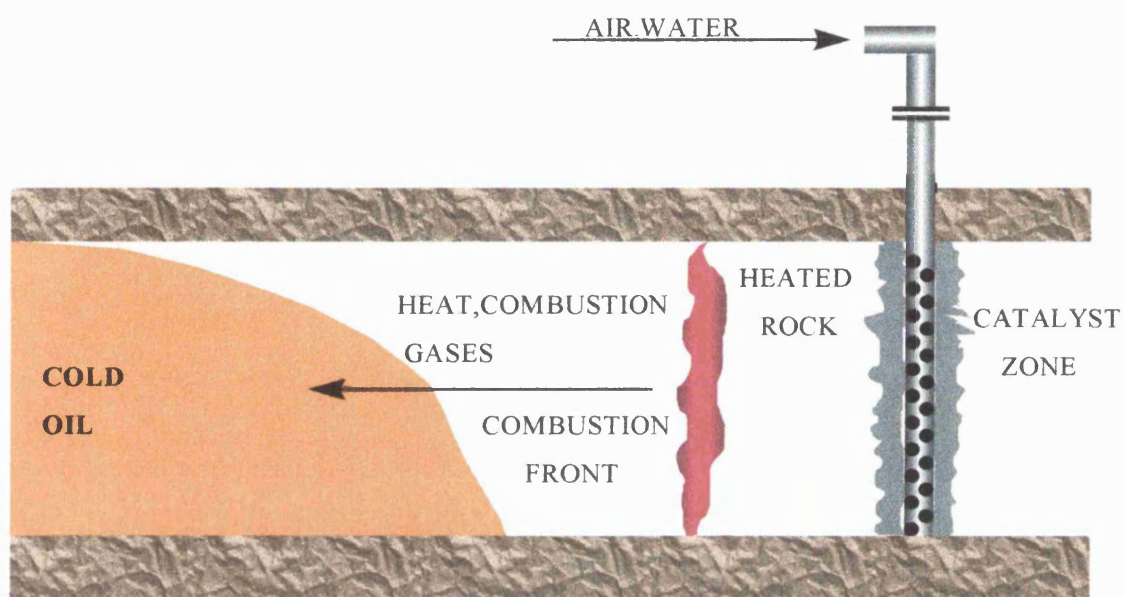


Figure 2.9A Injection mode of 'Burn and Turn' process (*Moore et al, 1996*)

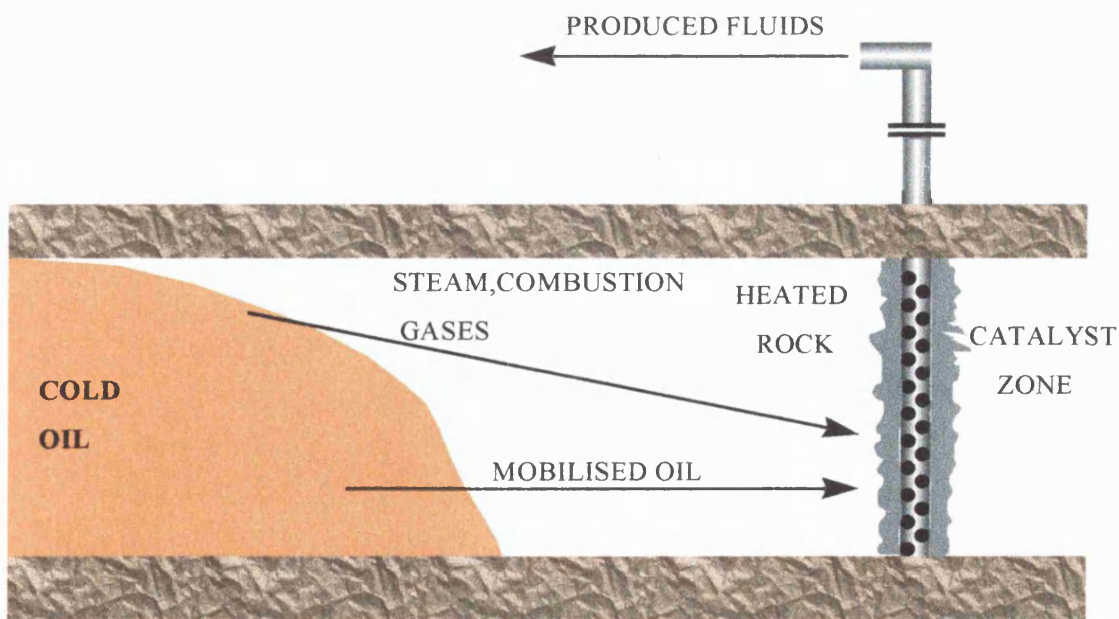


Figure 2.9B Production Mode of 'Burn and Turn' Process (*Moore et al, 1996*)

2. In-Situ Catalytic Upgrading Using Downhole Injection:

This process involves the injection of hydrogen, or other upgrading gases into a preheated catalyst bed located in the vicinity of the production well. Reservoir fluids pass over the heated catalyst zone and contact injected hydrogen; the oil is then upgraded. Diagram of the process is shown Figure 2.10. The injection of hydrogen, or other potentially explosive mixtures, is likely to be dangerous procedure in reservoir operation.

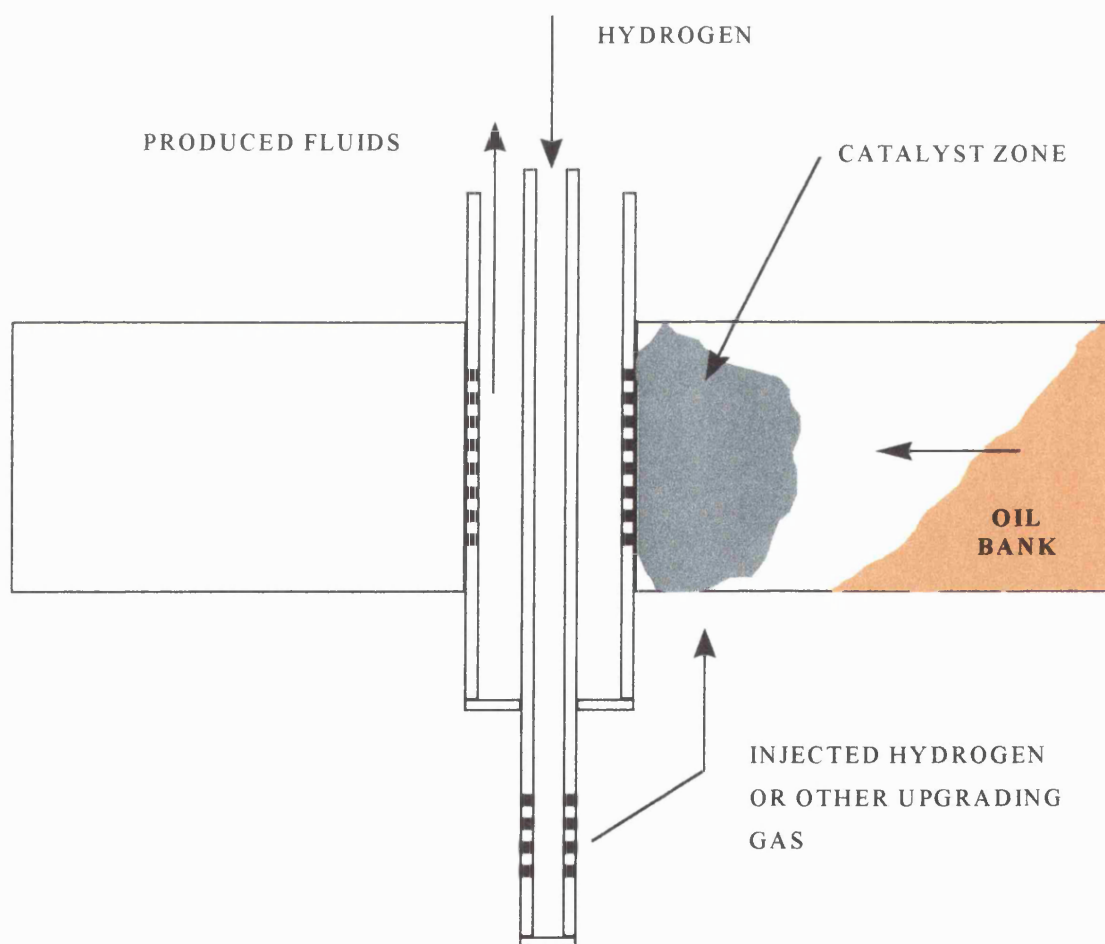


Figure 2.10 Diagram of *in-situ* catalytic upgrading scheme with downhole injection processing (Moore *et al*, 1996)

3. A Combustion-Assisted In-Situ Catalytic Upgrading

This process is conducted as a conventional dry or wet combustion, where combustion is triggered near the injection well; driving hot gases and fluids into the production well. At the production well, a catalyst bed is placed between the sand face and production casing. Thus produced fluids must pass through the catalyst bed, as a result, hydrogenation takes place and upgraded oil is produced. Heating of the catalyst bed can be provided either by gas override, or by electrical methods. Diagram of the process is shown in Figure 2.11.

One of the main disadvantages of this process is that all of the oil contacts the catalyst in one place, and by virtue of the high hold-up of oil, a high level of coking occurs.

Consequently, the catalyst activity deteriorates rapidly. In order to maintain catalyst activity and hence conversion, the catalyst must be frequently reactivated using a steam/air mixture.

Gravel packing is a widely used technique to minimise or prevent sand production.

Several techniques have been developed for placing the gravel, but the principle is to fill the annulus by specially selected grain size gravel. So gravel packs stop larger formation sand grains that in turn stop smaller formation sand grains.

Gravel packing of horizontal wells is conducted by squeezing gravel downhole to fill the lower part of the well bore. Then, once the gravel reached the end of the well, the gravel dune moved to fill the upper part of the well. Figure 2.12 illustrates the mechanism of horizontal well gravel packing.

The same technique can be used to place catalyst along the length of the horizontal producer in order to create a radial reactor around the producer well. The concept of 'Toe to Heel' downhole catalytic upgrading process is shown in Figure 2.13.

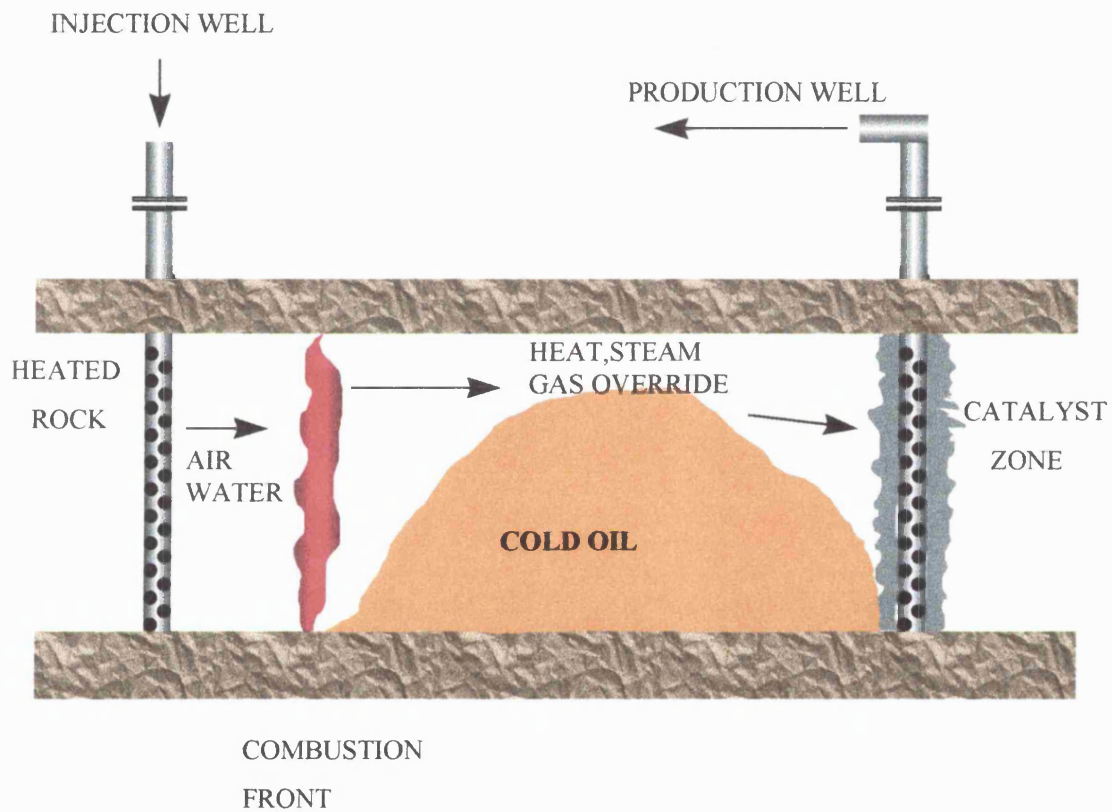


Figure 2.11 Diagram of a combustion assisted *in-situ* catalytic upgrading process
(Moore *et al*, 1996)

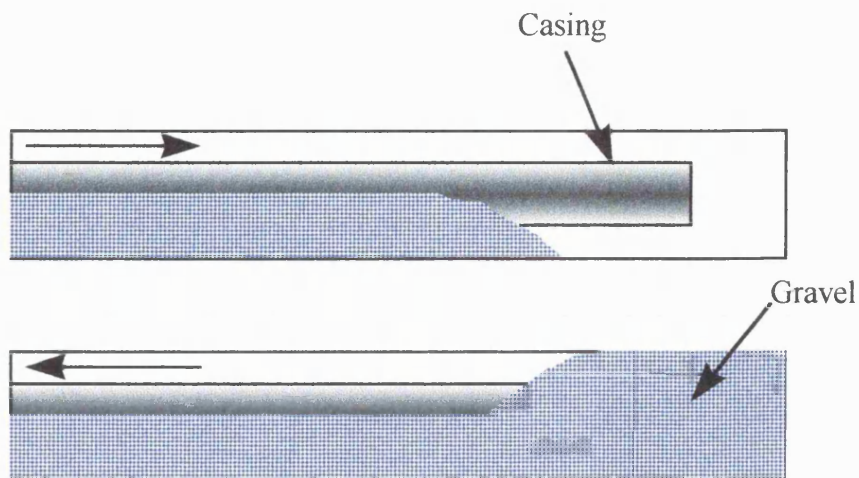


Figure 2.12 Mechanism of horizontal well gravel packing (*Butler et al*, 1986)

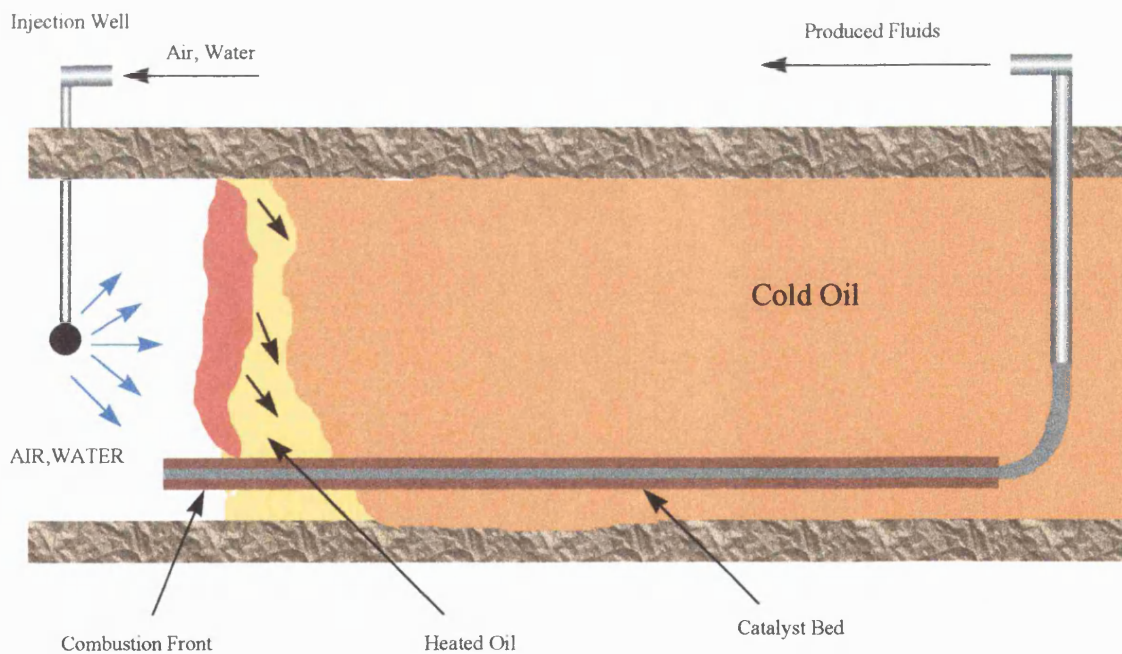


Figure 2.13 Diagram of Toe to Heel air injection process with downhole catalytic bed

CHAPTER THREE

EQUIPMENT AND EXPERIMENTAL PROCEDURE

INTRODUCTION

Three types of air injection/ *in-situ* combustion experiments were performed at low pressure using a 3-D physical model. The experiments were conducted using a horizontal well arranged in direct line drive. A first set of experiments was conducted to investigate the effect of the perforation density of the draining holes along the length of the horizontal producer on the combustion performance.

Two different crude oils were used, hence, two horizontal producer wells with different perforation densities were used, to take account of the different mobilities of the oils.

A second type of experiment involved using a modified horizontal producer well design to incorporate ‘sleeve-back’ principle which would enable the oil saturation downstream of the combustion front to be controlled.

A third type of experiment was carried out to investigate the feasibility of *in-situ* or downhole catalytic upgrading of heavy crude oil by using catalyst bed placed along the horizontal producer well. Both dry and wet combustion modes were conducted.

All experiments were conducted using unconsolidated sandpacks in a simple, 3-D rectangular semi-scaled combustion cell assembly, originally developed by *Tuwil* (1991), but modified during this study to enhance system performance

3.1 Equipment

The main elements of the air injection/ *in-situ* combustion system include the 3-D combustion cell, gas injection unit, water injection unit, fluid production unit, gas analysis unit, temperature control equipment and data acquisition unit are shown in the general flow diagram in Figure 3.1. The elements described separately as follows.

3.1.1 Combustion Cell

The combustion cell is a rectangular box having dimensions of 0.40×0.4×0.1m.

It is constructed from 316 stainless steel sheet with a wall thickness of 0.04 m with one removable end face. Figure 3.2 shows the 3-D combustion cell assembly.

A matrix of fifty five thermocouples K type are positioned at 0.06 m intervals, on the top surface of the cell and another five were arranged along the bottom center of the cell. The thermocouples were placed on three levels in the sand pack respectively at 0.02, 0.05, and 0.08 m from the top surface of the cell representing the TOP, MIDDLE and BOTTOM planes to monitor the combustion front movement during the experiment. Figure 3.3 show thermocouple positioning in the cell.

There are eighteen located on the top plane, twenty six on the middle and sixteen on the bottom plane.

The combustion cell was equipped with ten well ports and four ignition connections in order to incorporate different horizontal and vertical well configurations. Figure 3.4 shows the cell dimensions and position of the well ports.

The 3-D cell was designed to operate at a pressure of 172 Kpa (25 psig). A relief valve, with a cracking pressure of 193 Kpa (28 psig), is installed on the top of the cell to release any excess pressure that may develop during the experiment.

3.1.2 Gas Injection Unit

The gas injection unit consisted of high pressure gas supply cylinders, pressure regulators, mass flow meters, and a gas drier. This unit supply oxygen and nitrogen to the combustion cell via the high-pressure cylinders via two pressure regulators (D15 and D16).

The two Series 5850 mass flow meters were used to control and measure the gas injection flow rate of oxygen and nitrogen. A gas dryer (D10) was used to remove any moisture from the injected gas. A safety one-way valve was installed in the inlet gas line in order to prevent back flow from the combustion cell into the gas injection lines. An on-line relief valve (RV1) was also installed on the main injection line to avoid any damage to the cell that may result in case of a regulator malfunction.

3.1.3 Water Injection Unit

The water injection unit consisted of storage tank, metering pump, and non-return valve. The unit was used to introduce water to the combustion cell when operating in the wet combustion mode.

The pump suction line, was connected to water storage tank, which is located 0.4m

above the pump level. The pump discharge line was connected to the injection header on the 3-D cell. A non-return valve was installed just before the injection header to prevent back flow from the gas injection system.

3.1.4 Fluid Production Unit

The fluid production unit separates the produced fluids from the 3-D cell. It consisted of a first stage separator (V2), second stage separator(V3), first and second stage condensers, back pressure regulator, and fraction collector.

The two gas-liquid separators are made from cylindrical steel tube. Each separator had a fluid inlet pipe at the top and there are two outlet pipes. One at the top for gas and one at the bottom for liquid production. Both separators are surrounded by steel jacket, for water-cooling circulation. The condensation efficiency of the separators is thereby improved, maximising liquid recovery.

The first stage separator (V2) was connected directly to the production line from the combustion cell, whilst the second stage separator (V3) was connected via a back pressure regulator to the first stage separator.

The pressure, both upstream and downstream of the separators, was monitored by two pressure gauges (P5 and P6). The back pressure regulator (BPR) installed on the outlet line of V2 it was used to maintain a constant pressure in the combustion cell (maximum operating pressure of 2.9 bar). Fraction collector V5 was used to collect samples of the produced liquids. In order to provide fast and safe shutdown in case of an emergency, BV18 was used to release the separator(s) pressure directly to the vent.

3.1.5 Gas Analysis Unit

Gas analysis unit was used to analyse the composition of the gas produced and to measure its volume. The main parts of this unit are: a gas chromatograph (D2), gas analysers D7, D8, D9 (CO, O₂, and CO₂), wet test meter (D3), primary and secondary gas dryers (V6 and V8), sight glass (V7), and 3-way valve.

A primary gas dryer (V6) was connected to the second stage separator to absorb any liquid associated with the produced gas. A sight glass (V7) was connected into the primary gas dryer (V6), and used to monitor the gases that flow to the gas analysis system to ensure that they are free of entrained liquid. The gas analysers operate at a recommended pressure of 0.68 bar, which is adjusted by the pressure regulator (D1) installed after the sight glass. An insulation valve (BV9) was installed to protect the gas analysis system in case of an emergency, or, if there is any oil associated with the gas produced.

A 3-way valve (3WV) was installed after the pressure regulator D1 to direct the produced gas, either to the wet test meter, gas analysers, or to the gas chromatograph. A secondary gas dryer (V8), which was installed after the 3WV, used to absorb any liquids, which can not be removed in the primary dryer.

A Perkin Elmer 8500 gas chromatograph (D2), equipped with a thermal conductivity detector head for analysing N₂, O₂, CO, CO₂ and CH₄, was installed. The GC can also be fitted with an Alltech Heliflex AT-1 capillary column for measuring low levels of light hydrocarbons, using a flame ionisation detector. Figure 3.6 show photograph of the Gas Chromatograph.

The three separate Servomex gas analysers (type 1400 for CO and CO₂, and type 570A for O₂) D7, D8 and D9 were used to monitor oxygen, carbon monoxide, and carbon dioxide concentrations in the produced gas. The gases from each analyser eventually join the main gas production line, which was connected to the wet test meter. The wet test meter (D3) provides an accurate measurement of the cumulative gas volume.

Two pressure gauges (P8 and P9) were installed to monitor the inlet pressure to the analysers and wet test meter. Figures 3.7 shows a photograph of gas analysers and WTM unit.

3.1.6 Temperature Control Equipment

Three electrical heating tapes (1400 watt, 240volt) were wrapped around the cell to set the initial bed temperature, and to supplement the heat lost during the process.

The objective is to maintain the sandpack as near to adiabatic conditions as possible.

The temperature of the tapes, on the cell walls, was detected by three thermocouples installed on the external surface of the cell.

Three power regulators were used to adjust the temperature of the heating tapes independently, at the desired set. The manual control strategy, was always to keep the surface temperature of the cell 20 ° C less than the average temperature reading measured inside the sandpack. Also, in order to minimise heat loss, the 3-D cell is housed in an aluminum box filled with vermiculite powder. Figure 3.8 show the tape heaters positions on the cell body and Figure 3.9 show photograph of the insulation aluminum box.

3.1.7 Data Acquisition Unit

This unit was used to record all the measured data taken during an experiment.

Usually, sixty five readings taken from the sandpack and separate measurements of oxygen, carbon monoxide, carbon dioxide concentration of the produced gas. These measurements are acquired by National Instruments interface board SCXI-100, which converts the raw voltage signals to appropriately scaled values.

The National Instruments Labview software, 'Lab View' is a graphical programming language for instrumentation and control. It was installed on a Viglen IV/90 workstation.

Data is stored automatically during the experimental period on a hard disk, and also on a floppy disk. The Labview software has the facility for real-time screen display of the measured data. Figure 3.10 shows a photograph of the computer workstation.

3.1.8 Ignitor

A three-coil heater constructed from nickel-chrome wire was imbedded in the inlet section of the sandpack, positioned 1cm from the injection well. It was used to raise the inlet face of the sandpack to the required ignition temperature, usually about 400°C. The ignitor was arranged to cover the whole injection face in order to ensure a fast and uniform ignition. The ends of the coils were isolated electrically inside a ceramic tube to avoid any contact with the injector or the combustion cell body.

The electrical supply connections were made using conventional engine spark plugs. Figure 3.11 shows the ignitor position in the cell as well as the injector and producer wells.

3.2 Design of Horizontal Producer Wells

Conventional Design:

Three different types of horizontal producer wells were used in this study. Two were of conventional design, but each having different perforation densities along their length. The third type of horizontal producer was designed in order to physically simulate the condition of heavy oil inflow, but applied to light crude oil test where the use of a conventional design would cause excessive desaturation of the oil layer ahead of the combustion front. In all cases, the configurations used during this study are all direct-line drive, as shown in Figure 3.11.

The influence of a horizontal well producer arranged in line drive was the main focus in this study. In particular, its application to light oil reservoirs, wherein fuel availability during *in-situ* combustion considered to be a major problem.

Unfortunately, only a few details of the horizontal producer well used in previous studies have been reported (see Table 3.1).

In previous work by *Mahgoub* (1995) and *Wilson* (1998), 32 perforation drain holes along the horizontal producer well were used, mainly for medium-heavy and light crude oil experiments. Two new horizontal producers with different perforation density patterns were, therefore designed to investigate the effect of fluid entry along the horizontal producer well.

3.2.1 Design 1:

The first design employed a low hole perforation density, which used 17 holes of 1.5 mm diameter. They were uniformly arranged in a single row (phase angle of 360 °). This is equivalent to areal density of 1 hole/cm², based on the external well surface . This horizontal producer was used in Runs 961 and 963 on Clair and Forties Mix 1 oils (19.8 and 30.8 °API). For comparison, it was also used in the upgrading experiments conducted on heavy Wolf Lake crude oil (10.95 °API).

3.2.2 Design 2:

The second design used a high hole perforation density, which had 68 holes of 1.5 mm diameter arranged in four rows (phase angle of 90°). The perforation density for this design is 4 holes/cm² of the external well surface. This well was used only in experiments 963 and 964. Figures 3.12 and 3.13 show the perforation hole arrangements for horizontal producer well designs 1 and 2, also specifications are given in Table 3.2.

3.2.3 Design 3: Sleeve-Back Design of Horizontal Producer Well

In order to physically simulate, or mimic, the behaviour occurring during *in-situ* combustion of heavy crude oil, it was realised that the conventional horizontal well design (Design 2) would be inadequate when applied to *in-situ* combustion of lighter, and perhaps medium-heavy oils.

Principally, it has been observed in previous heavy oil experiments (see for example *Al shamali*, 1993), that ahead of the combustion front there appears to be a limited, an narrow, mobile zone from which fluids drain directly by gravity assisted pressure draw-down into the 'open' section of the horizontal well. Downstream of this, the heavy oil is essentially immobile with the oil saturation maintained at its original condition. This condition may also be assisted to some degree by the sealing effect of the heavy viscous oil on the well perforations.

The line drive arrangement of the horizontal producer well has unique flexibility in controlling the fluid entry profile along the horizontal producer, as it is traversed by the combustion front [so called 'toe-to heel' combustion/displacement]. The new design was achieved by using a co-aligned, two-well assembly as shown in Figure 3.14.

This arrangement provides two main advantages:

1. Hot gases and vaporised light fractions are prevented from displacing oil in the downstream sections of the sandpack, so that, the original oil saturation in downstream sections is maintained.
2. It divides the sandpack into two sections, which are perpendicular to the well, so enabling the flow in each section to be treated independently.

The upstream section of the horizontal well (detailed specifications are given in Table 3.3) has an adjustable internal production tube of OD 6.4mm, inserted inside a perforated outer casing having an ID of 6.4mm as shown in Figures 3.14 and 3.15.

There is, therefore, essentially no clearance between the production tubing and

exterior casing. The downstream section of the internal tubing therefore effectively 'shuts-in', or insulates that part of the reservoir, and no drainage can occur.

The downstream well section was connected to the production header assembly via a flexible stainless steel hose, which also incorporated a shut-off valve. The downstream section of the well assembly has an ID of 10mm and is isolated from the production header via a ball valve. Both sections were constructed from stainless steel tubing and perforated with a series of 1.5 mm diameter holes on a 4mm pitch. The phase angle was 180 ° for the upstream section and 360 ° for downstream section. The perforation density of upstream section is 3 holes/cm² of external well surface, and 1 holes/cm² for downstream section. For the upstream section, perforations were placed in two rows, opposite to each other, so that the interval between perforations in the same row is 8mm and between any opposing perforations is 4mm. Arrangements of perforations are shown in Figure 3.15 B.

The horizontal well sections were covered with a 250-gauge stainless steel mesh to prevent ingress of sand, which otherwise could have blocked the inside of the well.

A K type thermocouple was installed inside the production tubing of upstream well section to closely monitor the temperature in the high temperature zone.

A special mechanism for adjusting the sleeve back position of the horizontal producer was used. This assembly, which consists of collar, tubing pusher and a supporting bracket. The collar was welded onto the production tubing in the upstream well section of the horizontal well. This allows the movement of the tubing backwards according to the tubing pusher movement.

Tubing pusher is constructed from $\frac{3}{4}$ inch threaded tubing and equipped with an adjusting nut and mounted in a support bracket. The support bracket is made out of one-inch steel bar equipped with a threaded centre hole to accommodate the tubing pusher. The bracket is held by two steel bars 0.006m thick, which are screwed to the cell body by 0.02m nuts. Figure 3.16 A and B shows the main components and dimensions of the adjustable sleeve-back mechanism. The modified horizontal well assembly as installed on the combustion cell is shown in Figure 3.17.

The injection well used in this study had 20 holes of 1.5mm diameter, arranged in one row (phase angle of 360°) with a perforation density of 1 hole/cm². All wells were constructed from stainless steel tube and covered with a fine stainless steel mesh to prevent sand production. Diagram of the injector is presented in Figure 3.18 also, specifications of injection well are provided in Table 3.4.

3.2.4 Calibration of the Sleeve-Back Tubing

In order to achieve accurate adjustment of the tubing length, during an experiment, the threaded adjustment mechanism of the tubing pusher was designed to withdraw the internal tubing at a ratio of 8mm per 360° .

Several trials were made to achieve a smooth adjustment avoiding any high friction condition between the internal tubing and surrounding casing. The sleeve-back assembly was leak tested at room temperature up to 3.7 bar for 70 minutes to ensure no communication existed between internal tubing and outer casing.

3.3 Experimental Procedure

3.3.1 Preparation of Sandpack for In-Situ Combustion Experiments

Approximately 25 to 27 kg of washed Buckland silica sand together with kaolinite clay were used for each experiment. Sandpack properties for Runs 961, 962, 963 and 964 are given in Table 3.5 and for Run 966 is provided in Table 3.6. Chemical analysis of the Buckland silica sand is given in Appendix B.

Firstly, sand and clay were manually mixed thoroughly to ensure uniform distribution of the clay particles. Secondly, a pre-determined amount of water was introduced to the sand-clay mixture in small batches until the entire amount was thoroughly mixed. The wettability of the porous media was therefore assumed to be essentially water-wet. Then, oil was added to the mixture in small slugs (200 ml each) until the designed amount is mixed. During the mixing stage, special care was taken to prevent any losses of the mixture components. Once the mixture had been thoroughly mixed it was packed into the combustion cell. Packing was carried out by introducing small batches of the mixture (1.5 kg) into the cell, then tamped down firmly with a stainless steel rod fitted with a rectangular disc at its tamping end. Once the mixture level reached 1cm below the injection well port, the ignitor is then carefully inserted.

To ensure fast and uniform ignition 4 to 6 ml of linseed oil was poured on the injection face. Once the cell is charged, a gasket was placed and a thin layer of high temperature silicone rubber was applied to the gasket to ensure good sealing. Then the flange was bolted down in place with 36 bolts.

Both the injector and producer were inserted in the cell after a special tool has been used to create space for them.

After the bottom thermocouples were installed, and the heating tapes were wound, the 3-D cell was then housed inside the aluminum jacket box and positioned in horizontal level.

The top thermocouples and all the fittings were then installed. Finally, the cell was subjected to leak-test by injecting nitrogen at 2.9 bar for half-hour.

Then the aluminum box was filled with a Vermiculite isolation powder. The leads from the thermocouples, wet test meter, and gas analysers were connected to the interface board SCXI-100. Also, the leads from the heating tapes were connected to the power regulator.

3.3.2 Preparation of Sandpack for In-Situ Catalytic Upgrading Experiments

The HDS catalyst type used in the experiments was in the form of 1/16 inch extrudates. This was not convenient for placing in the sand pack due to the following reasons:

1. A large particle size will create a high permeability zone around the horizontal producer, which will effect the flow velocity within that zone.
2. The porosity in the catalyst layer around the producer will be much higher than the rest of the sand pack, which may reduce the residence time of hydrocarbon fluids and reactant gases with the catalyst surface.
3. The size of catalyst extudate is about 25 % of the external well diameter and hence it is not suitably scaled dimension.

The catalyst used in the experiments was supplied by Akzo Chemic, Netherlands. This is a pre-sulphided standard hydrotreating and HDS catalyst, applicable to a wide range of petroleum feedstocks, especially heavy fractions. It was a Co Mo type catalyst on an alumina support (composition is given in Appendix C). For use in the experiment, the catalyst was grained manually and sieved to 250 μm .

After preparing the catalyst, the sand-clay mixture is mixed with water and oil, the production well (Design 1) is then inserted into the cell and tightened, making sure that the perforations are directed to the top of the sandpack.

A one-inch ID stainless steel tube is then inserted inside the combustion cell in such way as form a jacket around the horizontal producer, providing a 0.97cm annulus for catalyst packing. The length of the packing tube exceeded the length of the horizontal producer by 2cm, in order to ensure complete coverage over the entire well length.

Thereafter, the packing started by mounting the cell in a vertical position and packed by introducing small batches of the sand-oil mixture (1.5 kg) to fill 2 cm of the cell height.

While sandpack is then tamped down firmly with a stainless steel rod fitted with a rectangular disc at its tamping end. The catalyst was then charged into the annular space between the horizontal producer and the packing tube, making sure that sufficient of the catalyst is introduced by observing the final height of catalyst in side packing tube. During catalyst charging, the packing tube is vibrated by gentle tapping on its external surface to ensure that there are no gaps between the sand-oil mixture and catalyst.

Once the catalyst level in the packing tube is above the sand-oil mixture by 3cm, the packing tube is pulled up 1 cm and secured in position by attaching it to the cell body. The sandpack is then tamped again to fill any gap created by pulling up the packing tube, this procedure minimises the possibility of empty pockets at the lowest limit around the horizontal well. This procedure is repeated until the level of the sandpack reaches 1 cm below the injection well location. Sandpack properties of this set of experiments are given in Table 3.7.

3.3.3 Normal Operating Procedure

Prior to the start of an experiment, all flow lines and separators are pressure tested. The test is accomplished by injecting nitrogen into the system at a pressure of 2.9 bar and holding it for a period of 1 hour. Thereafter, water supply to the condensers is initiated and regulated at the highest circulation rate to achieve maximum condensation efficiency. Summary of the operating conditions is provided in Tables 3.8 to 3.10.

Pressure regulators on the gas supply cylinders were then adjusted to the operating working pressure of the mass flow meters, which is 5 bar.

The back pressure controller of the system was then adjusted to 2.9 bar. Thereafter, nitrogen was introduced into the cell while the bed was still at room temperature to scavenge any trapped air from the pore space. Once no oxygen is detected by the analyser, the heating up phase is started. Practically, not all of the trapped air can be released and this resulted in producing low levels of carbon oxides before air injection was commenced.

The heating tapes are then turned on to raise the bed temperature to the desired level although subsequent practice, for both heavy and light oils, was to start the experiment at room temperature. The first heating tape, which covers the injection zone of the sandpack, was used to assist the ignitor during the ignition stage. This practice has proved to be effective in avoiding ignitor failure during the ignition stage. The ignitor was then switched on to increase the temperature of the inlet sand face to 400 °C. During this period, some liquids were produced and collected in labeled jars. The amount of produced fluids varied for each run, this will be discussed in detail later.

Once the temperature around the injection face reached 350-400 °C, air injection was commenced at the designed injection rate. Once vigorous combustion is confirmed, either by a rapid increase in temperature around the injection face, and/or by a sharp increase of CO₂ concentration in the produced gas, the ignitor power was reduced gradually approximately 10 % every 10 minutes and eventually shut-off. In some cases, the ignitor failed during later stages, but this did not affect the ignition phase. In this work, each experiment is divided into two periods; the ignition period and a stabilised period. The ignition period is the period in which the ignitor is still on regardless of its power input. The extent of this period depends mainly on the crude type, bed composition, and the general conditions of the experiment. The stabilised period is the period in which the ignitor is off and the combustion front is propagating without any external heat and the combustion front temperature has settled down to a stable level.

During the experiment, regular liquid samples were collected every 15 minutes. Most importantly, the temperature of the cell external surface was regularly adjusted according to the combustion front movement by regulating the heating tapes. The cell surface temperature was always kept 20° C less than the measured sandpack temperature. The experiment is allowed to proceed until temperature in the last row of thermocouples (approximately 6cm from end) reaches approximately 300 °C. This is done to avoid any unnecessary coke formation around the production well especially in the case of heavy crude oil (Wolf Lake). Finally, the air injection is switched to nitrogen and the shut down procedure is started.

3.3.4 Operating Procedure Using Sleeve-back Well Assembly

During the nitrogen injection phase of the experiment, both well sections were opened to production to displace any trapped air from the sandpack. Most of the trapped air in the sandpack is released through the downstream section of the horizontal producer. Adjustment to open section of the tubing in the upstream section, was accomplished using the special screw-bracket assembly described in Section 3.2.3 (see Figure 3.17). This was accomplished by using the temperature measured by the thermocouple located at the far end of the open part tubing in the upstream section. Temperature measured by this central thermocouple was always kept less than that measured in the high temperature zone by 10 to 20 ° C. This interval was kept by pulling back the tubing end into downstream zones using the screw-bracket assembly.

The upstream section of the horizontal well was continually adjusted as the combustion front propagated through the first half of the sandpack, whilst the downstream section was shut-in. When the combustion front reached the toe of the downstream well section, it was opened, and the upstream section was closed.

Along the length of the upstream section, at any segment of the bed, hot fluids were drained through the open perforations into the inner tubing, while the downstream perforations were closed. This mode of operation prevented the hot fluids displacing into the downstream sections of the sandpack. Thus, the oil saturation downstream of the mobile oil zone ahead of the combustion front should, ideally, remain at its initial condition.

The production tubing of the upstream section of the horizontal producer well passed through the production casing of the downstream well section. This configuration inevitably allows heat to transfer from the hot produced fluids flowing through the annular space. Thus, oil in the downstream zones, to some degree, will continually be heated by conduction of heat from the combustion front through the sand matrix and also by the 'heat exchange effect' of the production tubing and casing, from the start of the experiment. This will have the effect of causing a degree of displacement in the downstream sections of the sandpack, but it may be an effect which is less significant in the field.

3.3.5 Normal Shut Down Procedure

Shut down of the system is started by switching to 100 % nitrogen injection by closing BV1 and then increasing the nitrogen injection rate up to the actual design flux, in order to accelerate the shut down procedure. All of the heating tapes are switched off at the same time and reducing the back pressure of the cell. BV8 is opened to provide direct vent of the combustion gases. The water injection pump is turned off and when the gas analyser detects no oxygen, the mass flow controllers, gas analysers and wet test meter are switched off. Finally, the gas supply is shut off and the cell contents allowed to cool down. Full details to normal and emergency shut down procedures is provided in the COSHH sheet given in Appendix (H).

3.4 Experimental Plan

The main aim of the research was to investigate the effect of well completion design of the horizontal production well on the behaviour of *in-situ* combustion process in light oil reservoirs.

Firstly, two pairs of experiments were conducted with two different types of crude oil (medium-heavy and light). For each pair of experiment, one experiment was conducted using the low hole perforation density horizontal producer whereas a second experiment was carried out by using the high hole perforation density horizontal producer. Operating parameters were kept as constant as possible for each pair of experiment.

Secondly, a modified horizontal producer well was developed to minimise oil desaturation in the downstream zones. This was achieved by mimicking the process

behaviour observed to occur during heavy oil *in-situ* combustion, using the sleeve-back operation of the horizontal producer well. Experiments conducted with medium-heavy and light crude oils were performed at post- water flooded reservoir conditions. Finally, four experiments were performed to investigate the feasibility of *in-situ* upgrading of heavy crude oil by using a downhole catalyst bed in conjunction with horizontal producer well.

All of the experiments were conducted using a horizontal producer well arranged in direct-line drive, creating a ‘toe-to-heel’ displacement of the oil. Air was the only injectant used during the study.

Runs 961 and 962 were conducted using medium-heavy ‘Clair’ crude oil (19.8° API).

These experiments were designed to determine whether the perforation density has any effect on the combustion mode in such a fuel-rich crude oil (compared to light crude). Both of these experiments used coarse sand (W50) with 10 % clay with the same operating parameters. **Run 961** used the horizontal producer well with a perforation density of 1 hole/cm² (Design 1), whereas, **Run 962** used the horizontal producer with a perforation density of 4 holes/cm² (Design 2).

Runs 963 and 964 were carried out using ‘Forties Mix 1’ light crude oil (30.8 °API) in a sandpack consisting of fine sand (W150) with 10 % clay. Similar to the previous set of runs, **Run 963** used the low perforation density horizontal well (Design 1) and, **Run 964** used the high perforation density well (Design 2). This set of experiments was designed to investigate to the role of perforation density, or fluid entry points, on the oil desaturation rate under light oil reservoir conditions compared to the situation with medium-heavy crude oil (961 and 962).

Run 966 also used ‘Forties Mix 1’ light crude oil with the same operating parameters as used in Runs 963 and 964. The main aim of this experiment was to mimic the behaviour occurring during heavy oil recovery, wherein the downstream oil is essentially immobile at reservoir temperature. This was achieved by using the modified horizontal producer well, which has an internal adjustable tubing section allowing its perforations to be opened up as the combustion front moves through the sandpack (toe to heel with respect to the horizontal producer well). The results of these experiments are presented in Chapter Four.

Runs 971, 972, 975 and 976 were conducted to examine the feasibility and efficiency of a downhole catalytic upgrading process by using a catalyst bed along a horizontal producer well. Heavy Wolf Lake crude oil was used in this set of experiments and all experiments using the same horizontal producer well used in Runs 961 and 963 (i.e. Design 1, low hole perforation density well).

Runs 971 and 972 were conducted without a catalyst bed in dry and wet combustion modes, respectively. **Runs 975 and 976** were carried out in presence of a catalyst bed under the same operating conditions as in Runs 971 and 972. Results of this set of experiments are presented in Chapter Five.

Table 3.1 Specification of Horizontal Producer wells used in Previous Work

VARIABLE	ALSHAMALI (1993)	BENRAHIL (1994)	MAHGOUB (1995)	WILSON (1998)	TUWIL (1991)
Well Length (mm)	N/A	N/A	340	353	N/A
O.D (mm)	6.4	6.4	6.4	6.4	6.4
I.D (mm)	N/A	N/A	N/A	N/A	N/A
Perforation Diameter (mm)	1.6	N/A	1.5	1.5	1.5
Number of perforations	N/A	N/A	32	32	N/A
Row of perforations	N/A	N/A	ONE	ONE	N/A
Phase angle (deg)	N/A	N/A	360	360	N/A

Table 3.2 Specification of Production Wells (Design 1 and 2)

RUN No	961	962	963	964
Production well type	Horizontal	Horizontal	Horizontal	Horizontal
Well design	1	2	1	2
Material	SS 316	SS 316	SS 316	SS 316
Overall well length (mm)	375	375	375	375
Actual well length (mm)	340	340	340	340
O.D (mm)	6.4	6.4	6.4	6.4
I.D (mm)	4	4	4	4
Number of perforations	17*	68	17	68
Perforation diameter (mm)	1.5	1.5	1.5	1.5
Perforation pitch (mm)	20	10	20	10
Perforation density (hole/cm ²)	1	4	1	4
Phase angle (deg)	360	90	360	90
Rows of perforations	1	4	1	4
Well eccentricity (% of bed thickness)	25	25	25	25
Mesh gauge	100	100	250	250

*This well was also used in Runs 971,972, 975 and 976 (Catalytic Upgrading Experiments) covered with 300 mesh gauge screen.

Table 3.3 Specification of Horizontal Producer Well used in Run 966 (Design 3)

Well Section	UPSTREAM	DOWNSTREAM
Material	SS 316	SS 316
Overall well length (mm)	34	205
Perforated Interval (mm)	170	170
O.D (mm)	8.5	12.5
I.D (mm)	6.4	10
Annular volume (cc)	10.94	7.88
Annular clearance (mm)	0	3.6
Number of perforations	34	17
Perforation diameter (mm)	1.5	1.5
Perforation pitch (mm)	4	8
Perforation density (hole/cm ²)	3	1
Phase angle (deg)	180	360
Rows of perforations	2	1
Well eccentricity (% of bed thickness)	25	25
Mesh gauge	250	250
Distance from injector (mm)	40	210

Table 3.4 Specification of Injection Well

Injection well type	Horizontal
Overall well length (mm)	420
Perforated interval (mm)	395
O.D (mm)	6.4
I.D (mm)	4
Number of perforations	20
Perforation diameter (mm)	1.5
Perforation pitch (mm)	20
Rows of perforations	1
Phase angle (deg)	360
Well eccentricity (% of bed thickness)	50
Distance from producer (mm)	30
Well configuration	Line Drive

Table 3.5 Sandpack Properties for In-Situ Combustion Runs

RUN No	961	962	963	964
Sand type	Washed Silica. W50	Washed Silica. W50	Washed Silica. W150	Washed Silica. W150
Sand (wt %)	90	90	90	90
Clay content (wt %)	10	10	10	10
Grain volume* (cc)	61.16	61.16	52.96	52.96
Grain density* (cc)	2.546	2.546	2.553	2.553
Bulk volume* (cc)	96.36	96.36	92.14	92.14
Bulk density* (cc)	1.616	1.616	1.468	1.468
Matrix surface area* (m ² /kg)	1613	1613	1643	1643
Porosity* (%)	36.53	36.53	42.52	42.52
Permeability* (md)	1004	1004	616	616
S _o % (at packing)	60	60	60	60
S _w % (at packing)	40	40	40	40
S _v % (at packing)	0	0	0	0
Initial bed temperature (deg.C)	25	25	55	55
Crude type	Clair	Clair	Forties Mix 1	Forties Mix 1
Crude density (kg/m ³)	935	935	872	872
Crude viscosity (cp) @ 20 °C.	200	200	9.57	9.57
Crude gravity (deg. API)	19.8	19.8	30.8	30.8
S _o % (at ignition)	51	40.8	44.4	27.6
S _w % (at ignition)	38.6	36.5	38.4	36.4
S _v % (at ignition)	10.4	22.7	17.2	36

*Measured by AEA Technology, Winfrith

Table 3.6 Sandpack Properties for Run 966

Sand type	Washed Silica W150
Sand (wt %)	90
Clay content (wt %)	10
Grain volume* (cc)	52.96
Grain density * (cc)	2.553
Bulk volume* (cc)	92.14
Bulk density* (cc)	1.468
Matrix surface area* (m ² /kg)	1643
Porosity* (%)	42.52
Permeability* (md)	616
S _o % (at packing)	60
S _w % (at packing)	35
S _v % (at packing)	5
Initial bed temperature (deg.C)	55
Crude type	Forties Mix 1
Crude density (kg/m ³)	872
Crude viscosity (cp) @ 20 °C.	9.57
Crude gravity (deg. API)	30.8
S _o % (at ignition)	46.24
S _w % (at ignition)	38
S _v % (at ignition)	15.76

*Measured by AEA Technology, Winfrith

Table 3.7 Sandpack Properties for Catalytic Upgrading Runs

RUN No	971	972	975	976
Sand type	Washed Silica W50	Washed Silica W50	Washed Silica W50	Washed Silica W50
Sand (wt %)	97	97	97	97
Clay content (wt %)	3	3	3	3
Grain volume* (cc)	59.62	59.62	59.62	59.62
Grain density* (cc)	2.522	2.522	2.522	2.522
Bulk volume* (cc)	96.99	96.99	96.99	96.99
Bulk density* (cc)	1.551	1.551	1.551	1.551
Matrix surface area* (m ² /kg)	494	494	494	494
Porosity* %	38.5	38.5	38.5	38.5
Permeability* (md)	1042	1042	1042	1042
S _o % (at packing)	76	76	76	76
S _w % (at packing)	17	17	17	17
S _v % (at packing)	7	7	7	7
Initial temperature (deg.C)	18	17	18	17
Crude type	Wolf Lake	Wolf Lake	Wolf Lake	Wolf Lake
Crude density (kg/m ³)	993	993	993	993
Crude viscosity (cp) @ 15 °C.	100000**	100000**	100000**	100000**
Crude gravity (deg. API)	10.95	10.95	10.95	10.95
S _o % (at ignition)	72.94	70	72.2	72.6
S _w % (at ignition)	16.64	16.52	16.67	16.55
S _v % (at ignition)	10.42	13.48	11.13	10.85

*Measured by AEA Technology, Winfrith

** Hallam et al 1989

Table 3.8 Operating Conditions for In-Situ Combustion Runs

RUN No	961	962	963	964
Combustion mode	Dry	Dry	Dry	Dry
Air flux (sm ³ /m ² .hr)	5.7	5.7	4.5	4.5
O ₂ flux (sm ³ /m ² .hr)	1.19	1.19	0.95	0.95
N ₂ flux (sm ³ /m ² .hr)	4.51	4.51	3.55	3.55
Air injection rate (l/min)	3.9	3.9	3	3
O ₂ injected (%)	21	21	21	21
N ₂ injected (%)	79	79	79	79
Operating pressure (bar)	2.9	2.9	2.9	2.9
Overall run period (hr)	12	12.08	10.38	5.63
Air injection period (hr)	10.55	10.87	8.2	3.86

Table 3.9 Operating Conditions for Run 966

Combustion mode	Dry
Air flux ($\text{sm}^3/\text{m}^2.\text{hr}$)	4.5
O ₂ flux ($\text{sm}^3/\text{m}^2.\text{hr}$)	0.95
N ₂ flux ($\text{sm}^3/\text{m}^2.\text{hr}$)	3.55
Air injection rate (l/min)	3
O ₂ injected (%)	21
N ₂ injected (%)	79
Operating pressure (bar)	2.9
Pre-ignition period (hr)	1.6
Overall period (hr)	14.7
Air injection period (hr)	13.1

Table 3.10 Operating Conditions for Catalytic Upgrading Runs

RUN No	971	972	975	976
Combustion mode	Dry	Wet	Dry	Wet
Catalyst?	No	No	Yes	Yes
Air flux ($\text{sm}^3/\text{m}^2.\text{hr}$)	9	9	9	9
Oxygen flux ($\text{sm}^3/\text{m}^2.\text{hr}$)	1.89	1.89	1.89	1.89
Air injection rate (l/min)	6	6	6	6
Water injection rate (l/min)	0	0.0025	0	0.0025
Water Air Ratio	0	4.2×10^{-3}		4.2×10^{-3}
Initial temperature (deg.C)	18	17	18	17
Operating pressure (bar)	2.9	2.9	2.9	2.9
Well type	HIHP	HIHP	HIHP	HIHP
Well configuration	Line Drive	Line Drive	Line Drive	Line Drive
Overall period (hr)	12.7	7.5	12.53	7.3

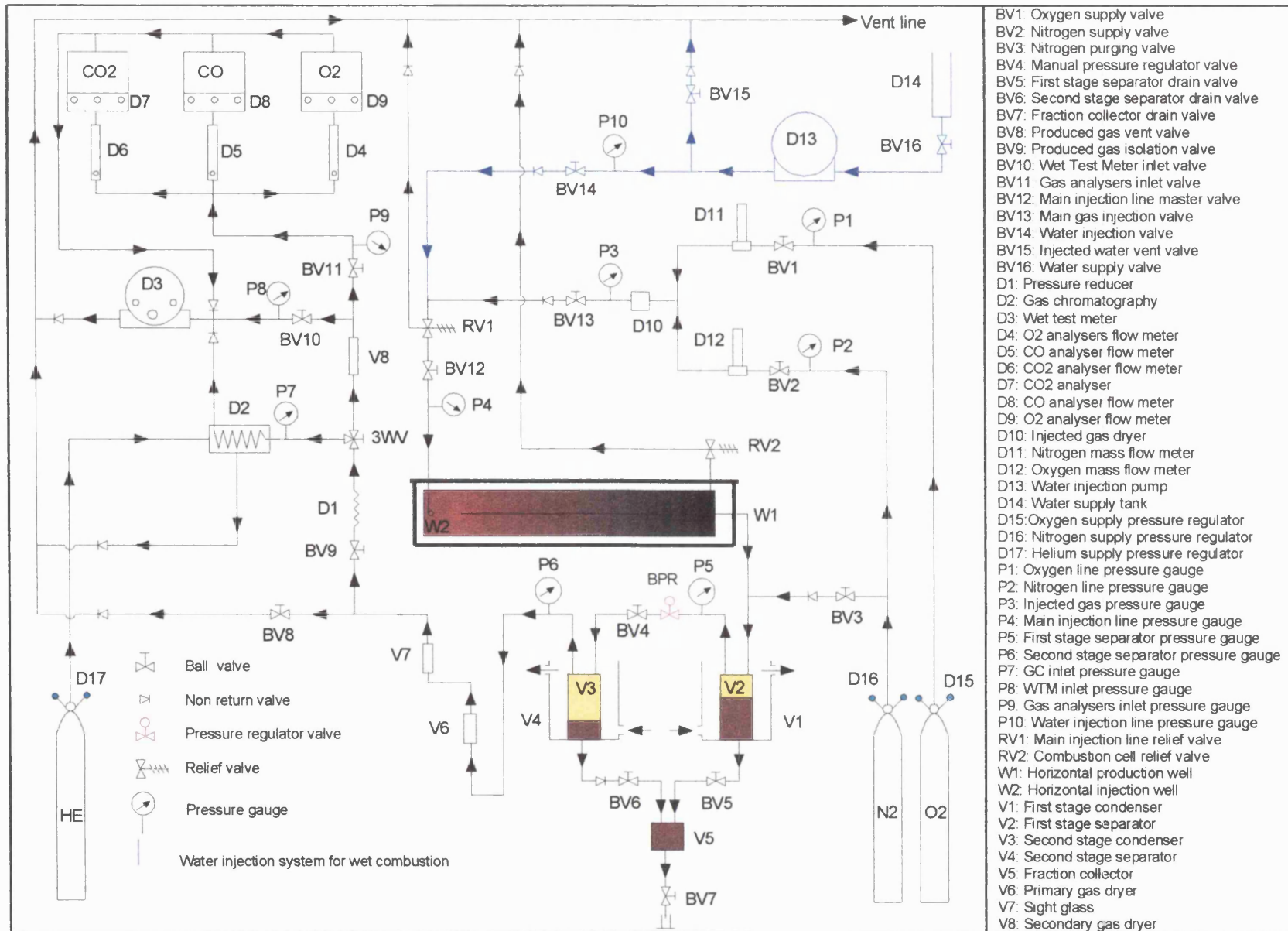


Figure 3.1 Flow diagram of 3D combustion model assembly

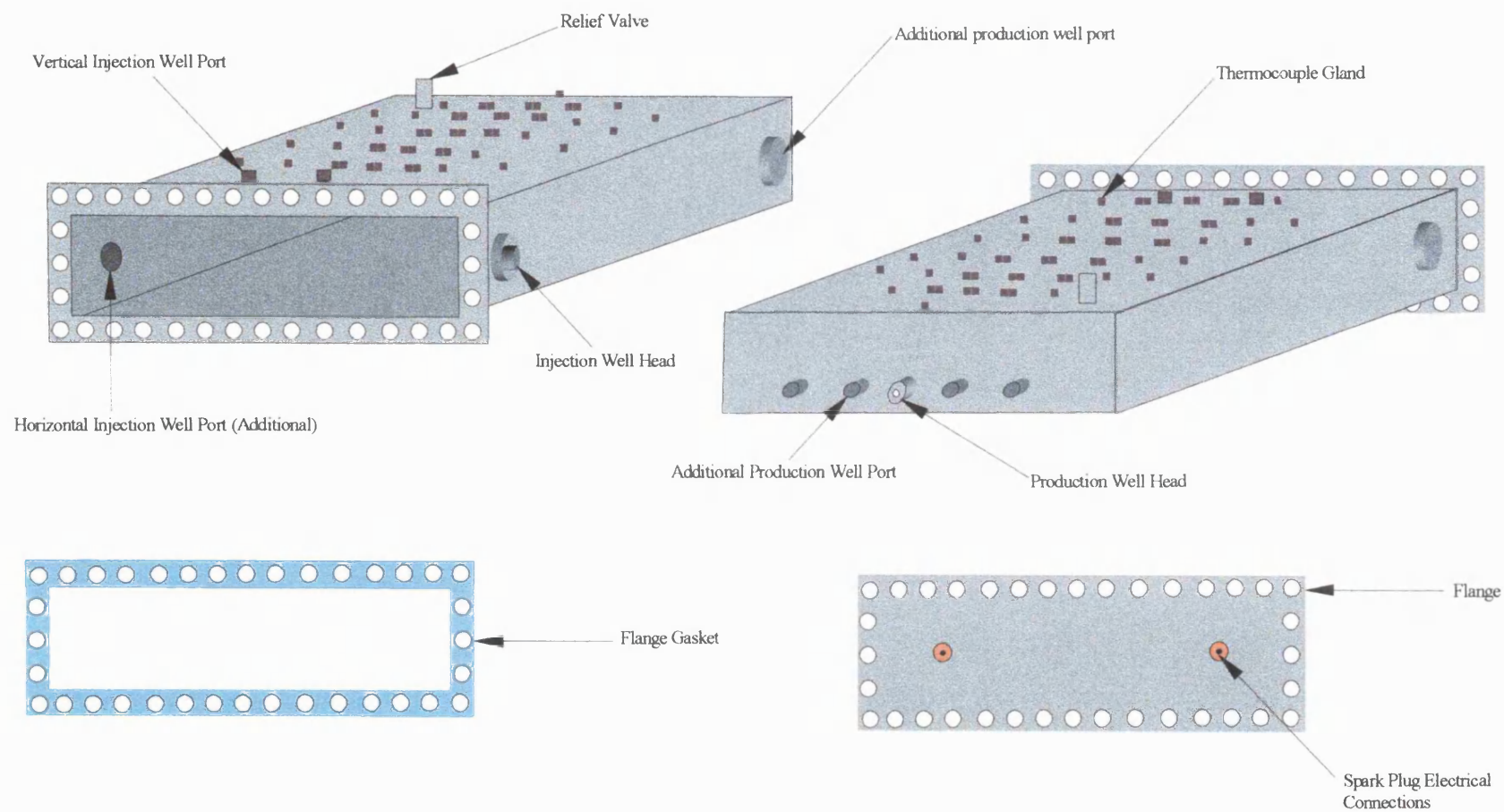


Figure 3.2 Combustion cell assembly

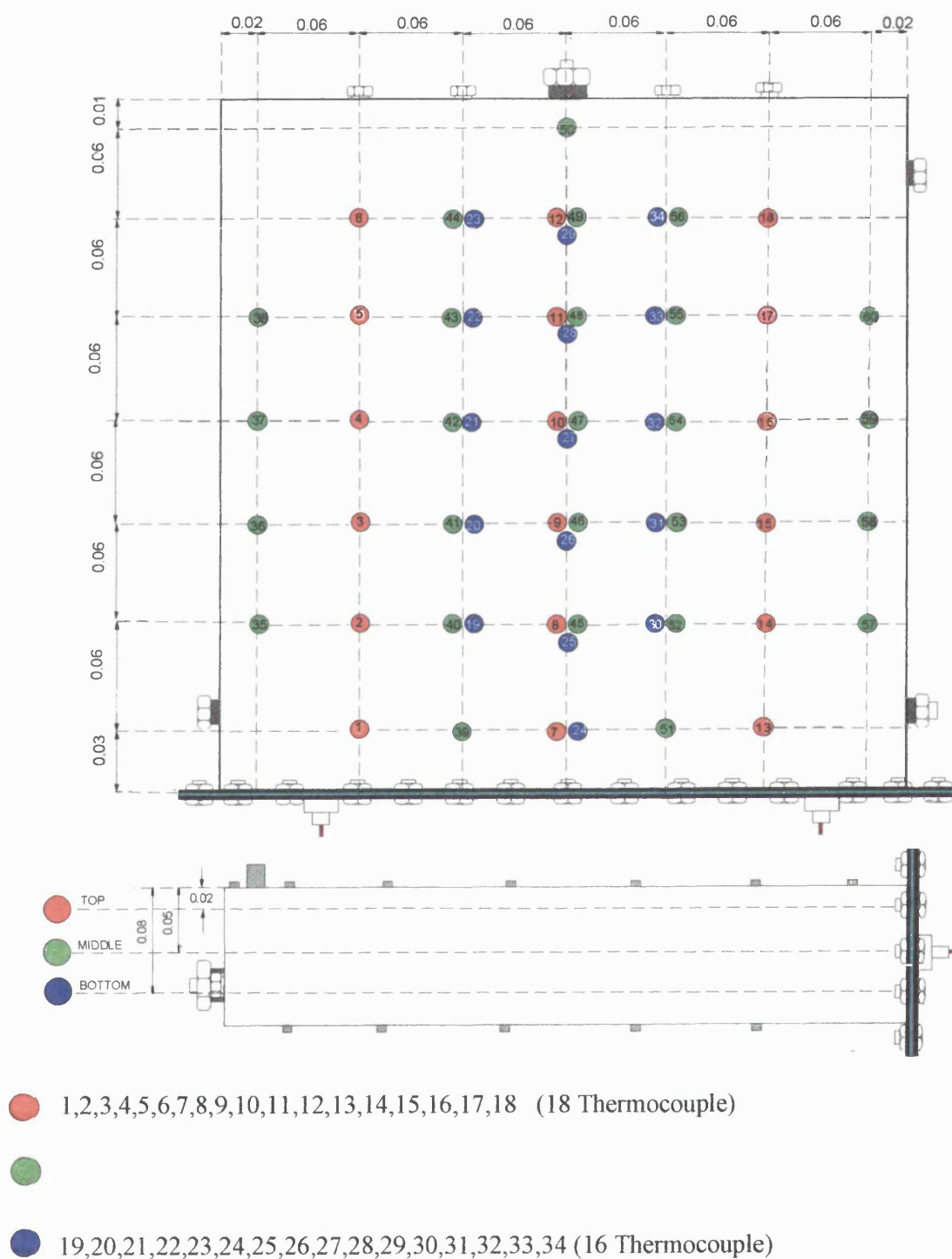


Figure 3.3 Thermocouple positions

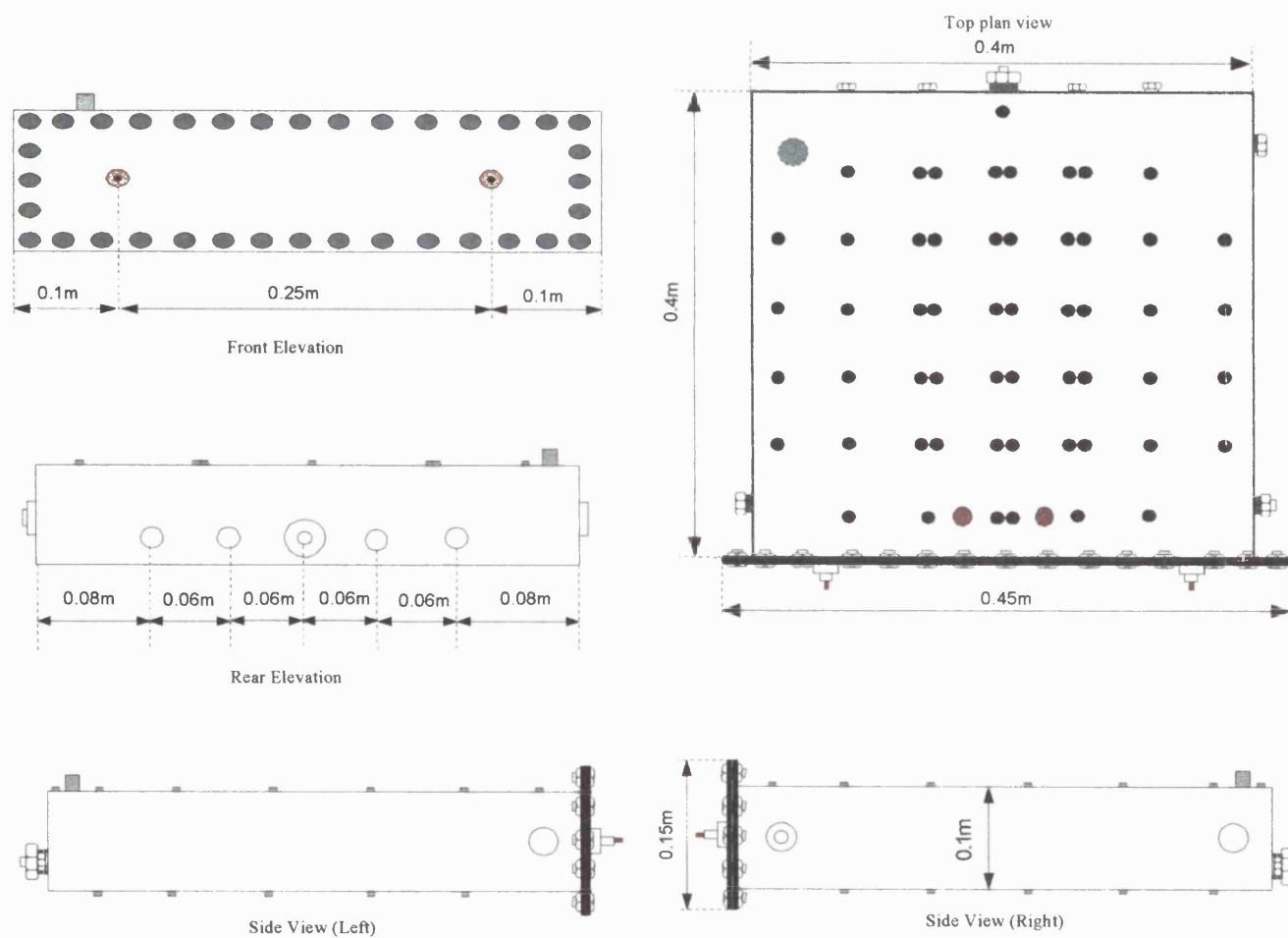


Figure 3.4 Combustion cell and location of well ports

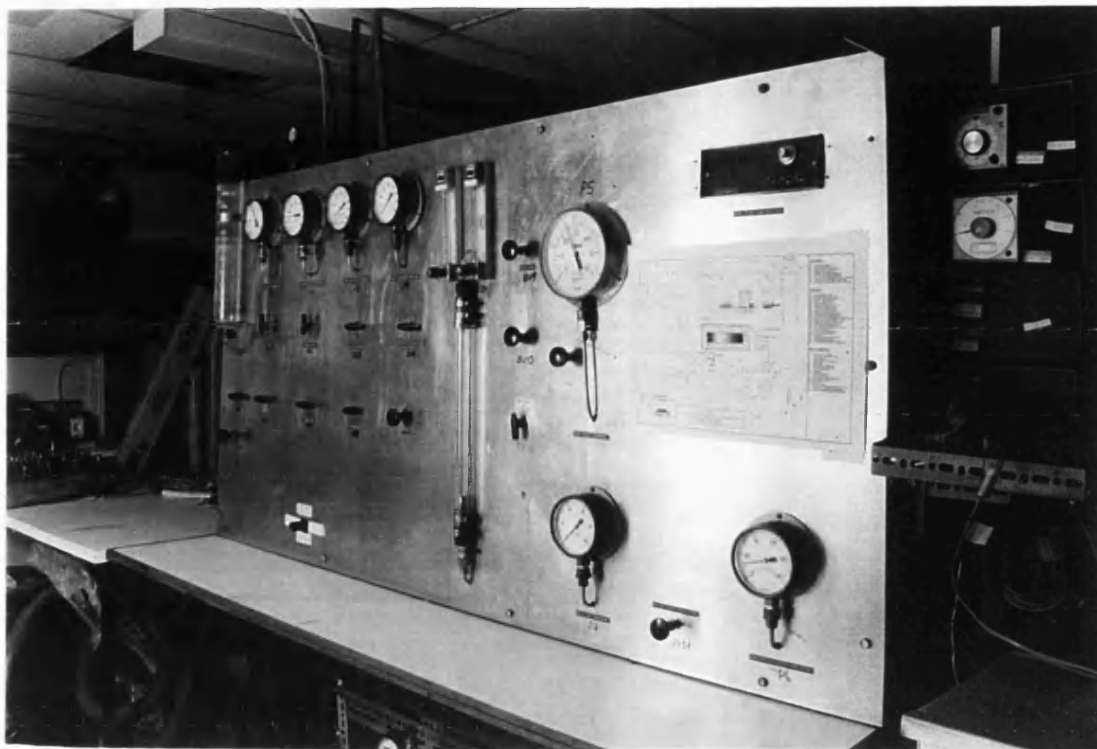


Figure 3.5 Photograph of control panel

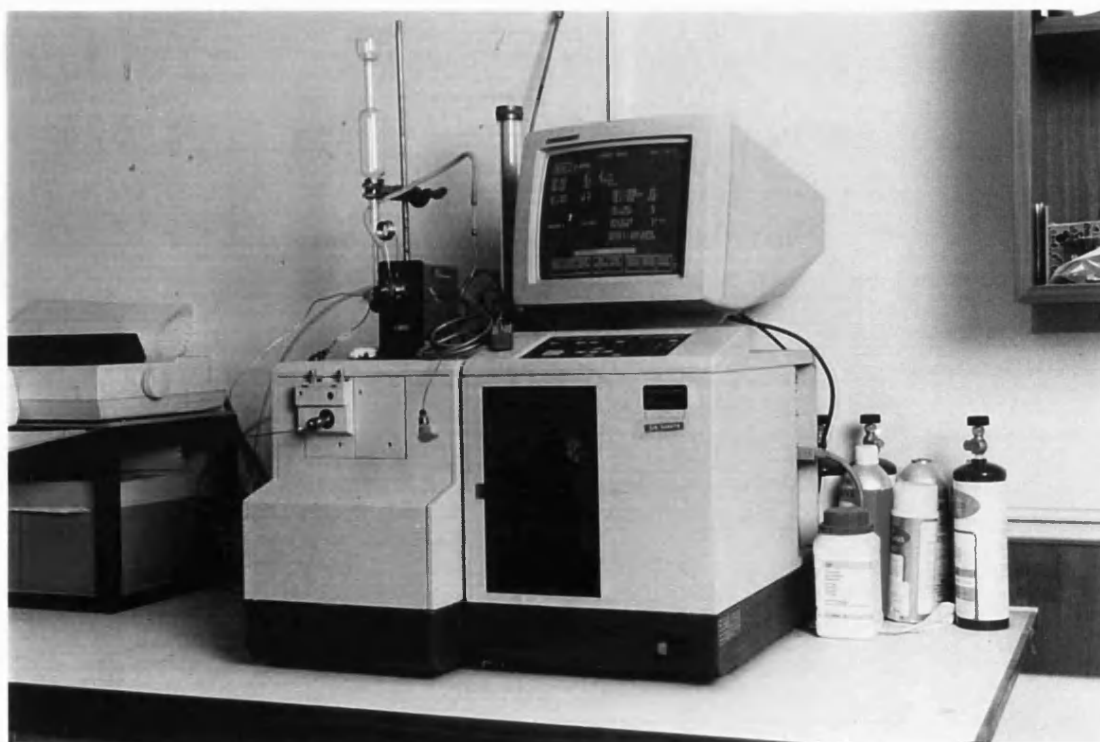


Figure 3.6 Photograph of Gas Chromatograph

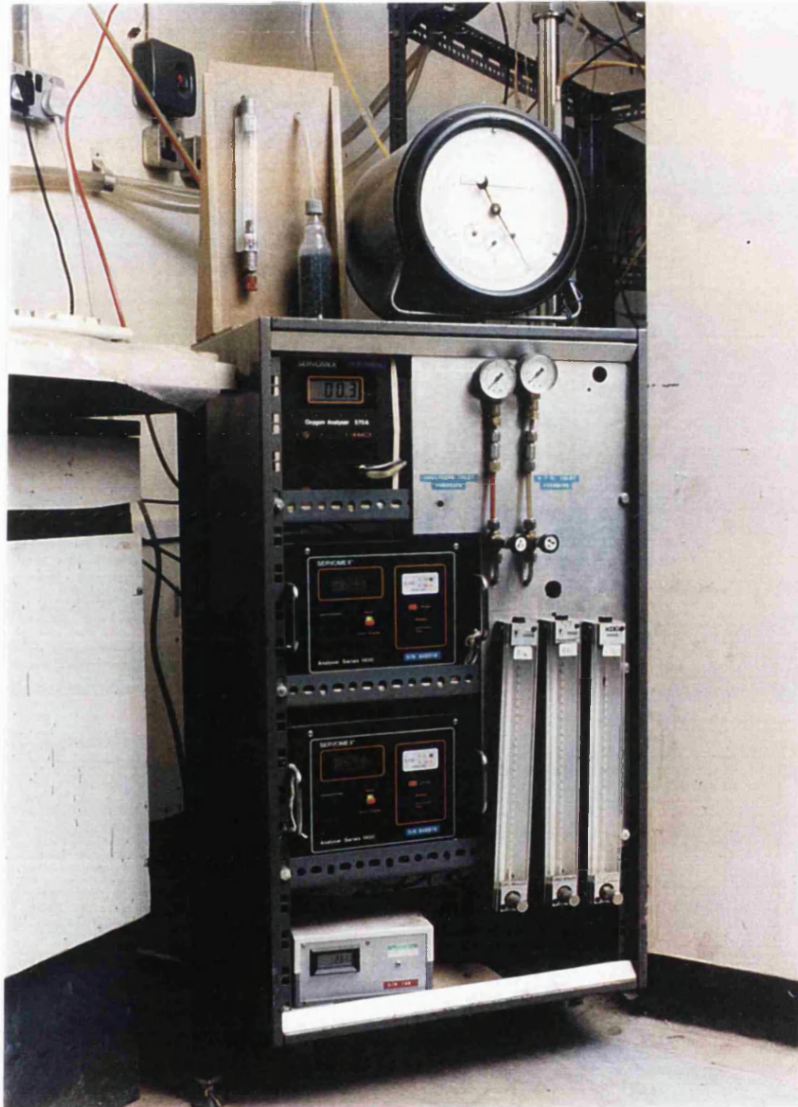


Figure 3.7 Photograph of gas analysers and Wet Test Meter

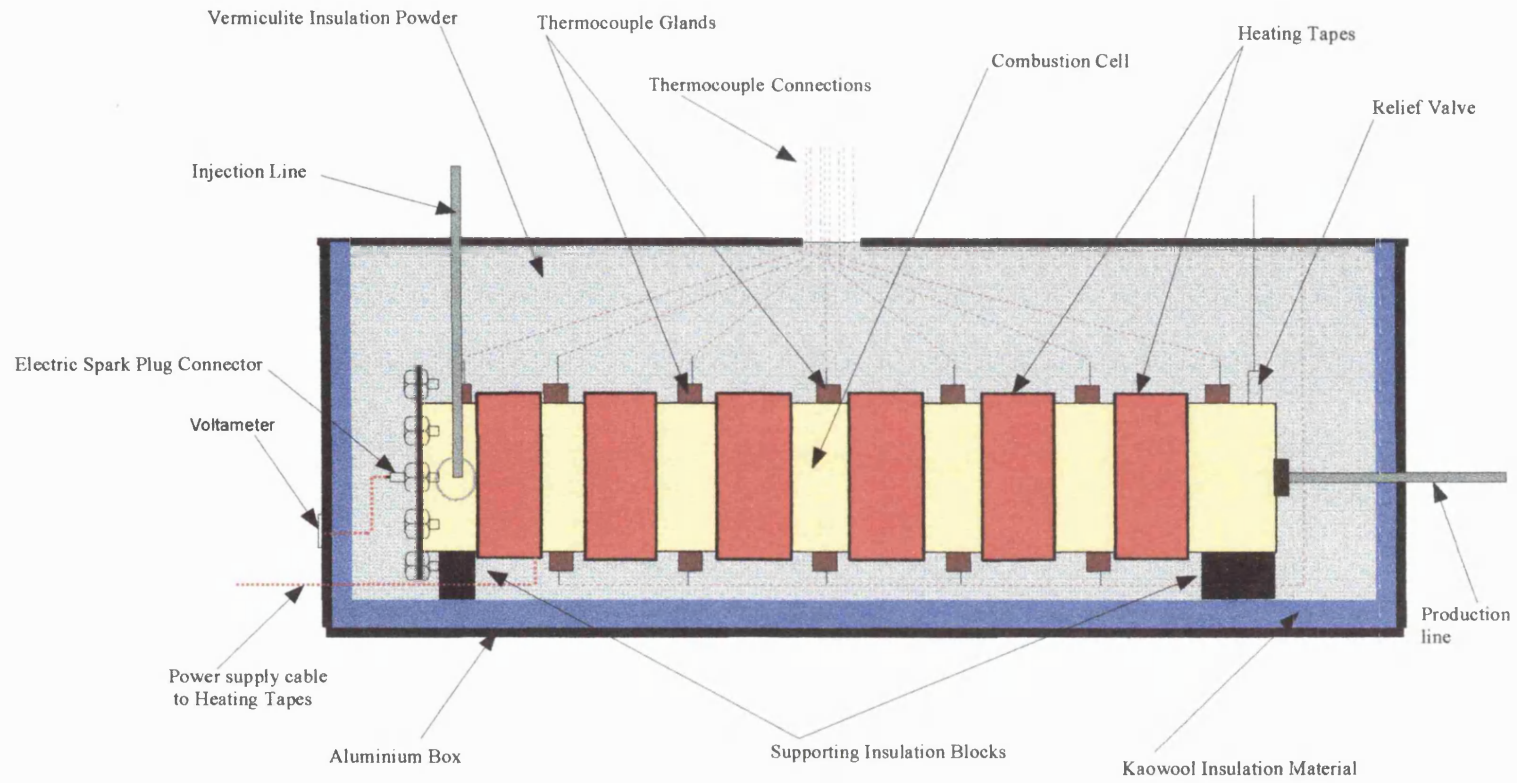


Figure 3.8 Combustion cell inside aluminium insulation box

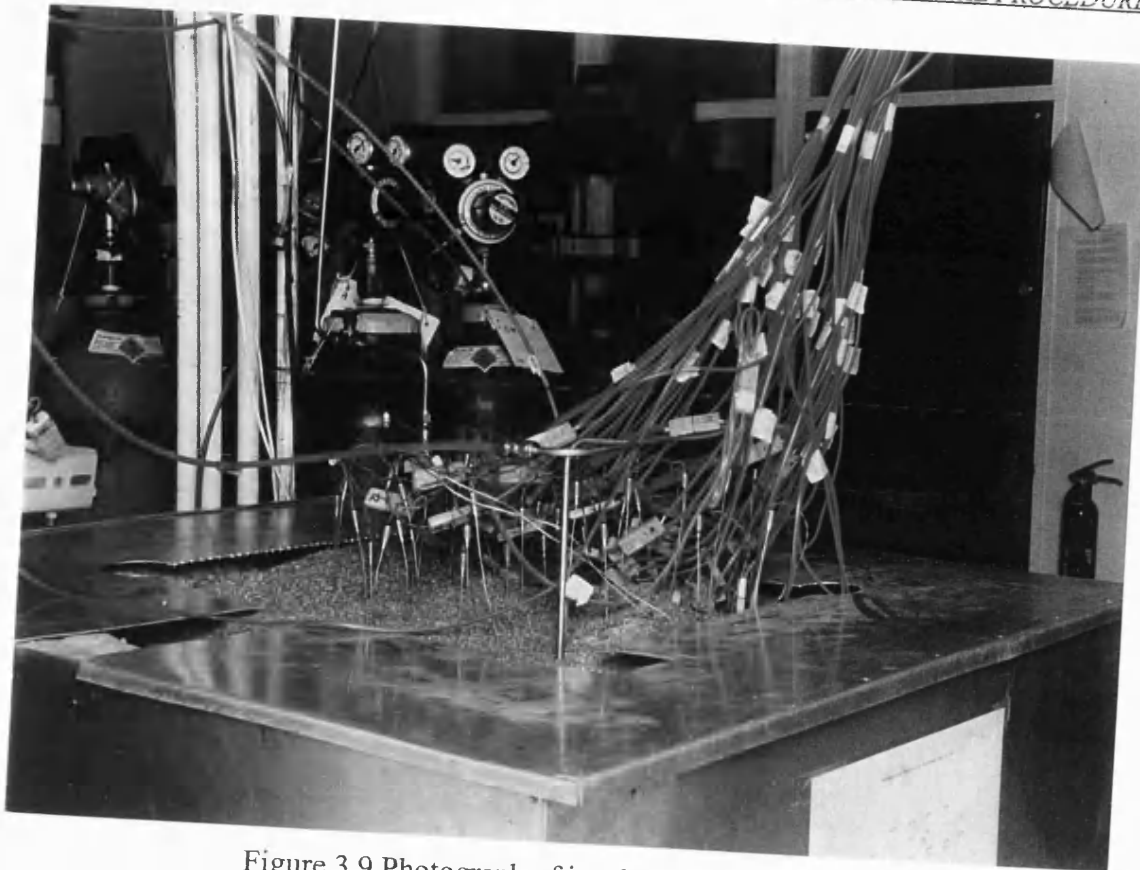


Figure 3.9 Photograph of insulation aluminum box



Figure 3.10 Photograph of computer workstation

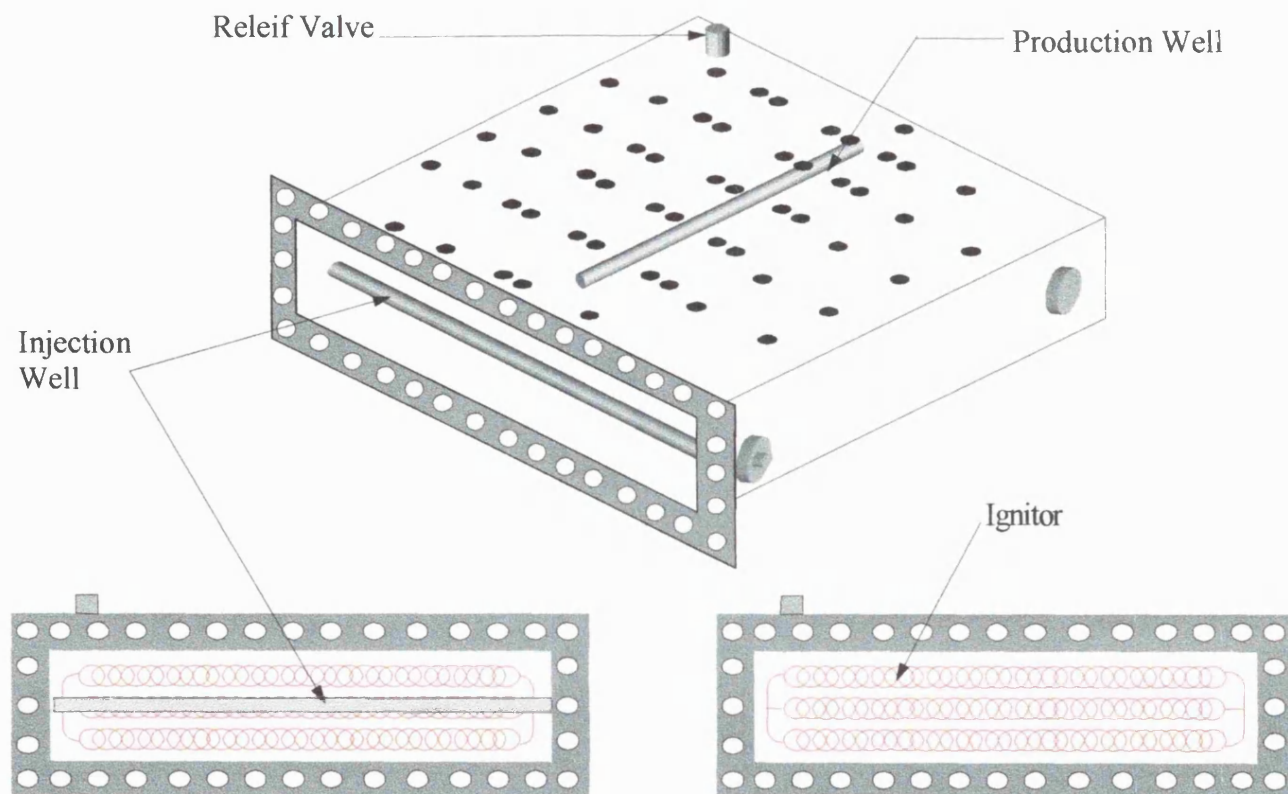


Figure 3.11 Well arrangement and ignitor position inside 3D cell

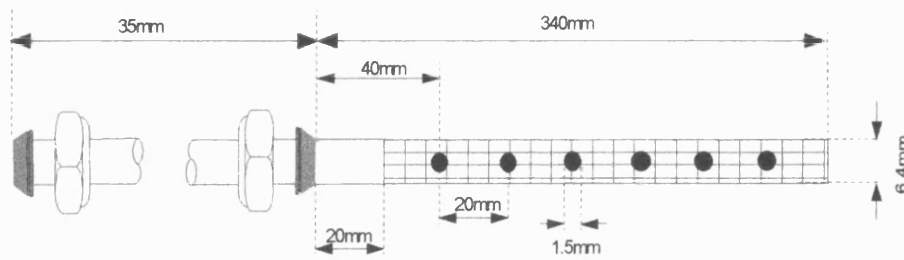


Figure 3.12 Horizontal producer well with low hole perforation density [Design 1]

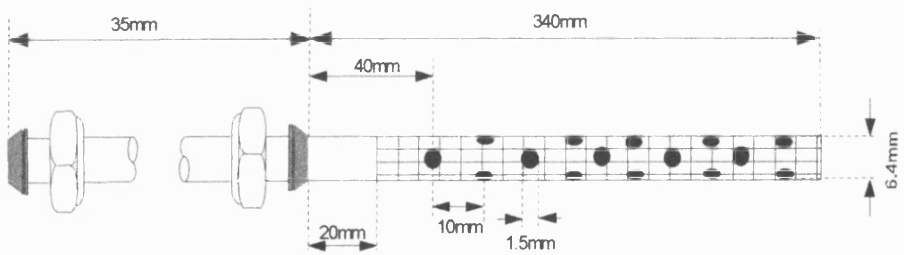


Figure 3.13 Horizontal producer well with high hole perforation density [Design 2]

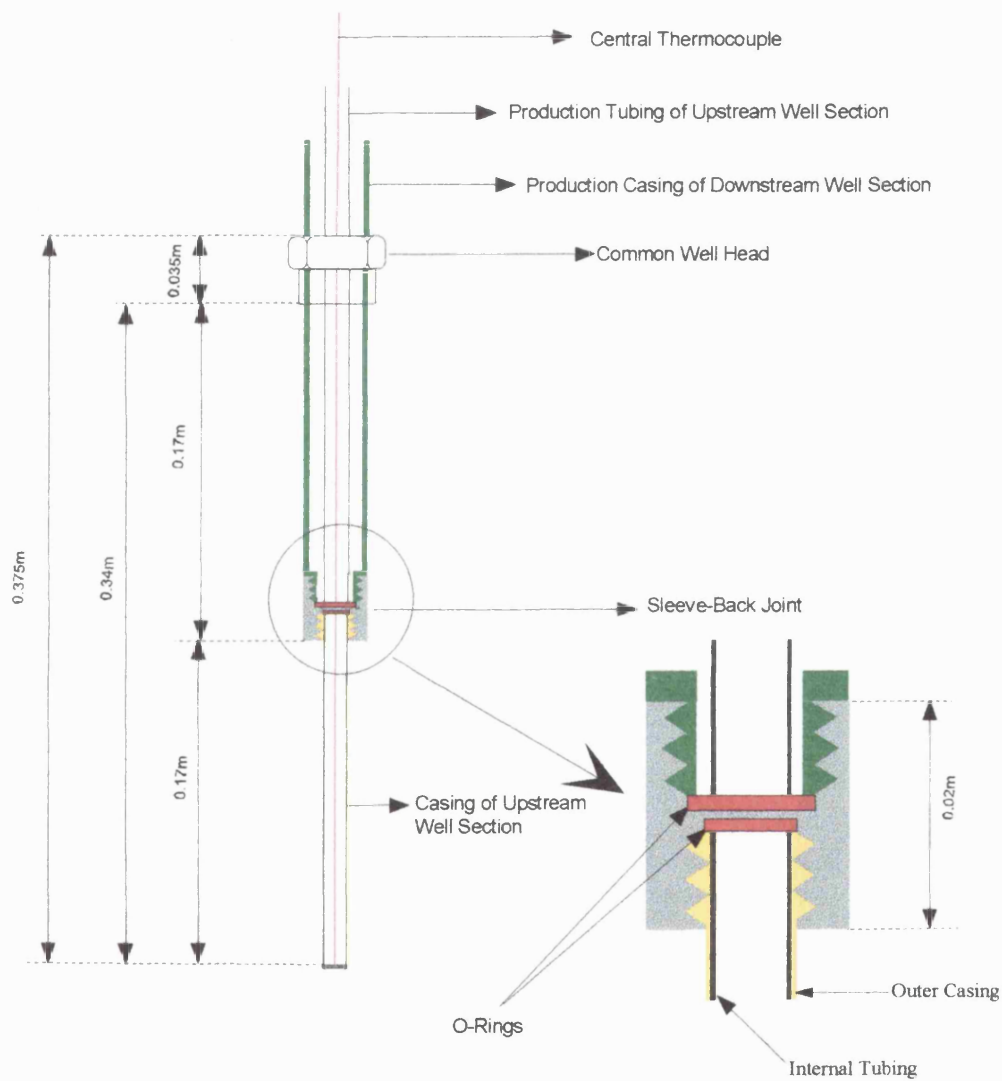


Figure 3.14 Co-aligned horizontal well assembly using sleeve-back mechanism

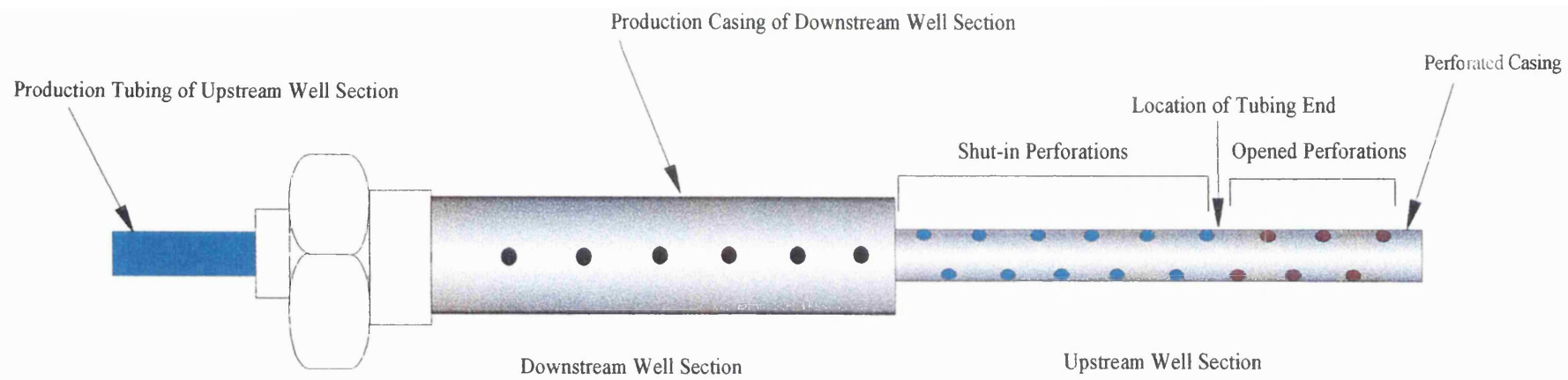


Figure 3.15A Operation regime for sleeve-back of horizontal producer well (Design 3)

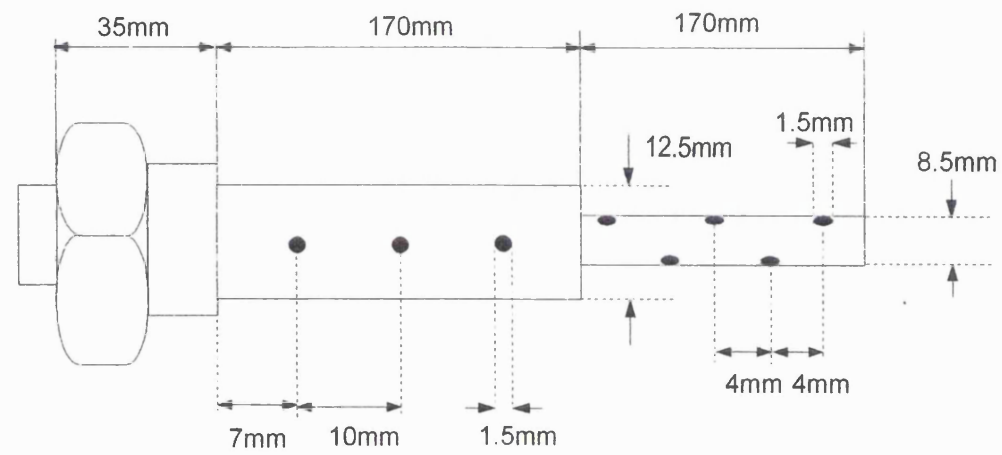
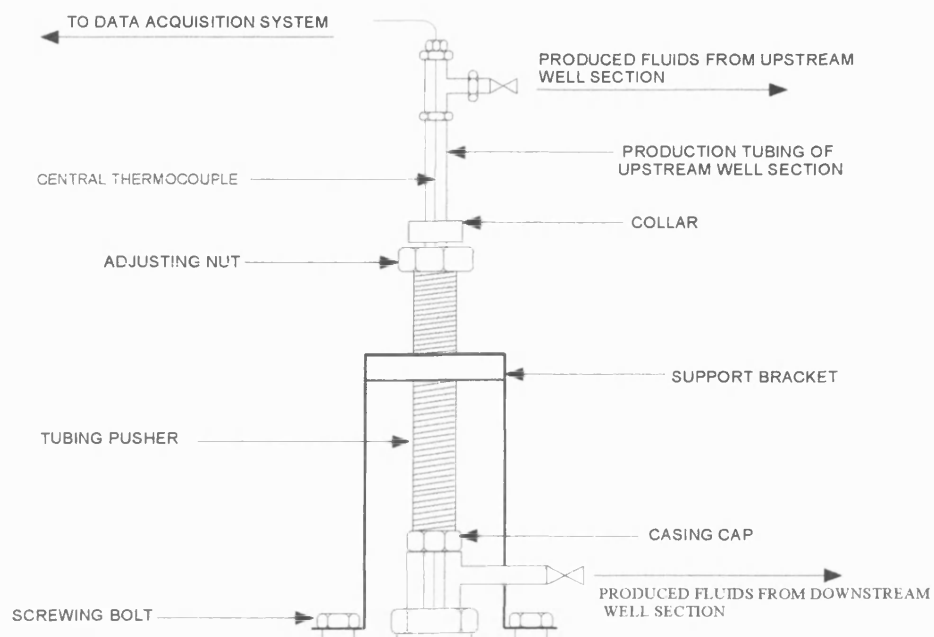
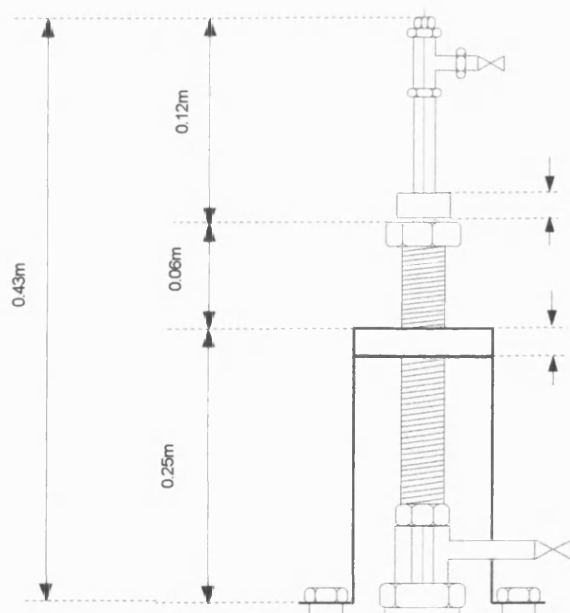


Figure 3.15B Arrangement of perforations



A. Arrangement of adjusting mechanism



B. Dimensions

Figure 3.16 Mechanism for adjusting sleeve-back of horizontal producer well (Design 3)

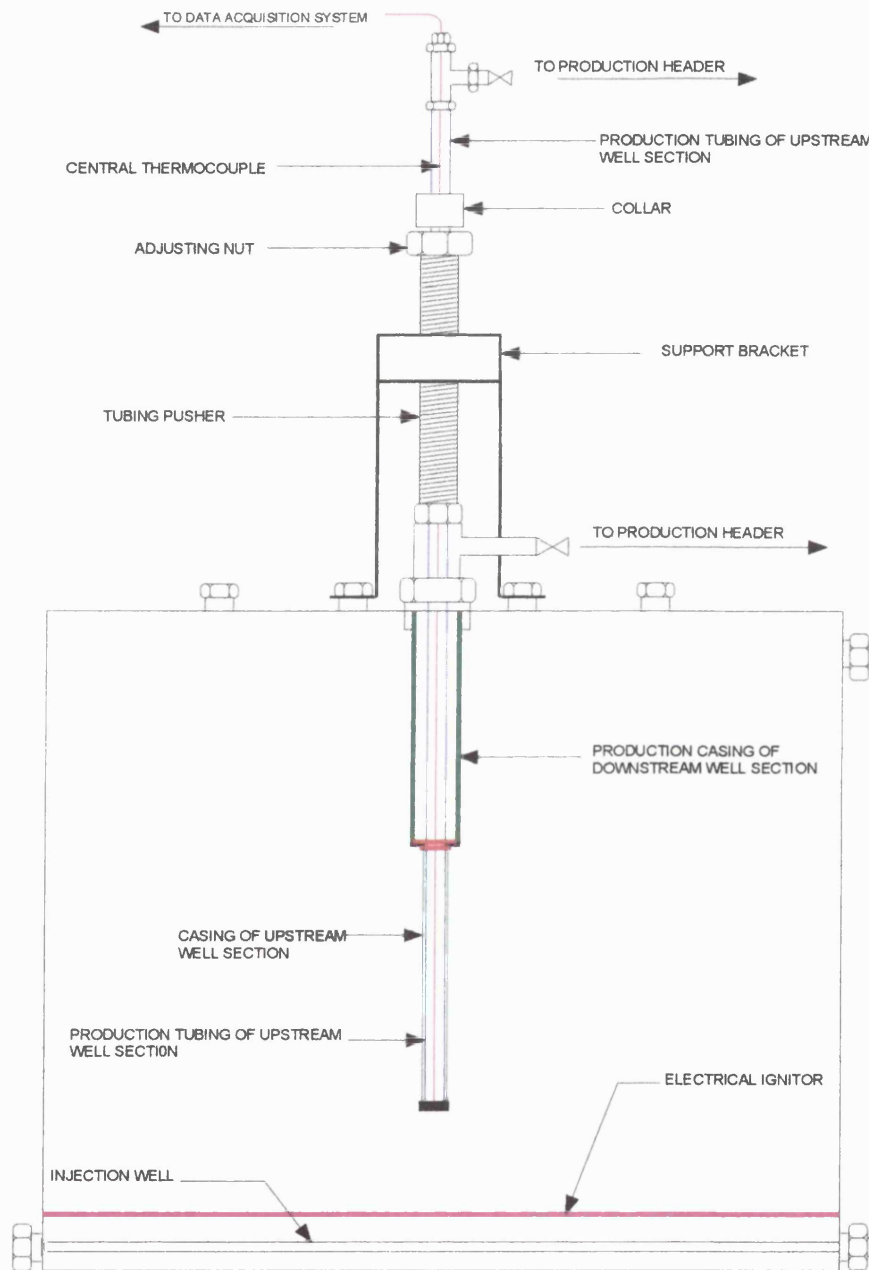


Figure 3.17 Horizontal producer well assembly (Design 3) as installed on 3D combustion cell

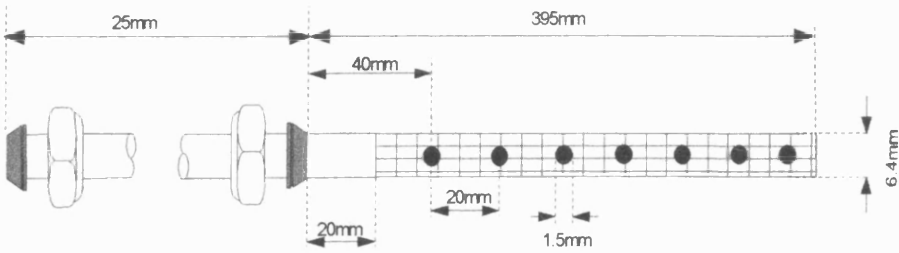


Figure 3.18 Horizontal injection well

CHAPTER FOUR

EXPERIMENTAL RESULTS AND DISCUSSION

PART I: Experiments with Conventional Horizontal Producer Well

This chapter deals with the experimental results, analysis and discussion. In part I, a total of four experiments were conducted to physically simulate the forward *in-situ* combustion process in a dry mode. In part II, one successful experiment was carried out by using a modified horizontal producer (Design 3). All of the experiments were carried out using the 'Toe-to-Heel' direct line drive configuration. Air was used as the oxidant gas for all of the experiments. Two pairs of experiments were conducted to investigate the effect on combustion performance of perforation hole density along the horizontal producer well. One set of experiment was conducted using a low perforation hole density and the second set was carried out by using a high perforation hole density.

The first set of experiments are designated Runs 961 and 962, using medium-heavy Clair crude oil (19.8 °API). The second pair of experiments are designated Runs 963 and 964, using light Forties Mix 1 crude oil (30.8 °API). One experiment (Run 966) was conducted using a modified horizontal producer well, incorporating the sleeve-back principle. This run also used the Forties Mix 1 crude oil.

The results from each run are analysed by comparing the following dependent parameters: produced gas composition, apparent hydrogen-carbon ratio and carbon molar ratio, oxygen utilisation and air-fuel requirement (AFR), carbon combustion rate, air requirement, fuel consumption, oil and water production histories, combustion front velocity, temperature profiles and also post-mortem analyses of the burnt sandpack.

A summary of the main results is tabulated in Tables 4.1 and 4.2. The detailed results for each individual experiment are presented graphically.

4.1 MAIN COMBUSTION PARAMETERS

4.1.1 Produced gas composition

The measured composition of the produced gas for each run is shown in Figures 4.1 to 4.4. Table 4.1 below summaries the values of CO₂, CO, and O₂ during the stabilised period, or average in the case of Run 964, when the combustion failed.

Table 4.1 Effect of Perforation Hole Density on Produced Gas Composition

Oil Type	Low Perforation Hole Density [H.W. Design 1]			High Perforation Hole Density [H.W. Design 2]		
Medium Heavy Clair (19.8 ° API)	Run 961			Run 962		
	CO ₂	CO	O ₂ (%)	CO ₂	CO	O ₂ (%)
	11.1	3.4	2.9	8	2.8	3.7
Light Forties Mix 1 (30.8 ° API)	Run 963			Run 964*		
	CO ₂	CO	O ₂ (%)	CO ₂	CO	O ₂ (%)
	8.85	2.35	4.8	6.1	1.9	7

*Average values because combustion not sustained

Only for Run 961, with Medium Heavy Clair oil was there a measure of vigorous combustion as demonstrated by a CO₂ level of 11.1%. The corresponding run with low perforation hole density (1/cm²), Run 963, but with Light Forties Mix 1 oil, achieved a significantly lower CO₂ level, at 8.85%. However, sustained propagating combustion was achieved, as can be seen in Figure 4.3.

The other light oil experiment, Run 964, using a higher perforation hole density (4/cm²), failed to sustain combustion, as shown in Figure 4.4.

The declining CO_2 trend in Run 964 shows that the combustion process starts to die after about 3 hours, even though the ignitor remained on. This is further evidenced by the sharp rise in the oxygen level at this time, which continues to rise to the end of the experiment.

It is evident from this set of results that, the perforation hole density along the horizontal well has a very significant effect on the combustion performance (as measured by the CO_2 level), and especially the ability to sustain combustion when a light oil is used. In a light oil reservoir, the mobility is higher, and consequently its ability to drain into the horizontal well is much greater than for a more viscous oil. This is further increased at higher perforation hole density, leading to desaturation of the oil layer downstream of the combustion front. The advancing combustion front therefore 'sees' a reducing fuel availability, causing the combustion front eventually to die.

It appears from the partial success with Run 963, that reducing the hole perforation density is advantageous for sustaining combustion of light, or medium heavy oils but at the possible expense of initial oil production.

4.1.2 Apparent atomic H/C and carbon molar ratios

The apparent H/C ratio and to a lesser extent the $\text{CO}/(\text{CO}+\text{CO}_2)$ ratio, are useful parameters for evaluating the combustion performance. A lower ratio for each, signifies more efficient combustion reactions occurring. The ratio of H/C for the fuel is calculated on the assumption that any unaccounted oxygen not participating in the carbon oxides production is consumed in the formation of water. This is not totally

correct because some of the oxygen will be consumed by LTO reactions downstream of the combustion front; for this reason the H/C ratio is considered an apparent value, rather than a true one. A low level of CO₂ in the produced gases and a high H/C ratio will tend to support this.

The apparent atomic H/C ratio is calculated by the following equation by *Burger et al* (1985):

$$H/C = 4 * [(O_{2\text{ cons }} - CO_{2\text{ formed }} - (CO_{\text{ formed }} / 2)) / (CO_{2\text{ formed }} + CO_{\text{ formed }})] \quad (4.1)$$

Where, O_{2cons} volume of oxygen used up, CO_{2 formed} and CO _{formed} are the volume of carbon oxides in the produced gases.

Figures 4.5 to 4.8 show that, the H/C is not constant, but varies as the combustion zone propagates into the downstream region. This is attributed, in part, to the variations in fuel availability and composition ahead of the combustion front. The high values of H/C observed during the ignition phase are artificial, and are not significant, except that in field operations (*Tsang, 1990*), it will be important if LTO is used to create ignition.

The stabilised apparent H/C value for Run 961 was 1.57, which is lower than that for Clair crude oil (H/C =1.8). Therefore, the fuel consumed is a coke-like material, and the process is combustion dominated. On the other hand, the H/C value for Run 962 was 2.42, indicating that significant LTO reactions occurred.

The fact that the CO/(CO+CO₂) ratio for Run 961 and 962 are similar (0.24 and 0.25), shows that this ratio is not a good indicator of combustion performance.

The apparent H/C ratio for Run 963, during the stabilised period, is 2.27, which is slightly higher than the H/C of the Forties Mix 1 crude oil (~ 2.0). In Run 964, the H/C value is much higher, averaging 4.7, but reaching to over 6 mid-way through the post-ignition period. This reflects a massive LTO effect occurring in the downstream region, especially in the steam zone. The values of H/C and CO/CO+CO₂ ratios are summarised in Table 4.2.

Table 4.2 Combustion Performance

RUN	961	962	963	964
Crude oil	Clair	Clair	FM1	FM1
H/C ratio	1.57	2.42	2.27	4.7
CO/CO+CO ₂ ratio	0.24	0.25	0.20	0.23
Combustion temperature (°C) Maximum Stabilised	631 450-510	602 440-490	535 350-390	448 †
Air to fuel requirement (sm ³ /kg)	10.56	11.51	11.58	12.08
O ₂ to fuel requirement (sm ³ /kg)	2.22	2.43	2.43	2.53
Fuel burned (% OOIP)	6.97	6.28	4.3	1.6
Oxygen utilisation (%)	90.3	81.4	80	67
Fuel consumption (kg/m ³)	24	21	9.4	3.5
Air Oil Ratio (m ³ /m ³)	908	958	484	271
Combustion front velocity (m/hr)	0.022	0.018	0.035	*
Air requirement (sm ³ /m ³)	259	317	129	*
O ₂ requirement (sm ³ /m ³)	54	67	27	*
Carbon combustion rate (g/hr)	9.28	9.17	9	7.4

† not stabilised; Max = 448 to Min = 329

*Combustion not sustained

4.1.3 Oxygen utilisation

The combustion performance can also be evaluated, in part, from the oxygen utilisation. This is defined as the fraction of oxygen consumed in the combustion reactions from the total oxygen injected.

Oxygen utilisation is calculated from the produced gas composition by Equation

Oxygen utilisation is calculated from the produced gas composition by Equation

4.2. The trends for the experiments are shown along side the air-fuel requirement in Figures 4.9 to 4.12.

$$\text{Oxygen Utilisation (\%)} = \left[\frac{O_{2IN} - O_{2OUT}}{O_{2IN}} \right] \times 100 \quad (4.2)$$

where O_{2IN} is the mole % of oxygen in the injected gas and O_{2OUT} is the oxygen concentration in the flue gases.

The oxygen utilisation in Run 961 declines from around 90 % down to approximately 80 %. For Run 962 it remains steady at approximately 82 %. Both of these values are reasonably high, but nevertheless; as shown in Figures 4.1 and 4.2 unconsumed oxygen in the produced gas is at the margins of safety, averaging around 3 to 4 %. Figures 4.9 and 4.10 also show the Air-fuel requirement for both runs.

The AFR for Runs 961 and 962 show quite different trends. In Run 961, the AFR settles down to a value of about 11, decreasing finally to 10 sm^3/kg . However, in Run 962, it increases up to 14.36 before undergoing a continues decline to a value of 11.5 sm^3/kg .

Oxygen consumed in LTO reactions for run 962 is calculated by Equation 4.3 which has been used by *Ramey et al (1992)*.

$$\text{O}_2 \text{ consumed in LTO \%} = \frac{100(X_{\text{Apparent}} - X_{\text{True}})}{4(0.2682N_2 - O_{2P})} \quad (4.3)$$

Where X apparent is the apparent H/C ratio for the fuel, and X true is the H/C value for the crude oil.

According to Equation 4.3, 78 % of the injected oxygen is consumed by LTO reactions in Run 962. This is probably the main reason for the high AFR in this case, i.e. highly oxygenated fuel was created by LTO reactions.

Run 963, which used light Forties Mix 1 crude oil, also exhibited a reasonably high oxygen utilisation, stabilising at around 80 %. However, in Run 964 the oxygen utilisation continually declined during the combustion period, from 78 down to 63 %. From Equation 4.3 the oxygen utilised in LTO reactions in Run 963 is about 38 %, so that combustion was the predominant reaction but, virtually all of the injected oxygen in Run 964 was consumed via LTO reactions. This evidence a lack of fuel availability due, in part, to increasing desaturation effect ahead of the front, because of increased drainage into the well.

Run 963, exhibits an almost steady AFR throughout the run, averaging 11.57 sm^3/kg . In Run 964 (Figure 4.12), there is an increasing trend after the ignition period, up to a maximum of 20 sm^3/kg , thereafter decreasing continuously to about 13 sm^3/kg .

Whilst LTO reactions can apparently increase fuel availability for a light oil, it is not necessarily advantageous because of the lack of control of combustion front propagation and, inevitably, the process dies.

In Runs 961, 962 and 963, (Figures 4.13 to 4.15), combustion front propagation and combustion intensity are maintained at a reasonable levels, achieving a carbon combustion rate of around 9g/hr. However, a combustion rate of only 7.4 g/hr is achieved in Run 964 which, clearly, is too low to sustain combustion front propagation.

4.1.4 Air requirement

Gas compression cost is a major factor contributor to the operating cost of all gas injection projects. For air injection projects, air availability is not in question, and so the chief concern is compression cost of the injected air. The air required to recover one cubic meter of oil (AOR) is the most important parameter determining the profitability of any air injection project.

The air requirement for each run is given in Table 4.2. The lowest value is for the light oil test in Run 963 at $129 \text{ m}^3/\text{m}^3$, ranging up to $317 \text{ m}^3/\text{m}^3$ for medium heavy Clair crude oil in Run 962. These values lie within the range reported by *Burger et al* (1985), of 150 to $600 \text{ m}^3/\text{m}^3$. Evidently, there is considerable potential for lower operating cost for air injection projects in light oil reservoirs. An example of the air requirement calculation is given in Appendix (F).

4.1.5 Fuel consumption

Fuel consumption is an extremely important factor in air injection projects.

Theoretically, the fuel deposited by thermal cracking ahead of the combustion zone should be consumed when the combustion front invades the cracked residual oil zone.

Fuel consumption is affected by the amount of fuel and also its composition. This in turn, determines the amount of air required to burn a unit bulk volume of reservoir.

The fuel consumption in kilograms of fuel per cubic meter of reservoir matrix, is calculated from the following equation:

$$\text{Fuel consumption (kg/m}^3\text{)} = \frac{\text{Fuel burned}}{\text{Volume of burned section}} \quad (4.4)$$

The fuel burned is calculated from the flue gas composition, whereas the volume of the burned section is measured from post-mortem inspection.

The amount of fuel burned as a percentage of the original oil in place is calculated using the equation:

$$\text{Fuel burnt (\% of OOIP)} = \frac{100 [\text{O}_{2c}/\text{Oxygen fuel requirement}]}{\text{OOIP}} \quad (4.5)$$

where O_{2c} is oxygen consumed in combustion reactions.

Table 4.2 gives the fuel consumption values for all runs. The fuel consumption for Runs 961 and 962 is 24 and 21 kg/m³, respectively. These values are higher than those reported by *Wilson* (1998), who reported a value of 14.9 kg/m³. The higher flux used in this study may be responsible for this. The amount of fuel burned as a percentage of OOIP was slightly different between the two runs, varying from nearly 7 % in Run 961 to 6.3 % in Run 962.

In Run 963, which used light Forties Mix 1 crude oil, a lower fuel consumption (9.4 kg/m³) was achieved, and the overall fuel burned was 4.3 % OOIP. However, in Run 964 it was only 1.6 % OOIP, which corresponds to 3.5 kg/m³. This very low fuel consumption may be related to the lower residual oil saturation ahead of the combustion front, limiting the process to an LTO mode, rather than self-sustained high temperature oxidation reactions. Thus, a well design which would help to limit,

or prevent, desaturation of the oil layer ahead of the combustion front, could help to improve fuel availability and sustain the process.

4.1.6 Oil and water production

The rate at which fluids are produced from the reservoir is affected by the fluid entry holes, or perforations, along the horizontal producer well. Thus the higher the drainage area exposed to the reservoir surface, the easier it will be for the oil to drain into the well. This can be even more pronounced in reservoirs with high vertical permeability in the case of horizontal producers, or where there is a higher horizontal permeability, if vertical wells are used. On the other hand, if the reservoir rock is sufficiently consolidated, and there is no risk of collapse, the producing wells are usually completed as open hole, in order to gain higher productivity. The fluid production history for all of the runs is presented in Figures 4.17 to 4.28.

Effect of ignition period on oil saturation

The oil produced during this period is mainly due to vaporisation of light fractions due to the heat generated by the ignitor. The percentage of oil produced during this period varies with each run according to the horizontal producer used. In Run 961 (Design1), oil equal to 15% OOIP was produced, whereas in Run 962 (Design 2), the oil produced during this period was 32% OOIP. A similar trend was also observed in Runs 963 and 964, using less viscous Forties Mix 1 crude oil.

In Run 963, oil produced was 26 % OOIP, whereas in Run 964 it was 54 % OOIP.

The amount of oil produced during this initial period significantly affects the fluid saturation distribution in the sandpack, but generally not to any major overall degree.

Table 4.3 summarises the average fluid saturation in sandpack at initial conditions and prior to air injection.

Oil saturation is more greatly affected than water saturation, typically around 15 to 25 % desaturation (Runs 961 and 963) using a low hole perforation density, increasing to nearly 32 % at high hole perforation density (Run 962), but even worse (> 50 %) for Run 964 using lighter oil.

Gas saturation (hydrocarbon gas) is developed within the sandpack in all runs, up to 36% in Run 964. Both this run, and Run 962 are characterised by high initial oil production. Consequently, the relative permeability to gas is increased, and therefore, oxygen residence time within the high temperature zone is reduced, limiting HTO and hence consumption of oxygen. Additionally, a higher gas saturation may cause channeling of air into downstream zones, and when the vertical permeability is low, this could increase oxygen contact time within the unreacted oil, resulting in LTO.

Table 4.3 Effect of Perforation Hole Density on Fluid Saturation in Sandpack

RUN	$S_{oi}(\%)$	$S_{oi}(\%)$	$S_{wi}(\%)$	$S_{w1}(\%)$	$S_{gi}(\%)$	$S_{g1}(\%)$
961	60	51	40	38.6	0	10.4
962	60	40.8	40	36.5	0	22.7
963	60	44.4	40	38.4	0	17.2
964	60	27.6	40	36.4	0	36

i = Initial fluid saturation (i.e. at packing)

1 = Fluid saturation prior to air injection

Production rate

From Table 4.4, it can be seen that oil production rate during the period when the sandpack is heated artificially is not constant. Higher production occurs when well Design 2 is used (i.e. Runs 962 and 964). Importantly, the fluid saturation in all runs is the same during this period ($S_{oi}=60\%$), i.e. at initial conditions. Therefore, the oil relative permeability is identical. This suggests that at a given oil saturation, the oil production rate is a function of the number of fluid entry points, or hole perforation density along the horizontal producer well. This is very evident, as shown by the high initial liquid production rates in Runs 962 and 964, which both used a high hole perforation density horizontal producer well.

This is in close agreement with results reported by *Brekke* (1992), in which he studied the effect of completion methods on horizontal well productivity. He reported that restricted flow through perforations reduced productivity of the well. Similar results were also reported by *Al Qahtani et al* (1996).

Table 4.4 Effect of Hole Perforation Density on Production Rate

Run		q_o (ml/hr)	q_w (ml/hr)	q_t (ml/hr)
961(Clair oil, H.W Design1)	Before ignition	295	45	340
	After ignition	198	183	381
962(Clair oil, H.W Design 2)	Before ignition	604	84	688
	After ignition	143	215	358
963(FM1 oil, H.W Design1)	Before ignition	505	71	576
	After ignition	233	220	453
964(FM1 oil, H.W Design2)	Before ignition	1135	144	1279
	After ignition	131	233	364

The oil production rate during the post-ignition period is lower than that during the ignitor-on period. For example, the oil production rate in Run 961 was 198 ml/hr, which is lower than that during the pre-ignition period by 33%. Similarly, in Run 962, the oil production rate before ignition was 604 ml/hr, but then declined during the post-ignition period, to 143 ml /hr. The reduction in oil production rates can be partially attributed to the reduction in oil saturation in the sand pack. Thus, if the oil relative permeability declines, oil flow through the sand matrix is also reduced (Darcy's law).

Higher oil production rates were sustained during the post-ignition period for Runs 961 and 963, which used Design 1 producer. This due to the higher combustion efficiency achieved in those runs.

The highest production rates were recorded during the pre-ignition period of Run 964, where the oil production rate peaked at 1135 ml/hr and the water production rate was 144 ml/hr. Here, the desaturation is equivalent to 31 % OOIP. Before air injection was started, the oil produced was equivalent to 54 % OOIP, and water only 9 % OWIP. In terms of pore volume, this means that almost 50 % of the sandpack is already 'swept' before ignition.

Particularly for the light Forties Mix 1 oil, it is obvious that part of the high oil influx, under the well configuration used, flows from the central region of the sand pack. Therefore, the maximum oil saturation is located at the edges of this central region, whereas the minimum oil saturation is in the middle of the sand pack in the vicinity of the horizontal producer where there is the possibility of a lighter oil saturation because of the draw-down effect into the horizontal producer.

A high depletion rate of oil in the down stream zones creates a low residual oil saturation ahead of the combustion front. Thus, there is less oil left in the sandpack to be thermally cracked to produce coke and so sustain the process in HTO mode. This was confirmed in post-mortem inspections, discussed later in Section 4.2.10.

The average oil saturation at ignition for Run 963 was 44.4 %, which is 38 % higher than that in Run 964. This was sufficient to sustain a reasonable efficient process for about 8 hours.

Recovery factor

Although a high total oil recovery is achieved in all of the runs, the actual recovery during the combustion period varies for each run. From Table 4.6, the maximum oil recovery during the combustion period was achieved in Runs 961 and 963, for which the combustion performance was more efficient. On the other hand, the lower oil recovery was recorded in Run 964 which produced only 15 % OOIP by combustion. The extra “assist” when the ignitor is “on” during the combustion period, amounts to an increase in temperature of a 60 to 100 °C. This means that the combustion is mainly dominated by the natural in situ combustion process, since

$$\Delta H_{\text{HTO}} \propto \Delta T_{\text{stabilised}} / \Delta T_{\text{ignitor on period}}$$

which is 76, 77, 84 and 73 % in Runs 961, 962, 963 and 964, respectively.

Table 4.5 Oil Recovery (% OOIP)

RUN	Pre-ignition period	Combustion period with ignitor on	Combustion period with ignitor off	Overall
961 Oil recovery (% OOIP)	15	47	23	85
Water recovery (% OWIP)	3.4	49.7	38.9	92
962 Oil recovery (% OOIP)	32	34	17	83
Water recovery (% OWIP)	8	57.3	21.7	87
963 Oil recovery (% OOIP)	26	35	21	82
Water recovery (% OWIP)	4	38.1	42.9	85
964 Oil recovery (% OOIP)	54	12	3	69
Water recovery (% OWIP)	9	26.8	10.2	46

Physical properties of produced oil

The physical properties of the produced oil changed according to the experimental conditions. In all of the runs, the oil produced before ignition was similar to the original crude oil.

In Run 961, the oil produced after ignition was upgraded by 2 points as compared with the original crude. In Run 962, the oil produced 2 hours after ignition was also upgraded by 2 points. As the experiment proceeded, lower gravity crude oil was produced (18.3 API) indicating that the oil had been oxygenated.

A similar trend was also observed in Run 964 but no upgraded oil was produced post-ignition, due to the failing combustion condition.

In Run 963, oil produced after ignition has an API gravity of 32 ° which is one point higher than the original crude. Table 4.6 summaries physical properties of produced liquids for all runs.

Table 4.6 Physical Properties of Produced Liquids

Run No	Sampling Time	Oil Gravity °API	Oil viscosity cp	Water pH
961	Before ignition	19.8	212	7
	At ignition	24	53	4.2
	7 hours later	22	31	3.1
962	Before ignition	19.8	210	7
	At ignition	25.5	45	3.85
	2 hours later	23	28	3.6
	7 hours later	18.3	98	6.2
963	Before ignition	30.8	9.57	7
	At ignition	34.6	5.8	6.83
	5 hours later	32	7.2	5.43
964	Before ignition	30.8	9.57	7
	At ignition	32.2	6.4	6.68
	2 hours later	29.3	12.2	7.08

4.1.7 Combustion front velocity

Combustion front velocity is mainly governed by the rate of fuel deposition and hence its consumption. In an ideal combustion mode, fuel should be burned by high temperature oxidation reactions at the same rate it is formed. The burning rate is dependent on the local oxygen flux and carbon concentration. Excessive fuel deposition can result in a lowering of the combustion front advancement rate and increased air requirement. On the other hand, optimum fuel deposition results in a steady and smooth advance of the combustion front.

The combustion front velocity was determined by measuring the time required for the stabilised combustion front to travel, a certain distance, detected from the peak temperature as measured by the thermocouples located between the second and fifth row.

As presented in Table 4.2, the average combustion front velocity for Runs 961 and 962 was 0.022 and 0.018 m/hr, respectively. For Run 963, which used light Forties Mix 1 crude oil, combustion front velocity was higher at 0.035 m/hr. This is appreciably lower than normally observed from combustion tube experiments, which are one-dimensional experiments. However, the 3-D flow regime associated with the present experiments more closely represent the level of combustion front advance which would occur in an actual reservoir conditions.

4.1.8 Temperature contours

Figures 4.29 to 4.49 show the temperature two-dimensional contour maps measured along the horizontal and vertical mid-planes starting from the second row of thermocouples.

They show that the peak temperature is varying according to type of crude oil.

In Runs 961 and 962, using Clair crude oil, the peak temperature was in the range 550 to 630 °C initially, which stabilised at 450-500 °C until the end of the experiment. In Runs 963, 964, which used light Forties Mix 1 crude oil, the peak temperature was in the range 450 to 535°C, falling to 375 °C during the stabilised period of Run 963.

In each of the four experiments, we can observe the distinguishing, unique features of Toe-to Heel combustion displacement. This is represented by the elongated, approximately linear, temperature profiles ahead of the combustion front, stretching across the entire width of the sandpack. It is considered that this is due to gas displacement being forced-out to the edges of the sandpack because of the resistance

imposed by the more viscous oil in the downstream, cold regions. These easiest, and shortest, communication path for the gas and mobilised oil, of course, directly into the exposed, or active section of the horizontal producer well.

None of the contour plots (Figures 4.29 to 4.49) reveal a zone of very tight contours immediately ahead of the combustion front, except during the early stages of the tests on Clair oil (Runs 961 and 962), Figures (4.29-31 and 4.35-37). Although these temperatures are artificially high, because of the energy supplied from the ignitor, nevertheless, they are indicate of the 'narrow' mobile zone condition likely to be created in a heavy oil reservoir, in which the downstream part of the reservoir remains cold and the oil therefore has a very high viscosity.

Both the medium heavy Clair oil and the light Forties Mix 1 oil have fairly low viscosities and so are not very efficient at providing any liquid seal along the downstream part of the horizontal producer well. The consequence, is that, oil drains and desaturates the sandpack and therefore, overall, we do not see the higher temperatures that would be observed in a more nearly adiabatic reservoir.

In most cases, at least up to the time when the sandpack first seriously desaturates, the vertical contours (taken along the mid-vertical axis) are nearly vertical over the height of the sandpack. Thus, Toe-to- Heel displacement is very effective because the combustion gases and mobilised fluids are caused to flow directly into the horizontal well below, stabilising any tendency towards gas override. If the 'Toe-to-Heel' process can be designed to achieve the potentially high sweep displacement, both longitudinally and also laterally, then excellent oil recovery is possible.

Run 961 was extended over twelve hours and air was injected when average temperature in the injection face was 470 °C. Figures 4.29 to 4.34 present the temperature profiles covering air injection period of the experiment, which extended for 10 hours. Figure 4.29 show that vigorous combustion occurred in the middle of the injection face with a region of closely-spaced contours ahead of the combustion front, which extend laterally towards the edges of the sandpack with full extent in the vertical plane.

Figure 4.32 shows temperature contours at 360 minutes combustion time. At this time, the high temperature zone is located in the central region of the sandpack with closely-spaced contours a head of it ranges from 360 to 405 °C. In the vertical mid-plane section, a tonguing effect is clearly shown ahead of the high temperature zone, which properly resulted from drainage of hot fluids into the producer.

At 480 minutes combustion time (Figure 4.33), combustion zone has travelled about 55 % of the sandpack and is located in the central region. There is a small tendency for gas override in the downstream zones. At 600 minutes combustion time, the combustion zone reached its maximum size with leading edge temperature of 420 °C. Meanwhile, temperature in the burnt out zone is declined to 390 °C due, in part, to cooling effect of the injected air.

Run 962 was also extended for twelve hours and air injection was started when average temperature of the injection face averaged 465 °C. Figures 4.35 show vigorous ignition is occurred along 60 % of the injection face. Thereafter, the stability of the combustion front gradually improves and at 480 minutes, the front reached its maximum size and approached closely to a vertical orientation in the vertical plane as shown in Figure 4.39 b.

At 600 minutes combustion time, the front had travelled about 25cm of the cell length but diminished in size to approximately 60% of its previous size. It can be seen in Figure 4.40 b that moderate degree of gas override effect has occurred at this stage of the run.

Run 963 was conducted with Forties Mix 1 crude oil by using the low hole perforation density horizontal producer. When the average temperature of the inlet face reached 390 °C, air was commenced into the sandpack and rapid increase in temperature was observed. Temperature near the injection face has risen to 530 °C indicating vigorous ignition has occurred. This was also confirmed by a stable rise in CO₂ level mirrored by a drop in O₂ concentration.

The temperature profiles of this run, Figures 4.41 to 4.45, covering 500 minutes of the combustion time. Ignition mainly occurred in the middle of the sandpack and approximately covered 50 % of the injection face as shown in Figure 4.41 a.

At 120 minutes combustion time (Figures 4.42 a and b), the horizontal and vertical mid-plane contours show that there is a region of closely-spaced contours (360 to 420 °C)

ahead of the combustion front. These contours are expanded linearly towards the edges of the sandpack with vertical extend covering the entire thickness of the sandpack.

The controlling factor responsible for the development of such uniform high temperature region ahead of the front is the drainage of the hot fluids into the exposed well section. This fluid encroachment is created by the pressure controlled draw down provided by the producer.

At 240 minutes combustion time, Figures 4.43 a and b, the front has travelled 37 % of the sandpack length and is mainly located in the central region. Immediately ahead of the combustion zone, several contours are uniformly distributed in downstream zones with no sign of gas override, evidencing that hot gases are being drained effectively by the draw down action of the horizontal producer. At 360 minutes combustion time, combustion zone has diminished in size but still advancing in the central region of the sandpack as shown in Figures 4.44 a and b.

At 500 minutes, Figures 4.45 a and b, the combustion zone and trailing hot region has essentially achieved its maximum size. Immediately ahead of the combustion zone, the contours are widely-spaced because this region was extensively desaturated since the early stage of the run, and hence, limited amount of fluids is drained into the horizontal producer well. In the horizontal plane, the combustion zone expanded into the edges of the cell, whereas in the vertical plane, moderate degree of gas override is observed.

Run 964 was conducted under the same operating parameters in run 963 but with high hole perforation density horizontal producer. Air was introduced into the cell when average temperature near the injection face reached 400 °C. Successful ignition was achieved as evidenced by steady rise in CO₂ level mirrored by very low O₂ concentration in the produced gas.

In addition, temperature near the injection face continued to rise and reached 448 C. Figures 4.46 a and b show that about 50 % of the injection face was well ignited and the overall ignition performance is similar to Run 963.

At 60 minutes combustion time, the ignited section is restricted to the central region of the injection with closely-spaced contours developed immediately ahead of it. These contours ranged from 150 °C in the middle of the sandpack to 270 °C near the combustion zone during which CO₂ level was 9.5 %.

At 120 minutes combustion time, the combustion zone is still locating in a narrow region in the central section of the injection face with temperature of 345 °C.

Meanwhile, several contours are developed in the downstream zones, most probably by hot gases and generated steam, which results in more heat being transferred to down stream region as shown in Figure 4.48 a.

The vertical mid-plane profile in Figure 4.48 a show clearly the uniform distribution of heat waves along the entire thickness of the sandpack with essentially no sign of gas override. At this stage, CO₂ concentration in the produced gas declined to 7 % whereas O₂ concentration increased to 5 %.

At 180 minutes combustion time, peak temperature could not be maintained, and more importantly, did not move into downstream zones any further as shown in

Figure 4.49a but a band of elongated contours can be seen stretching across the width of the sandpack.

Meanwhile, the vertical mid-plane profile in Figure 4.49 b, shows the tonguing effect created by the draw-down of the horizontal producer, which captured most of the fluid along the entire length of the sandpack. As oxygen concentration continued to rise, the run was terminated after 232 minutes from ignition.

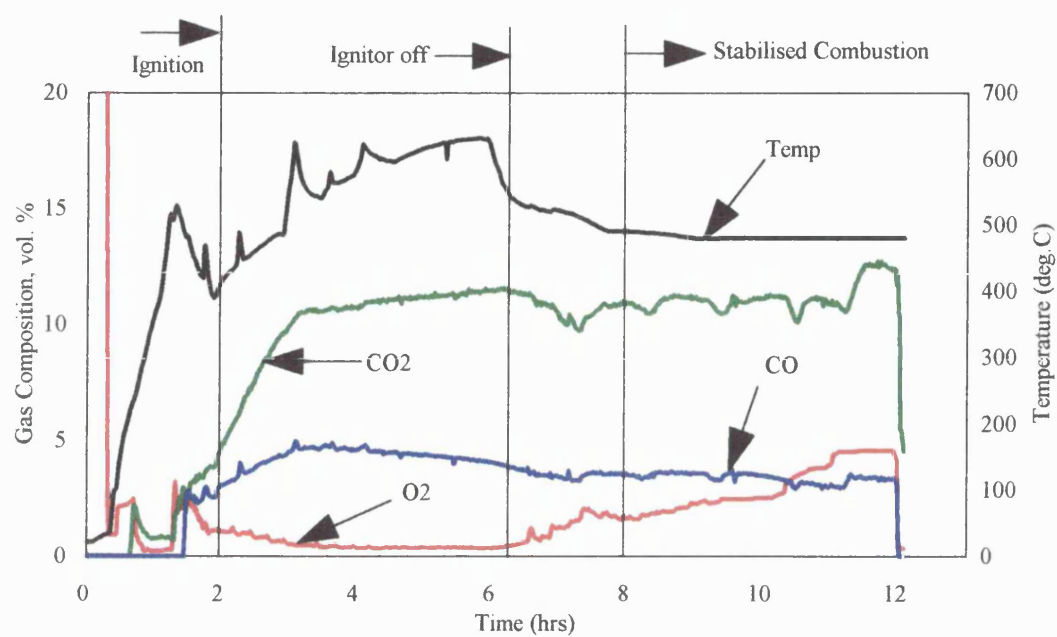


Figure 4.1 Produced gas composition for Run 961 (Clair oil, H.W. Design 1)

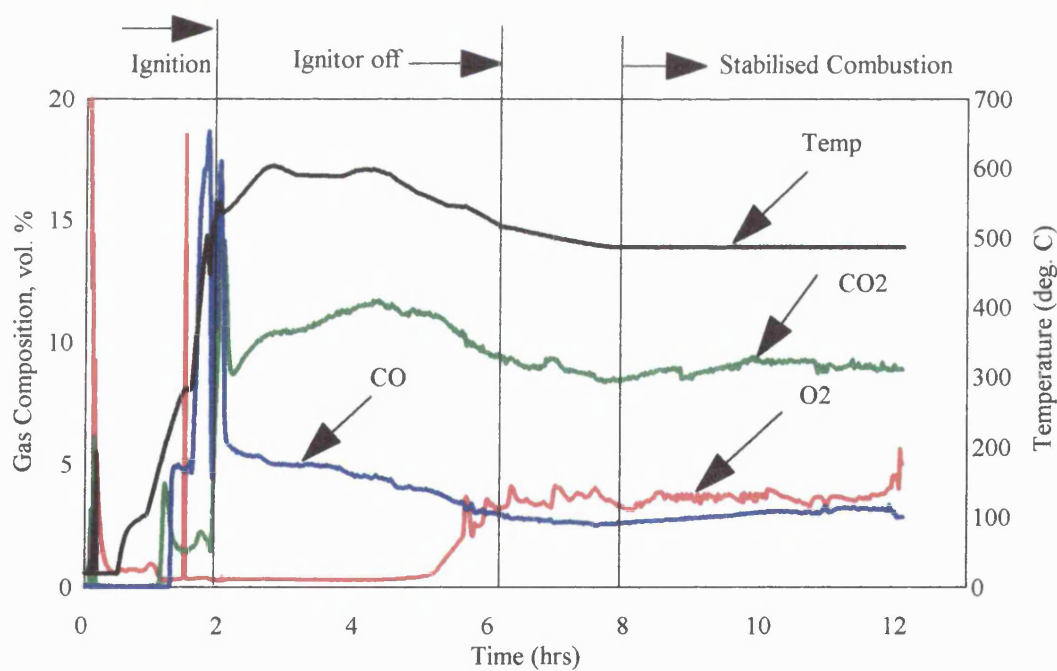


Figure 4.2 Produced gas composition for Run 962 (Clair oil, H.W. Design 2)

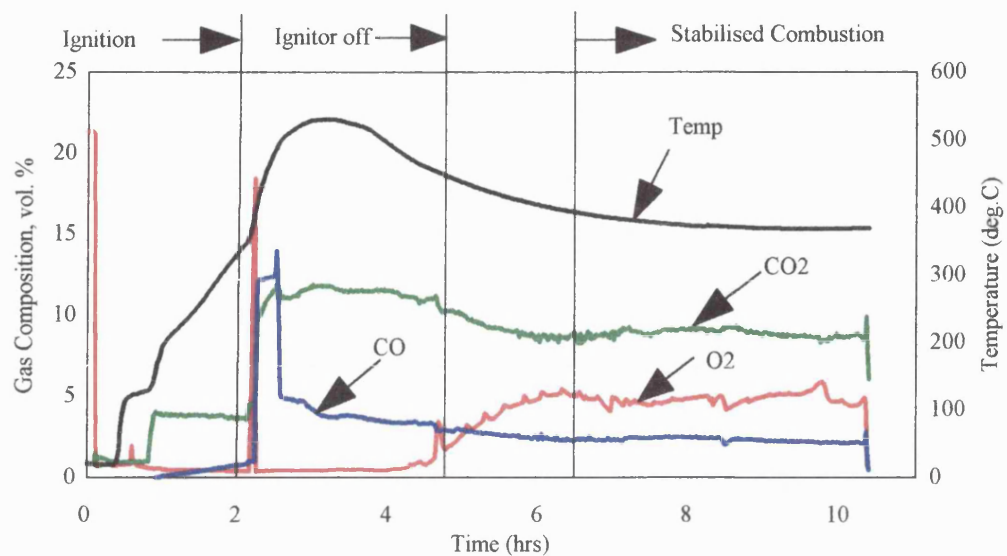


Figure 4.3 Produced gas composition for Run 963 (Forties Mix1 oil, H.W. Design1)

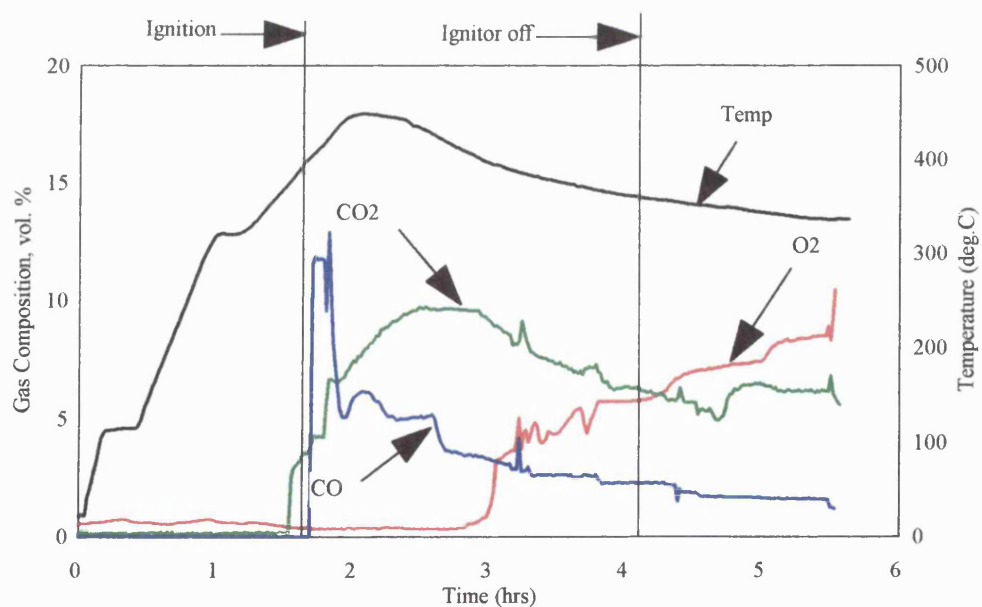


Figure 4.4 Produced gas composition for Run 964 (Forties Mix 1 oil, H.W. Design 2)

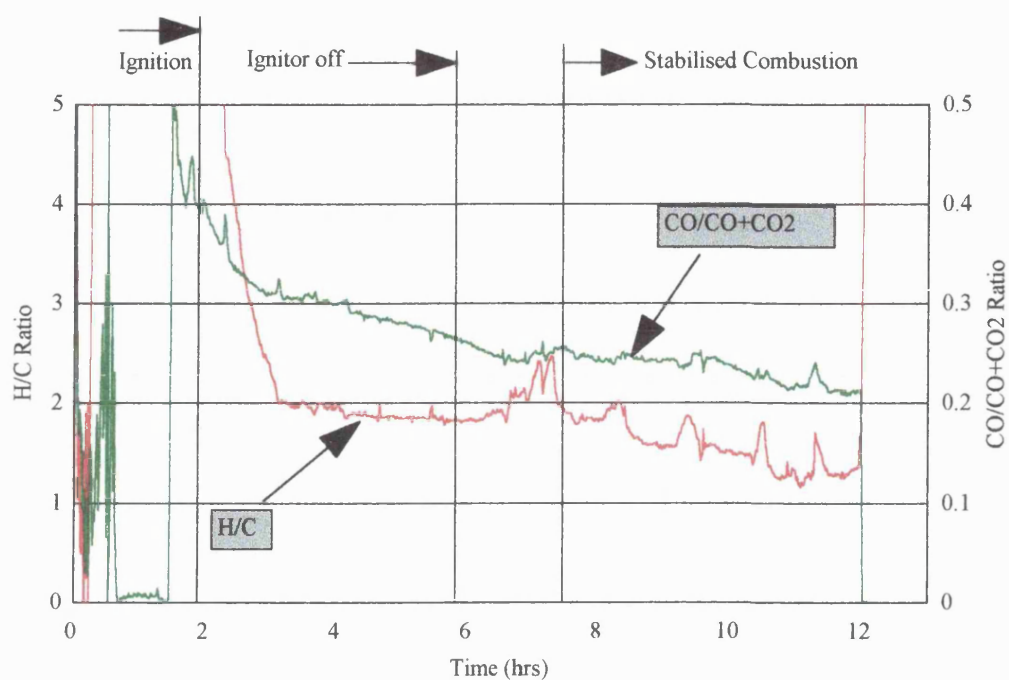


Figure 4.5 H/C and CO/CO+CO₂ ratio for Run 961 (Clair oil , H.W. Design 1)

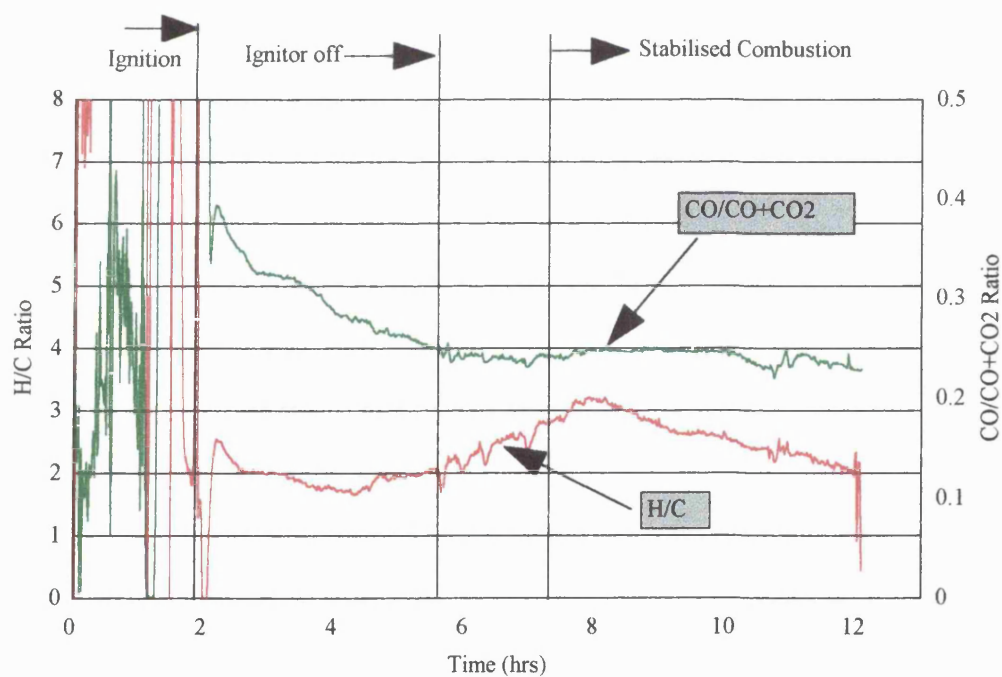


Figure 4.6 H/C and CO/CO+CO₂ ratio for Run 962 (Clair oil , H.W. Design 2)

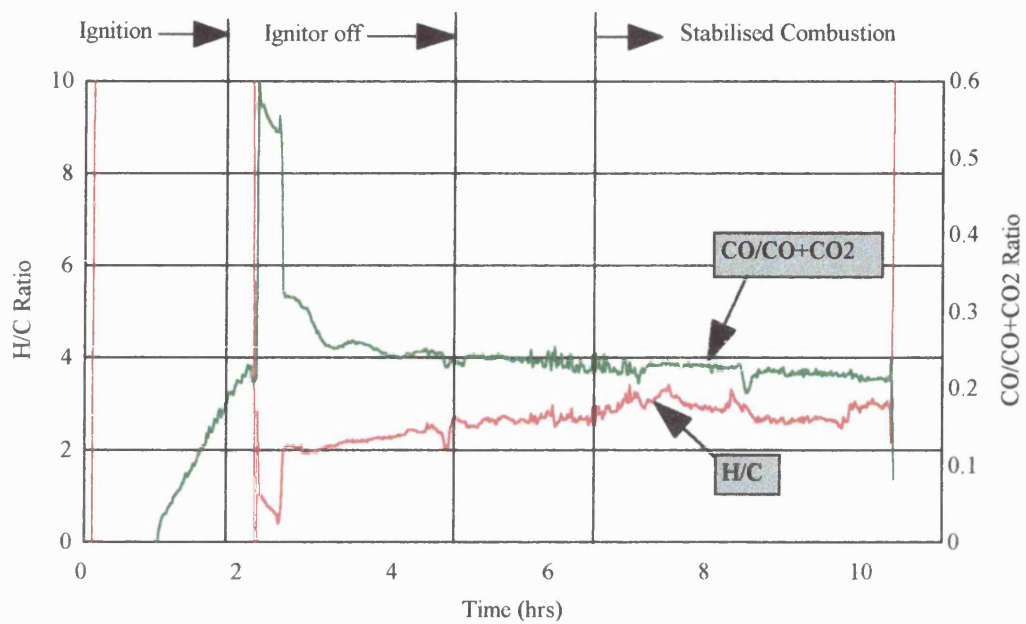


Figure 4.7 H/C and CO/CO+CO₂ ratio for Run 963 (Forties Mix 1 oil, H.W. Design)

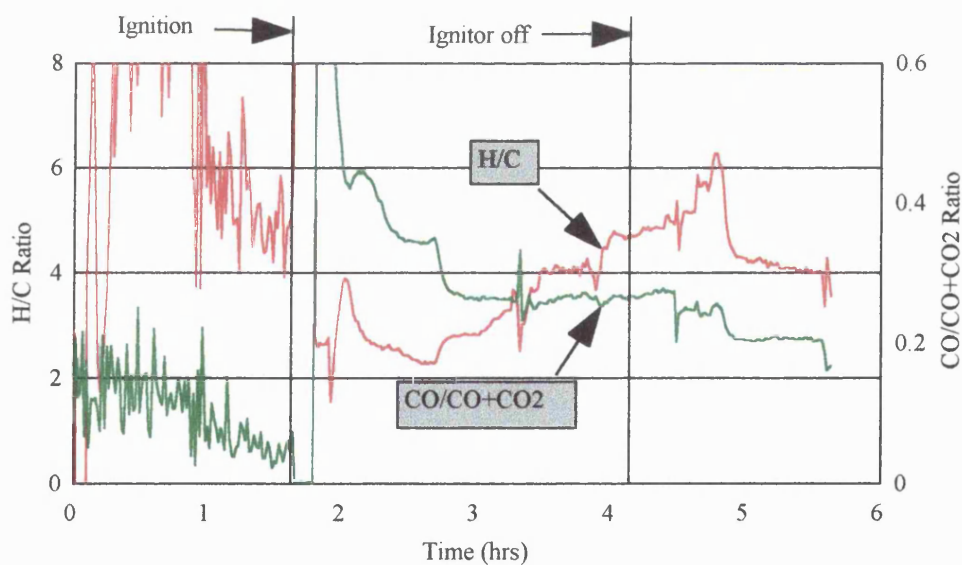


Figure 4.8 H/C and CO/CO+CO₂ ratio for Run 964 (Forties Mix 1 oil, H.W. Design 2)

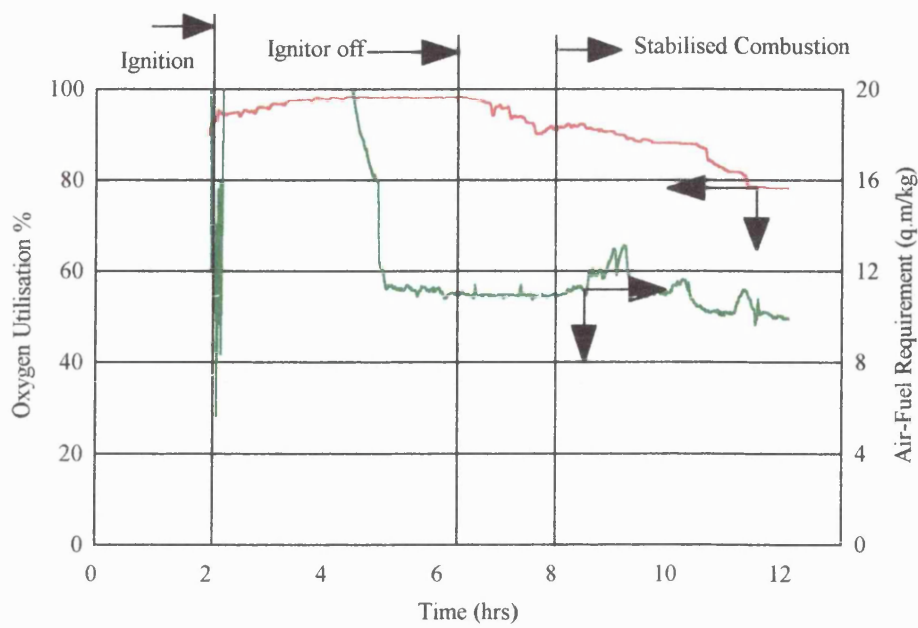


Figure 4.9 Oxygen utilisation and AFR for Run 961 (Clair oil, H.W. Design 1)

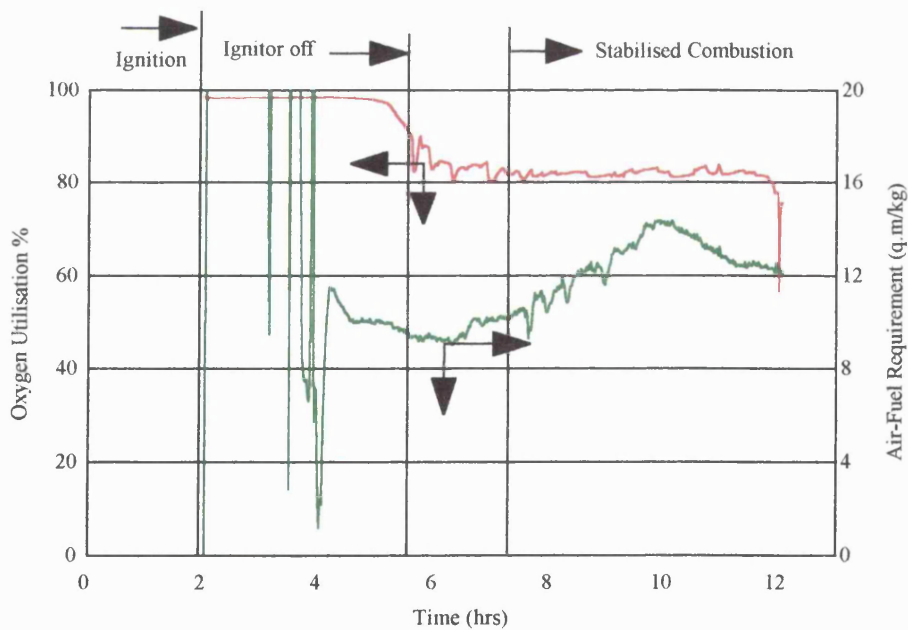


Figure 4.10 Oxygen utilisation and AFR for Run 962 (Clair oil, H.W. Design 2)

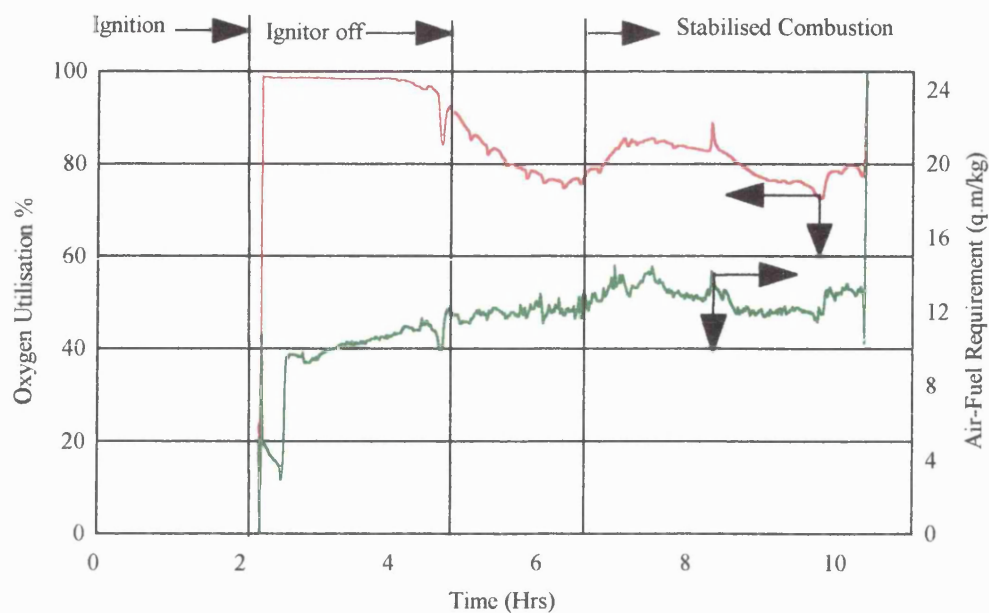


Figure 4.11 Oxygen utilisation and AFR for Run 963 (Forties Mix 1 oil, H.W. Design 1)

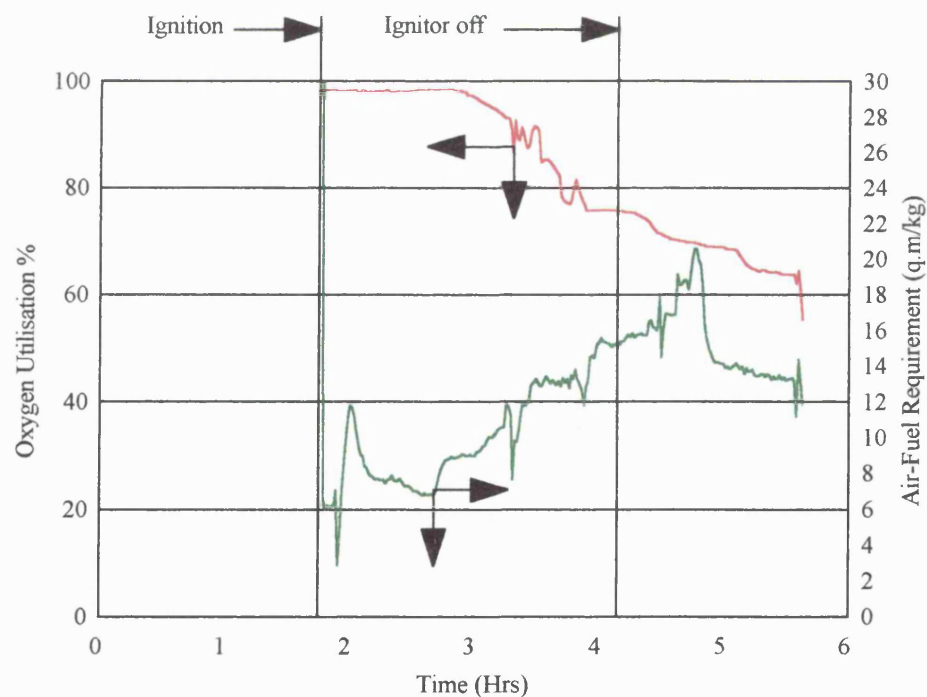


Figure 4.12 Oxygen utilisation and AFR for Run 964 (Forties Mix 1 oil, H.W. Design 2)

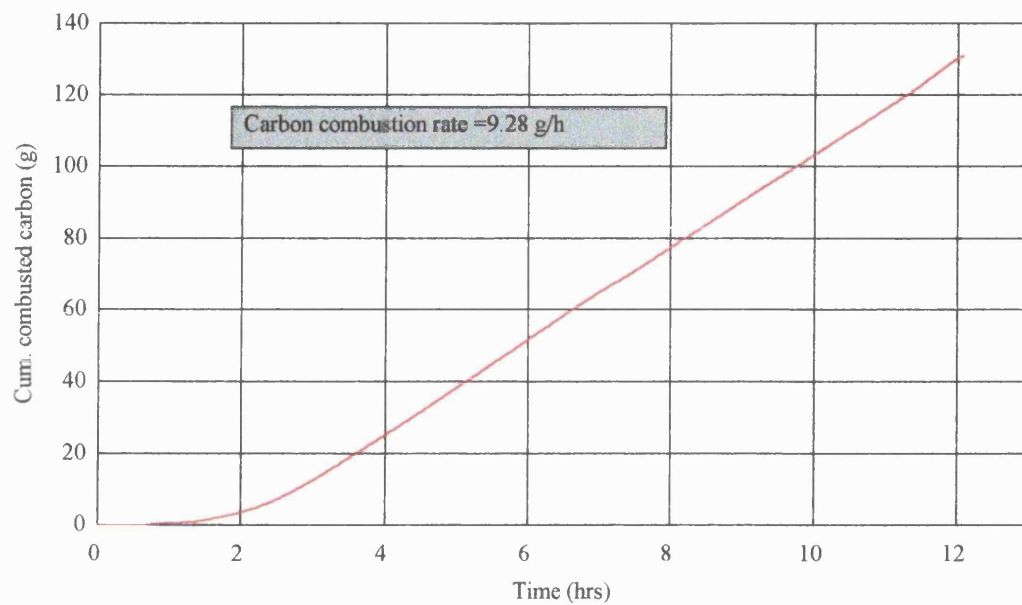


Figure 4.13 Carbon combustion rate for Run 961 (Clair oil, H.W. Design 1)

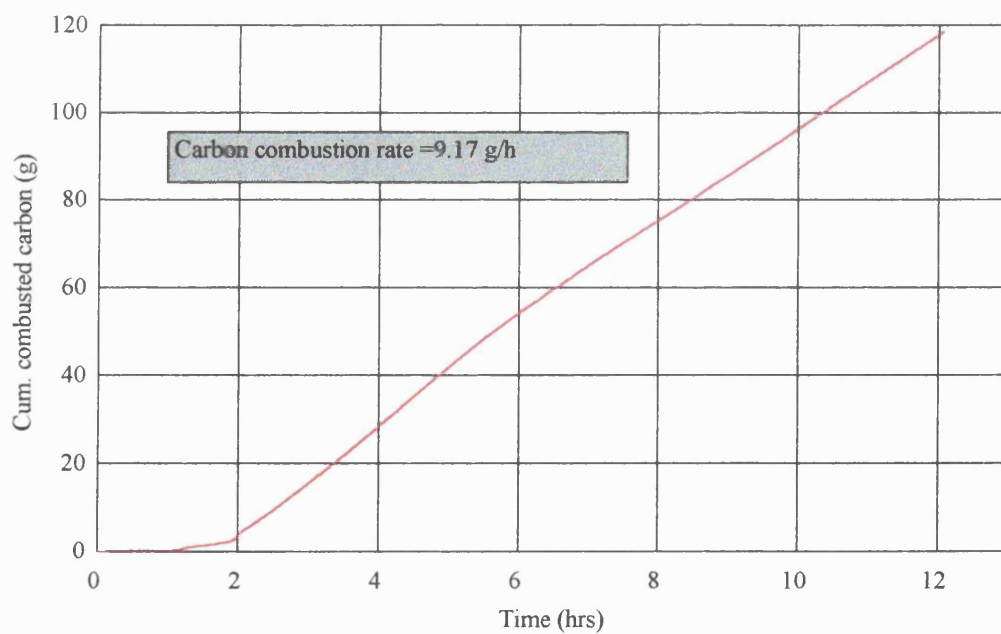


Figure 4.14 Carbon combustion rate for Run 962 (Clair oil, H.W. Design 2)

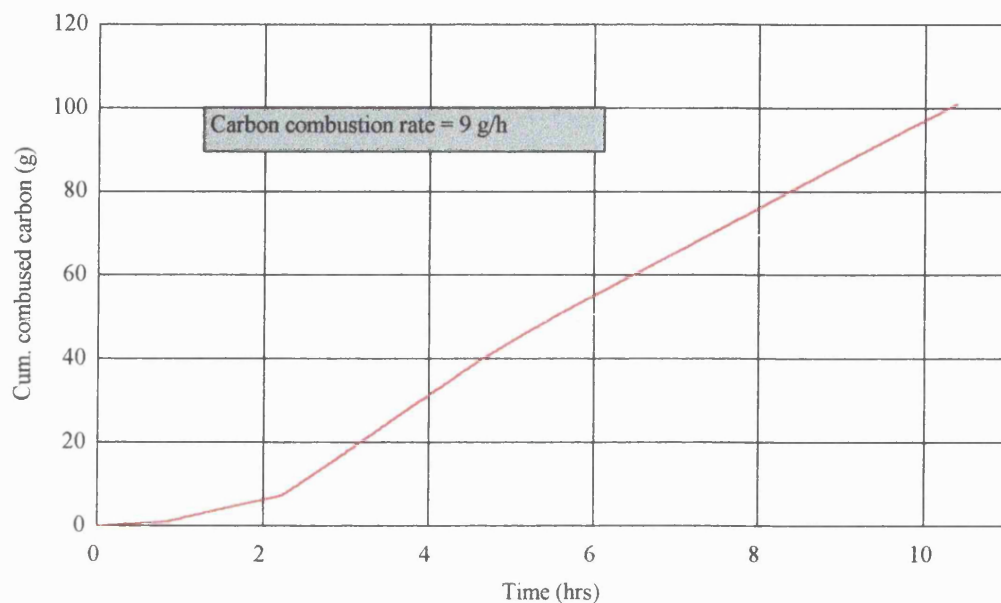


Figure 4.15 Carbon combustion rate for Run 963 (Forties Mix 1 oil, H.W. Design 1)

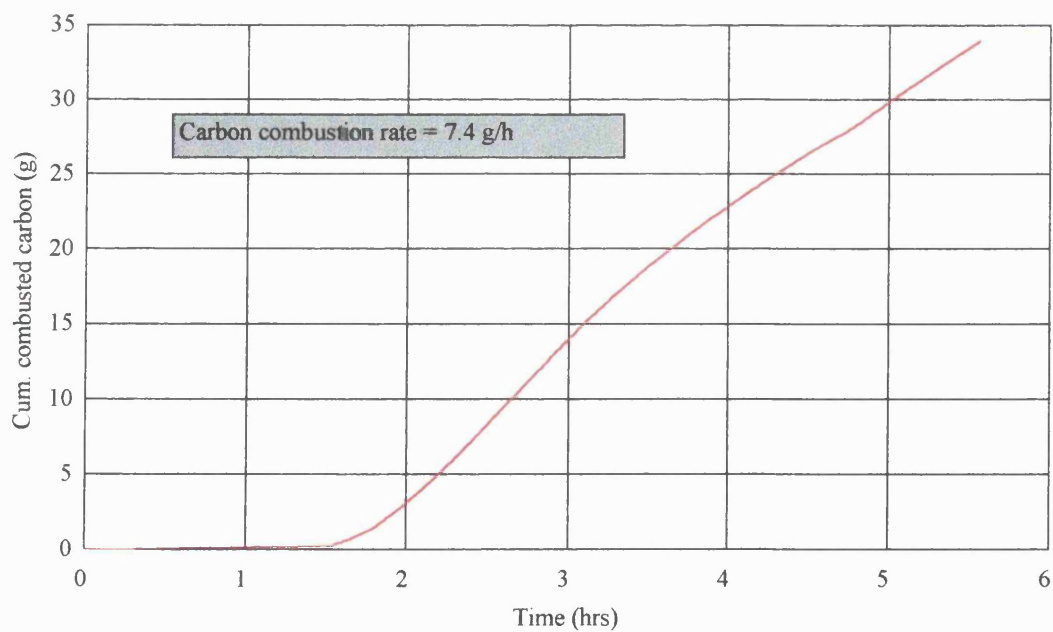


Figure 4.16 Carbon combustion rate for Run 964 (Forties Mix 1 oil, H.W. Design 2)

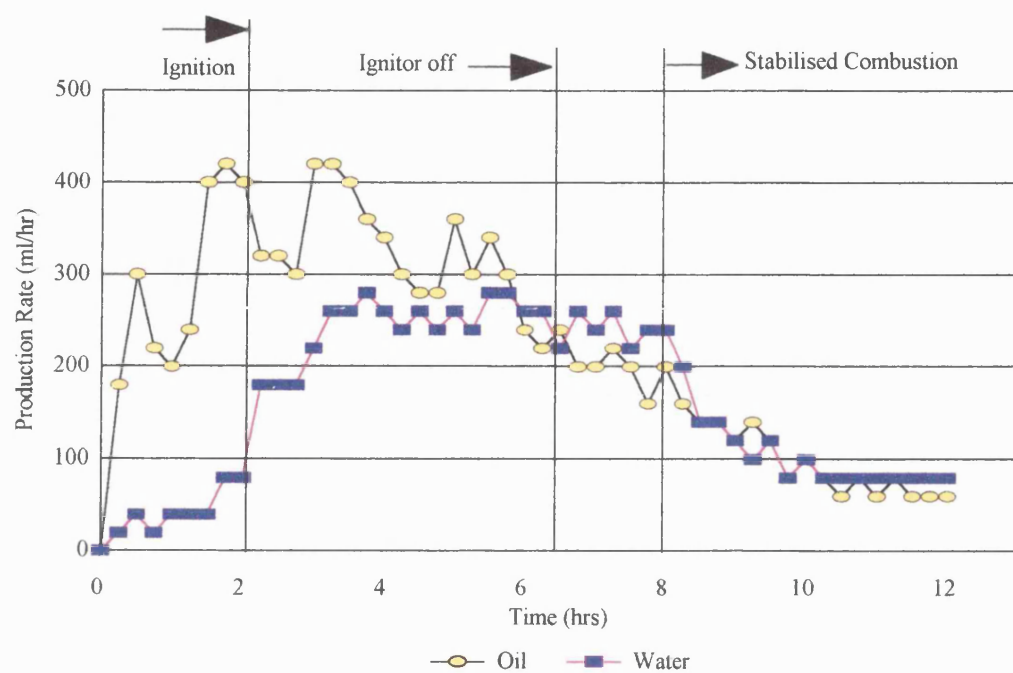


Figure 4.17 Oil and water production rate for Run 961 (Clair oil, H.W. Design 1)

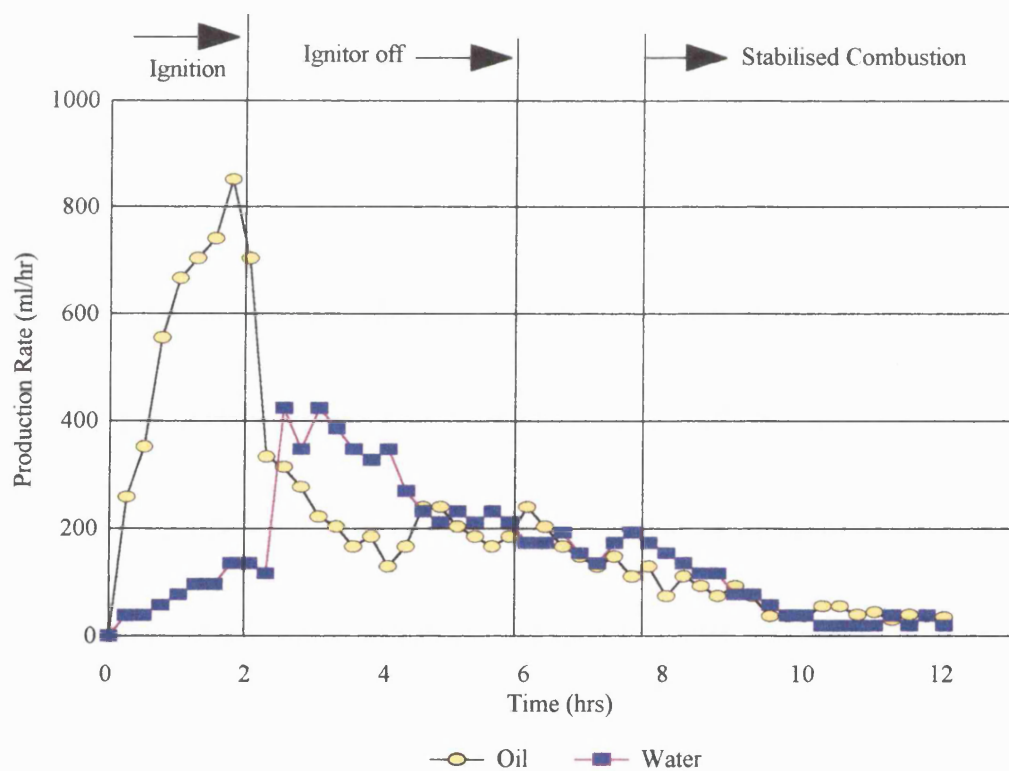


Figure 4.18 Oil and water production rate for Run 962 (Clair oil, H.W. Design 2)

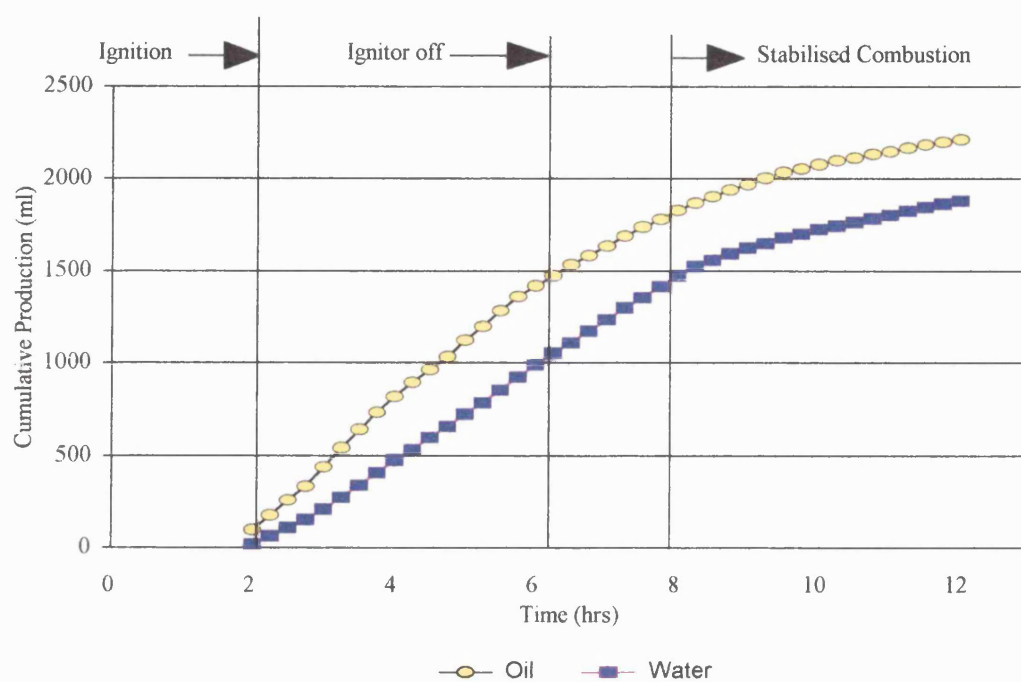


Figure 4.19 Cumulative production for Run 961 (Clair oil, H.W. Design 1)

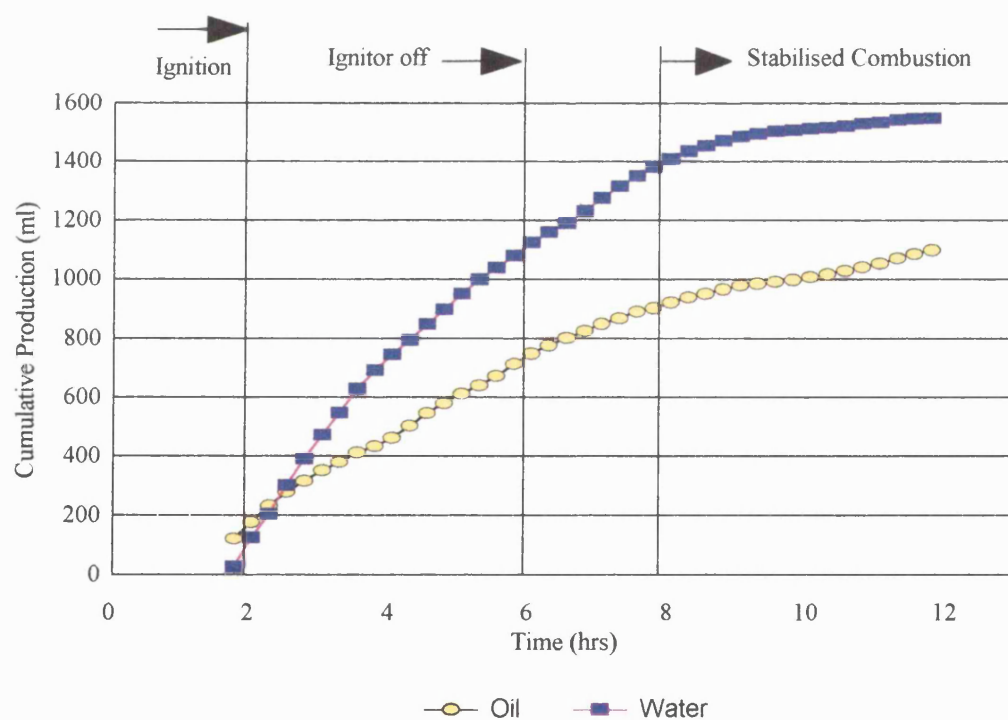


Figure 4.20 Cumulative production for Run 962 (Clair oil, H.W. Design 2)

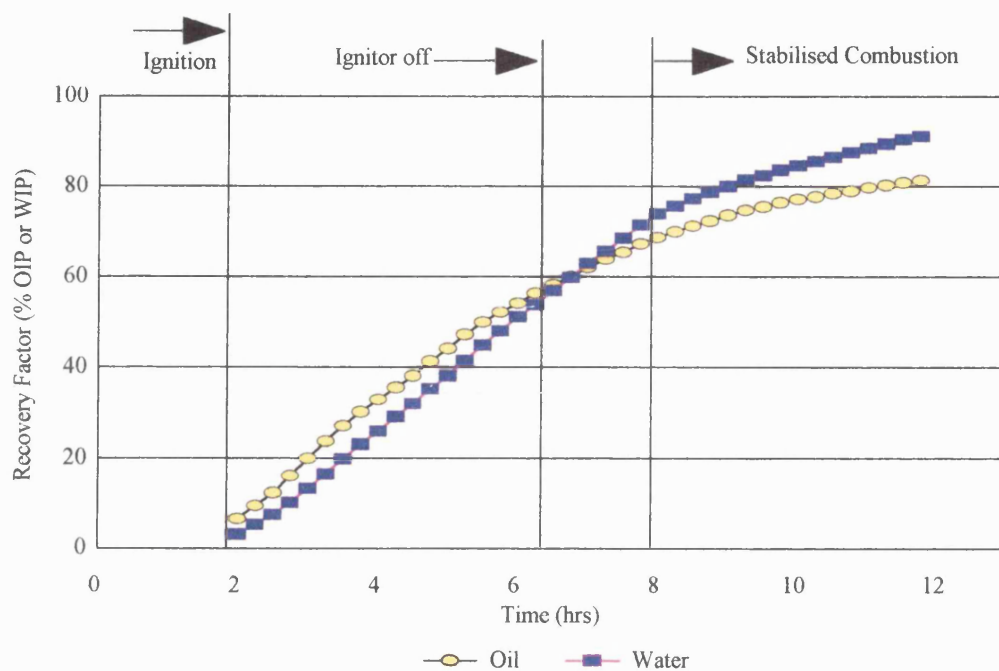


Figure 4.21 Oil and water recovery for Run 961 (Clair oil, H.W. Design 1)

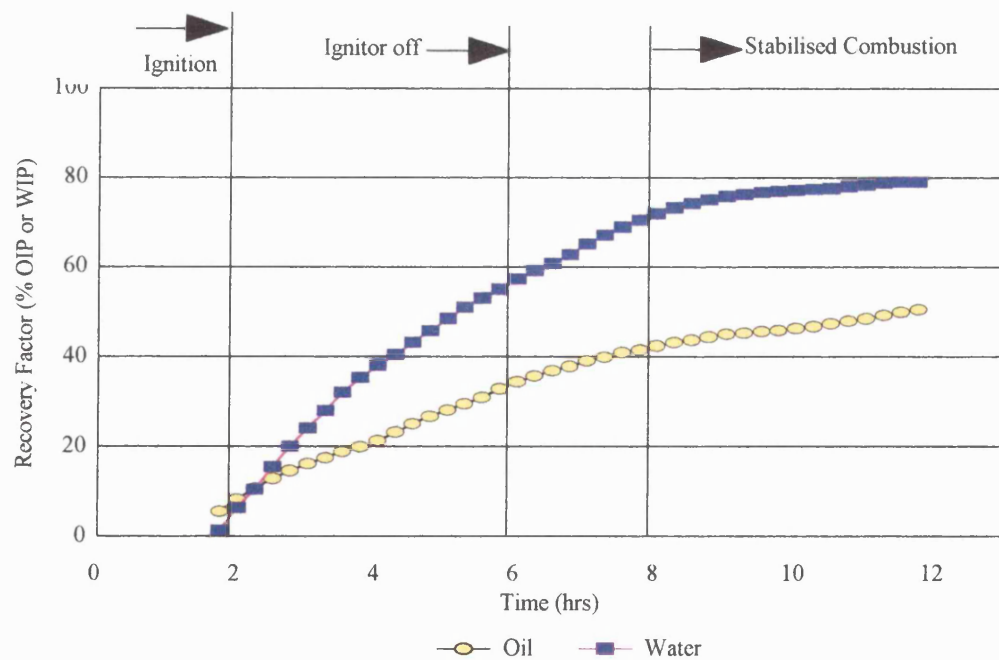


Figure 4.22 Oil and water recovery for Run 962 (Clair oil, H.W. Design 2)

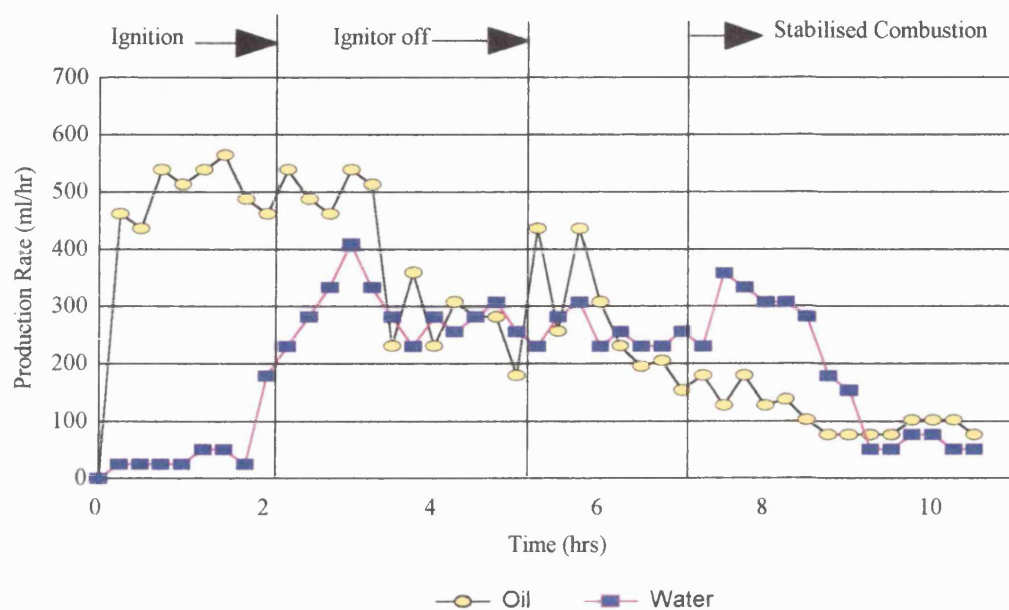


Figure 4.23 Oil and water production rate for Run 963 (Forties Mix 1 oil, H.W. Design 1)

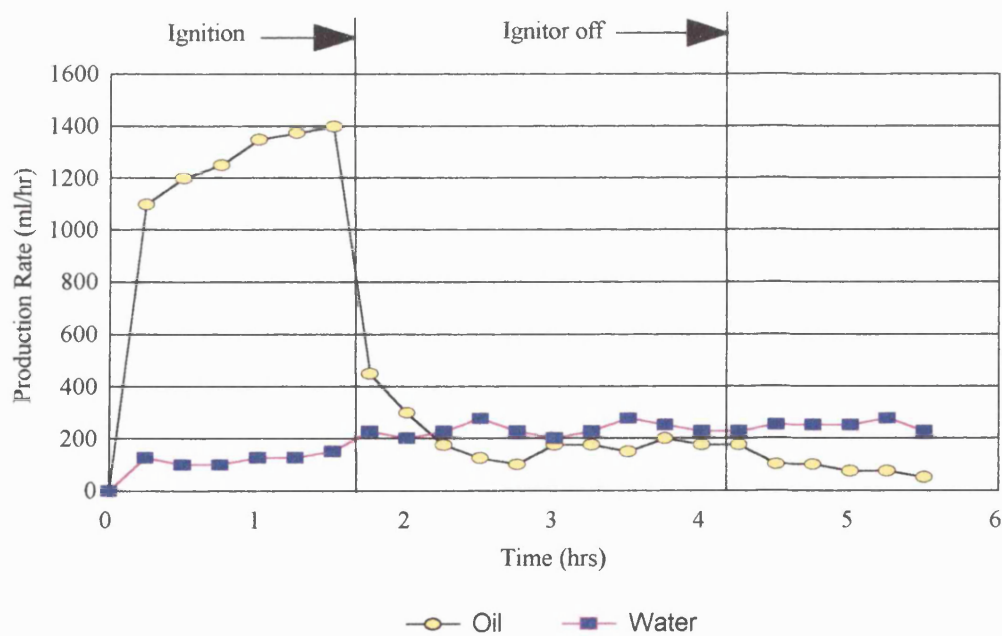


Figure 4.24 Oil and water production rate for Run 964 (Forties Mix 1 oil, H.W. Design 2)

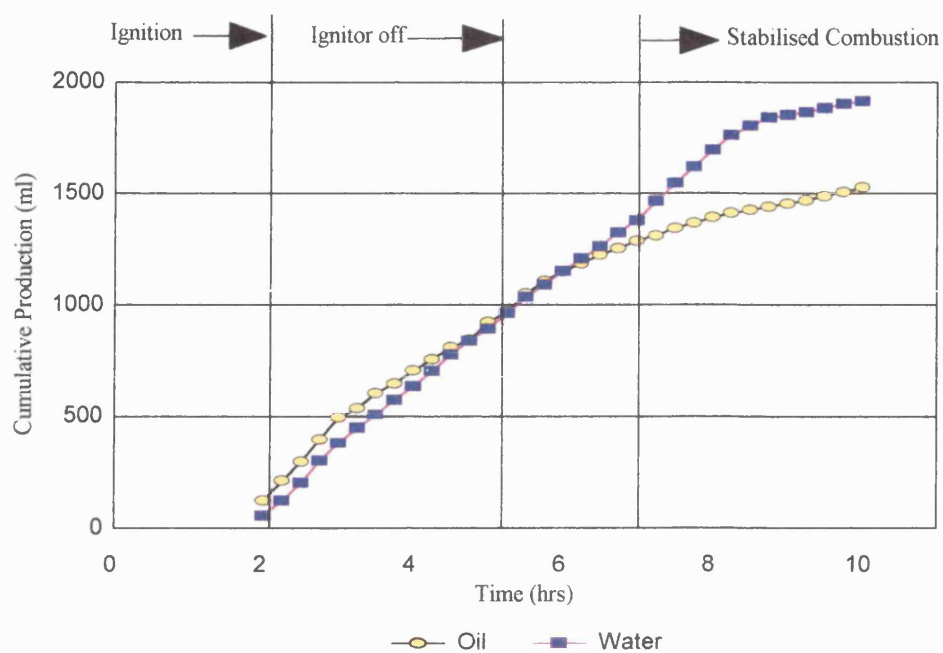


Figure 4.25 Cumulative production for Run 963 (Forties Mix1 oil, H.W. Design 1)

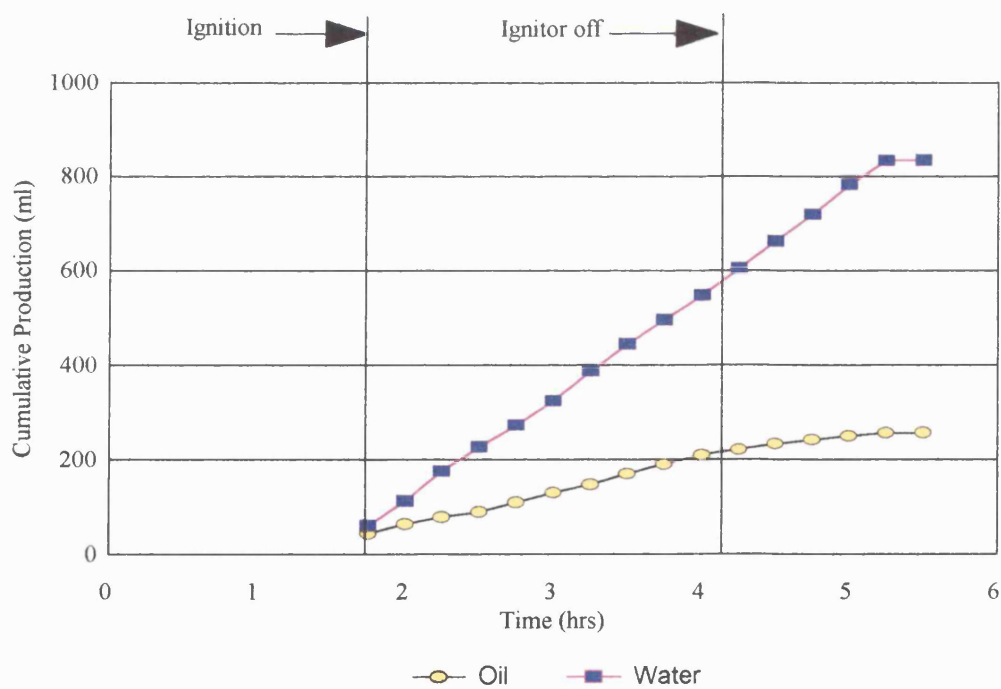


Figure 4.26 Cumulative production for Run 964 (Forties Mix1 oil, H.W. Design 2)

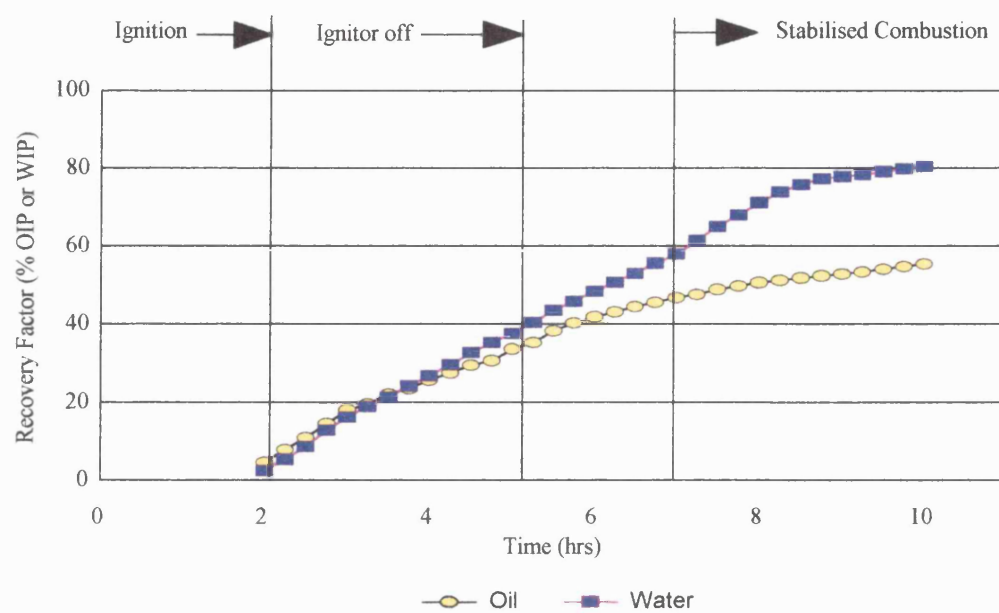


Figure 4.27 Oil and water recovery for Run 963 (Forties Mix 1 oil, H.W. Design 1)

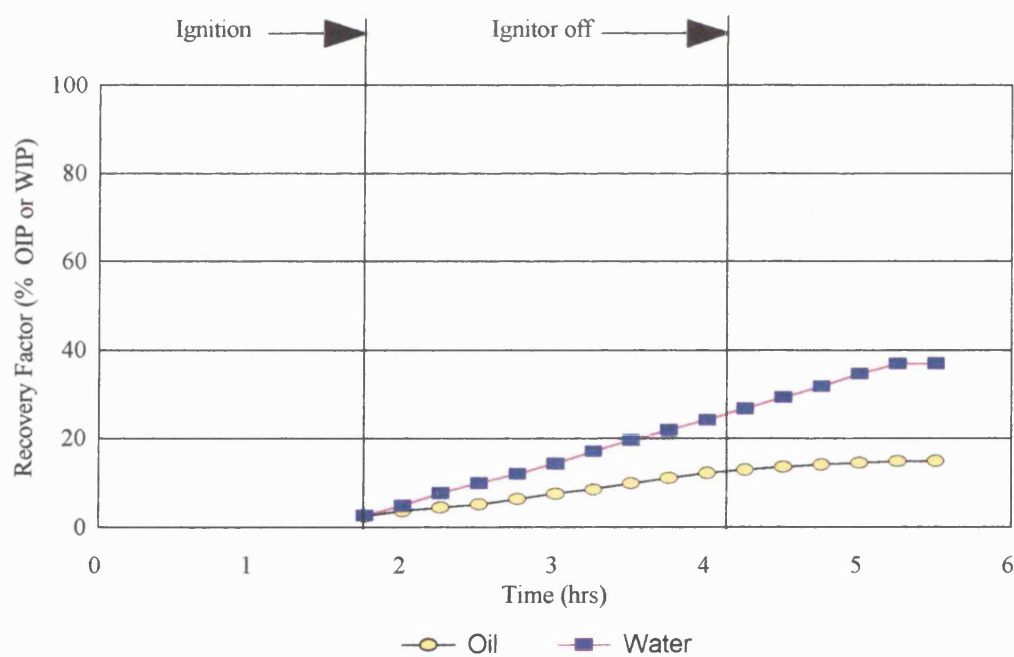


Figure 4.28 Oil and water recovery for Run 964 (Forties Mix 1 oil, H.W. Design 2)

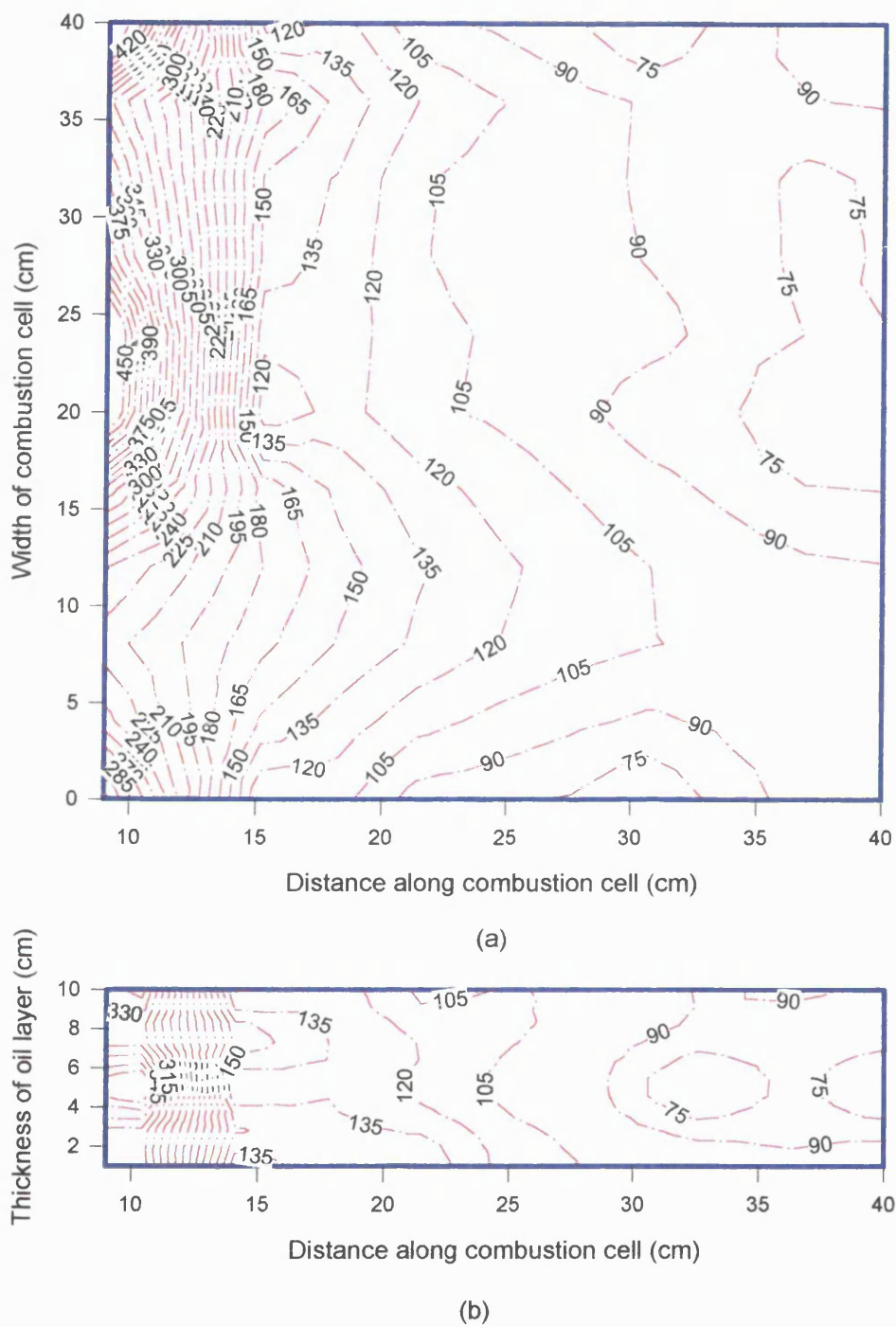


Figure 4.29 Run 961: Temperature profiles in sandpack (a) Horizontal mid-plane, (b) Vertical mid-plane. [Clair oil, H.W. Design 1]. Combustion Time = 0 minutes

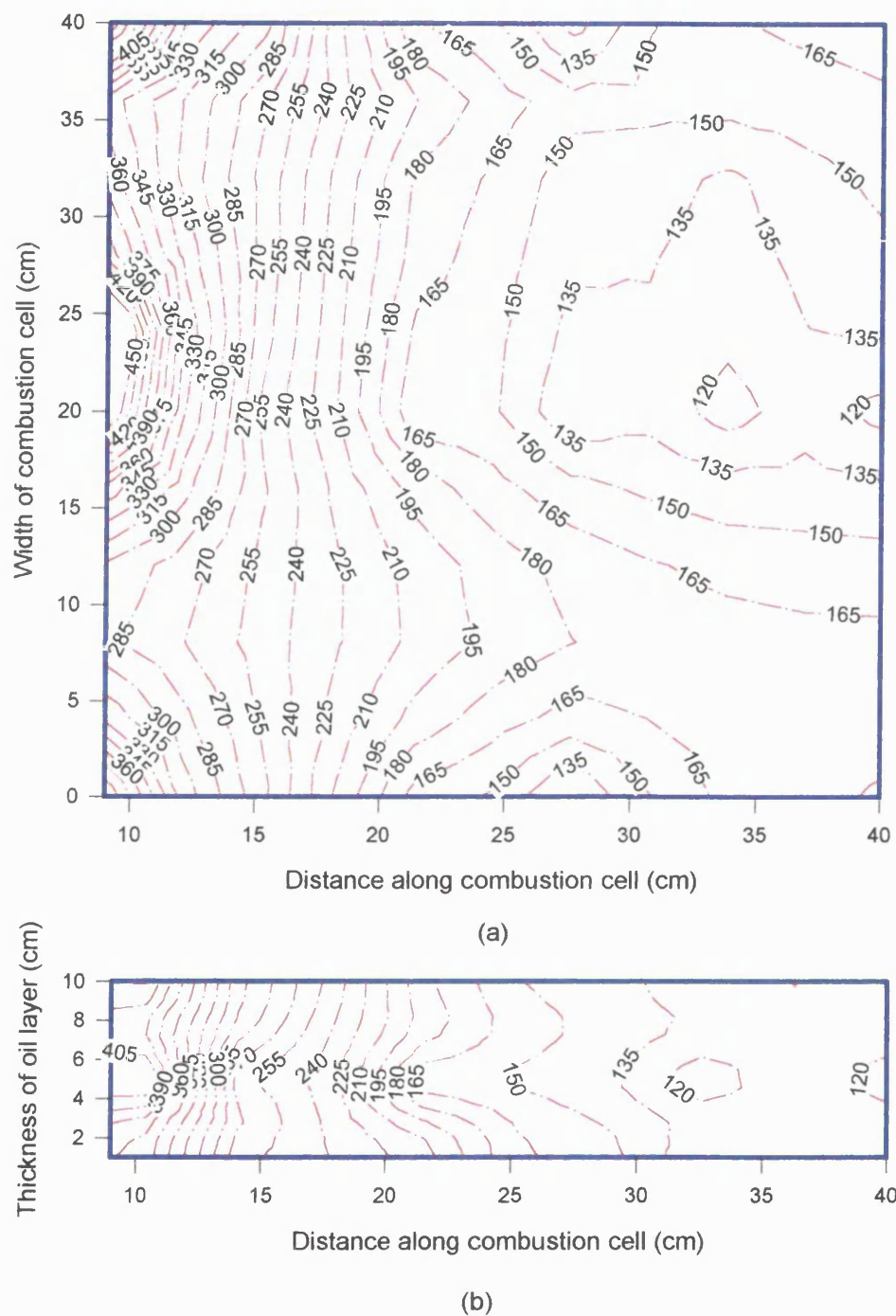
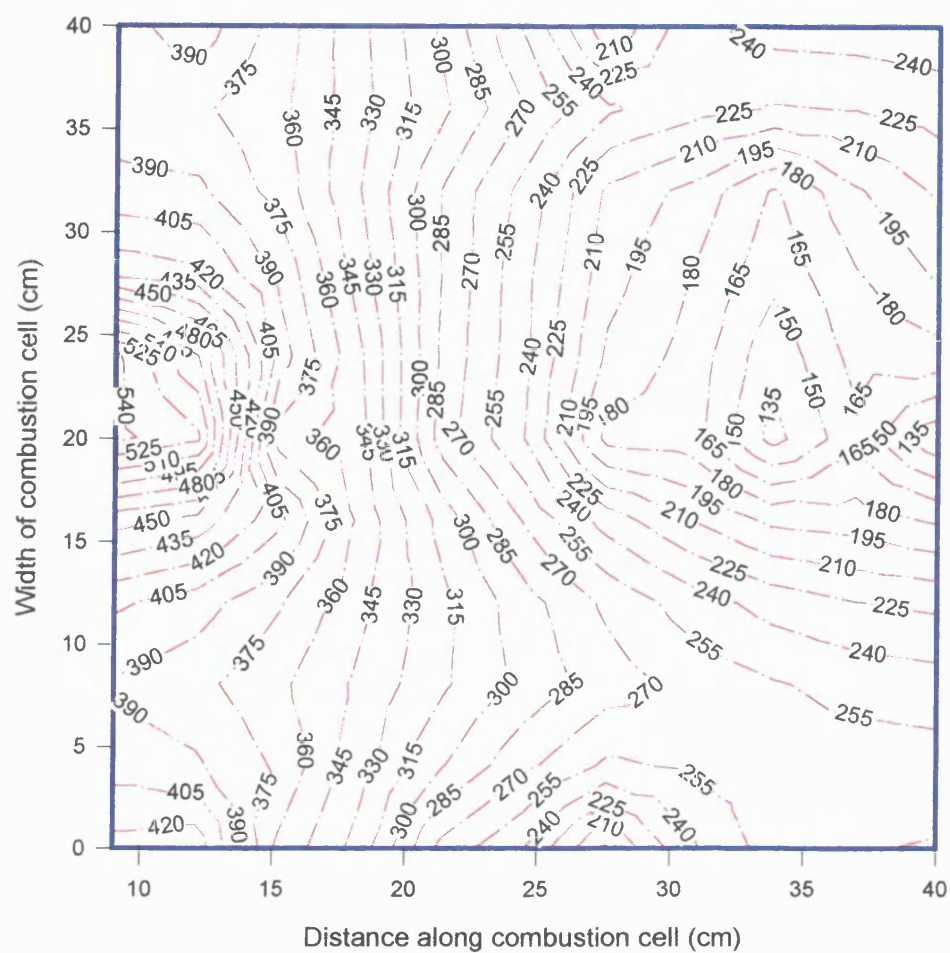
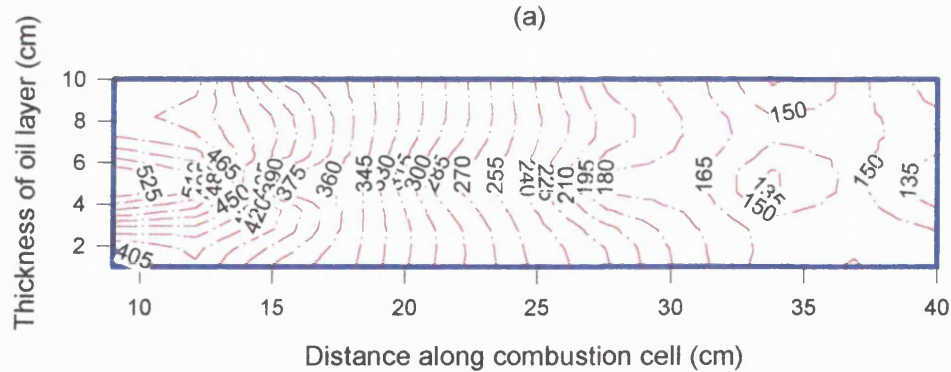


Figure 4.30 Run 961: Temperature profiles in sandpack (a) Horizontal mid-plane, (b) Vertical mid-plane. [Clair oil, H.W. Design 1]. Combustion Time = 120 minutes

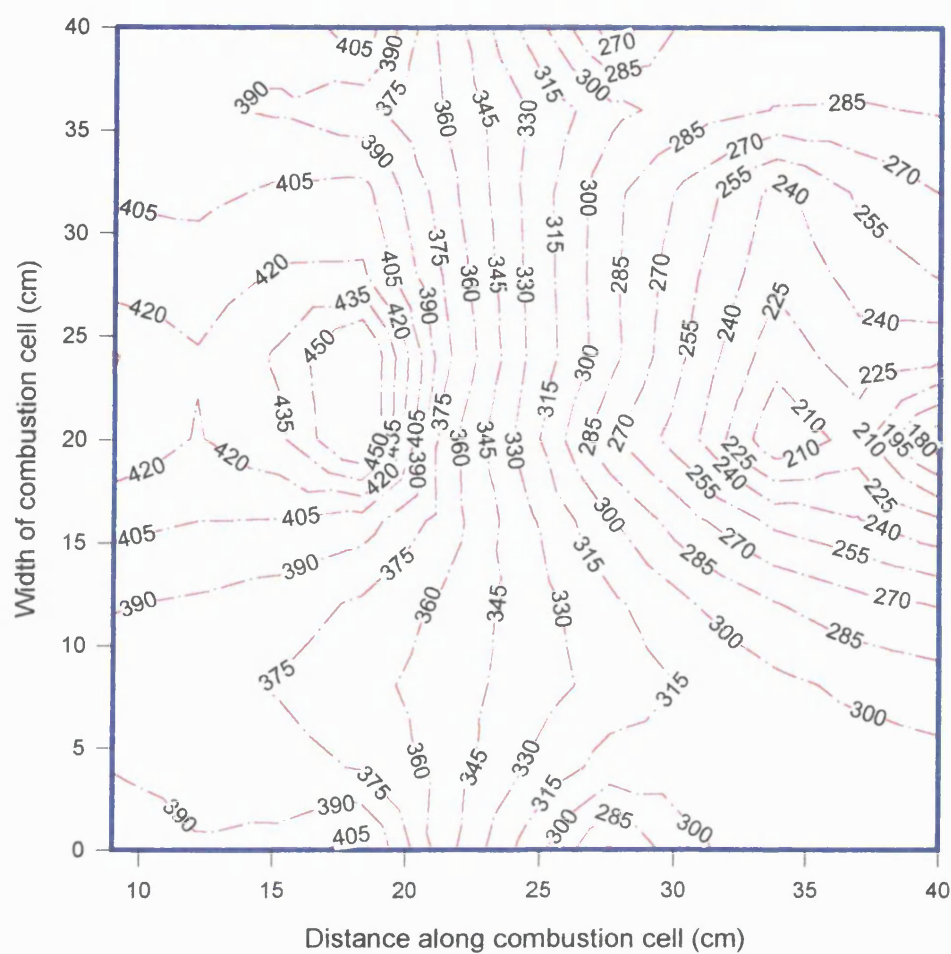


(a)

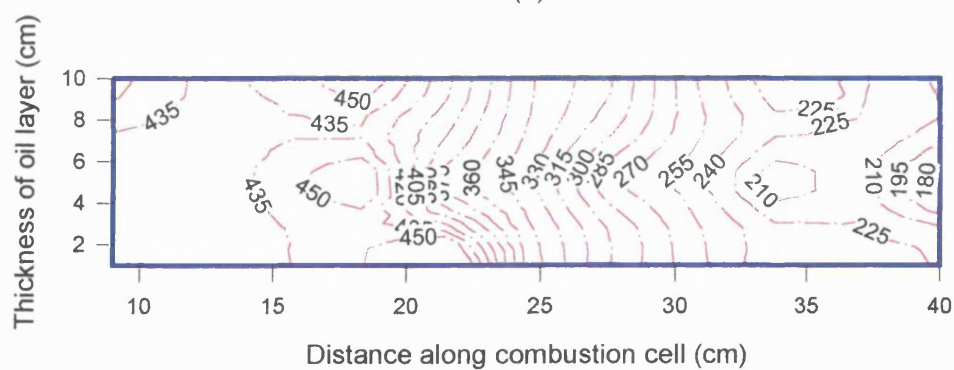


(b)

Figure 4.31 Run 961: Temperature profiles in sandpack (a) Horizontal mid-plane, (b) Vertical mid-plane. [Clair oil, H.W. Design 1]. Combustion Time = 240 minutes



(a)



(b)

Figure 4.32 Run 961: Temperature profiles in sandpack (a) Horizontal mid-plane, (b) Vertical mid-plane. [Clair oil, H.W. Design 1]. Combustion Time = 360 minutes

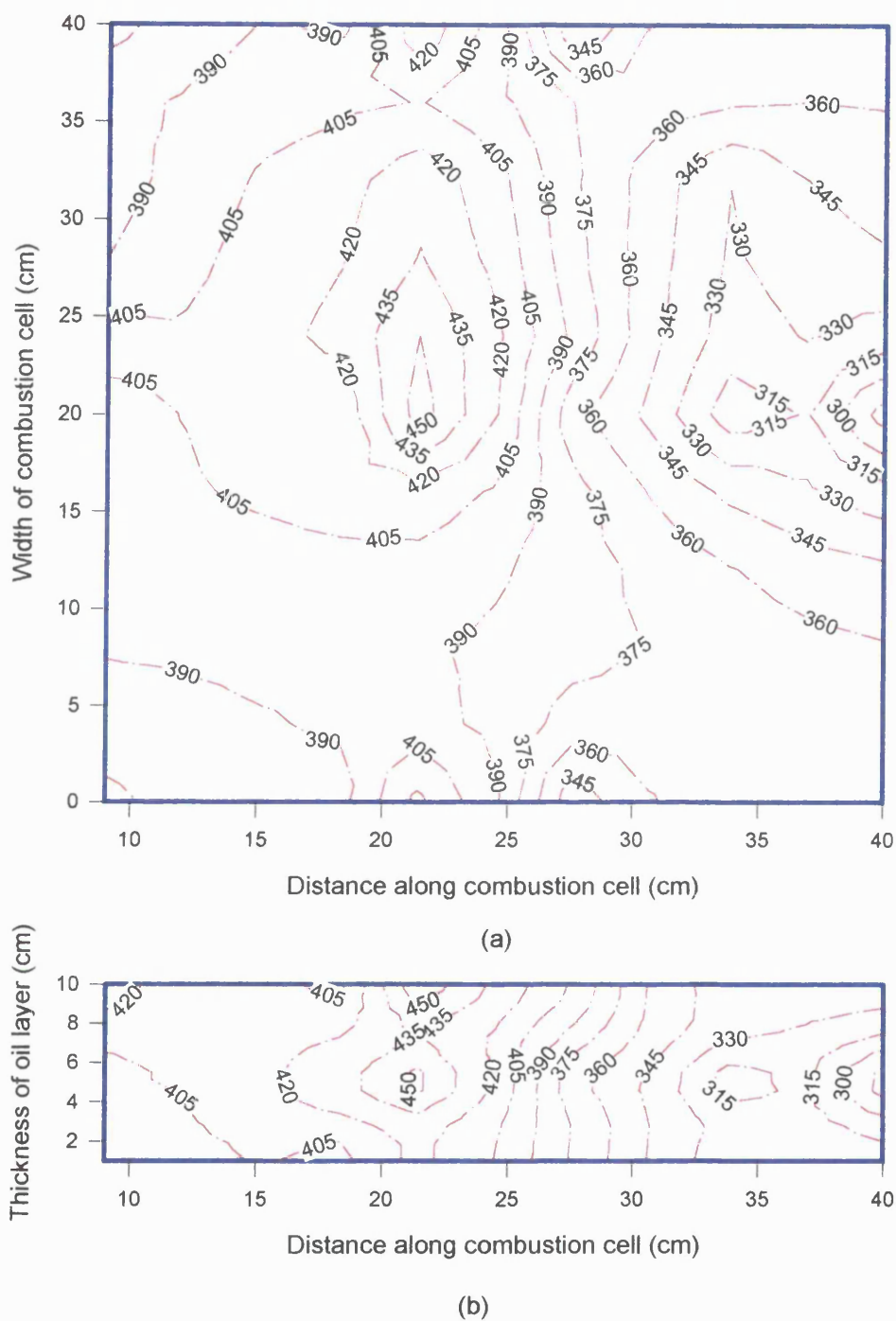
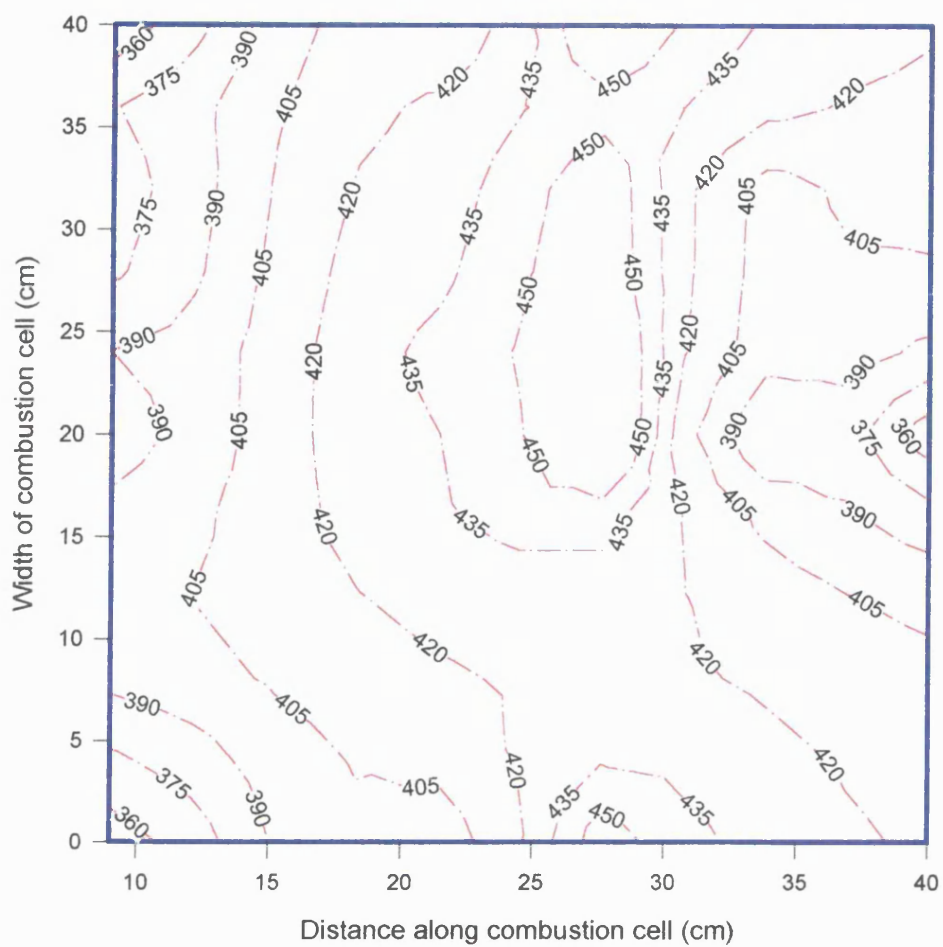
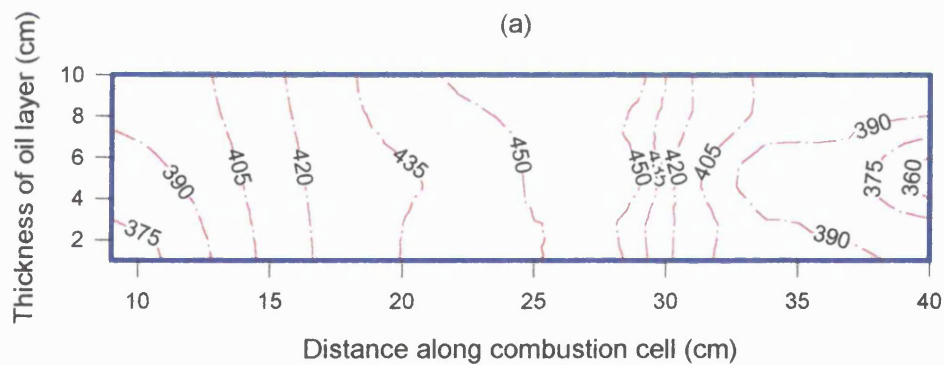


Figure 4.33 Run 961: Temperature profiles in sandpack (a) Horizontal mid-plane, (b) Vertical mid-plane. [Clair oil, H.W. Design 1]. Combustion Time = 480 minutes



(a)



(b)

Figure 4.34 Run 961: Temperature profiles in sandpack (a) Horizontal mid-plane, (b) Vertical mid-plane. [Clair oil, H.W. Design 1]. Combustion Time = 600 minutes

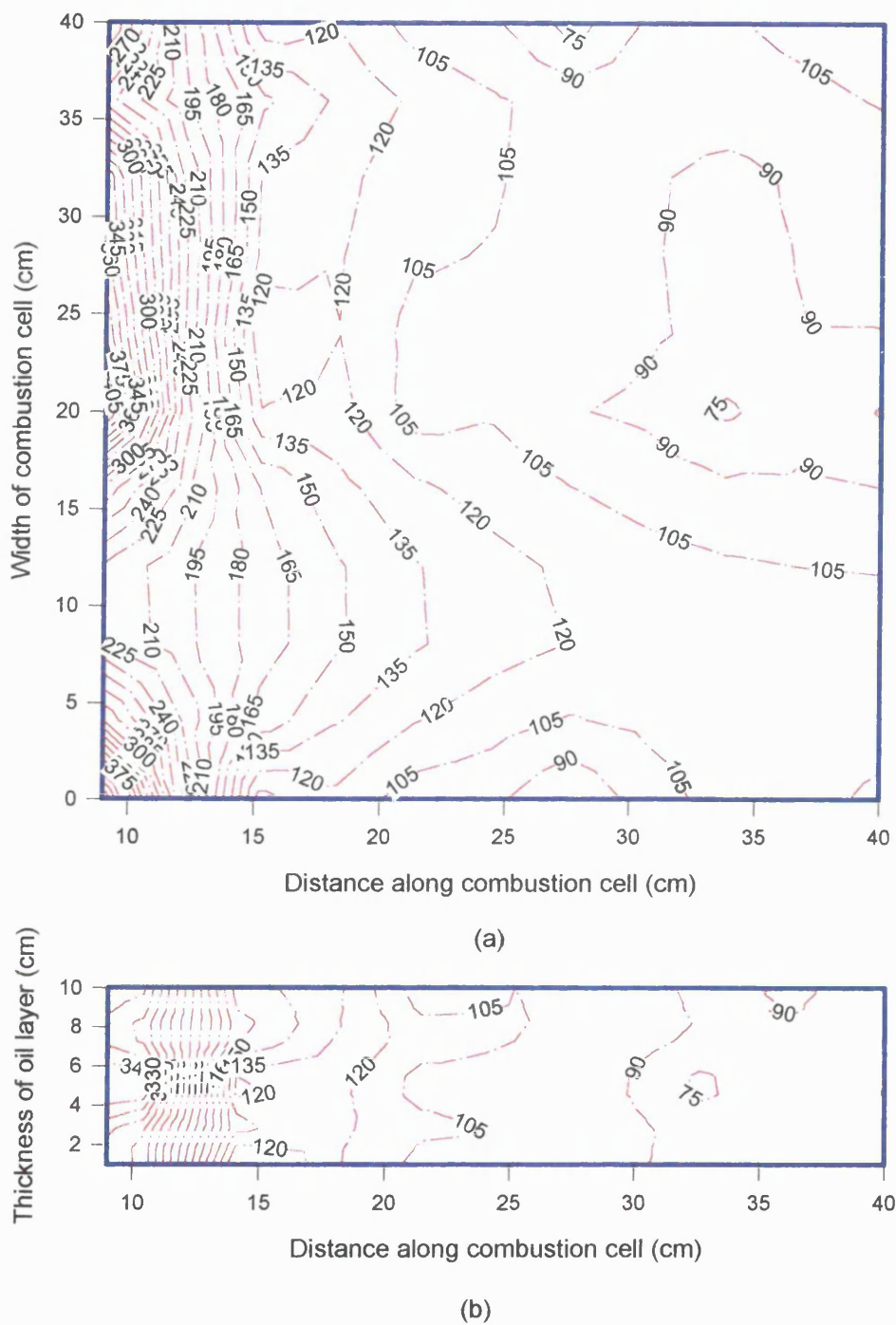


Figure 4.35 Run 962: Temperature profiles in sandpack (a) Horizontal mid-plane, (b) Vertical mid-plane. [Clair oil, H.W. Design 2]. Combustion Time = 0 minutes

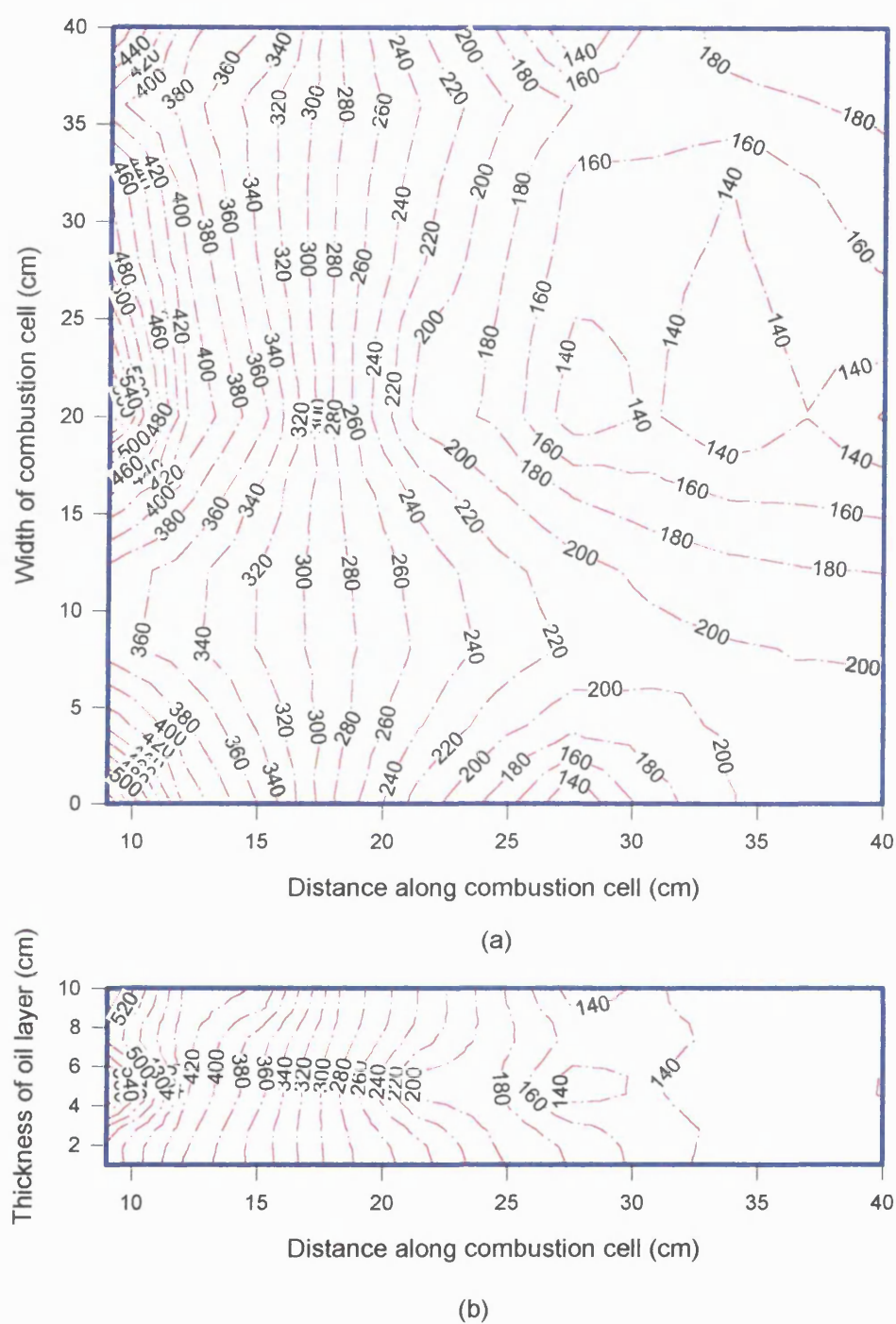
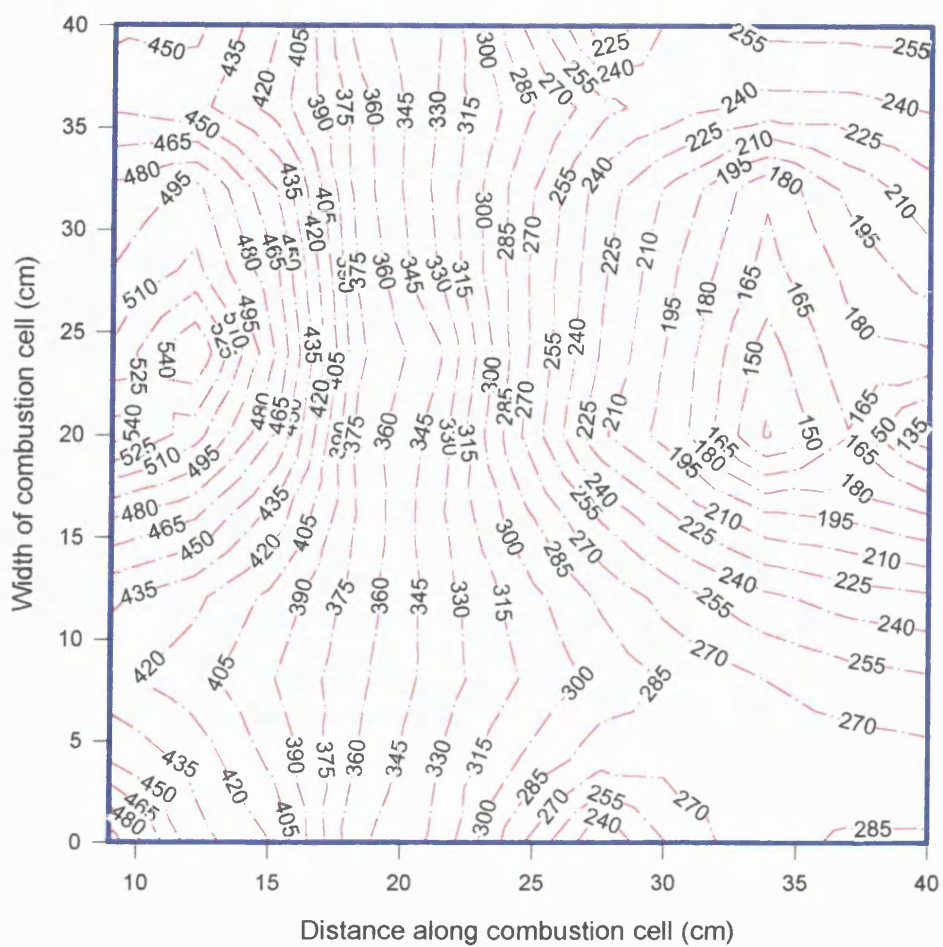
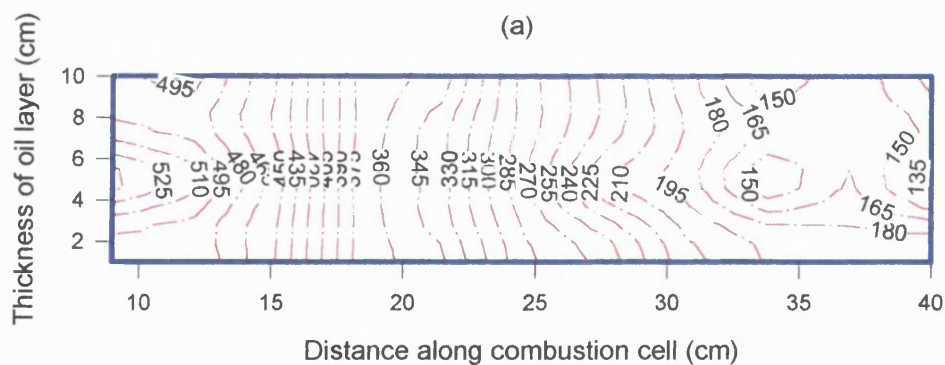


Figure 4.36 Run 962: Temperature profiles in sandpack (a) Horizontal mid-plane, (b) Vertical mid-plane. [Clair oil, H.W. Design 2]. Combustion Time = 120 minutes

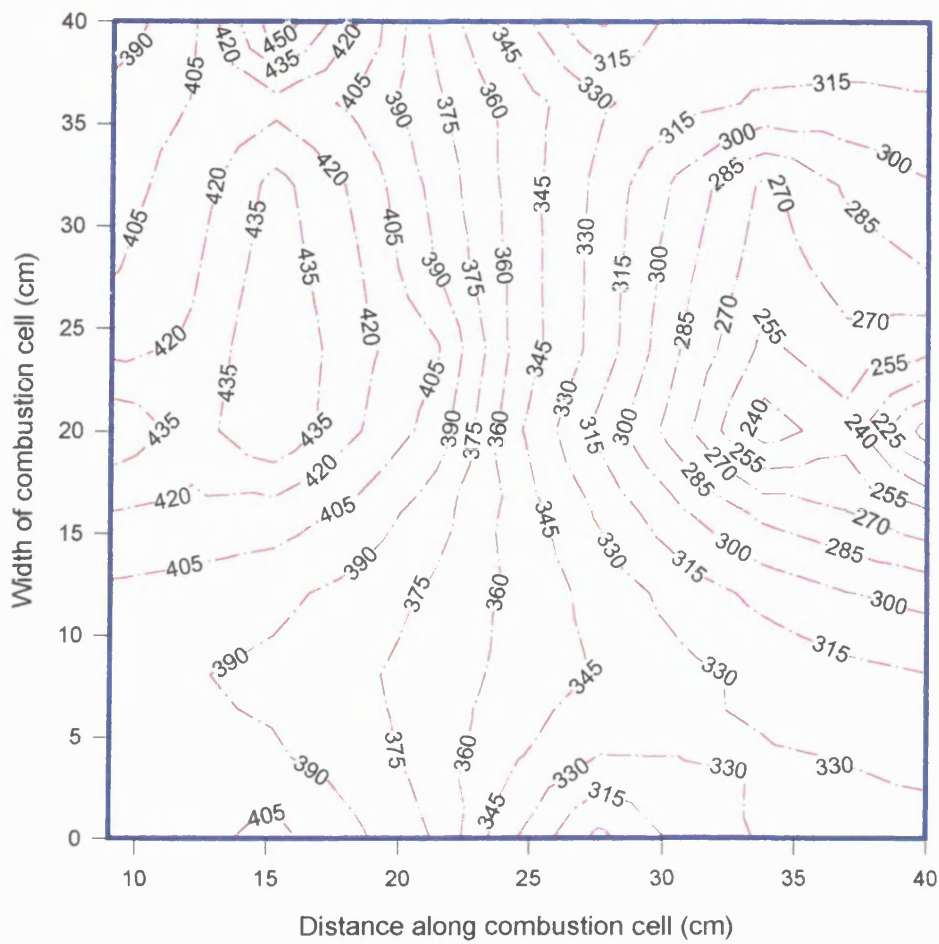


(a)

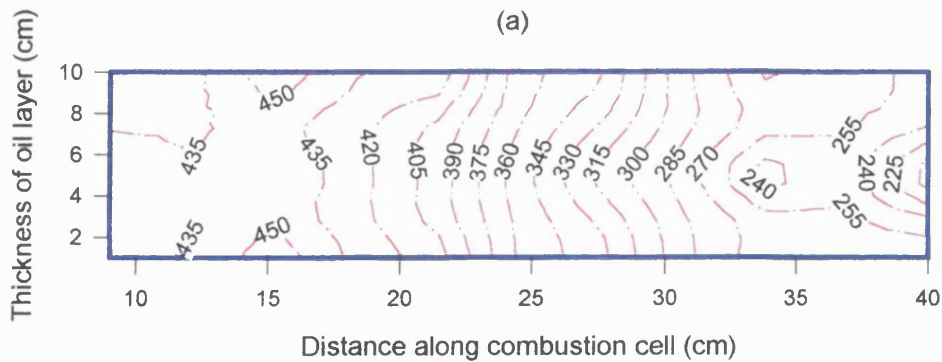


(b)

Figure 4.37 Run 962: Temperature profiles in sandpack (a) Horizontal mid-plane, (b) Vertical mid-plane. [Clair oil, H.W. Design 2]. Combustion Time = 240 minutes

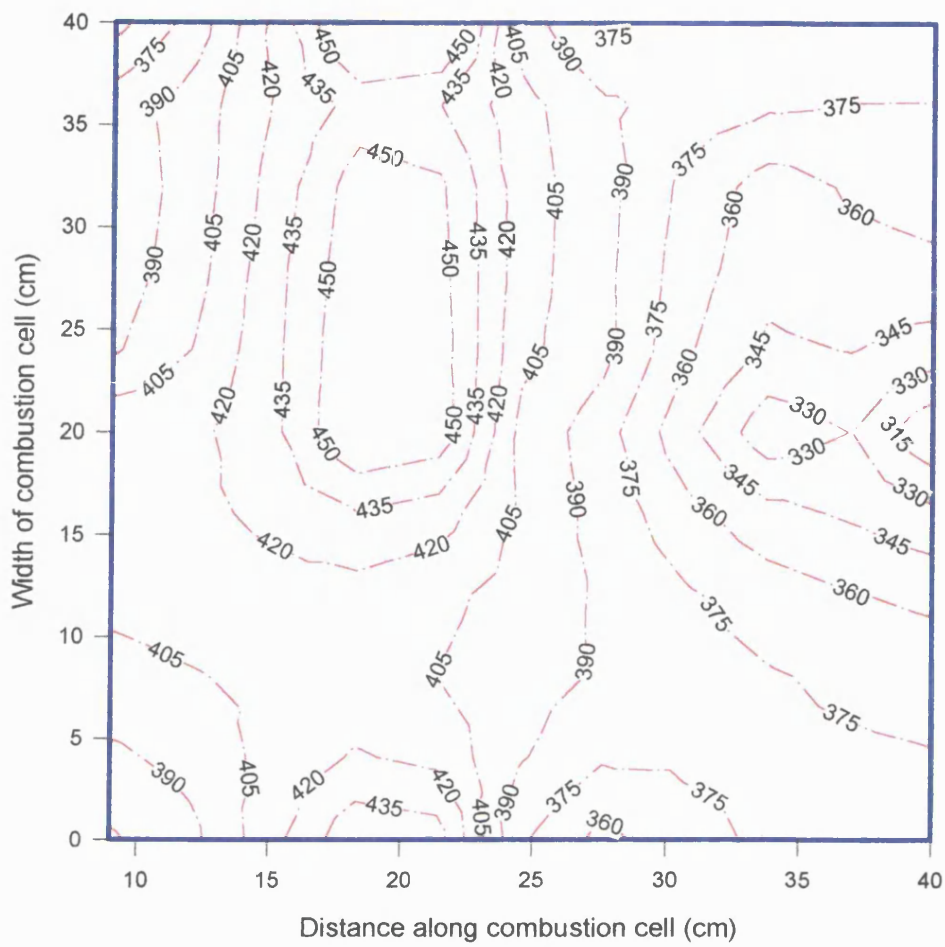


(a)

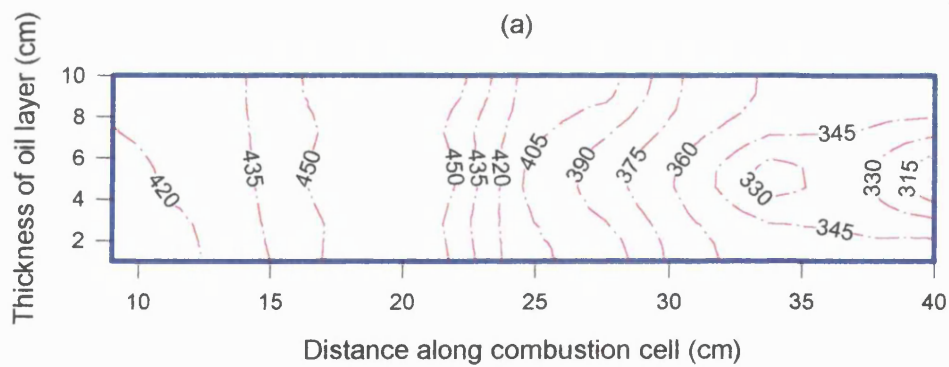


(b)

Figure 4.38 Run 962: Temperature profiles in sandpack (a) Horizontal mid-plane, (b) Vertical mid-plane. [Clair oil, H.W. Design 2]. Combustion Time = 360 minutes



(a)



(b)

Figure 4.39 Run 962: Temperature profiles in sandpack (a) Horizontal mid-plane, (b) Vertical mid-plane. [Clair oil, H.W. Design 2]. Combustion Time = 480 minutes

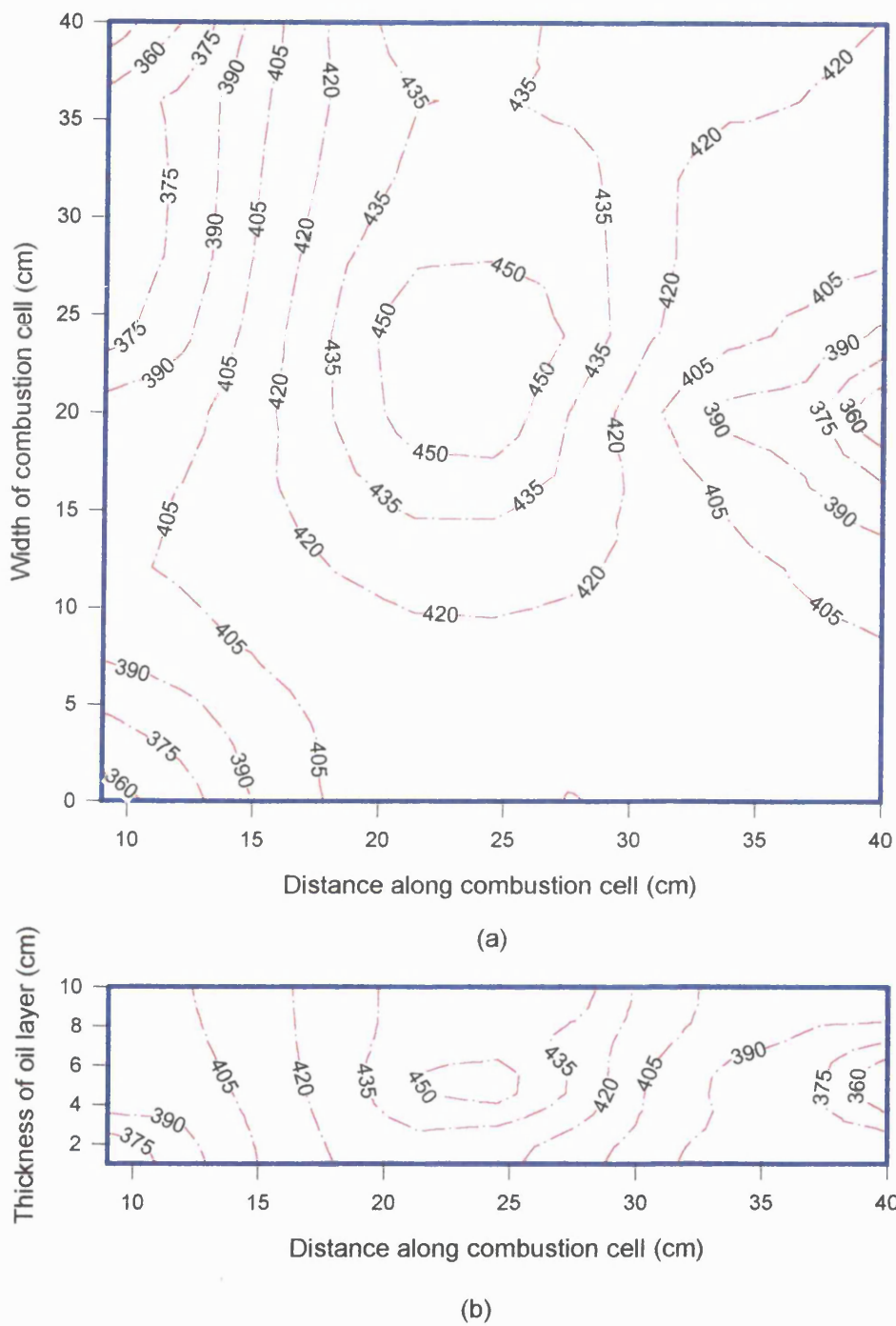
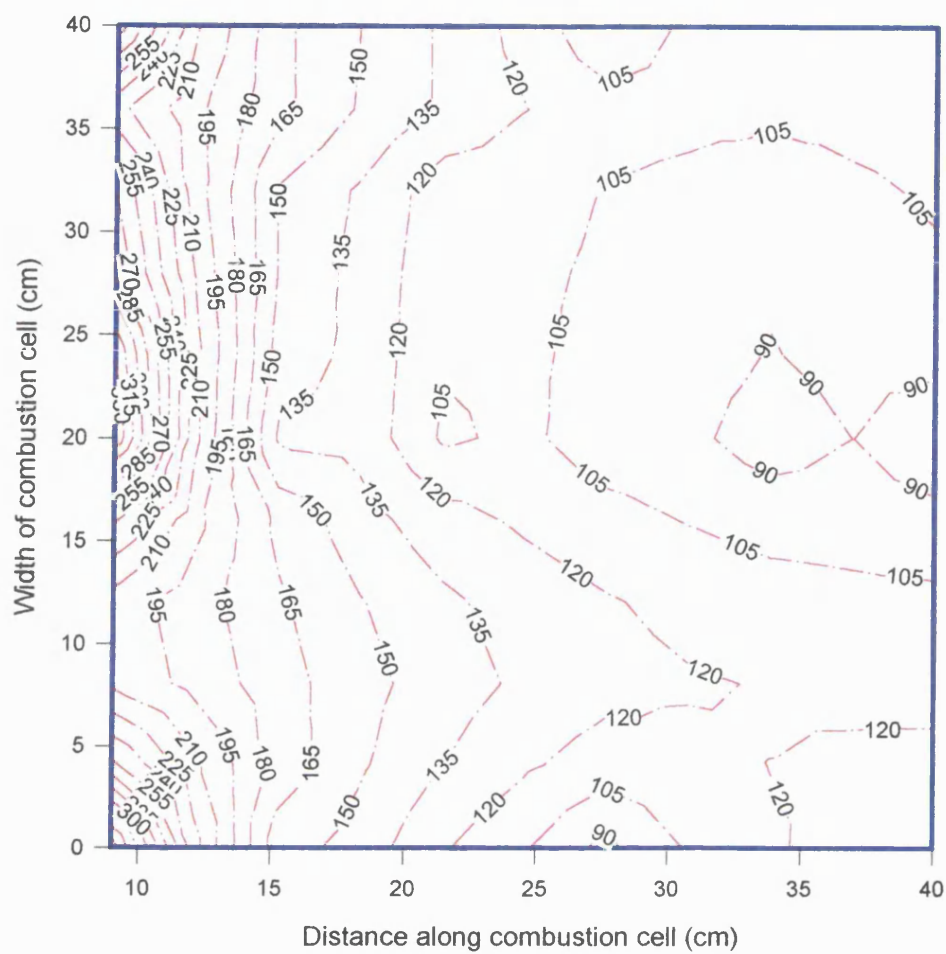
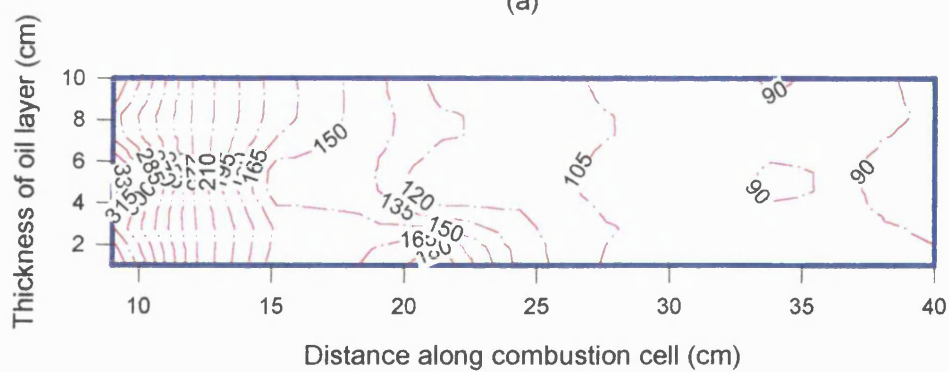


Figure 4.40 Run 962: Temperature profiles in sandpack (a) Horizontal mid-plane, (b) Vertical mid-plane. [Clair oil, H.W. Design 2]. Combustion Time = 600 minutes

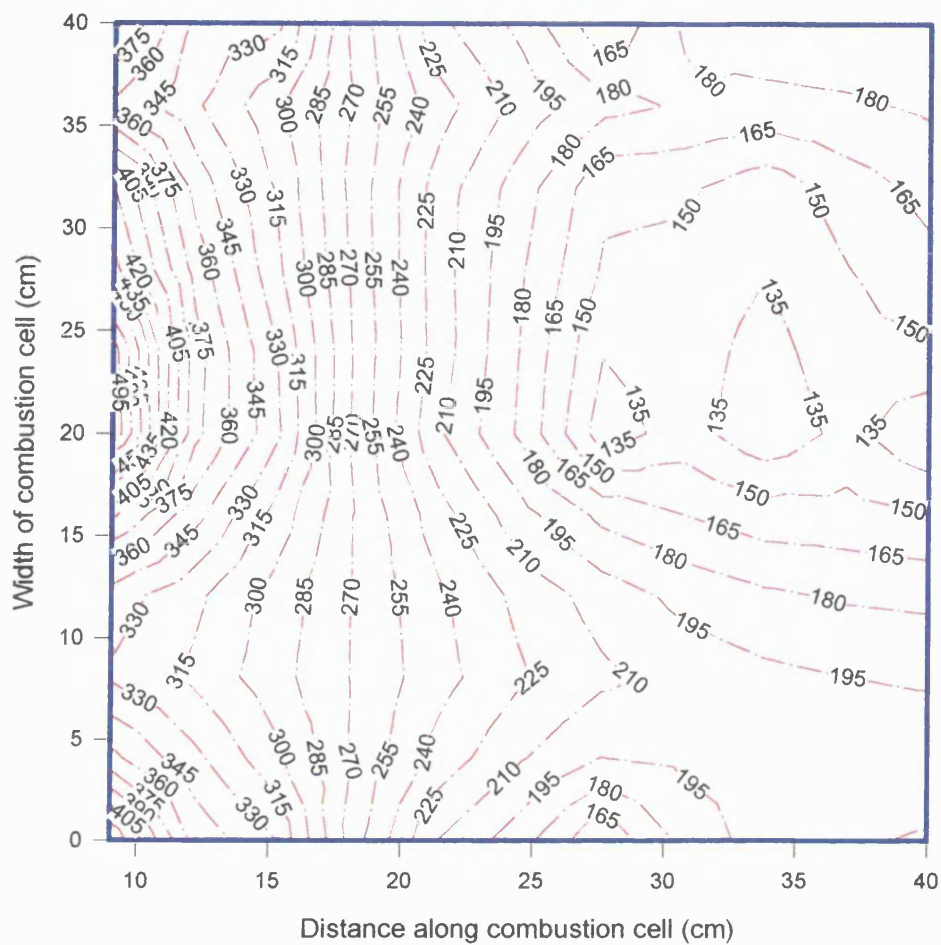


(a)

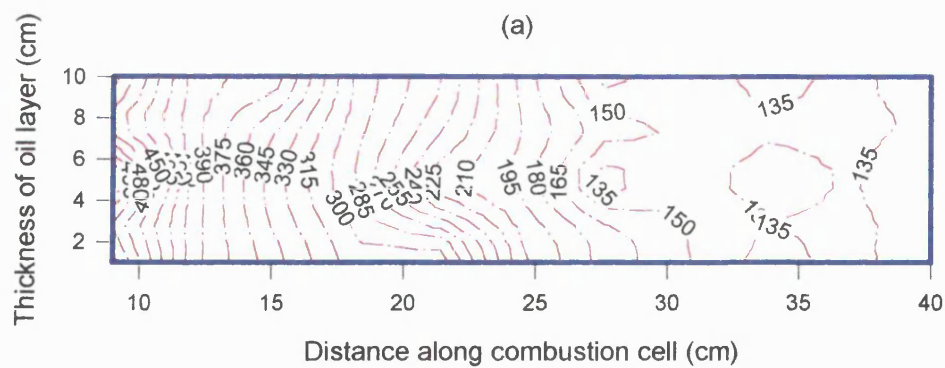


(b)

Figure 4.41 Run 963: Temperature profiles in sandpack (a) Horizontal mid-plane, (b) Vertical mid-plane. [Forties Mix 1 oil, H.W. Design 1]. Combustion Time = 0 minutes

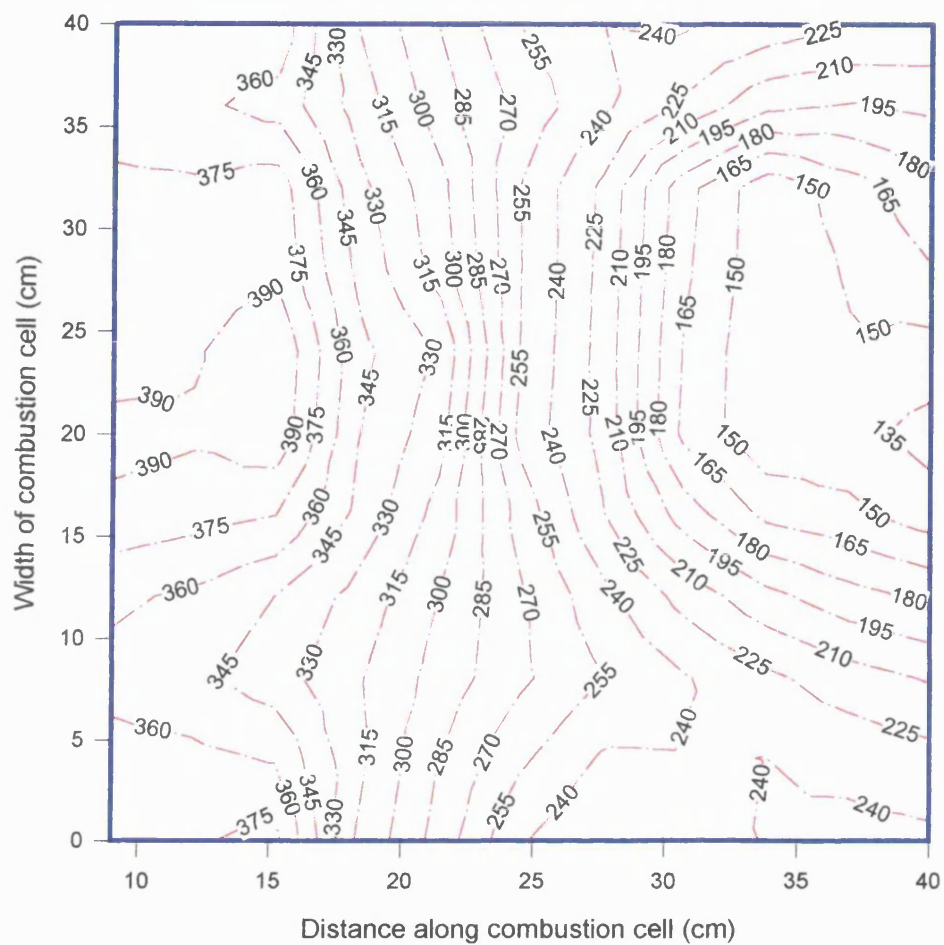


(a)

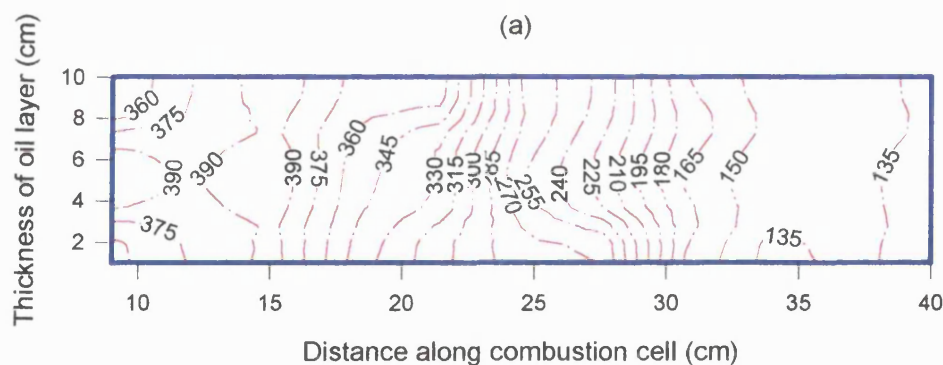


(b)

Figure 4.42 Run 963: Temperature profiles in sandpack (a) Horizontal mid-plane, (b) Vertical mid-plane. [Forties Mix 1 oil, H.W. Design 1]. Combustion Time = 120 minutes

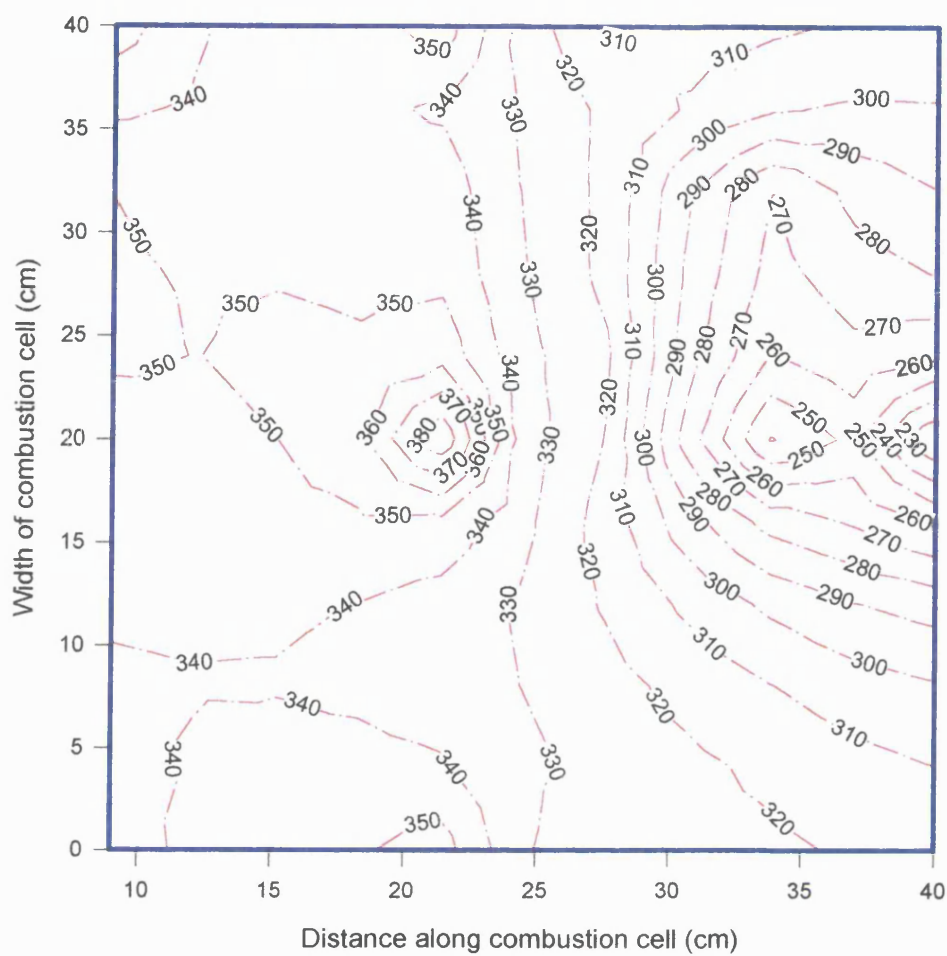


(a)

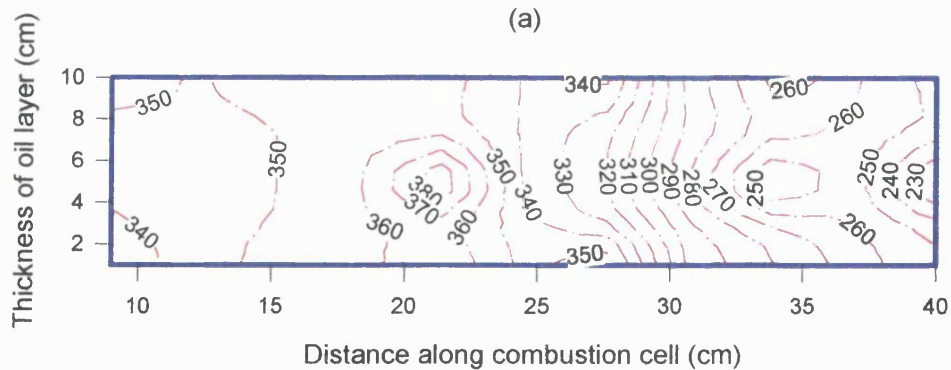


(b)

Figure 4.43 Run 963: Temperature profiles in sandpack (a) Horizontal mid-plane, (b) Vertical mid-plane. [Forties Mix 1 oil, H.W. Design 1]. Combustion Time = 240 minutes

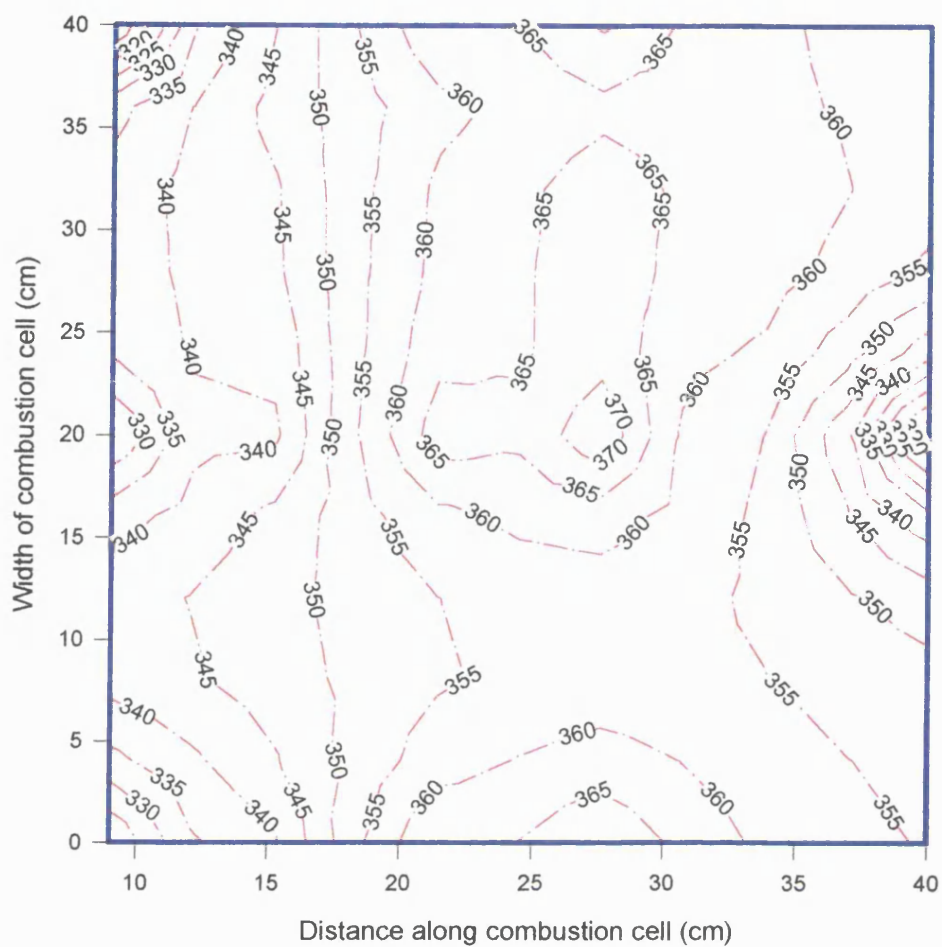


(a)

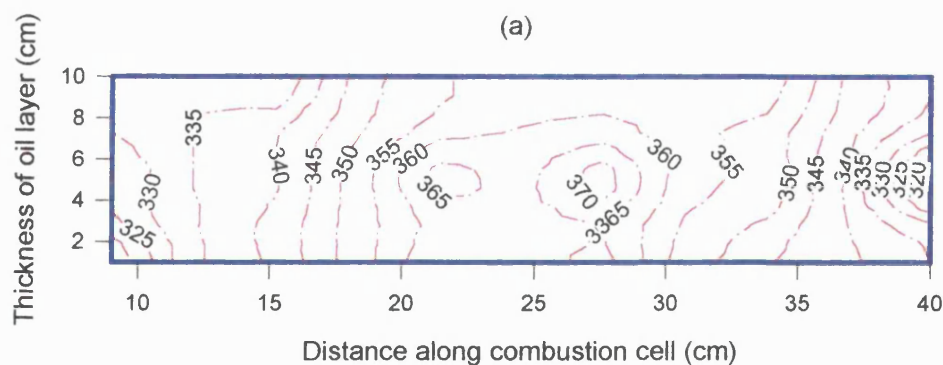


(b)

Figure 4.44 Run 963: Temperature profiles in sandpack (a) Horizontal mid-plane, (b) Vertical mid-plane. [Forties Mix 1 oil, H.W. Design 1]. Combustion Time = 360 minutes

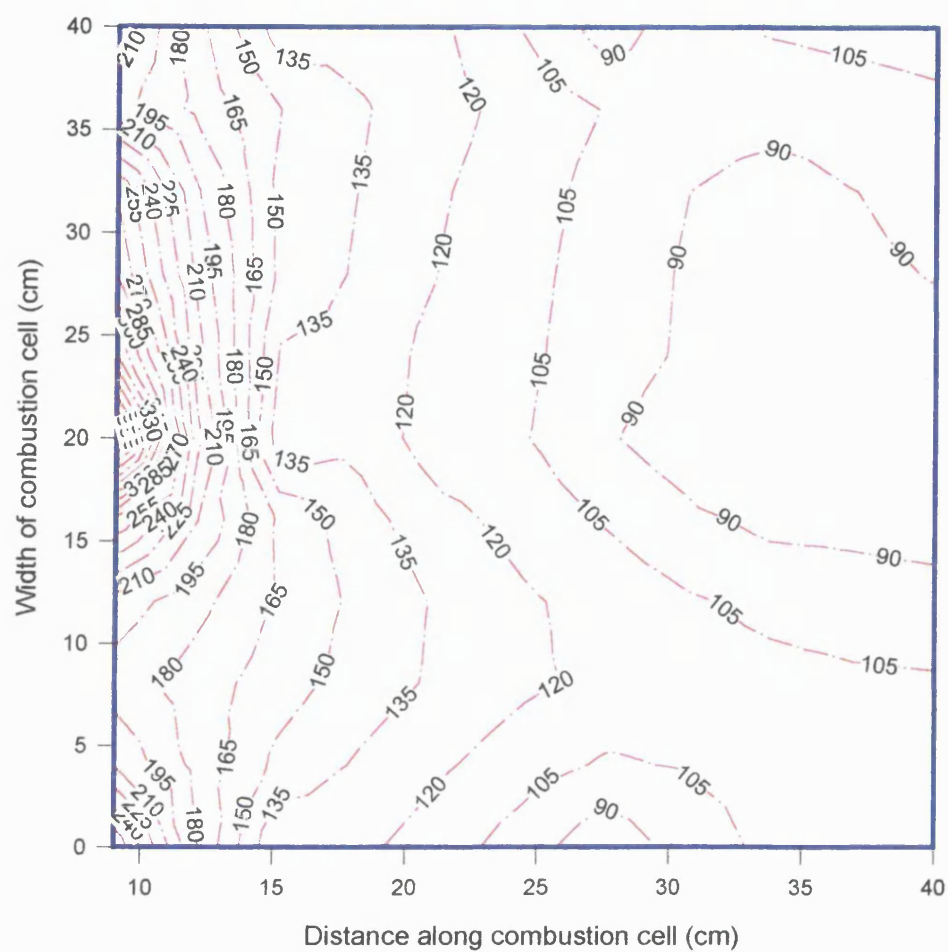


(a)

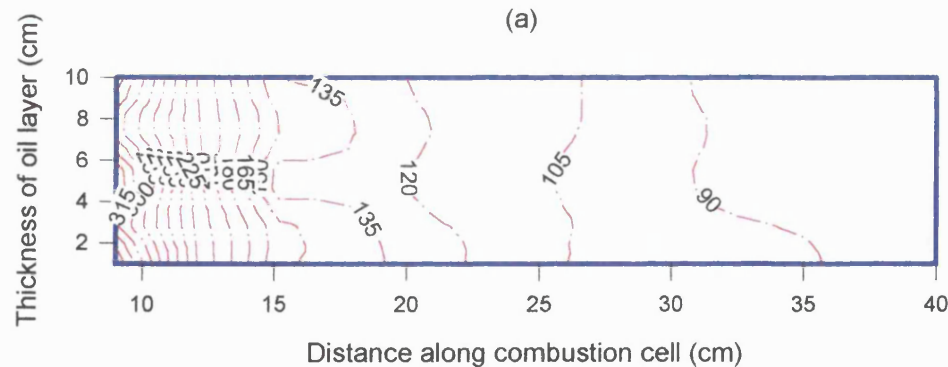


(b)

Figure 4.45 Run 963: Temperature profiles in sandpack (a) Horizontal mid-plane, (b) Vertical mid-plane. [Forties Mix 1 oil, H.W. Design 1]. Combustion Time = 500 minutes

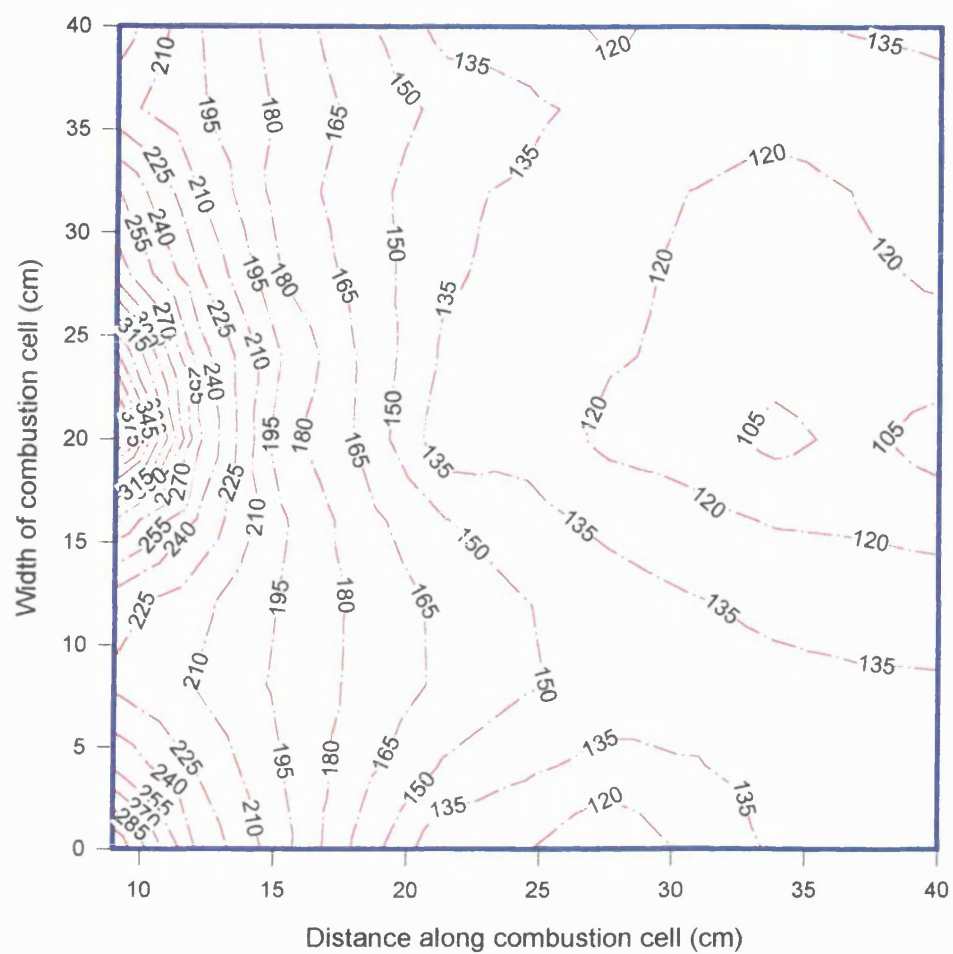


(a)

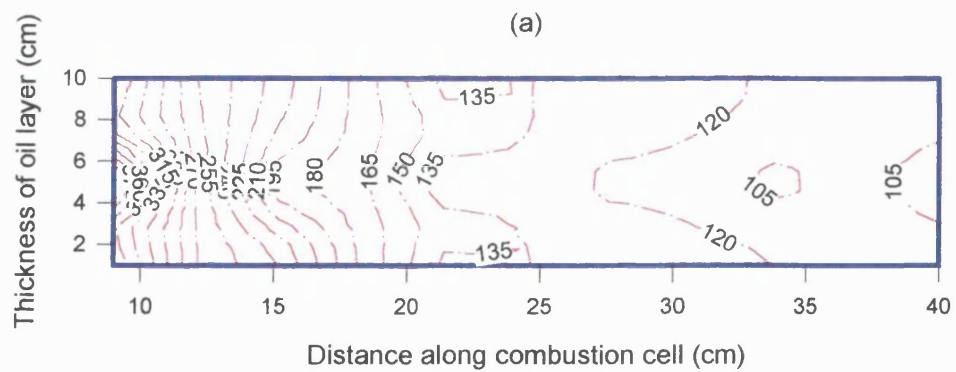


(b)

Figure 4.46 Run 964: Temperature profiles in sandpack (a) Horizontal mid-plane, (b) Vertical mid-plane. [Forties Mix 1 oil, H.W. Design 2]. Combustion Time = 0 minutes

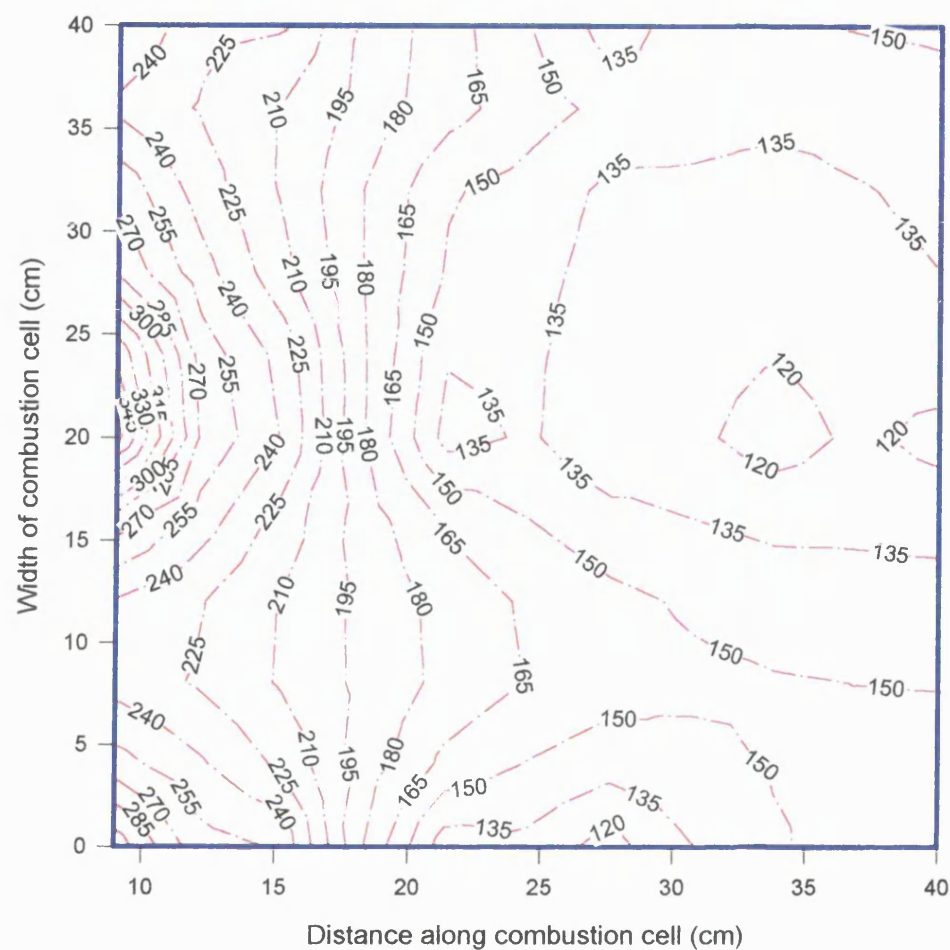


(a)

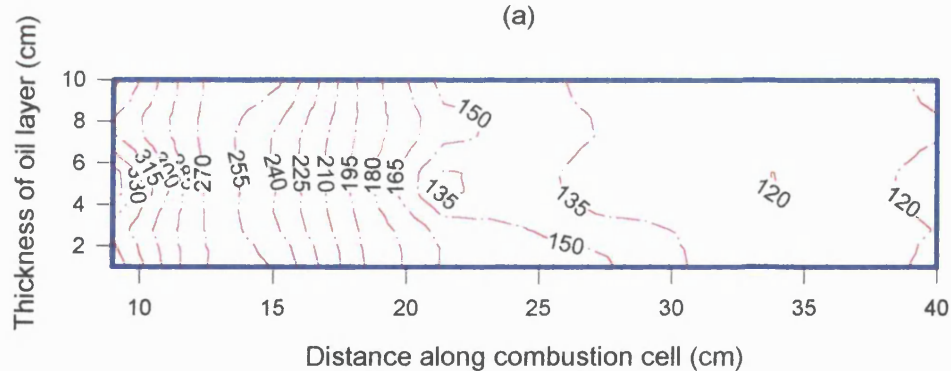


(b)

Figure 4.47 Run 964: Temperature profiles in sandpack (a) Horizontal mid-plane, (b) Vertical mid-plane. [Forties Mix 1 oil, H.W. Design 2]. Combustion Time = 60 minutes

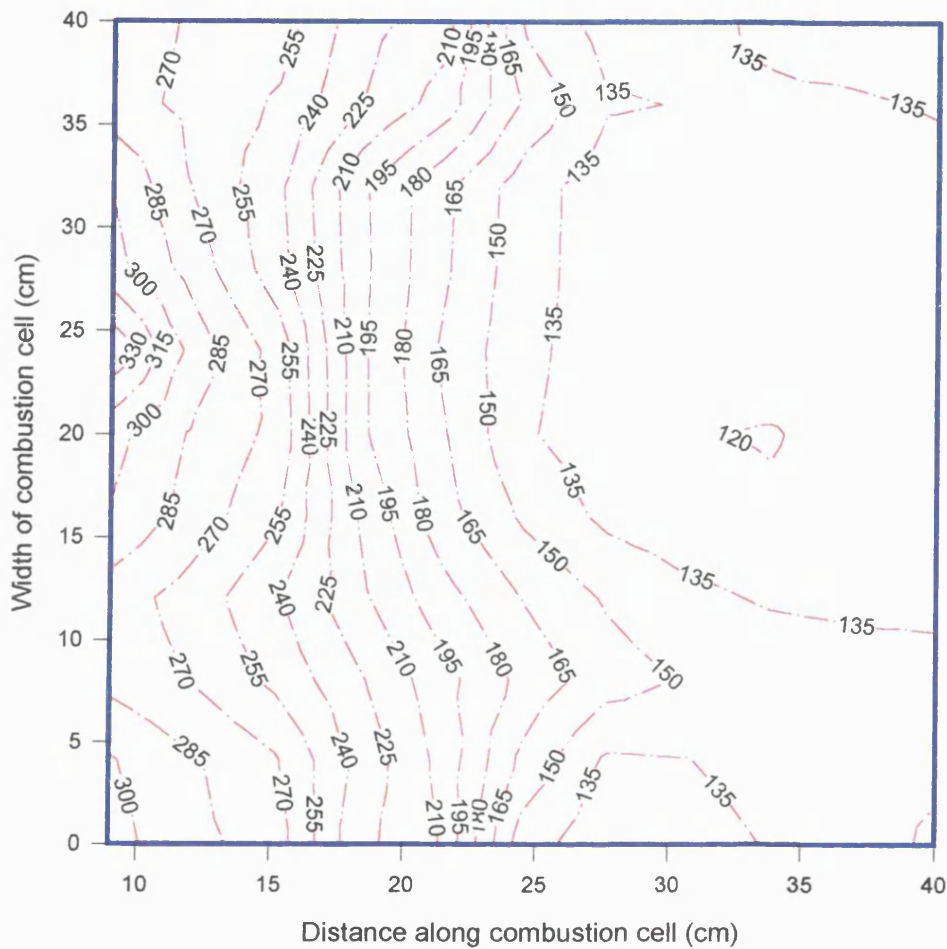


(a)

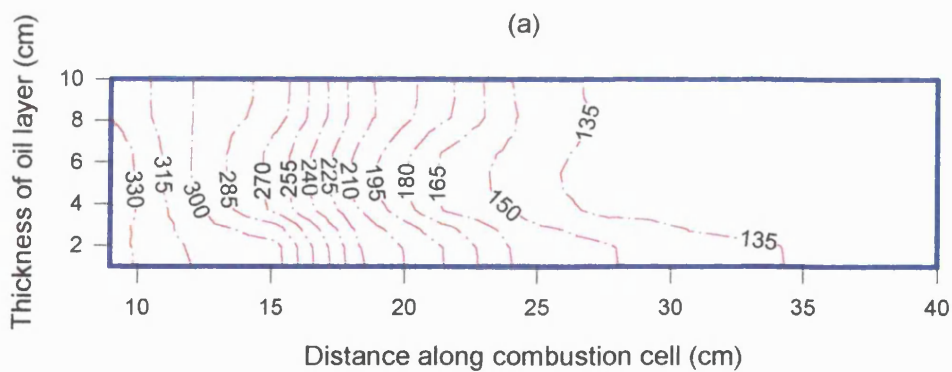


(b)

Figure 4.48 Run 964: Temperature profiles in sandpack (a) Horizontal mid-plane, (b) Vertical mid-plane. [Forties Mix 1 oil, H.W. Design 2]. Combustion Time = 120 minutes



(a)



(b)

Figure 4.49 Run 964: Temperature profiles in sandpack (a) Horizontal mid-plane, (b) Vertical mid-plane. [Forties Mix 1 oil, H.W. Design 2]. Combustion Time = 180 minutes

Table 4.7 Production Performance and Sweep Efficiency

Run	961	962	963	964
Oil type	Clair	Clair	FX1	FX1
Oil recovery (% OOIP)	85	83	82	69
Water recovery (% OWIP)	92	87	85	46
Gas Oil Ratio (m ³ /m ³)	902	992	481	269
Water Cut (%)	72	69.8	69	44.4
Areal sweep efficiency (%)	77.3	71	74	44
Vertical sweep efficiency (%)	67	58	68.4	38
Volumetric sweep efficiency (%)	51.8	41.2	50.6	17

FM1=Forties Mix 1

4.1.9 Post-mortem Analysis of Sandpack

After each experiment, the combustion cell was allowed to cool down to room temperature. The thermocouple connections and flow lines were then disconnected and the cell removed from the insulation box. The inlet flange of the cell was removed and the sandpack was subjected to a visual inspection in order to evaluate the combustion effect and sweep efficiency. This was done by removing vertical layers from the sandpack, with the cell mounted in a horizontal position, and measuring the extent of the burned zone and also to take photographs.

The areal sweep efficiency is measured from the horizontal burnt area of the sandpack divided by the total horizontal area, whereas the vertical sweep is obtained from the vertical cross-section burnt area divided by the total vertical cross-section area. The volumetric sweep efficiency is the product of the areal sweep efficiency times the vertical sweep efficiency. These results are given in Table 4.7.

In addition, samples from the combusted porous media were collected in order to determine the amount of residual oil. This was conducted by heating the samples inside an oven at a temperature of 800 °C for 8 hours. The resulting decrease in mass, before and after heating, provided an average value for the residual material.

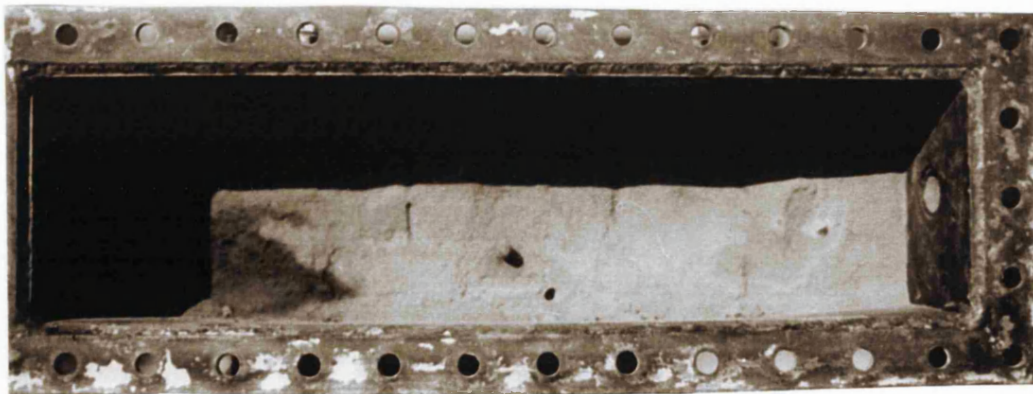
A summary of the visual observations of the post-mortem analysis is provided in the following section, together with accompanying photographs, from Runs 961, 962, 963, and 964.

1. Post-mortem Analysis for Run 961 (Clair Oil, H.W. Design 1)

Distance from inlet (mm)	Observations
60	A clean, loose sand zone covers the entire inlet face, indicating symmetrical ignition on the start of the run.
90	There are two distinct zones. A light grey zone, which is completely clean, covers about 83 % of the sand face. The second zone contains dark brown sand containing residual oil and restricted in a triangular area at the left hand side of the sand face, opposite the extreme end of the injector. This may have been caused by insufficient air supply to this part of the sand face because of lower injection pressure at this end position.
140	The clean burned sand zone covers about 75 % of the sandpack, with a uniform intensity at the top and bottom of the sandpack. This indicates good control of gas override. A thin, solid coke layer is located between the clean sand zone and dark brown zone, defining the boundary of the combustion zone. The dark brown area covers 25 % of the sandpack in the bottom left-hand corner, approximately 2.5cm distance from the horizontal producer.

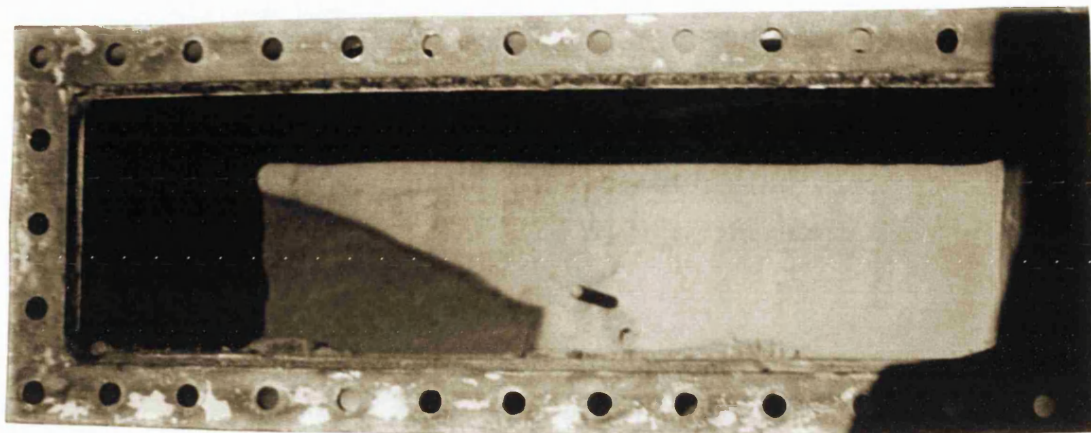


(A)

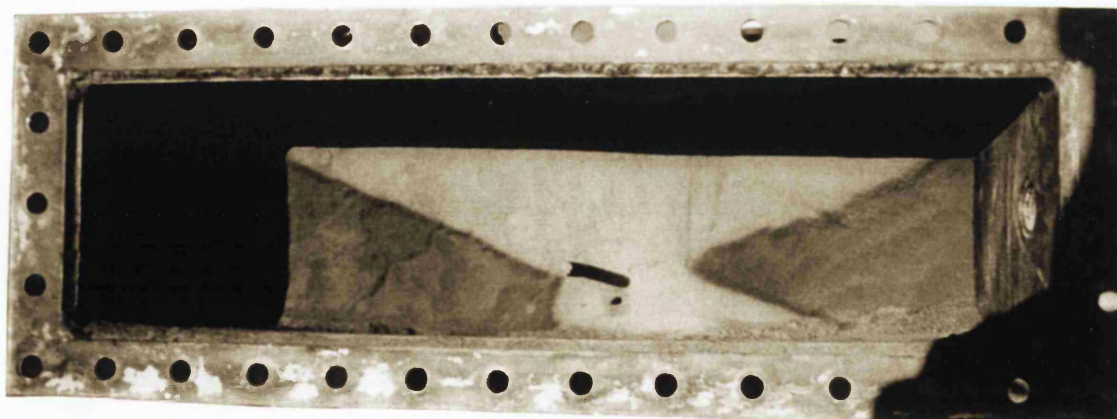


(B)

Figure 4.50 Post-mortem analysis photographs for Run 961 (Clair oil, H.W. Design 1)
(A) at 60mm, (B) at 90mm from inlet face of the combustion cell



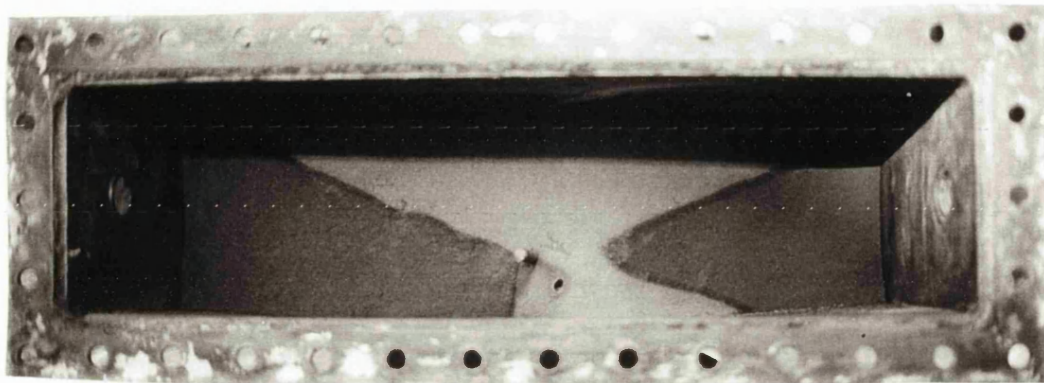
(A)



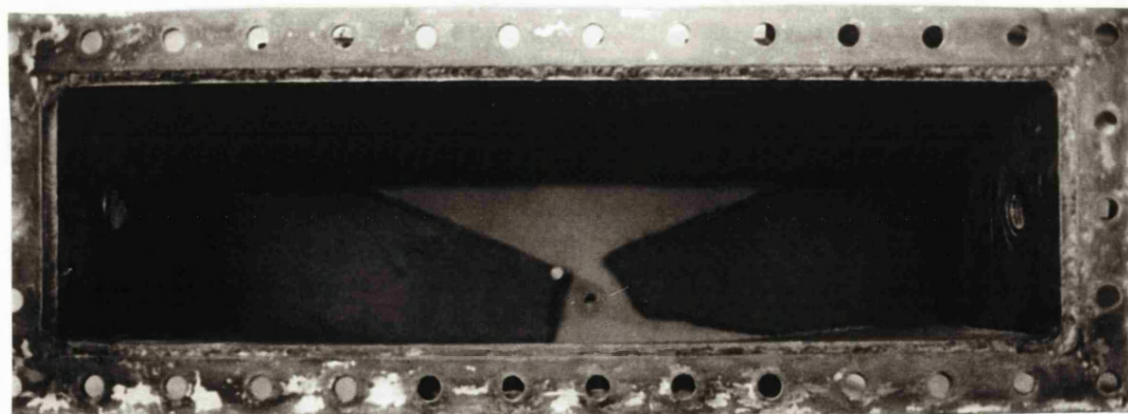
(B)

Figure 4.51 Post-mortem analysis photographs for Run 961 (Clair oil, H.W. Design 1)
(A) at 140mm, (B) at 170mm from inlet face of the combustion cell

170	<p>A dark brown area casts in the right side of the sandpack, which is smaller than that in the left-hand side one, which extends to upper part of the sandpack.</p> <p>The clean sand zone is reduced in size and is mainly located in the upper section but extends well into the horizontal production well area because of the draw-down effect. A thin-coke layer can be clearly seen separating the burned and unburned regions.</p>
200	<p>The dark brown area in the left side has reached the horizontal producer, whereon the right-hand side one it is still 5cm away from it.</p> <p>The dark brown area now covers about 55 % of the sand face and is mainly located on the edges of the sand face. The clean sand area covers the upper section and also an area surrounding the horizontal producer well.</p>
230	<p>Dark brown area on the right-hand side has extended more towards the horizontal producer, whereas that on the left-hand side one is still touching it. The triangular shape is created by the draw-down effect of the horizontal producer, draining mobilised fluids over a large part of the upper central region of the sandpack. Regions towards the edges of the sandpack could be drained more efficiently by placing an extra well at those locations. There is still a clean sand zone under the horizontal producer and in the top section of the sand face.</p>



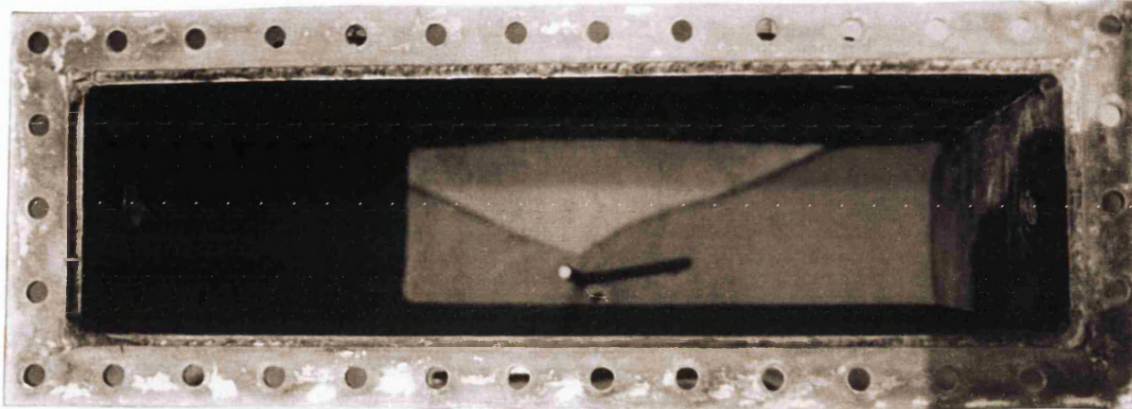
(A)



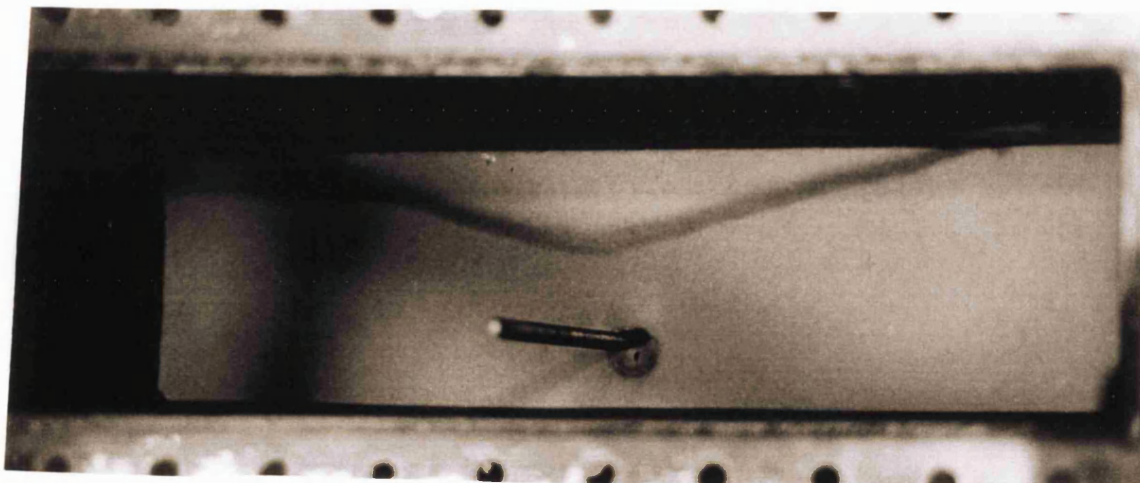
(B)

Figure 4.52 Post-mortem analysis photographs for Run 961 (Clair oil, H.W. Design 1)
(A) at 200mm, (B) at 230mm from inlet face of the combustion cell

270	Dark brown areas on the left and right sides have almost joined together, and now cover about 70 % of the sandpack. At this stage, the combustion front has travelled 17cm along the horizontal well and a clean sand zone mainly exists only in the top part of the sandpack. The much reduced clean sand area around the producer at this stage marks the end of highly controlled gas override, as gases approach the production end.
300	The dark brown colour has changed to a lighter one and covers about 80% of the sand face. This indicates that the area has been effectively swept by steam flood and vaporised light fractions since the early stages of the experiment. The clean sand zone is found only in the top part of the sandpack, indicating severe gas override conditions because of the approach of the production end.



(A)

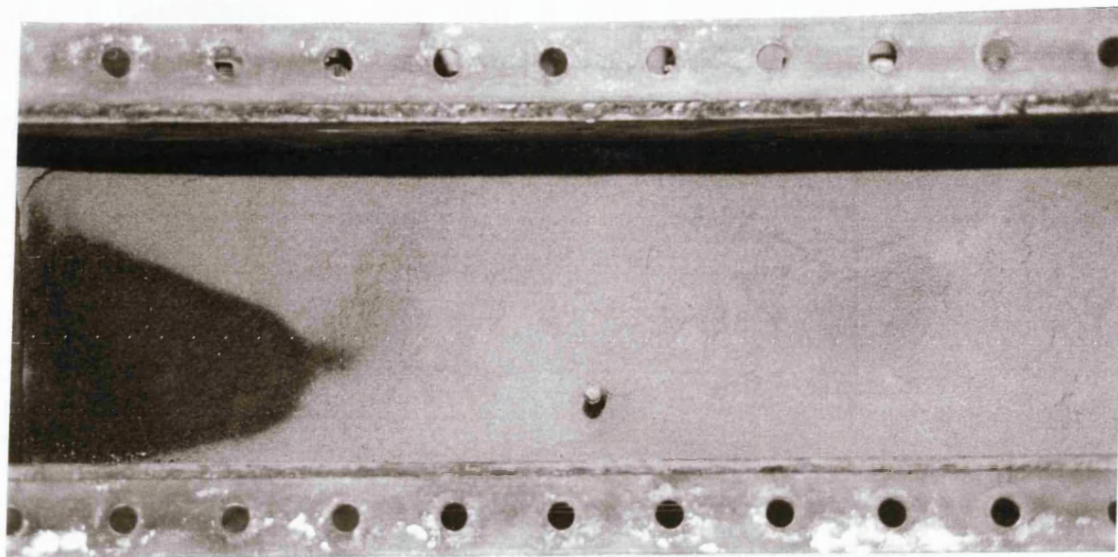


(B)

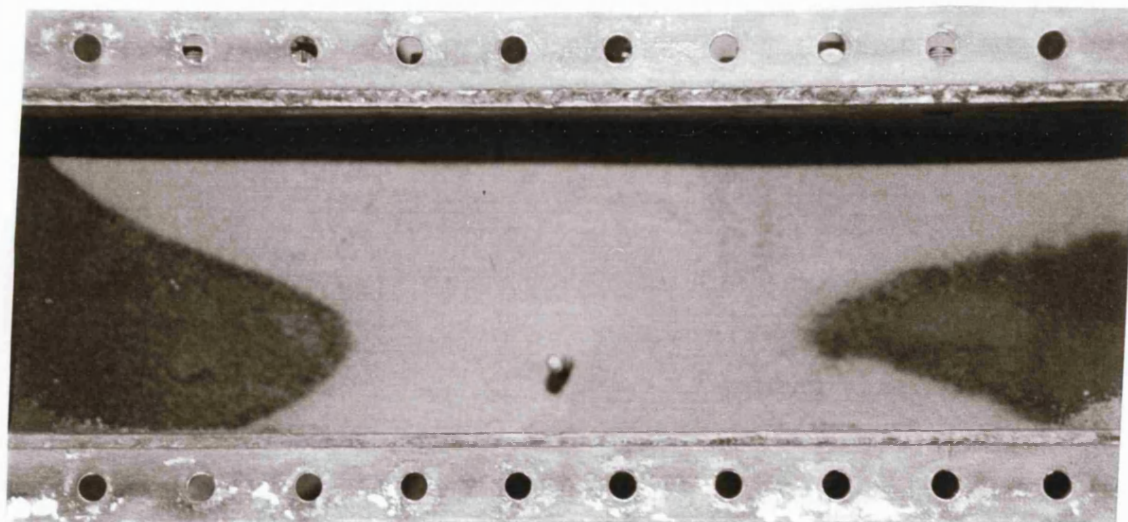
Figure 4.53 Post-mortem analysis photographs for Run 961 (Clair oil, H.W. Design 1)
(A) at 270mm, (B) at 300mm from inlet face of the combustion cell

2. Post-mortem Analysis for Run 962 (Clair Oil, H.W. Design 2)

Distance from inlet (mm)	Observations
60	Clean sand zone is covers 80 % of the sandpack, with a triangular-shaped area of dark-brown colour located at the far, left-hand side of the sandpack.
90	Dark brown area appear also on in the right-hand side of the sandpack. Clean sand covers about 65 % of the sandpack. The clean sand zone is uniformly distributed on both sides of the sand-pack indicating vigorous combustion.
110	Two clean sand zones exist in the top and bottom of the sandpack separated by dark brown area, which cover about 55 % of the sandpack. A thin coke layer separates the clean sand from the dark brown areas, indicating the edges of the combustion front. Thus, what appears to be a second combustion front has formed and propagated in the lower section of the sandpack.
140	The clean sand zone(s) have reduced in size, mainly located in the top part of the sandpack, and below the horizontal producer. Clean sand now cover about 45 % of the sandpack. The dark brown area have become wider in the central region. It is now clear evidence that there are two separate combustion regions, above and below the horizontal producer.

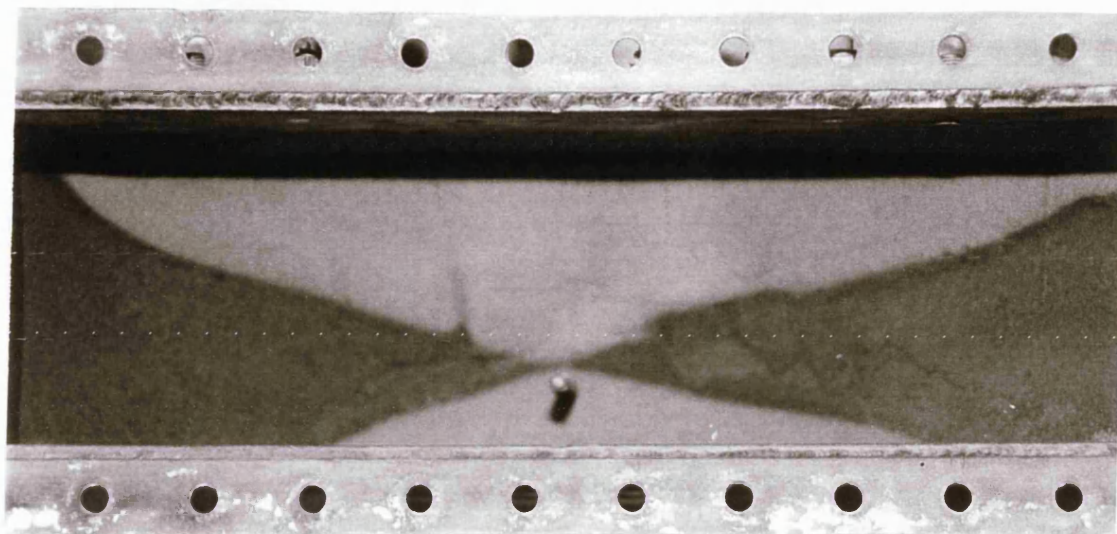


(A)

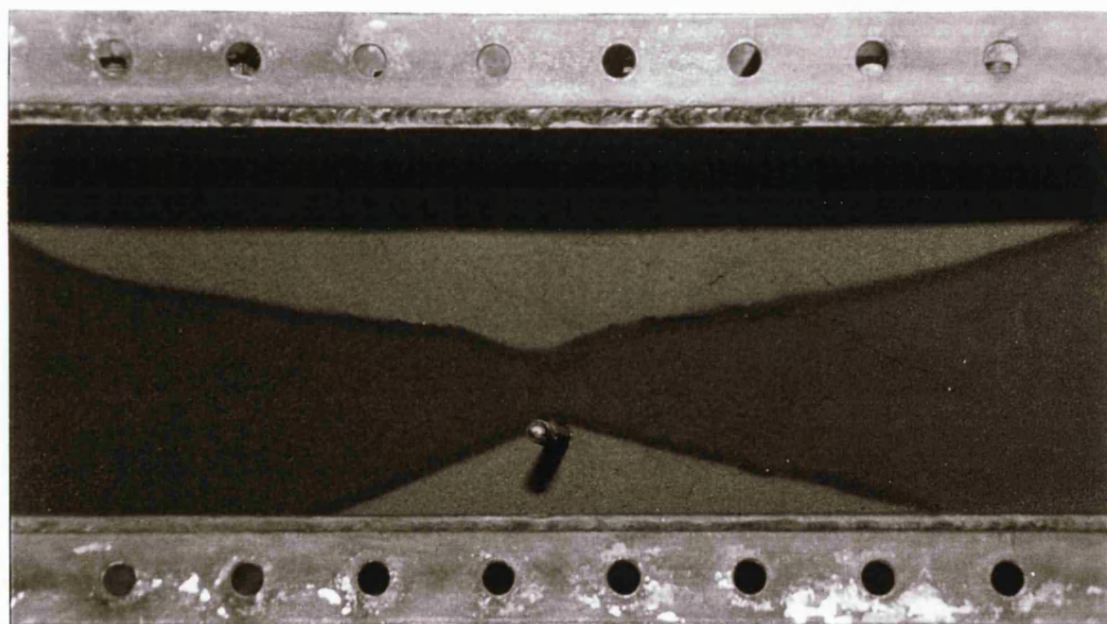


(B)

Figure 4.54 Post-mortem analysis photographs for Run 962 (Clair oil, H.W. Design 2)
(A) at 60mm, (B) at 90mm from inlet face of the combustion cell



(A)



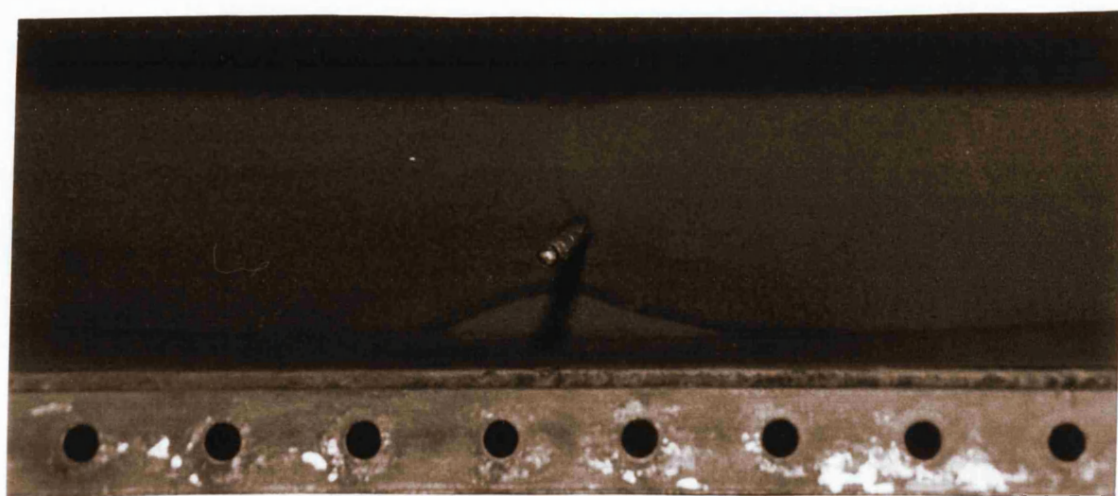
(B)

Figure 4.55 Post-mortem analysis photographs for Run 962 (Clair oil, H.W. Design 2)
(A) at 110mm, (B) at 140mm from inlet face of the combustion cell

170	The dark brown areas have increased, but there are still two clean sand zones located in the top section and beneath the producer.
220	<p>Only a small area of clean sand exists beneath the producer well and another larger area covers the top section (not clear in the picture).</p> <p>They cover about 10 % of the sandpack. Between the two clean sand zones, a light brown coloured zone exists, which indicates either an effective steam flood and gas displacement, and/or accelerated drainage due to high pressure drop.</p>
300	<p>The clean sand zone is found only in the top section of the sandpack.</p> <p>Thus, the second combustion region ended at this location. About 95 % of the sandpack is covered by light brown colour, which indicates oil in this region has been efficiently displaced by steam flooding and hot gases since early stages of the experiment.</p>

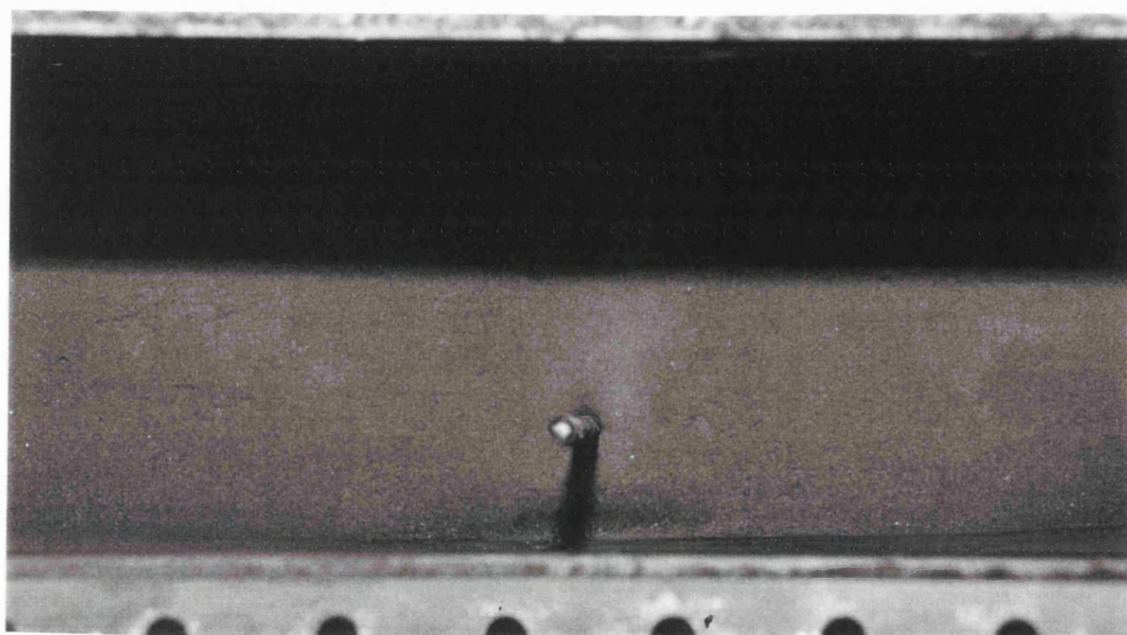


(A)



(B)

Figure 4.56 Post-mortem analysis photographs for Run 962 (Clair oil, H.W. Design 2)
(A) at 170mm, (B) at 220mm from inlet face of the combustion cell

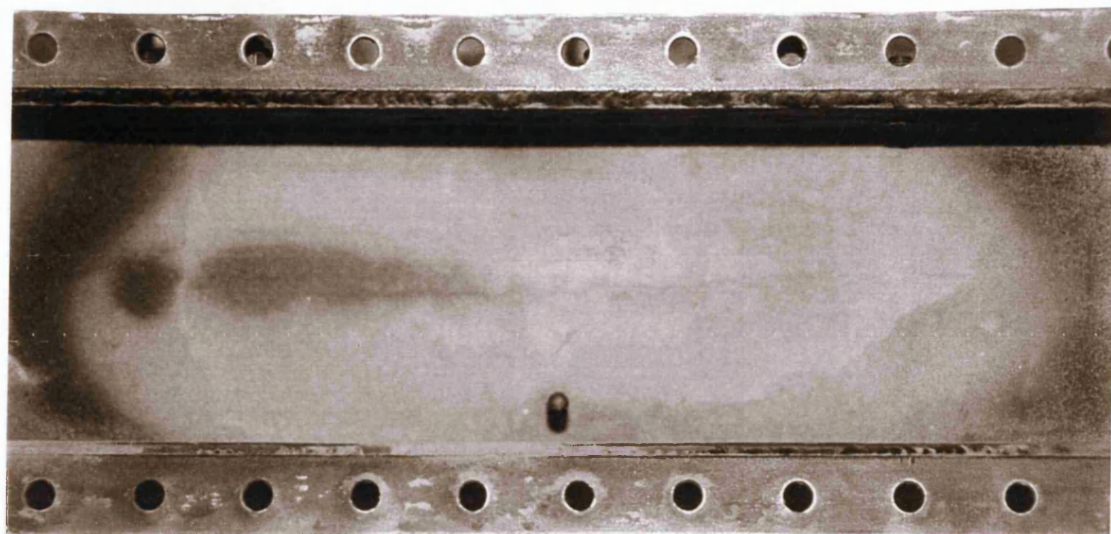


(C)

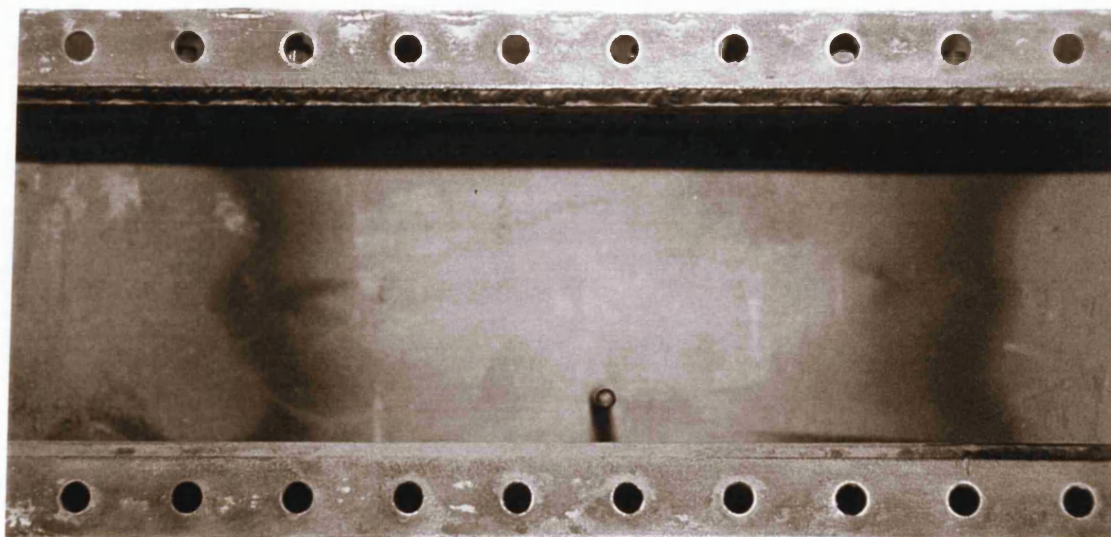
Figure 4.56 Post-mortem analysis photograph for Run 962 (Clair oil, H.W. Design 2)
(C) at 300mm from inlet face of the combustion cell

3. Post-mortem Analysis for Run 963 (Forties Mix 1 Oil, H.W. Design 1)

Distance from inlet (mm)	OBSERVATIONS
60	A clean, semi-consolidated sand covers the sandpack, indicating a vigorous, uniform ignition and combustion.
90	The very clean sand zone is mainly located in the centre of the sandpack indicates good sweep in the top and bottom sections. Some residual oil is trapped at the edges.
130	Two distinctive zones exist. A light brown areas of residual oil exist on the left and right-hand sides of the sandpack and extended towards the producer. The very clean, grey coloured zone covers about 60 % of the sandpack with similar intensity in the top and bottom sections, indicating highly controlled combustion front. The dark brown colour strip surrounding the clean sand zone is defining the side boundaries of the combustion front.
170	The light brown areas have extended towards the producer; whereas the clean sand zone has maintained its pervious position but is reduced in size.

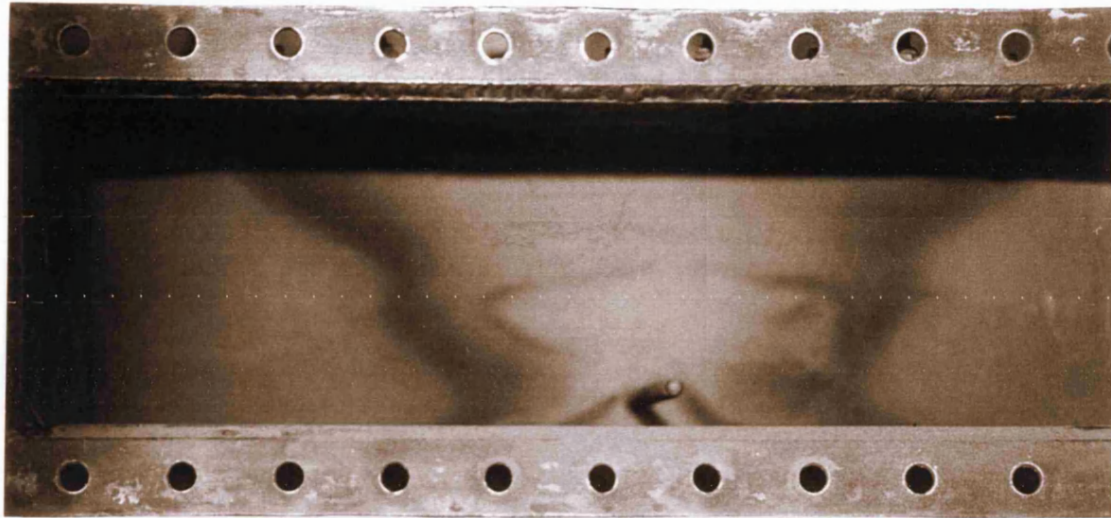


(A)

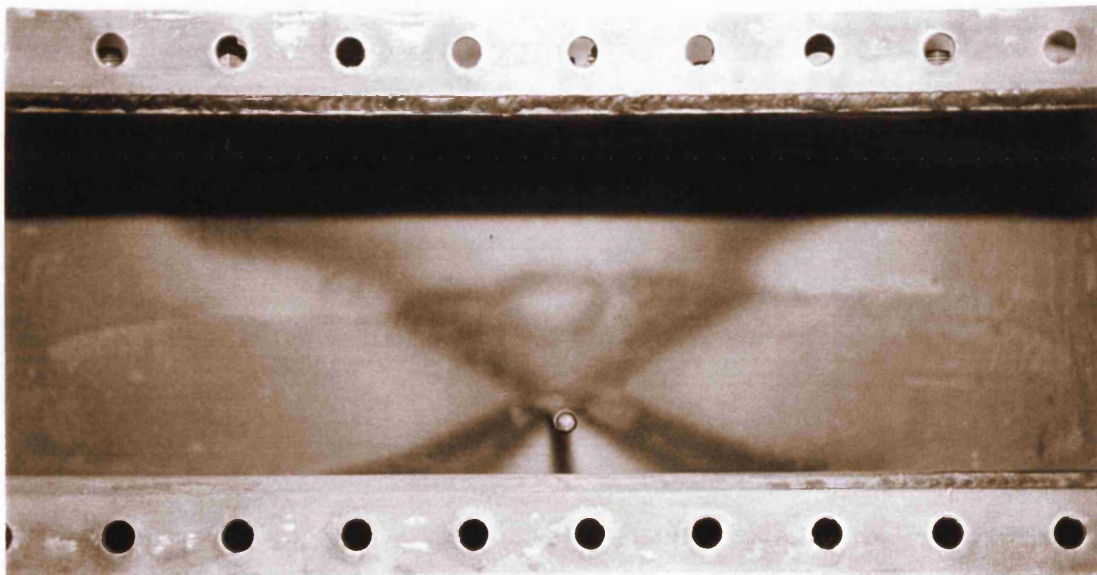


(B)

Figure 4.57 Post-mortem analysis photographs for Run 963 (Forties Mix 1 oil, H.W. Design 1)
(A) at 60mm, (B) at 90mm from inlet face of the combustion cell



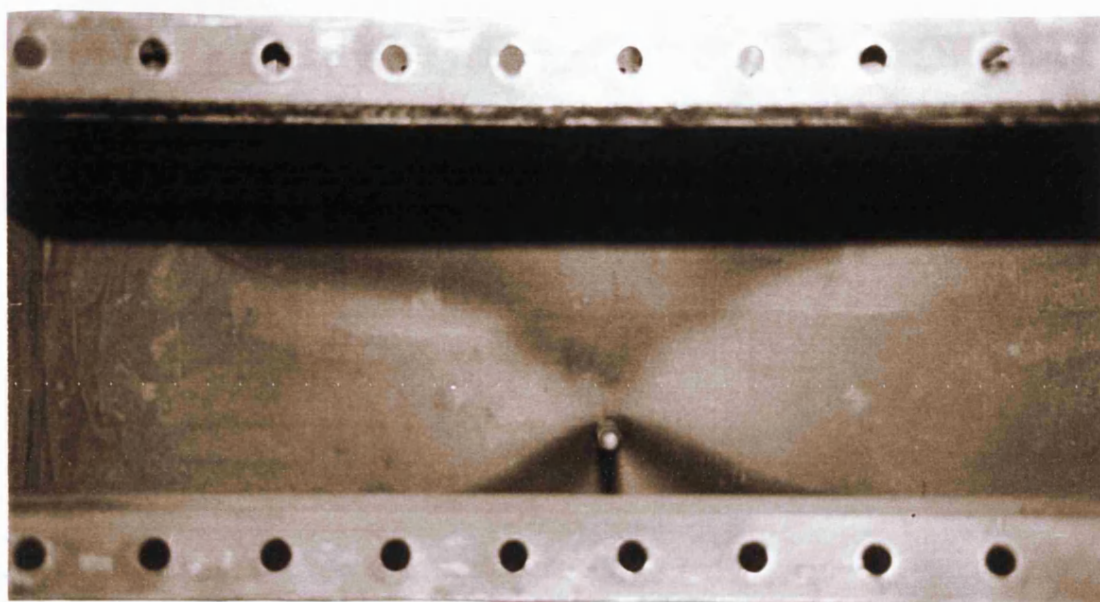
(A)



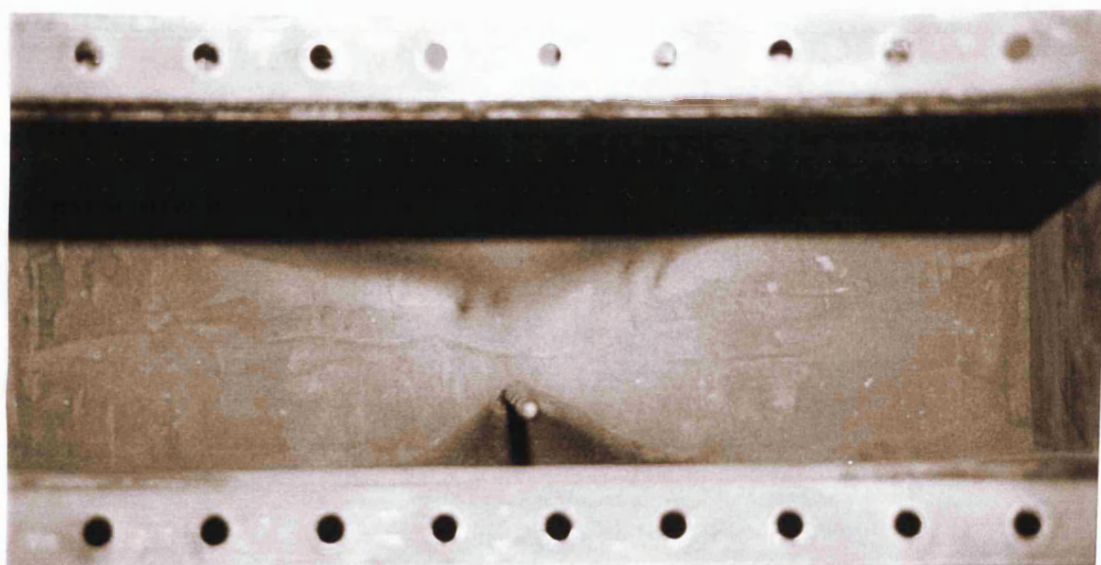
(B)

Figure 4.58 Post-mortem analysis photographs for Run 963 (Forties Mix 1 oil, H.W. Design 1)
(A) at 130mm, (B) at 170mm from inlet face of the combustion cell

200	<p>The light brown areas have joined together, 1.5cm above the producer, indicating the start of some gas override effect. At this stage, the combustion front has travelled about 14cm of the interwell distance.</p> <p>A clean sand zone exists in the top section indicating moderate degree of gas over ride. An arch shaped black layer underlies the producer well with clean sand in the centre, suggesting the formation of a secondary combustion front.</p>
240	<p>The light brown area extends further into the upper section of the sand pack, indicating a moderate degree of gas override.</p>
270	<p>Clean sand zone is restricted in the top section of the sand pack whereas light brown colour is covering 80 % of the sand face indicating that most of the oil has been continually displaced by steam and hot gases since early stages of the experiment.</p>

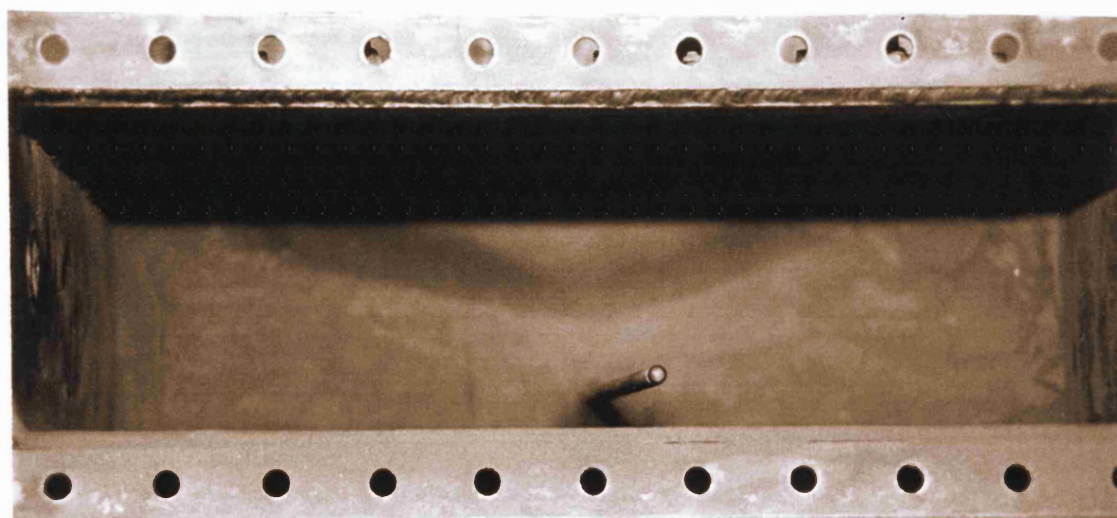


(A)



(B)

Figure 4.59 Post-mortem analysis photographs for Run 963 (Forties Mix 1 oil, H.W. Design 1)
(A) at 200mm, (B) at 240mm from inlet face of the combustion cell

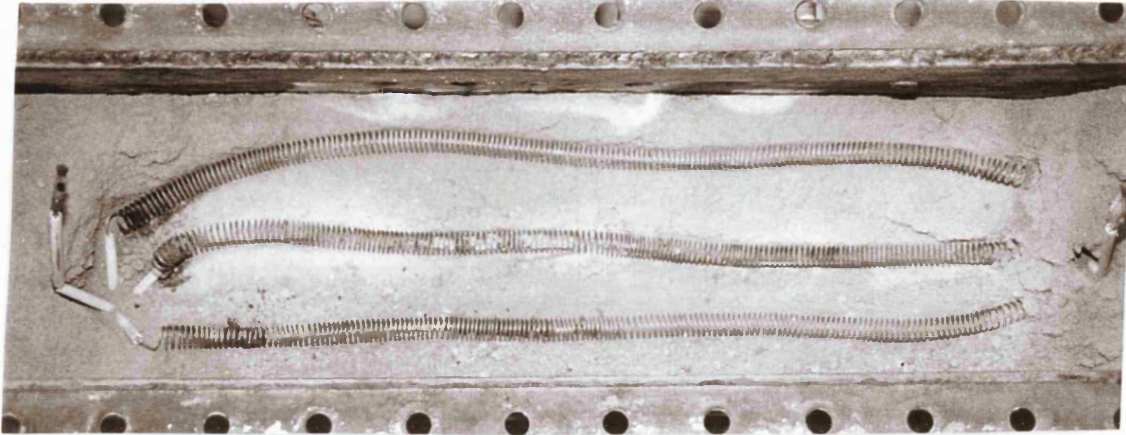


(C)

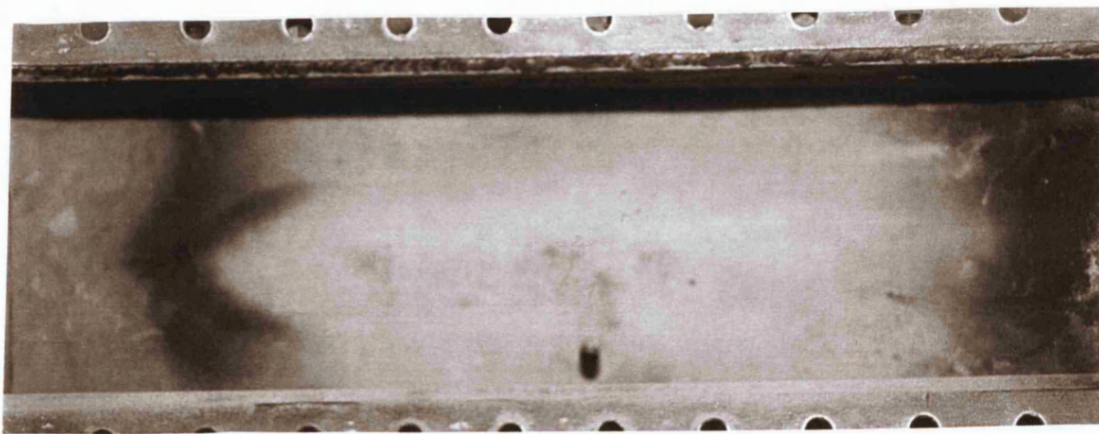
Figure 4.59 Post-mortem analysis photograph for Run 963 (Forties Mix 1 oil, H.W. Design 1)
(C) at 270mm from inlet face of the combustion cell

4. Post-mortem Analysis for Run 964 (Forties Mix 1 Oil, H.W. Design 2)

Distance from inlet (mm)	OBSERVATIONS
30	Clean sand covering the entire area of the sand face, indicating uniform and vigorous ignition along the injection face.
70	A burnt zone is present at the centre of the sandpack and covering about 60% of the sand face with uniform distribution in the top and bottom sections. It is bounded by a thin coke layer indicating that the combustion front was propagating in a steady state mode. Also it suggests that there is high fluid down flow from the centre of the sand pack towards the producer. may have occurred. Residual oil is left at both sides of the sandpack, indicating some degree of LTO may have occurred.
140	A light brown colour covers the entire area of the sandpack, with no sign of combustion front movement, in and beyond this region. Oil displacement in this region may have resulted partially from steam generated during the initial phase of the experiment and also, by hydrodynamic displacement of hot gases.

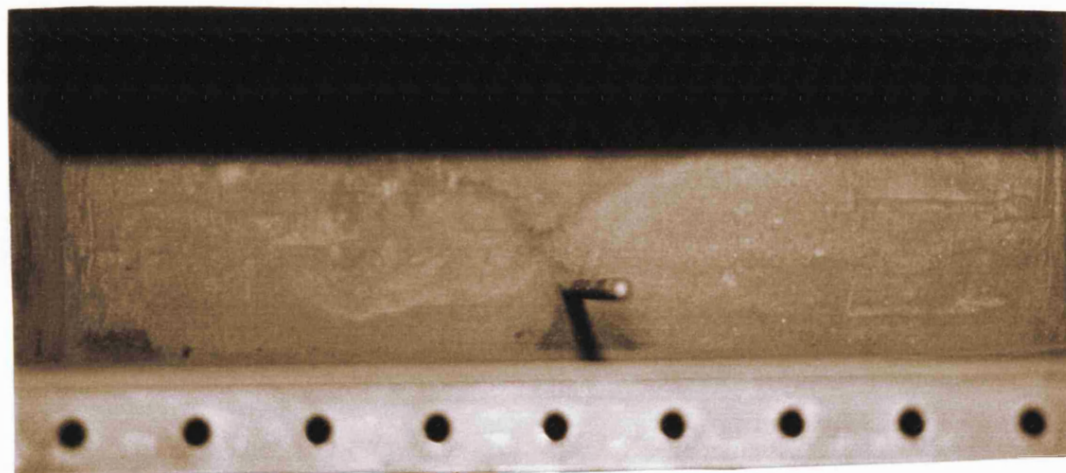


(A)



(B)

Figure 4.60 Post-mortem analysis photographs for Run 964 (Forties Mix 1 oil, H.W. Design 2)
(A) at ignitor, (B) at 70mm from inlet face of the combustion cell



(C)

Figure 4.60 Post-mortem analysis photograph for Run 964 (Forties Mix 1 oil, H.W. Design 2)
(C) at 140mm from inlet face of the combustion cell

PART II : Experiments with Modified Horizontal Producer Well

4.2 Experimental Results of Run 966

In this experiment, the effect of oil desaturation downstream of the combustion front, due to vaporisation and gas stripping, was subjected to a ‘practical test’, in order to evaluate the effect on displacement mechanisms. This was achieved by using a modified horizontal producer well (Design 3) to mimic the process behaviour occurring in heavy oil reservoirs, wherein the high viscosity (several hundred to thousands of centi poise) prevent the oil draining and effectively seals the flow into the horizontal producer. Design 3 producer is in fact a combination well of Designs 1 and 2 producers used in Runs 963 and 964, respectively. The benefit of this design is that it has the capability to be adjusted along the first half of the well length, using an internal tubing sleeve.

Run 965 was carried out to test the new well assembly. This experiment was terminated in the early stages because the tubing sleeve mechanism became stuck.

Run 966 was conducted using Light Forties Mix1 crude oil and under similar operating conditions to Runs 963 and 964.

The results of this experiment are presented in Figures 4.61 to 4.77 and also summarised in Tables 4.8 to 4.11.

4.2.1 Produced gas composition

The produced gas composition for Run 966 is shown in Figure 4.61, together with the peak temperature profile. A vigorous ignition was achieved, with the ignitor shut-off after 2.7 hours. Thereafter, the combustion front stabilised quickly, achieving a constant temperature of 370 °C throughout the whole experiment. The produced CO₂

level is higher than that achieved in Run 964 which used a non-sleeve back design.

The produced oxygen level is also lower. Values of produced gases are given in

Table 4.8.

4.8 Produced gas composition for Runs 963,964 and 966

Run	963	964	966 Upstream	966 Downstream
CO ₂ %	8.85	6.1	8.4	9.3
CO %	2.35	1.9	3	3.6
O ₂ %	4.8	7	5	4.7
CO/CO+CO ₂ Ratio	0.20	0.23	0.26	0.21
H/C Ratio	2.27	4.7	2.32	1.9

The ‘spike’ in the CO₂ profile,(Figure 4.61), at 431 min occurs when the downstream section of the horizontal well is opened. Thus, the sleeve-back operation in the upstream section of the horizontal producer well, effectively “shutting-it-in” to a position slightly ahead of the combustion front, prevent the oil from draining and desaturating the sandpack downstream. The internal tubing sleeve was adjusted by keeping an approximately 10-15 °C difference between the temperature measured on the sleeve tip and the combustion front temperature. In Run 964, the CO₂ level continuously decreased from a maximum of nearly 10 %, down to around 5 % due to poor combustion and falling combustion peak temperature as a result of reduced fuel availability. The oxygen level in the produced gas also continues to increase to about 8 % which is beyond the stabilised level of 5 % seen in upstream section of Run 966. The main reason for the poor combustion in Run 964 is desaturation of the oil layer downstream in the sandpack, owing to excessive drainage caused by the high hole perforation density (Design 2). Thus, if the downstream oil saturation can be

maintained, then combustion front propagation can be sustained at a fairly vigorous level. This is clearly demonstrated in Run 966, which used a similar perforation density in the upstream well section to Run 964 but had the benefit of the internal tubing sleeve-back to prevent the downstream oil layer desaturating.

4.2.2 Combustion behaviour

The summary of results in Table 4.9 show that the atomic H/C ratio of the fuel burned during Run 966 in the upstream section was 2.32, which is higher than the value of 1.9 for the downstream section. A post-mortem analysis of the sandpack revealed that there was a substantial amount of coke near the heel of the upstream section. Since oxygen utilisation during this experiment was relatively low at around 75 %, it is clear that significant oxygen bypassed into the downstream zones, undergoing low temperature oxidation. Considering that all of the original oil-in-place is virtually accounted for by the fuel burned and the oil produced (a difference of only 1.6 %), this effect was not very extensive during the experiment. However, for the light Forties Mix 1 crude, the amount of fuel consumed is not unduly low, at around 5 % OOIP and 1.6 % of pre-oxidised fuel amounts to 25 % of the total fuel burned. Therefore, the air flux used may have been too low to burn this amount of fuel efficiently, or else, pre-oxidised fuel produced by LTO reactions was more difficult to burn at the low combustion temperature prevailing in the experiment.

Table 4.9 Combustion Performance

Well Section	Upstream	Downstream
Air to fuel requirement (sm^3/kg)	11.6	10.9
O_2 to fuel requirement (sm^3/kg)	2.44	2.3
Fuel burned (% OOIP)	4.7	5.1
Oxygen Utilisation (%)	75.6	77.5
Fuel Consumption (kg/m^3)	11	12.2
Combustion front velocity (m/hr)	0.028	0.025
Air requirement (sm^3/m^3)	161	180
O_2 Requirement (sm^3/m^3)	33.8	37.8
Carbon Combustion Rate (g/hr)	8.6	11.3

4.2.3 Oil and water production

The oil and water production achieved in the experiment are shown in Figures 4.65 to 4.69, and Table 4.10 summaries the oil and water recovery in both well sections. The overall recovery performance is given in Table 4.11.

Oil and water production rates were steady at a low rate during the initial three hours of the experiment, as shown in Figure 4.65. During the stabilised combustion period, oil and water production begins to increase sharply up to about 8 hours. The total oil produced at the end of the first part of the experiment when the sleeve-back was operated was 36.4 % OOIP the water recovery was 31.8 % OWIP. The overall oil recovery for the upstream and downstream section of the sandpack is 93.5 % OOIP, i.e. 36.4 and 57.1 % OOIP for both sections respectively. Accordingly, 114.2 % oil recovery was achieved from the downstream section. This was most probably due to the fact that oil was retained in the upstream section of the sandpack because the sleeve-back operation was too tightly controlled. Utilising only a 10 to 15 °C temperature difference between the tubing sleeve tip temperature and the upstream

combustion front temperature resulted in the active drainage length of the exposed horizontal well being over-constrained.

The temperature profile in Figure 4.73 indicates that the overall temperature drop over the mobile oil region is more like 60 to 80 °C and hence more accurate control of the tubing sleeve movement would create a bigger exposed section of the horizontal producer well.

Table 4.10 Production Performance for Run 966

Well Section	Upstream	Downstream
Average oil production rate (ml/hr)	73	229
Average water production rate (ml/hr)	62	176
Average liquid production rate (ml/hr)	135	405
Water Cut (%)	58	63
Oil recovery (% OOIP)	36.4	57.1
Water recovery (% OWIP)	31.8	54
Areal sweep efficiency (%)	75	73
Vertical sweep efficiency (%)	88	75
Volumetric sweep efficiency (%)	66	54.7

Overall, the ‘sleeve-back’ principle controlled the drainage of light oil in the downstream section of the sandpack, thereby maintaining oil saturation close to, or even higher, than its original saturation. Clearly, if the objective is to keep oil saturation ahead of the combustion front constant and thereby maintain combustion front propagation throughout the reservoir length, sleeve-back of the horizontal producer is a very effective means for achieving this. The very high sweep efficiency and recovery achieved in this way may be weighted against a non-sleeve-back operation (i.e. Run 964), in which lower oil recovery was achieved (69 %OOIP), but without the sleeve-back. In watered-out light oil reservoirs, often there is considerable displacement efficiency achieved by the massive stream drive created.

Table 4.11 Overall Recovery for Run 966

Produced liquid	Pre-ignition period	Combustion period with ignitor on	Combustion period with ignitor off	Overall
Oil recovery (% OOIP)	23	6.4	64.1	93.5
Water recovery (% OWIP)	4.7	3	78.1	85.8

4.2.4 Temperature contours

The temperature contours at the horizontal and vertical mid-planes of the sandpack are shown in Figures 4.72 to 4.76. There is a band of tightly-spaced contours

immediately ahead of the combustion front (360°C), grading down to about 270 °C.

This effect is even more dramatic at the later time of 431 minutes (Figure 4.74) when the combustion front has reached just over half-way through the sandpack. Here, the downstream section is open and the upstream sleeve-back section is now closed. It would appear that the downstream section is still benefiting from the shut-in effect of the sleeve-back operation. In part, this is probably because, as explained in the previous section, it has been too tightly-controlled in the experiment. The continuous sleeve-back procedure was operated on the basis of an approximately 15 °C difference between the combustion front temperature measured at the TOP, MIDDLE and BOTTOM layers of the sandpack, expand to that measured at the ‘toe’ inside the horizontal well at the leading shut-in position. It can be seen in Figure 4.73 a and b, that the actual temperature drop across the controlled mobile oil (drainage) region, immediately ahead of the combustion front, is approximately 80 °C, over a distance of 2cm of the sandpack. Based on 100m horizontal well length, the exposed, or active drainage length, of the horizontal producer well would be approximately 5meters. In this mobile oil zone, because of the high temperature, the fluid is mainly gas. With all

the factors constant, (Darcy's law), drainage from the reservoir is largely governed by the fluid viscosity (if no restrictions on drainage into the horizontal producer well) and therefore, the active well drainage length of only 5m, is able to drain more oil, over the entire length than at approximately higher viscosity at lower temperature, approximately $5/100 \times (1/10^{-3})$, or a factor of 50.

This is obviously an overcomprehensive, but even allowing for increased pressure loss in the horizontal well because of higher gas velocity or liquid condensation downstream (condensed fluid) this is still have a large margin for maintaining oil productivity.

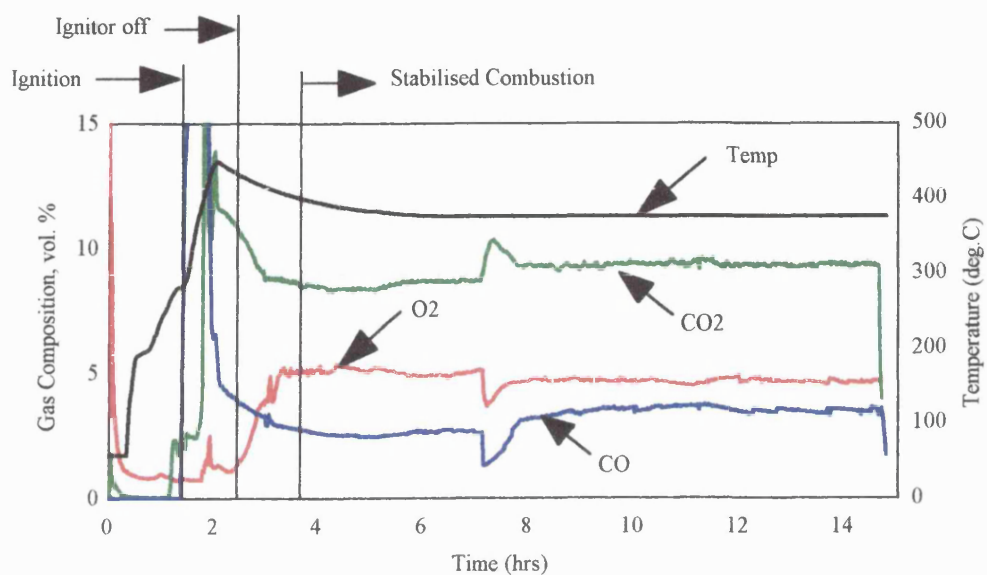


Figure 4.61 Produced gas composition for Run 966 (Forties Mix 1 oil, H.W. Design 3)

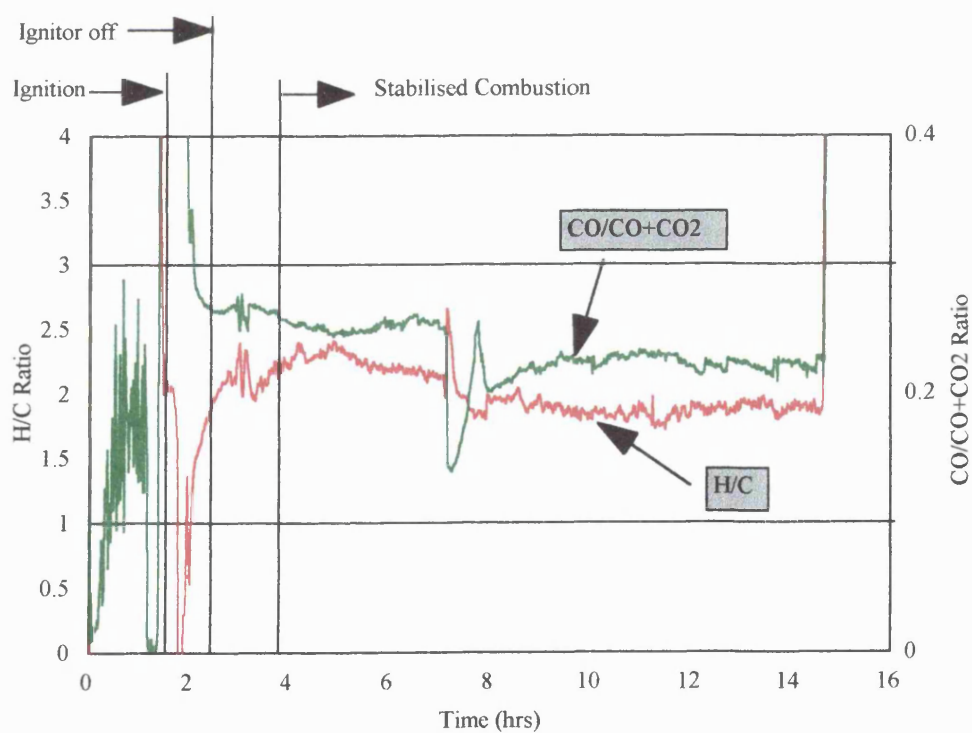


Figure 4.62 H/C and CO/CO+CO₂ ratio for Run 966 (Forties Mix 1 oil, H.W. Design 3)

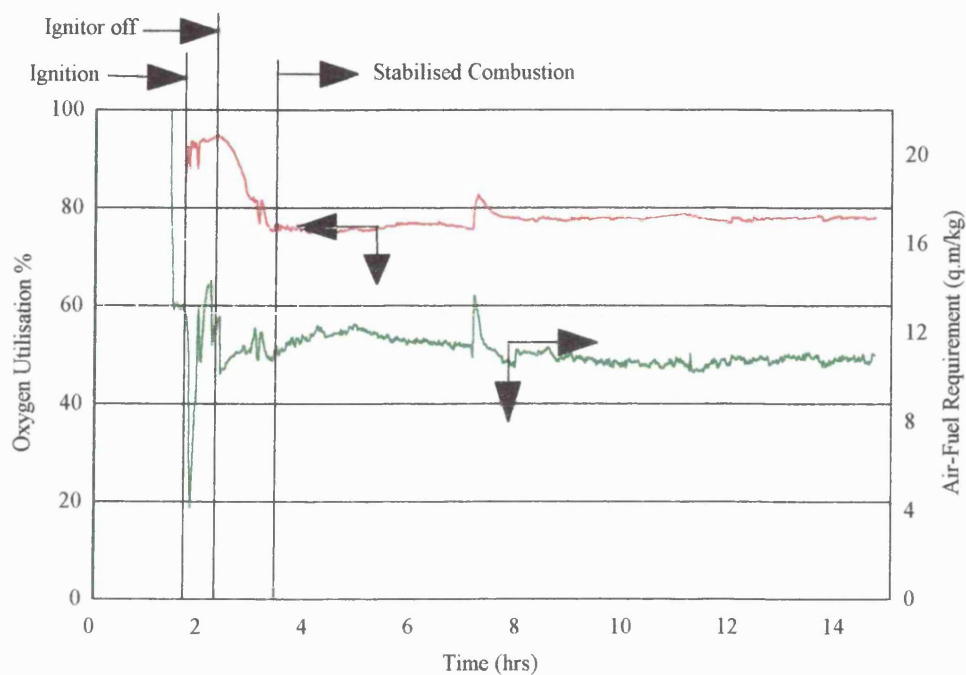


Figure 4.63 Oxygen utilisation and AFR for Run 966 (Forties Mix 1 oil, H.W Design 3)

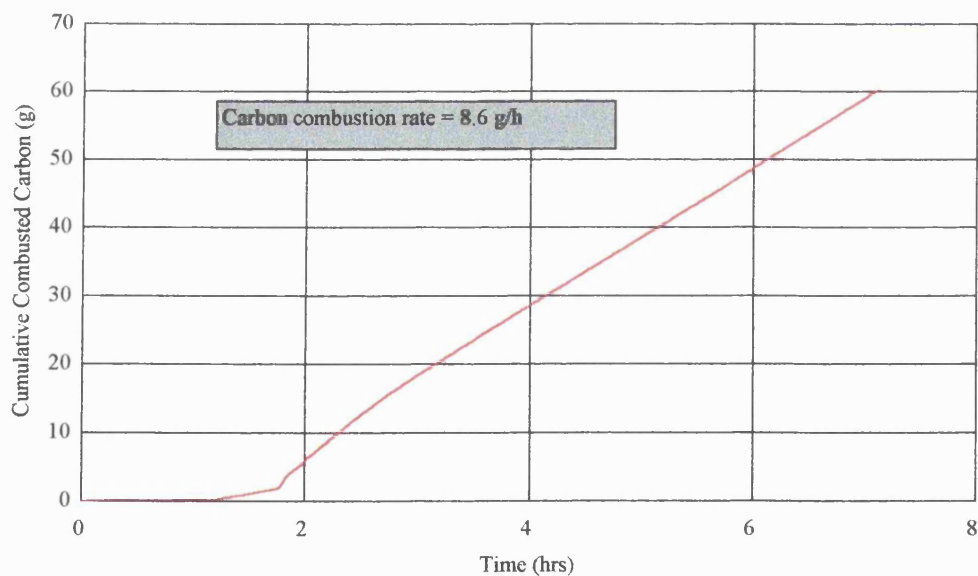


Figure 4.64 Carbon combustion rate for Run 966 [upstream well section]
(Forties Mix 1 oil, H.W. Design 3)

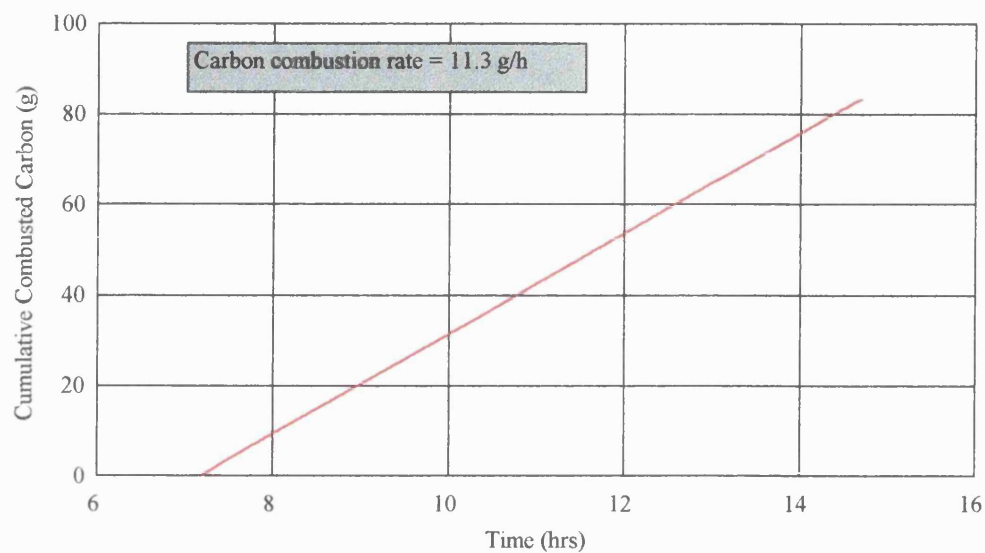


Figure 4.65 Carbon combustion rate for Run 966 [downstream well section]
(Forties Mix 1 oil, H.W. Design 3)

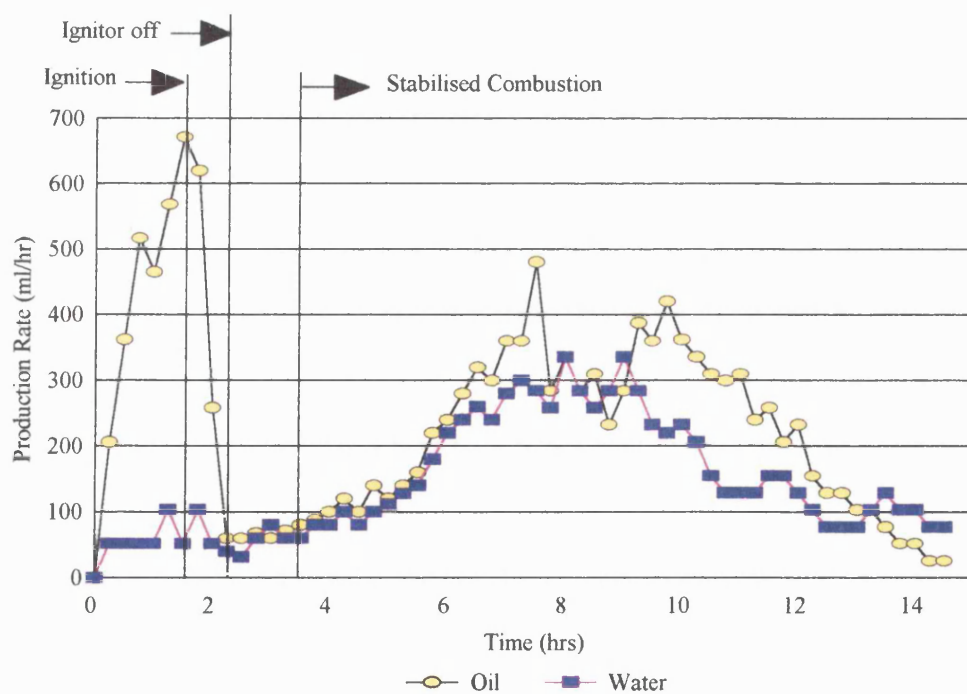


Figure 4.66 Oil and water production rate for Run 966 (Forties Mix1 oil, H.W. Design 3)

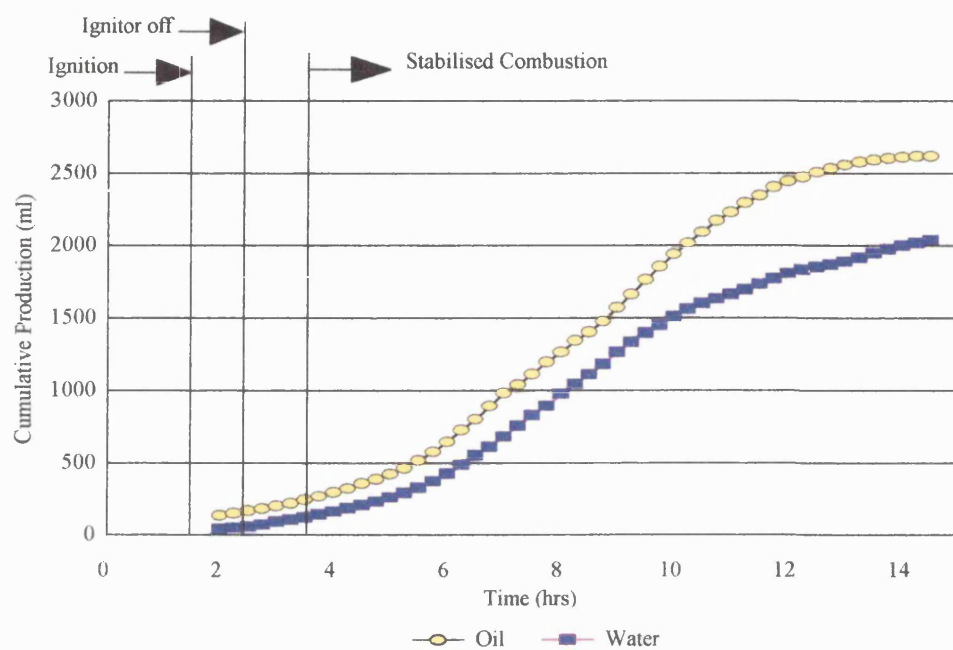


Figure 4.67 Cumulative production for Run 966 (Forties Mix 1 oil, H.W. Design 3)

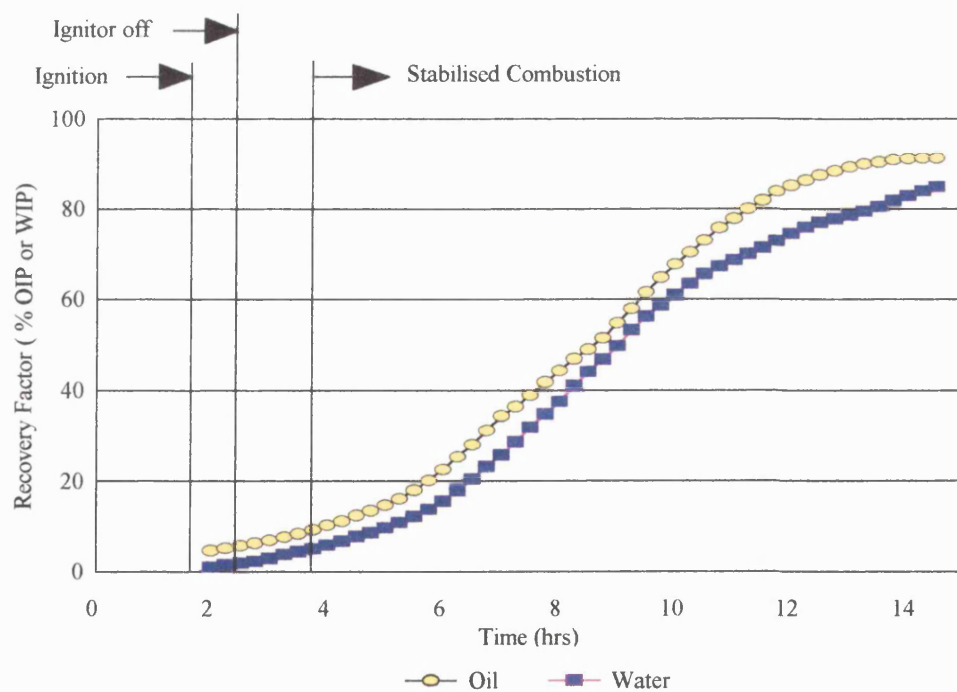


Figure 4.68 Oil and water recovery for Run 966 (Forties Mix 1 oil, H.W. Design 3)

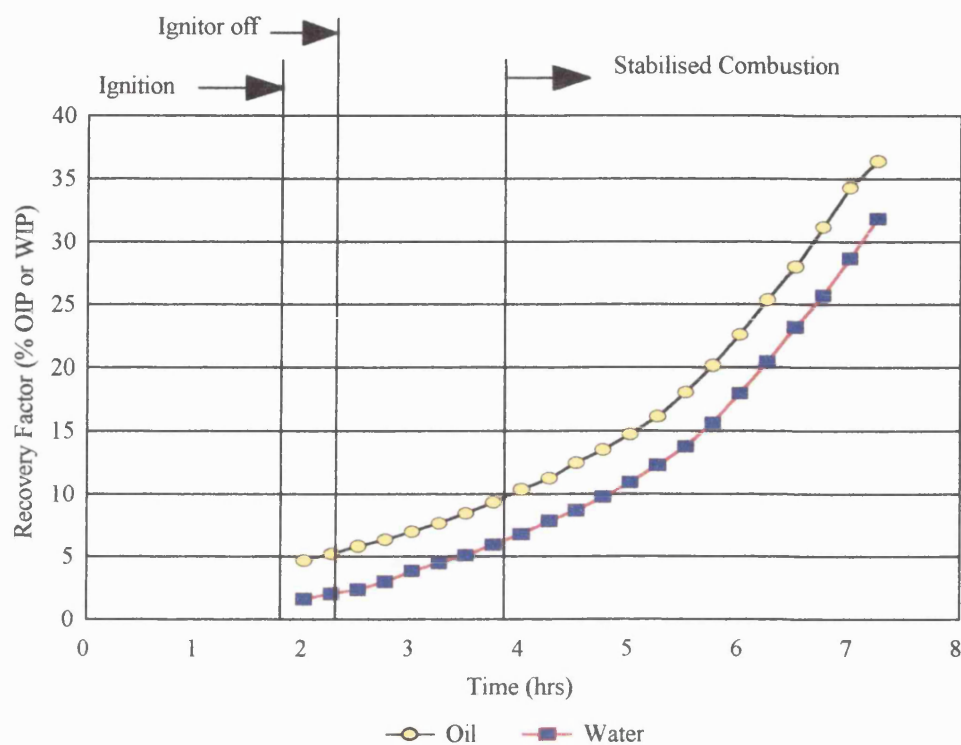


Figure 4.69 Oil and water recovery for upstream well section (Run 966, H.W. Design 3)

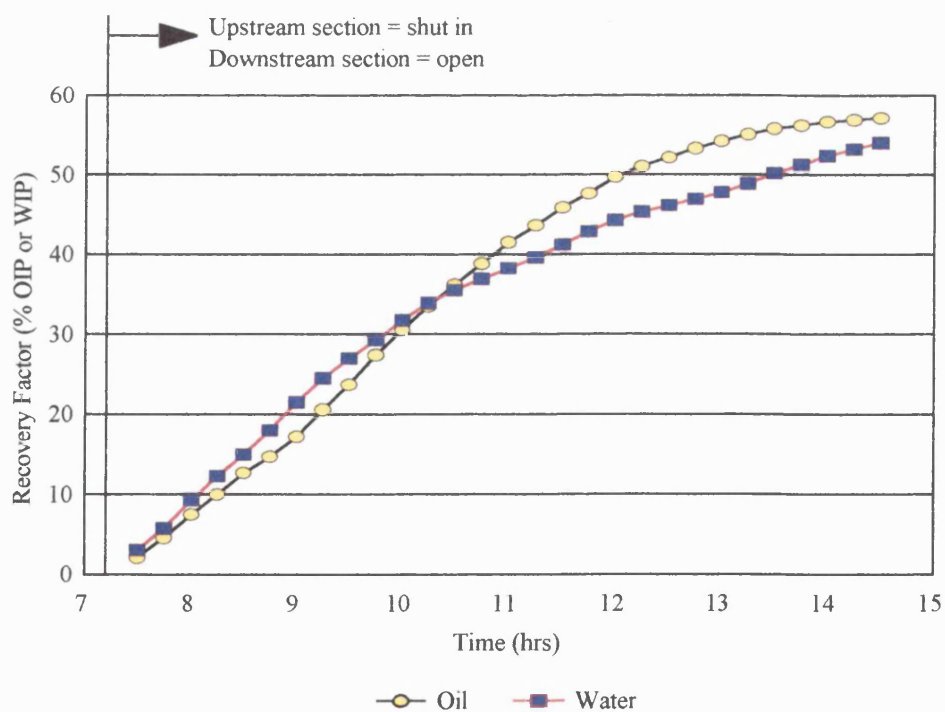


Figure 4.70 Oil and water recovery for downstream well section (Run 966, H.W. Design 3)

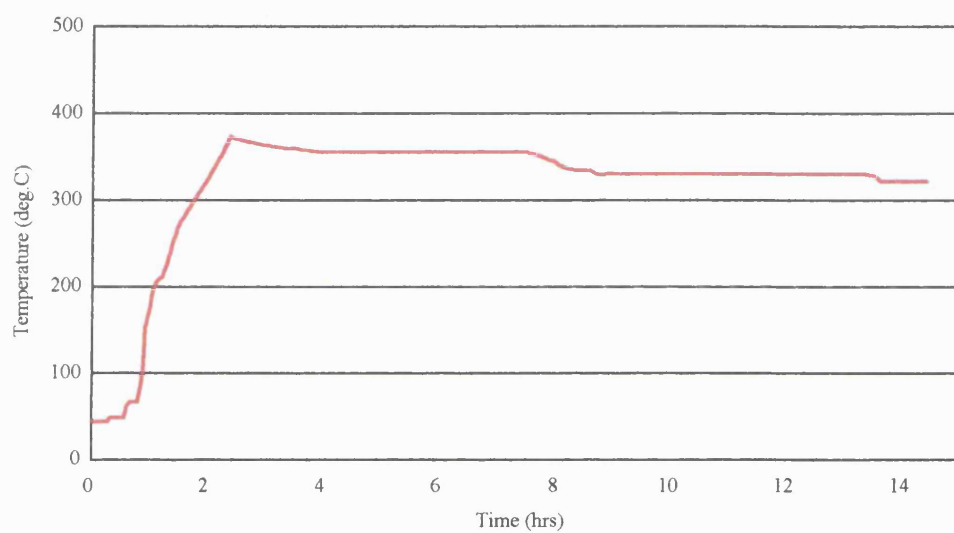
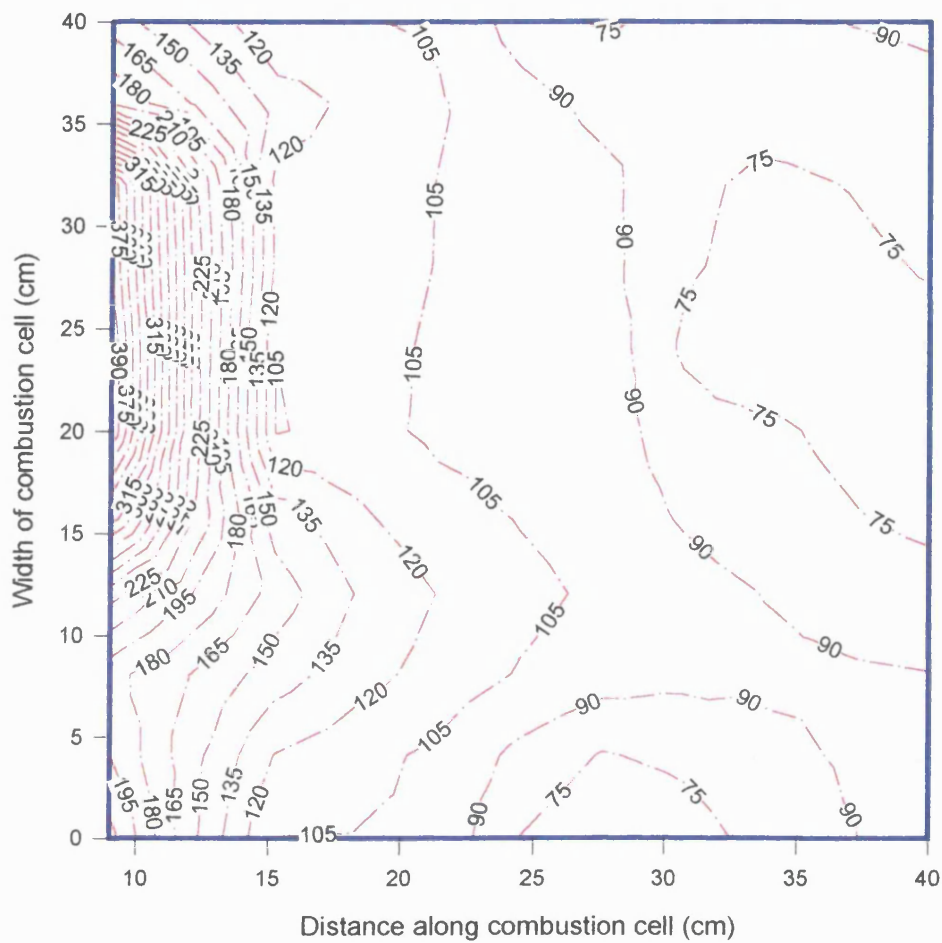
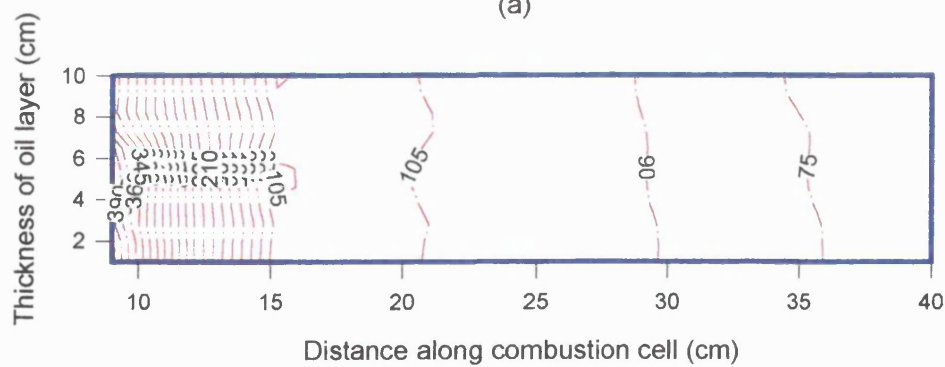


Figure 4.71 Temperature measured by central thermocouple (Run 966, H.W. Design 3)

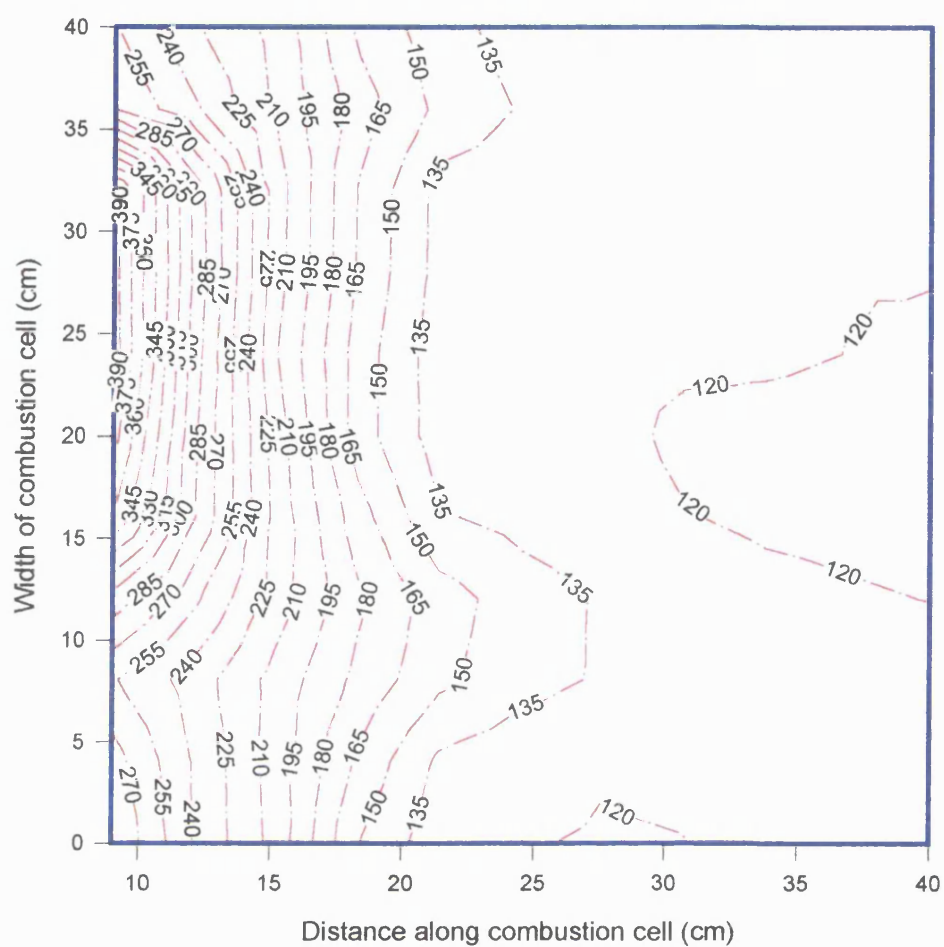


(a)

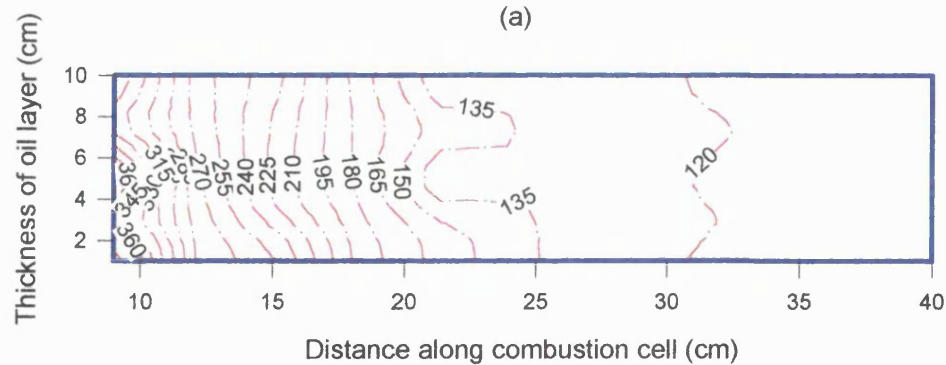


(b)

Figure 4.72 Run 966: Temperature profiles in sandpack (a) Horizontal mid-plane, (b) Vertical mid-plane. [Forties Mix 1 oil, H.W. Design 3]. Combustion Time = 0 minutes

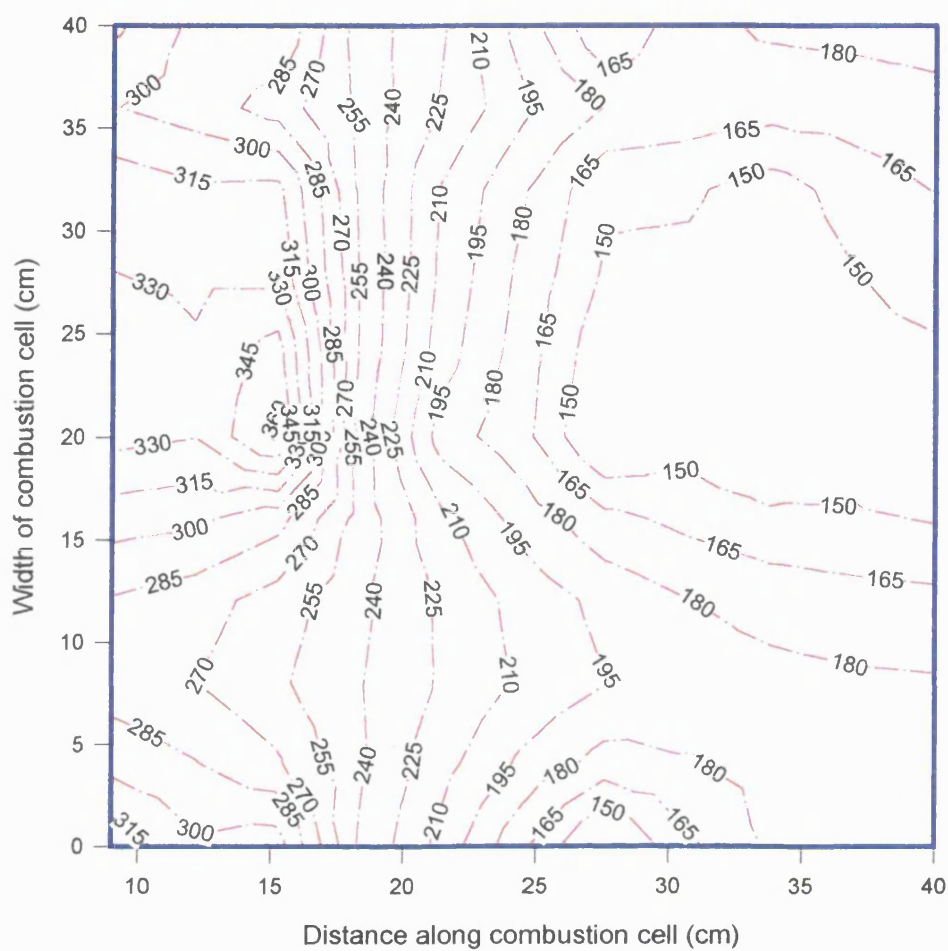


(a)

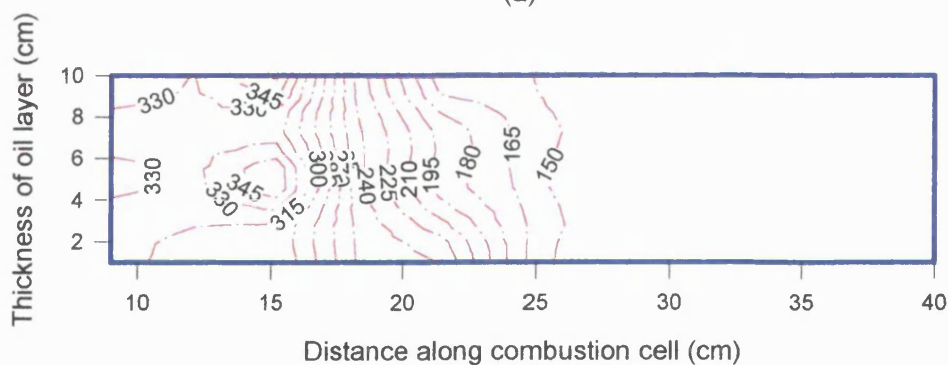


(b)

Figure 4.73 Run 966: Temperature profiles in sandpack (a) Horizontal mid-plane, (b) Vertical mid-plane. [Forties Mix 1 oil, H.W. Design 3]. Combustion Time = 120 minutes

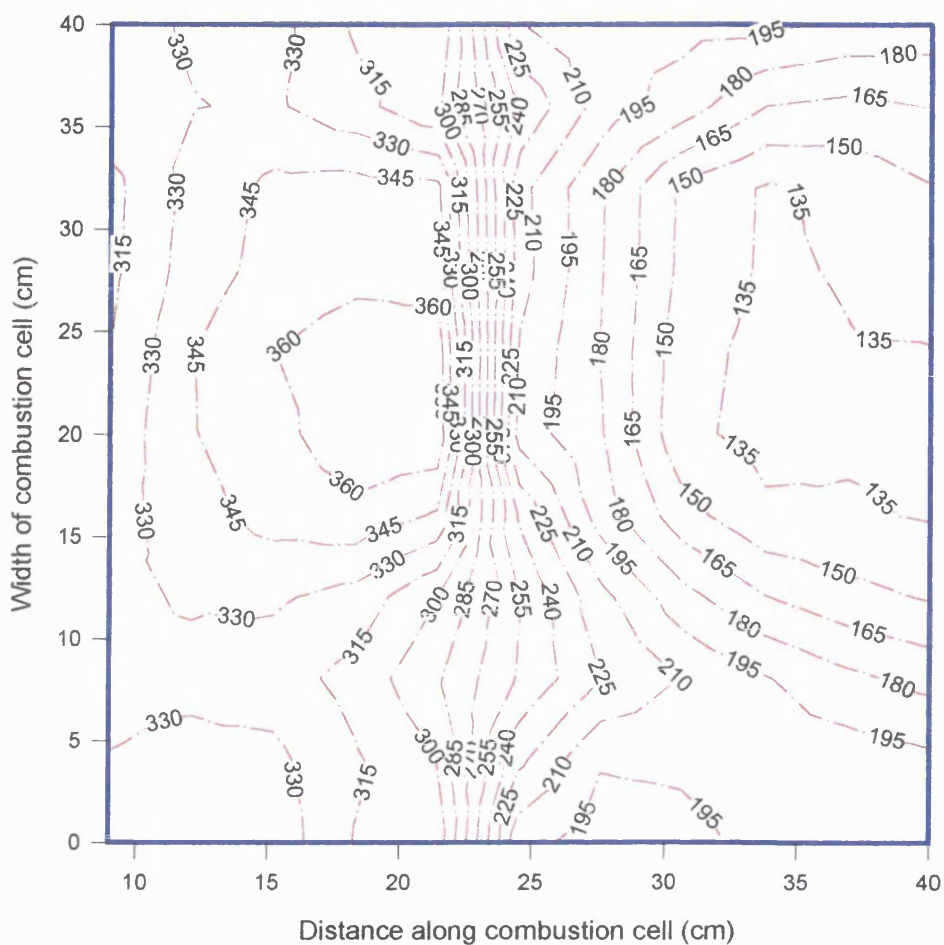


(a)

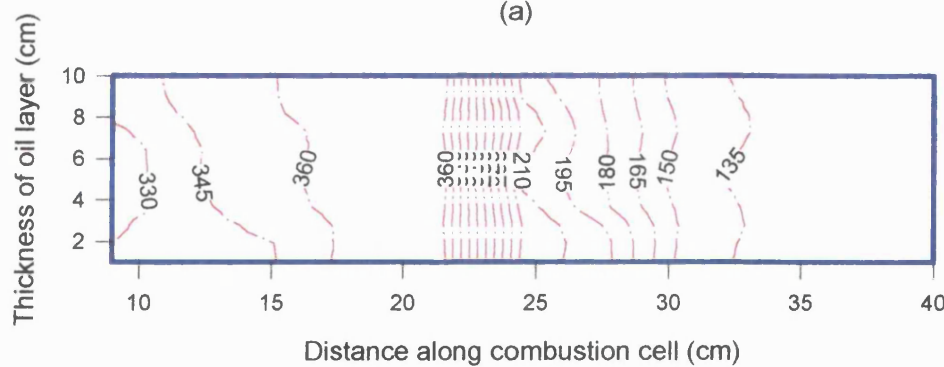


(b)

Figure 4.74 Run 966: Temperature profiles in sandpack (a) Horizontal mid-plane, (b) Vertical mid-plane. [Forties Mix 1 oil, H.W. Design 3]. Combustion Time = 240 minutes

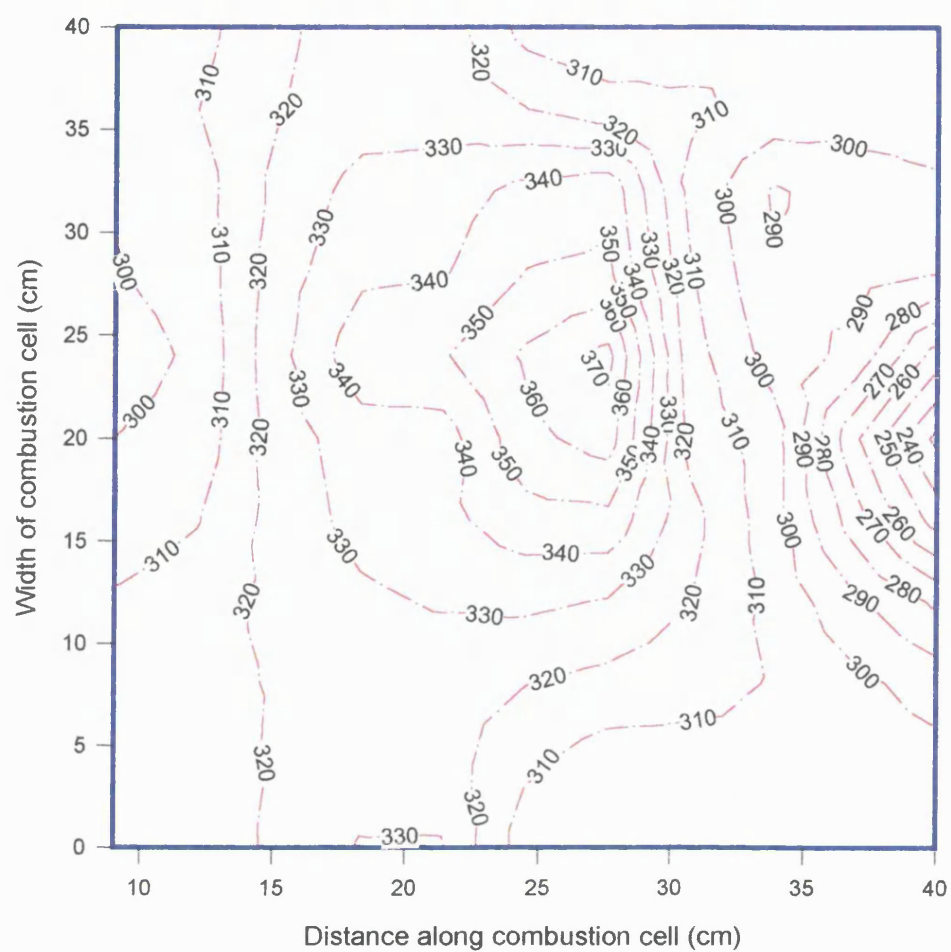


(a)

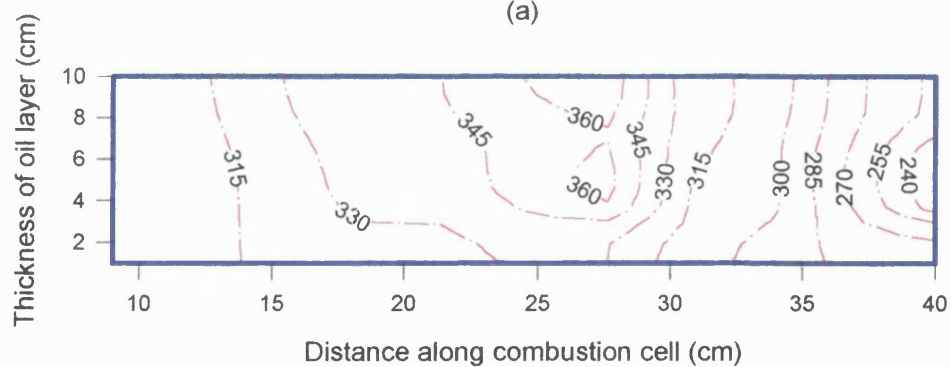


(b)

Figure 4.75 Run 966: Temperature profiles in sandpack (a) Horizontal mid-plane, (b) Vertical mid-plane. [Forties Mix 1 oil, H.W. Design 3] Combustion Time = 431 minutes



(a)



(b)

Figure 4.76 Run 966: Temperature profiles in sandpack (a) Horizontal mid-plane, (b) Vertical mid-plane. [Forties Mix 1 oil, H.W. Design 3]. Combustion Time = 600 minutes

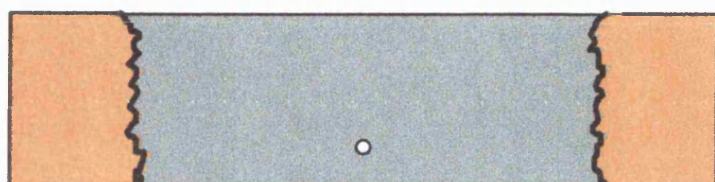
4.2.5 Post-mortem Analysis

Post-mortem analysis of this experiment is based on visual observations recorded during the post-run inspection. At 60mm from the inlet face, Figure 4.77a, clean sand covered the entire sand face, indicating symmetrical ignition during the ignition phase. At 90mm, Figure 4.77b a rectangular shaped burnt zone formed in the central region, covering the entire height of the sandpack, indicates good control of gas override. In addition, a thin coke layer marked the boundary of the clean sand zone. There were two areas of light brown colour restricted at the far sides of the sand pack and covers about 10 % of the sandpack. This is resulted from the lateral expansion of combustion zone as a result of the limited gas flow into downstream zones. At 210mm, Figure 4.77c, a substantial amount of coke surrounding the heel of the upstream well section. Clean sand is still covering wide area above and below the producer, but slightly reduced in size. At 300mm, Figure 4.77d, the clean sand covers 25% of the sandpack and it is located in the top and middle sections of the sandpack. This part is opened to production at later stages of the experiment but it seems to be that this section was efficiently utilized from the shut-in effect of the sleeve-back operation by enlarging the combustion zone size. Thus, more efficient heat distribution is achieved which resulted in higher sweep efficiency than that observed in this section of the sand pack in conventional experiments.

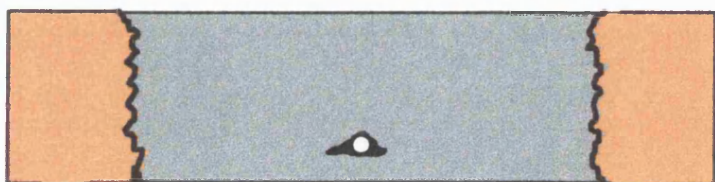
At 350mm, two distinctive zones exist. A light brown coloured zone is restricted in a narrow arch-shaped area in the top section of the sandpack, indicating some degree of gas override may have developed in this part of the sandpack. The second zone has a darker brown colour and covers about 90% of the sandpack.



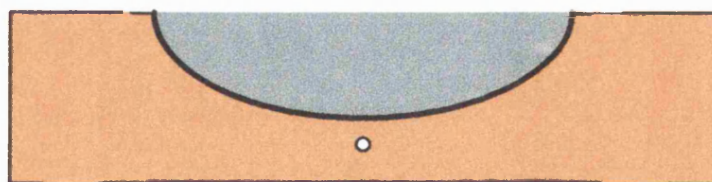
(a)



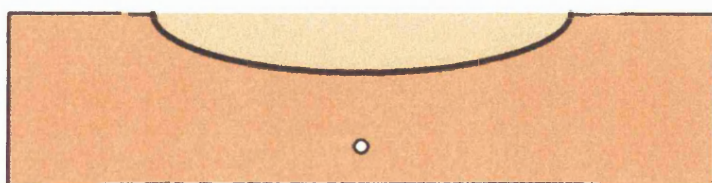
(b)



(c)



(d)



(e)

Figure 4.77 Post-mortem analysis for Run 966 (a) at 60mm, (b) at 90mm, (c) at 210mm, (d) at 300mm, and (e) at 350 mm from inlet of the combustion cell

CHAPTER FIVE

DOWNHOLE CATALYTIC UPGRADING

A total of four forward *in-situ* combustion experiments were made using horizontal wells arranged in a line drive configuration. Two experiments were conducted in a dry mode (Runs 971 and 975) and a further two were carried out in a wet combustion mode (Runs 972 and 976). One dry (Run 975) and one wet (Run 976) combustion experiment involved the use of a catalyst bed surrounding the horizontal producer well. Each experiment was conducted using heavy Wolf Lake crude, having an API gravity of 10.95°.

The following parameters were kept constant during the experiments: air injection flux, water injection rate or WAR, and total combustion time. The operating and initial sandpack conditions are given in Table 3.10.

Before initiating wet combustion, a period of stable dry combustion front was achieved. In both of the wet combustion runs (972 and 976), the time that the ignitor was left on after achieving ignition was minimised by reducing the ignitor power about 25 % every 10 minutes. During the dry phase, the combustion front was travelled about 18 % of the entire sandpack length. Water injection into the sandpack was then commenced at a rate of 2.5 ml/min, equivalent to WAR of $4.2 \times 10^{-3} \text{ m}^3/\text{m}^3$. The wet phase of these runs was allowed to proceed until the temperature at the last row of thermocouples reached 300 °C.

All four experiments were analysed by comparing the properties of the produced fluids, especially the density, API gravity, viscosity, produced gas composition, apparent H/C atomic ratio, carbon molar ratio, oxygen utilisation, oil and water recovery, and the temperature profiles.

5.1 Main Combustion Parameters

5.1.1 Produced gas composition

Figures 5.1 to 5.4 show the composition of the produced gases (CO_2 , CO, O_2) and the maximum combustion temperature as a function of time. Table 5.1 below summarises the produced gas composition for each run.

Table 5.1 Produced Gas Composition

Run		971	972	975	976
Combustion mode		Dry	Wet	Dry	Wet
Catalyst		No	No	Yes	Yes
CO_2 %	(Overall)	14.43	14.24	16.67	16.52
	(Stabilised)	14.30	13.85	16.45	17.1
CO %	(Overall)	4.2	3.95	3.1	2.3
	(Stabilised)	4.0	3.5	2.4	0.31
O_2 %	(Overall)	0.97	1.18	0.80	0.93
	(Stabilised)	1.1	2.3	0.85	1.62

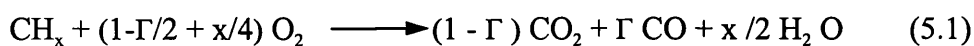
Run 971 was conducted as a conventional dry in situ combustion experiment. From Figure 5.1, the CO_2 and CO concentrations stabilised at 14.3 % and 4.0 % respectively and the O_2 concentration is stable at approximately 1.1 % throughout the experiment time. The very low O_2 level, indicates that most of the oxygen has been consumed by combustion reactions.

Run 975 which also was conducted in dry combustion mode but with a catalyst bed around the horizontal producer well (Figure 5.2) which shows steady levels of CO_2 and CO at 16.45 % and 2.4 % respectively. Comparing with Run 971, the CO_2 level is significantly higher and this effects a lower value of CO and also oxygen at 0.85 %.

Importantly, the smaller amount of CO produced in Run 975 suggests that some conversion of CO to CO₂ has occurred, giving rise to a higher value of CO₂ than produced in Run 971. Similar trends of gas composition are reported by *Moore et al* (1996), who attributed it to the effectiveness of the heated catalyst zone in converting CO and H₂O into CO₂ and H₂ via the water-gas shift reaction.

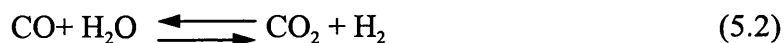
The important reactions taking place are given by Equations 5.1 to 5.4 below:

Combustion Zone:



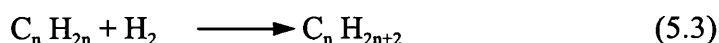
Mobile Oil Zone:

Water-gas shift reaction (WGS):



Annular Catalytic Bed:

Hydrogenation:



Hydrodesulphurisation (HDS):



The gas composition profiles under wet combustion for Runs 972 and 976 are shown in Figures 5.3 and 5.4. They exhibit very similar level as Run 971 and 975 during the dry combustion phase.

When water injection commenced, in **Run 972**, the combustion temperature increased slightly to 477° C. The CO₂ concentration is peaked up and then sharply decreased

before stabilised at 13.85 %. The CO exhibited similar trend, stabilising at 3.5 %, which is lower than that produced in Run 971. During this time, the O₂ value increased from 1.18 to 5.2 %, stabilising at 2.3 %. These fluctuations in gas composition indicate that the combustion was partially quenched since the peak temperature decreased from its dry combustion value of 455° C down to 393 °C.

In **Run 976**, as soon as water injection took place, the combustion temperature increased slightly to 468 °C, but then declined gradually stabilised at 402 °C. The reduction in combustion peak temperature, confirms that the process was operating in a partially quenched mode.

Clearly, the rise in CO₂ concentration from 16.52 to 17.1%, with the drop in CO concentration from 2.3 to 0.31 % is a confirmatory evidence (in addition to the upgrading effect discussed later) that during wet combustion, conversion of CO to CO₂ is promoted by water gas shift. Thus, the increased efficiency of catalyst is, in part, attributed to the effect of the HDS/HDC, when contacted by vaporised water.

In addition, conversion of CO to CO₂ is higher in the catalytic test (Run 976), which suggests that the presence of catalyst may accelerated this conversion.

Johnson and Bright (1985), and *Stapp* (1989) demonstrated the importance of water in upgrading, reporting successful upgrading of heavy oil in the presence of water and brine, with either H₂ or CO, using heterogeneous or homogeneous catalysts.

5.1.2 Apparent H/C and carbon molar ratios:

Figures 5.5 to 5.8 shows the trends of H/C ratio and CO/CO+CO₂ ratio. In all cases, the H/C ratio for the fuel burned was lower than the original value for Wolf Lake crude oil (H/C =1.5), i.e the fuel was of heavier composition and high temperature oxidation was the dominant reaction. A summary of the main combustion results for all of the four runs is given below in Table 5.2.

Table 5.2 Combustion Performance

Run	971	972	975	976
Combustion mode	Dry	Wet	Dry	Wet
Catalyst	No	No	Yes	Yes
Combustion temperature (°C) Maximum	621	625	629	627
Stabilised	452	393	455	402
H/C ratio	0.73	0.71	0.44	0.33
CO/CO+CO ₂	0.22	0.20	0.13	0.017
Air to fuel requirement (sm ³ /kg)	9.485	9.544	9.457	9.81
O ₂ to fuel requirement (sm ³ /kg)	2	2	2	2.06
Fuel burned (% OOIP)	9.1	4.4	8.74	4.27
Oxygen Utilisation (%)	94.8	89	96	92.3
Fuel Consumption (kg/m ³)	40.42	24.8	38.65	24.46
Combustion front velocity (m/hr)	0.016	0.024	0.015	0.022
Air requirement (m ³ /m ³)	563	375	600	409
O ₂ requirement (m ³ /m ³)	118	78	126	86

The H/C ratio for Run 975 was 0.44, which is approximately half than for Run 971.

One possible explanation for this is that a fraction of the hydrogen was consumed to form H₂S and therefore not accounted for in the H/C calculation. A similar effect is observed in the wet combustion runs (Figure 5.7 and 5.8), where the H/C value is lowest at 0.33 for the catalytic test (Run 976) compared to 0.71 in the wet test (Run 972).

The lower value of $\text{CO}/(\text{CO}+\text{CO}_2)$ ratio in both of the catalytic tests compared to the non-catalytic tests, is due to low CO level, especially in the wet combustion test. This is clear evidence for CO consumption in water gas shift reaction.

5.1.3 Oxygen utilisation

Figure 5.9 to 5.12 shows the oxygen utilisation of all of the runs along side with AFR.

Oxygen utilisation is very high during dry combustion, typically greater than 95 %, showing a slight reduction during wet combustion. These high values indicate that very satisfactory combustion was achieved.

The calculated values of oxygen utilisation and AFR are presented in Table 5.2. The AFR for all of the runs lie in the range reported in the literature (*Burger et al*,1985), which is 10 to 12 sm^3/kg .

5.1.4 Fuel consumption and air requirement

The fuel consumption values and air requirement are given in Table 5.2. For the dry runs, the oil consumed as fuel ranged from 8.74 to 9.1 % OOIP, corresponding to 40.42 and 38.65 kg/m^3 for Runs 971 and 975, respectively. The air requirement was high at end of the range 563 and 600 sm^3/m^3 , but consistent with values reported in the literature, which range from about 150 to 600 sm^3/m^3 when air is the injectant gas(*Burger et al*,1985).

The wet combustion runs gave fuel consumption values about one-half those during dry combustion 4.27 and 4.4 % OOIP for Runs 972 and 976, respectively.

Similarly, air requirement was 375 and 409 sm^3/m^3 . Clearly, wet experiments consumed less fuel and required less air because of the high displacement efficiency provided by steam generated during the wet runs. This is also confirmed by high recovery achieved in wet runs, even though the duration was much lower than dry ones.

5.1.5 Oil and water production

Figures 5.13 to 5.24 show the production history for all of the runs. The production performance summarised in Tables 5.3 and 5.4. The amount of oil produced prior to ignition is very small in all of the runs, ranging from 4 to 6.2 % OOIP. The dry combustion runs are characterised by a sharp increase in oil production after ignition, which then peaks and gradually declines during the rest of the run. The trend of oil production during the wet combustion tests is different overall. Figures 5.19 and 5.20 show that after ignition the oil production has already plateaued (Run 972), or only increased by a small amount to reach the first sustained period of high rate production (Run 976) during the dry combustion period of these tests. After commencing water injection, oil production increases to a new higher level, before exhibiting a sharp decline towards the end of each experiment.

The oil recoveries are reasonably high for the non catalytic runs, but slightly lower (11 to 14 %) for the catalytic runs. It is possible that the small particle size of the catalyst (about 250 μA) may have provided additional resistance to inflow to the horizontal producer well compared to the non catalytic runs.

In an actual field application, it is possible that the catalyst could be used in unmodified extrudate form, which has a porosity of about 40 %.

Both of the wet runs achieved high oil recovery (62.3 and 53.2 % OOIP) in about half time compared with the dry runs. This is because of the extensive steam generated during the those runs.

Table 5.3 Production Performance and Sweep Efficiency

RUN	971	972	975	976
Oil produced before ignition (% OOIP)	5	6.2	4	4.5
Water produced before ignition (% OWIP)	2.6	3.3	2.4	3.1
Average oil production rate after ignition (ml/hr)	260	429	222	384
Average water production rate after ignition (ml/hr)	81	135	61	113
Average liquid production rate after ignition (ml/hr)	341	564	283	497
Gas Oil Ratio (m ³ /m ³)	1324	741	1443	715
Total oil recovery (% OOIP)	67.9	62.3	60.4	53.2
Total water recovery (% OWIP)	91.25	86.4	71.14	69.8
Areal sweep efficiency (%)	68	73	64	71
Vertical sweep efficiency (%)	60	59	61	55
Volumetric sweep efficiency (%)	40.8	43	39	39.05

Table 5.4 Oil Recovery (% OOIP)

RUN	Pre-ignition period	Combustion period with ignitor on	Combustion period with ignitor off	Overall
971 Oil recovery (% OOIP)	5	22.2	40.7	67.9
Water recovery (% OWIP)	2.6	18.8	69.85	91.25
972 Oil recovery (% OOIP)	6.2	17.5	38.6	62.3
Water recovery (% OWIP)	3.3	9.3	73.8	86.4
975 Oil recovery (% OOIP)	4	23.4	33	60.4
Water recovery (% OWIP)	2.4	19	49.74	71.14
976 Oil recovery (% OOIP)	4.5	16	32.7	53.2
Water recovery (% OWIP)	3.1	6	60.7	69.8

5.2 Analysis of Produced Liquids

The properties of the produced liquids are very important parameters in this study, and hence, special effort was made to subject the collected samples to a wide range of analysis. In this respect, for example, separation of the oil was conducted via four stages. Firstly, primary separation of free water was carried by heating the samples in a hot water bath at 80°C, then allowing the water to settle down for 2 hours in a specially fabricated glass separator equipped with tap in the bottom end. Depending on the presence of emulsions, some of the samples were centrifuged three times to remove water. The density was measured using a Paar DMA35 density meter and viscosity was measured using Brookfield DV2 viscometer. The density, API gravity, and viscosity are plotted versus time in Figures 5.25 to 5.32. The pH for the produced water was measured by a hand held pH meter, and is presented graphically in Figures 5.33 to 5.36. Tabulated values are given in Appendix (D). One sample of the crude oil and one sample from Run 976 (wet/catalytic), were analysed by British Petroleum Plc by using high temperature GC/SIMDIS and elemental analysis. These results are given in Appendix E and presented graphically in Figure 5.37 and 5.38.

One sample from each run was subjected to SARA analysis (Saturated, Aromatic, Resins, Asphatenes) carried out by the Petroleum Recovery Institute, Calgary. These results are presented in Table 5.7.

5.2.1 Oil Density

In Figures 5.25 to 5.28, the density of the produced oil reduces sharply after ignition. This is more dramatic in the catalytic runs (Run 975 and 976). Except for Run 976, the density then undergoes a slight increase and is then more or less steady for the rest of the experiment. In contrast, Run 976 shows a further reduction in oil density occurred about 1 hour after water injection commences. These trends are mirrored, but in a contra-manner, by the API gravity. The most important finding is that a substantial increase in API gravity of the produced oil is achieved and sustained throughout the experiment. The upgrading achieved due to thermal cracking alone (Runs 971 and 972) is approximately 2 to 3 API points. However, for the catalytic runs (975 and 976) it is much more dramatic, achieving increases of 7 API point (dry catalytic) to 10 API point (wet catalytic).

The upgrading achieved for normal ISC runs (non-catalytic) is lower than that reported in previous studies (see Table 5.5), in which up to 10 API points gravity increase have been reported. The variation in upgrading achieved by these workers can, in part, attributed to the following effects:

1. Air flux
2. Initial bed temperature
3. Clay content

At higher air flux, channelling into downstream zones is more likely to occur due to mobility variations between air and the reservoir oil. This could increase partial oxidation of the oil, causing an increase in the density and viscosity.

Table 5.5 Experimental conditions and upgrading achieved in previous 3-D ISC Experiments

Variable	Present Study	Tuwil (1991)	Wang (1993)	Al-Shamali(1993)	Haweesa (1998)
Reference Test	Run 971	Run 1	Run 4*	DL215	Run 5
Crude type	W.L	M.L	W.L	W.L	W.L
API gravity	10.95	11	10.2	10.95	10.95
Injected gas	Air	Air	Air	Air	Air
Clay content (wt %)	3	0	0	0	10
Initial temperature (°C)	18	90	60	60	70
O ₂ flux (m ³ /m ² .h)	1.89	1.26	2	1.3	1.05
Well configuration	HIHP	VIHP	VIVP	HIHP	HIHP
Oil recovery (% OOIP)	67.9	66.3	37.35	71.57	61.4
Average temperature(°C)	452	402	300	495	452
API of produced oil	13.28	19	9.73	17.3	20.9

* With bottom water layer (50 % of oil layer thickness)

W.L = Wolf Lake

M.L = Marguerite Lake

At lower air flux, the increased oxygen residence time within the high temperature zone, allow combustion reactions to proceed more nearly to completion, minimising or eliminating contact between unreacted oxygen and oil in the downstream zones.

The higher initial bed temperature used in Runs 1,5 and DL 215 (90, 60,70°C respectively) will have significantly affected the combustion temperatures attained and have resulted in a higher level of thermal cracking.

The amount of clay used in Hwessa's Run 5, amounted to 10 wt % of the bed. This may have created some extra catalytic effect, causing more upgrading. On the other hand, it is not certain why the achieved thermal upgrading in Runs 1 and DL215 is so high, because no clay was used.

The variations in separation techniques used to separate the water from the oil , may have significantly affected the measurements. However, this is more likely to give lower API values. Table 5.6 summaries the average API gravity and viscosity measurements during the stabilised combustion period of each run.

Table 5.6 Density and Viscosity of Produced Oil During Stabilised Period

Run	971	972	975	976
Density (g/cc) @ 18 °C	0.975	0.980	0.945	0.928
Viscosity (cp) @ 18 °C	9246	9970	118	34
API gravity	13.61	12.86	18.29	21

The average API gravity, for Run 975, was 18.29 °, which is higher than that obtained in Run 971 by almost 5 points and higher than the original crude oil by 7 points.

At the same stabilised temperature in both runs (452 and 455° C), the efficiency of thermal cracking should, ideally, be similar. But the produced oil in Run 975 has been more highly upgraded and therefore it cannot only be attributed to thermal cracking alone. Hence, this upgrading is due to the presence of the catalyst bed around the horizontal producer well. As the combustion front propagates, CO produced by combustion is reacted via water-gas shift to produce H₂ and CO₂ at the prevailing sandpack temperature of 455 °C. The oil is then upgraded by hydroconversion, involving hydrocracking of large molecules and hydrogen addition. Any excess hydrogen is then available to react with the sulphur present in the crude oil to produce H₂ S.

In surface upgrading operations, the catalyst is normally charged in the oxide state, but optimum activity is not reached until the catalyst becomes sulphided (*Phillipson*, 1970). Production of highly upgraded oil in Run 975 during the early stages of the experiment is partially attributed to the fact that the catalyst used was already pre-sulphided.

The small particle size of the catalyst used (250 µm) could have improved the catalyst performance in two ways. Firstly, it formed a dense catalyst zone around the producer, which had a restricting effect on the production rate, since the total oil recovery was lower in the catalytic runs.

Secondly, the small particle size may have increased the residence time of the oil within the catalyst zone, thereby increasing hydroconversion and HDS.

It is well known that the catalyst activity is proportional to the total external and intra-diffusional surface area of the catalyst, and so, in terms of activity, it is desirable to

have as small particle as possible. This is not practical in large fixed-bed reactors because excessive power would be required to force the reactant through a bed of very fine particles (Pearce *et al*, 1981). Frost *et al* (1971) have noted a marked improvement in desulphurisation rate when catalyst particle size was reduced and Alpert *et al* (1969) have reported the use of a powdered catalyst in an ebullated bed reactor.

In **Run 972**, after combustion stabilised, the oil density exhibited a decreasing trend. The average API gravity during the stabilised period was 12.86 ° API. The density and API gravity trends are shown in Figure 5.27.

In **Run 976**, high API gravity oil was produced in the period following ignition, peaking at 20.5 ° API. Once the combustion stabilised, produced oil density exhibited a relatively steady trend until water was injected into the sandpack. The introduction of water into the sandpack resulted in the highest API gravity achieved in this study. An oil of 22.14 ° API gravity was produced just after 36 minutes from commencing water injection, at a temperature of 453 ° C.

The production of this highly upgraded oil continued until the end of the run. During this period, the reduction in CO was mirrored by an increase in CO₂. These effects can be attributed to the following:

- Increased hydrogen generation due to coke gasification and water-gas shift reactions as the injected water vaporises and contacts the residual coke ahead of the combustion front.
- Stimulation effect by the injected water on the catalyst activity.

Shihabi (1983) has demonstrated that, catalyst activity can be restored by water. Also one of the regeneration methods is by using a steam/air mixture to remove deposits from the catalyst surface, thus restoring their activity (*Goodman et al*,1970). This explains the production of highly upgraded oil in this run.

The average density and API gravity of the produced oil during the wet phase of Run 976 were 0.928 g/cc and 21.0 ° API , whereas the average values during the combined dry and wet periods were 0.944 g/cc, 18.49 ° API, respectively.

5.2.2 Oil Viscosity

Figures 5.29 to 5.32 show the viscosity trends for each run. Generally, the oil viscosity values exhibit a similar trend to the density. During the pre-ignition period, the viscosity of produced oil was similar to the original crude oil. In **Run 971** (dry non-catalytic), Figure 5.29, the lowest viscosity value was recorded during the ignition period, thereafter, it exhibits increasing trend with time, reaching maximum value of 9820 cp by the end of the run, which represents a reduction of 90 % compared to the initial viscosity. In **Run 975**, (dry catalytic), Figure 5.30, a massive reduction in viscosity occurred during the ignition period, indicating that other factors, rather than the higher temperature created by the ignitor, are affecting the oil viscosity. As the run proceeded, the viscosity exhibited an increasing trend for about 6 hours, and then stabilised at about 118 cp, which is about 100 % lower than that achieved in Run 971. Clearly, this large difference in viscosity between the two runs is not due to thermal cracking alone, as the stabilised temperature in both runs is almost identical at 452 and 455 C, respectively.

In **Run 972**, (wet non-catalytic), Figure 5.31, viscosity exhibits a similar trend to that in Run 971 with average value of 9970 cp during the stabilised period. In **Run 976**, (wet catalytic), Figure 5.32, the oil viscosity is very low during the ignition period, averaging 62 cp. After water is injected, the viscosity undergoes a further reduction to 34 cp.

In all runs, except Run 976, there is a trend for the produced oil viscosity to increase following an artificially low value (ignitor effect) and then to level-off to an approximately stable plateau value.

For Run 976 (wet catalytic), from already very low value (62 cp) the oil undergoes a further sharp reduction in viscosity of about 50 % after water injection.

This is an exceedingly low value compared to the original crude, and 70 % lower than that achieved in the dry catalytic run. This can only be explained by the extra hydroconversion occurred as a result of hydrogen produced by water gas shift, enhanced by reaction at the catalyst surface.

Figures 5.33 to 5.36 show the pH of produced water for each run. The water became much more acidic during the dry combustion runs (Run 971 and 975), at a pH of around 2.7. Interestingly, the pH in the wet tests (Run 972 and 976) tends to reach a steady value earlier than in the dry test and also does not fall to such low values, stabilising around a pH of 4. This is due to the effect of the injected water on the acidity of produced water.

5.2.3 Boiling Range Distribution

High temperature GC SIMDIS analysis was conducted on the crude oil and the produced oil from Run 976. The detailed measurements of boiling range distribution are given in Appendix E. Figure 5.37 and 5.38 shows the simulated percent off against the boiling point distribution. The initial boiling point of the produced oil is lowered by 44 C. The final boiling point (FBP) of the Wolf Lake crude is 720 °C with a total distilled amount of 83.11 wt %, whereas analysis of the produced oil has a lower FBP of 619 °C and total distilled amount of 99.5 wt %. The decrease in the boiling point, and reduction in the amount of residue is consistent with the significant upgrading achieved.

5.2.4 Elemental Analysis

The elemental analysis of the produced oil, Figure 5.39, shows a huge reduction in the sulphur content from 43400 mg/kg to 5100 mg/kg compared to the crude oil. This is equivalent to nearly an order of magnitude reduction. In addition, the heavy metal content is considerably reduced from 195 to just 8 mg/kg for the vanadium, and from 73 to 3 mg/kg for nickel. Importantly, Molybdenum in the produced oil is dropped from 7 to 3 mg/kg indicating stability of the catalyst used.

The lower sulphur content in the produced oil indicates vigorous hydrodesulphurisation (HDS) occurred. But, because no oil sample from the non-catalytic runs was elementally analysed, so the reduction in sulphur observed could be due to thermal cracking and the catalytic effect of the catalyst used. This can be verified by analysing the produced oil from the non-catalytic runs (Run 971 and 972) and analysis

of the porous media for sulphur deposition, as well as completing a sulphur mass balance on the produced water and gas.

The much lower metal content in the produced oil indicates that hydrodemetalisation (HDM) occurs and there appeared to be no reduction of catalyst activity during the experiments. In surface upgrading processes, the catalyst is normally deactivated simultaneously by coke and metal deposition, but it not always clear which effect and operating conditions are dominating at different stages of the catalyst life (Bartholomew, 1994).

Takaushi *et al* (1985) have also concluded that deposited metals (from the oil) could interact with the active phase and be themselves active in HDM. It has been also proposed that sustained activity is due to a combination of sulphides of vanadium, nickel and molybdenum, creating new active sites (Simpson *et al*, 1996).

Nonetheless, activity of the catalyst bed used along the horizontal well in this study should be viewed differently because in surface upgrading processes the whole catalyst is at the reactor operating temperature, and hence, the whole catalyst is subjected to deactivation when the reactor is put on operation. In the annular reactor bed along the horizontal well, the catalyst is located near, or within, the combustion zone. It is activated in a sequential manner and HDS and HDM reactions take place with the catalyst in that region only. Therefore, the full active catalyst is provided along the exposed section of the well ahead of the front and this helps to preserve reactivity throughout the run. Because of this, production of highly upgraded oil in the catalytic runs (975 and 976) is maintained throughout the runs even though the hydrogen partial pressure was low.

HDS activity of the Co/Mo catalyst has been tested at Salford University at pressure of 1, 20 and 40 bar over a range of temperatures. It was found that at 1 bar the HDS activity was between 20 and 30 %, whereas at 20 and 40 bars the HDS activity was 60 to 70 %. The conversion was not very sensitive to temperature over a range of 200 to 300°C. Therefore, using the pre-sulphided catalyst in the ISC experiment at 2.9 bar there should be significant HDS activity occurring.

Weissman et al (1996) have found that regardless of the catalyst composition or age similar sulphur removals were obtained. The equivalent activities of different catalysts seems to indicate that feed reactivity controls the extent of sulphur removal. They reported 20-30 % sulphur removal when the oil is processed without a catalyst, probably arising from thermal degradation or volatility of low molecular weight sulphur compounds contained in the crude oil.

5.2.5 Compositional Analysis

One oil sample collected during the stabilised period of each run was subjected to a SARA analysis (Saturates, Aromatics, Resins and Asphaltenes). Results of this analysis are given in Table 5.7. The amounts of saturates and aromatics increased from 69 % in the crude oil to 76 % in Run 971 and up to 79 and 84 % in the catalytic Runs 975 and 976 respectively. Clearly, the highest increase is in Run 976, in which the amount of heavy residuals (resins) is reduced to 16 % from 31 % in the crude oil. This is consistent with the density, viscosity and metal content analysis for Run 976, which indicating that oil in this run has been highly upgraded. On the other hand, Run 972 which conducted without catalyst bed, has recorded the lowest amounts of

saturates and aromatics, it decreased to 65 % from 69 % in the original crude oil.

Similarly, the amount of resins increased to 35 %. This may explain the low API gravity achieved in this run.

Generally, the overall compositional trend of the produced oil is consistent with that reported by *Behar et al* 1988 who used Infrared Spectroscopy to show the different geochemical compositions that affect the crude oil composition after oil samples were produced by *in-situ* combustion. He reported that the amounts of saturates and aromatics increased from 51.4 % in the original crude oil to 72.4 % for the recovered oil. Also, the quantity of asphaltenes and resins decreased from 8.1 % in the crude oil to 4.1 % for the samples produced at the end of the test.

Clearly, the saturates increased very substantially in the catalytic runs to 35 and 46 % in Run 975 and 976, respectively. There is a significant decrease in the aromatic content in the wet combustion runs, but no effect during the dry catalytic test (Run 975).

There is almost a 100 % reduction in the polar A resins in both of the catalytic runs, and also the dry non-catalytic test (Run 971). Only in the wet catalytic test, is there a substantial decrease in resins (polars).

Table 5.7 SARA* Type Compositional Analysis

Parameter	Original Crude Oil	Run 971 Dry Normal	Run 975 Dry Catalytic	Run 972 Wet Normal	Run 976 Wet Catalytic
Saturates Mass %	25	29	35	30	46
Aromatics Mass %	44	47	44	35	38
Polars A Mass %	15	8	7	11	7
Polars B Mass %	16	16	14	24	9
Total Resins	31	24	21	35	16

* Performed by PRI, Calgary

5.2.6 Gas Chromatograph Analysis

Two oil samples were analysed by GC using a flame ionisation detector FID (analyses conducted by BP). The analysis involves applying of an electric current to the poles of the FID, causes the ions to generate an electric current with an intensity proportional to the amount of each hydrocarbon fraction. Results of the analysis are given in Figure 5.40 and 5.41. The GC analysis obtained for the wet catalytic test in Run 976 provides very clear evidence of the substantial upgrading of Wolf Lake crude during this run. Comparing the GC traces shown in Figures 5.40 and 5.41, we can see that the extensive range of heavy species is largely removed and replaced predominantly by lighter components, exhibited by the lighter peaks in the left-most part of the GC chart.

5.3 Temperature Contours

Figures 5.42 to 5.66 show the two-dimensional temperature contour measured in the middle layer of the sandpack starting from the second row of thermocouples. They show the propagation path of the combustion front and leading high temperature zones at various experimental times as a function of distance through the sandpack and also areal extent.

In **Run 971**, Figure 5.43 show vigorous combustion is occurring in the central region of the sandpack, with the combustion front defined by the leading edge of 440-450 °C contour. It is important to note that the combustion zone is located in the centre of the sandpack (vertical section, Figure 5.43 b). This represents a highly stable combustion. At 240 minutes combustion time, the ignitor effect is diminished and the process now is 100 % combustion dominated. Ahead of the combustion zone (Figure 5.44) there is a band of closely-spaced contours, which expanding almost linearly ahead of the combustion zone towards the edges of the cell. It can be seen clearly in Figure 5.44 b and 5.45 b that the contour orientation is almost vertical. These vertical contours ahead of the combustion front indicate the effective drawdown of combustion gases (and mobilised oil) directly into the exposed section of the horizontal well. This gravity-assist, is largely responsible for the control of gas override and the stable combustion front propagation.

It can be seen in Figure 5.45 (a) that the tightly-spaced contours are located in the central region of the sandpack (i.e. above the horizontal producer) whereas they are diminishing towards the sandpack edges where no direct communication into the horizontal producer is exist. The flow of hot gases and oil directly into the horizontal

producer is created by the pressure controlled draw-down of the mobilised fluids. The hot fluids are drained immediately into the horizontal producer, which is the main factor for controlling gas override tendency.

At 480 minutes, Figure 5.46 a, the combustion front has travelled about 16cm of the sandpack length and is still located in the central region, forwarded by tightly- spaced contours downstream. In the vertical mid-plane, Figure 5.46 b, the contours are vertical ahead of the combustion front covering the entire depth of the sandpack.

In Runs 961,962 and 963, performed with much lighter Forties Mix 1 and medium heavy Clair oil, there was initially a mobilised oil zone ahead of the front as we have seen in Run 971, but this then disappeared because the sandpack is became desaturated (see Figs 4.31, 4.37 and 4.42). The very high oil viscosity of the heavy Wolf Lake oil acts to maintain the initial high oil saturation in the downstream region, effectively acting as a 'viscous barrier' to displacement and also providing a measure of sealing along the horizontal well. This was the basic idea on which the sleeve-back design was tested in Run 966.

Comparing the temperature contour of the sleeve-back experiment of Run 966 (Figs 4.73 and 4.74), we can see clearly the similarity in the inflow behaviour with Run 971.

At 600 minutes, the high temperature zone is well stabilised in the central region and the tightly-spaced contours are still located ahead of the front. In the vertical mid-plane section, Figure 5.47, there is a small tendency of gas override in the last third of the sandpack. This may partially be attributed to the production end approach, wherein the lower pressure point is exist. At 720 minuets, Figure 5.48 a and b, the

combustion front still located in the central region, whereas temperature near the production end is about 300 °C. The narrow mobilised zone still exists with no change in its length (about 2cm) whereas it is reduced in width to about 7cm. This may be attributed, in part, to the increased distance from the injector and hence, less uniform air distribution occurred. Also, the increased heat loss near the edges of the sandpack may account for this shrinkage in the mobilised zone width.

Figures 5.49 to 5.54 show the temperature contour maps for **Run 975**. The contours are similar to those observed in Run 971.

In the wet experiment **Run 972**, Figure 5.55 and 5.56 shows that vigorous ignition occurred at the inlet face of the sandpack and a band of tightly-spaced contours is located ahead of the high temperature zone. At 180 minutes combustion time, Figure 5.57 a, the combustion front temperature is declined from about 430 to 390 °C due to the water injection. Most importantly, the mobilised oil is now much more extended than in the dry combustion case, as indicated by the widely-spaced contours. This is due to the much more extensive steam flood in the downstream region. The steam creates a more efficient displacement, desaturating the oil layer downstream. Thus the oil viscosity in the downstream region is substantially reduced and the mobile oil zone is extended over a larger area compared to the dry runs (Run 971 and 975). This may explain the loss of the tightly-closed contours immediately ahead of the combustion front.

Interestingly, in Figure 5.57 b, there is a band of closely-spaced vertical contours ahead of the combustion zone, located about 10cm away downstream. This probably marks the boundary of the “invaded zone”, beyond which the oil is still relatively

immobile (viscous), upstream of this, fluid is drained under pressure controlled gravity assist into the horizontal producer.

At 240 minutes, Figure 5.58 a and b, the temperature near the injection well head has reduced, but the temperature near the toe of the horizontal producer well is still high. This is because of the very low water rate in that section of the horizontal injector well. A similar effect was observed during the post-mortem inspections in dry runs (for example Run 961 and 962), where the left side section of the sandpack was found to contain substantial amounts of residual oil, while the right side section (opposite to the injection well head) was completely clean (see post-mortem photographs in Figures 4.51a and 4.54 a). Therefore, it is poor air distribution, due to non-uniform pressure drop through the injection well.

At 240 minutes, Figure 5.58 a, the high temperature zone has moved further into downstream region, and the temperature near the production end is now around 240°C. Comparing with Run 971, Figure 5.44 a, at the same time, the corresponding temperature was 150 °C. Therefore, there has been a 100°C increase in the wet combustion test. This is obviously due to the expanded steam zone created by water injection.

At 300 minutes, Figure 5.59 a, the high temperature zone (360 to 380°C) is now deviated slightly to the left of the central axis of the sandpack, covering about 20 % of the sandpack. The cooling effect of the injected water is evident in the bottom left-hand corner of the graph (inlet of injection).

At 330 minutes, (Figure 5.60) the high temperature zone expanded further whereas temperature near the injection face declined to about 160 ° C.

In a wet 3D combustion experiment by *Greaves et al* 1998 using a WAR of 7.5×10^{-3} , the temperature in the downstream zones was increased up to 475 °C in the final stages of the run. This may be attributed, in part, to the higher WAR used, which recovered more of the stored heat in the burned out zone, transporting it downstream.

Run 976 (wet catalytic) shown a greater symmetry of temperature compared to the other wet combustion test Run 972 (non-catalytic). At 120 minutes (Fig. 5.62) there is an extensive mobile drainage region ahead of the combustion front, extending across the whole sandpack, over an axial distance of about 10cm. As wet combustion became more stabilised after 70 minutes of water injection (Fig. 5.64), the combustion zone is now about one-third into the sandpack. As the temperature in the downstream region increases due to steam displacement, the controlling effect of the viscous barrier is diminished, and we now have a more extensive inflow along a greater length of the horizontal producer well.

In the field, it is likely, based on these experiments, that the mobile drainage zone ahead of the combustion front would be in order of 10 to 20 meters in width.

Thus, in the absence, or minimal effect of heat exchange from the horizontal producer well transporting heat downstream, we would expect to see a well-controlled mobile during wet combustion. However, if the displacement into the downstream region by steam and consequent substantial heat transport was a large effect, it may be necessary to sleeve-back the horizontal well (as discussed in Section 4.2) in order to preserve a

‘viscosity barrier’ and restrict drainage to the exposed section of the horizontal well.

This is very important for catalytic upgrading, in order that the length of the annular reactor is kept constant and conditions in the mobilised oil zone are also maintained constant.

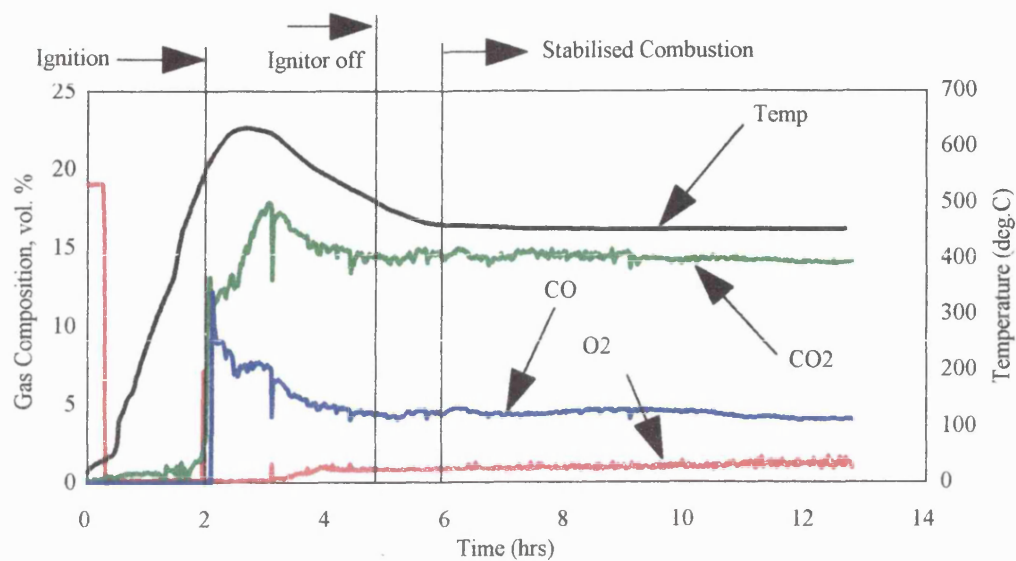


Figure 5.1 Produced gas composition for Run 971 (Dry normal, Wolf Lake)

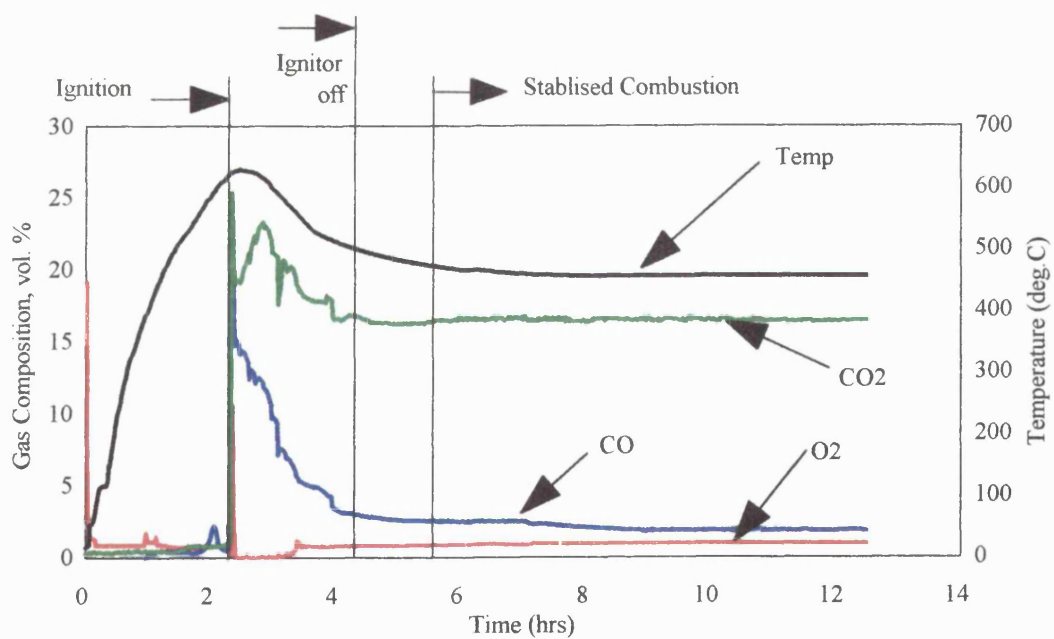


Figure 5.2 Produced gas composition for Run 975 (Dry catalytic, Wolf Lake)

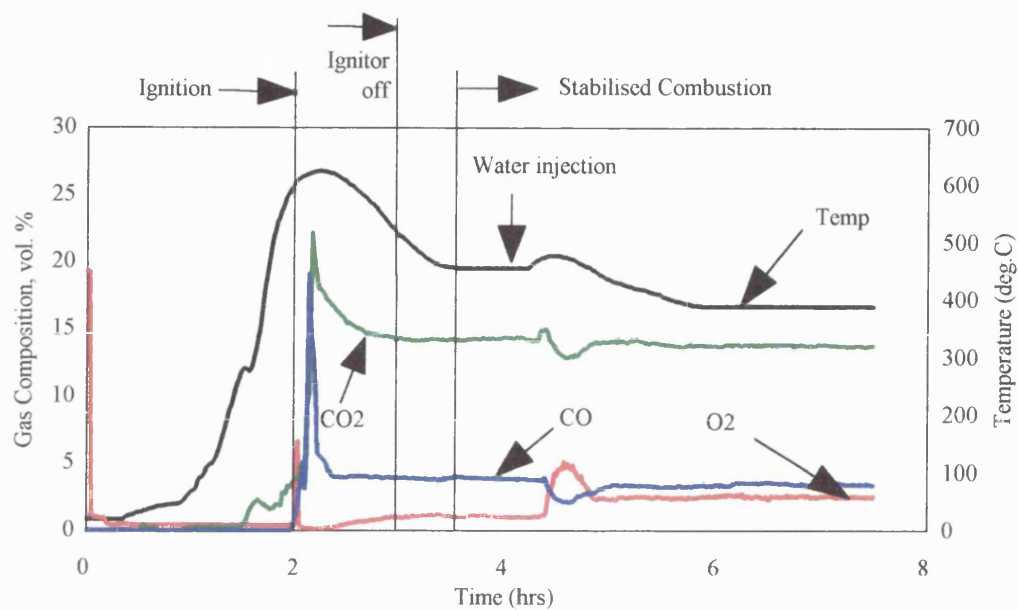


Figure 5.3 Produced gas composition for Run 972 (Wet normal, Wolf Lake)

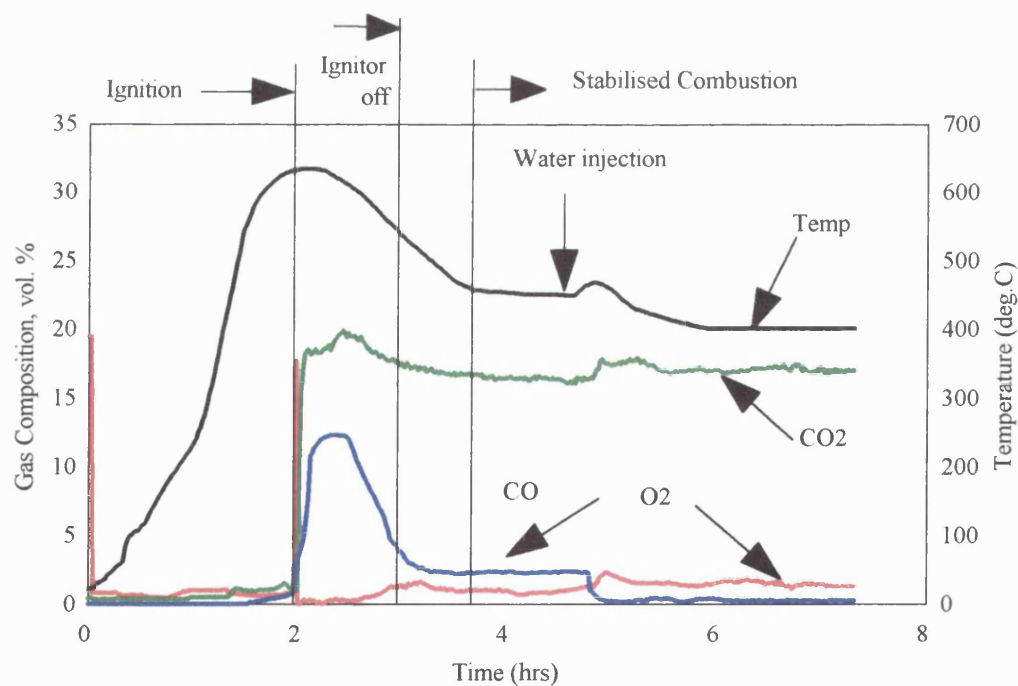


Figure 5.4 Produced gas composition for Run 976 (Wet catalytic, Wolf Lake)

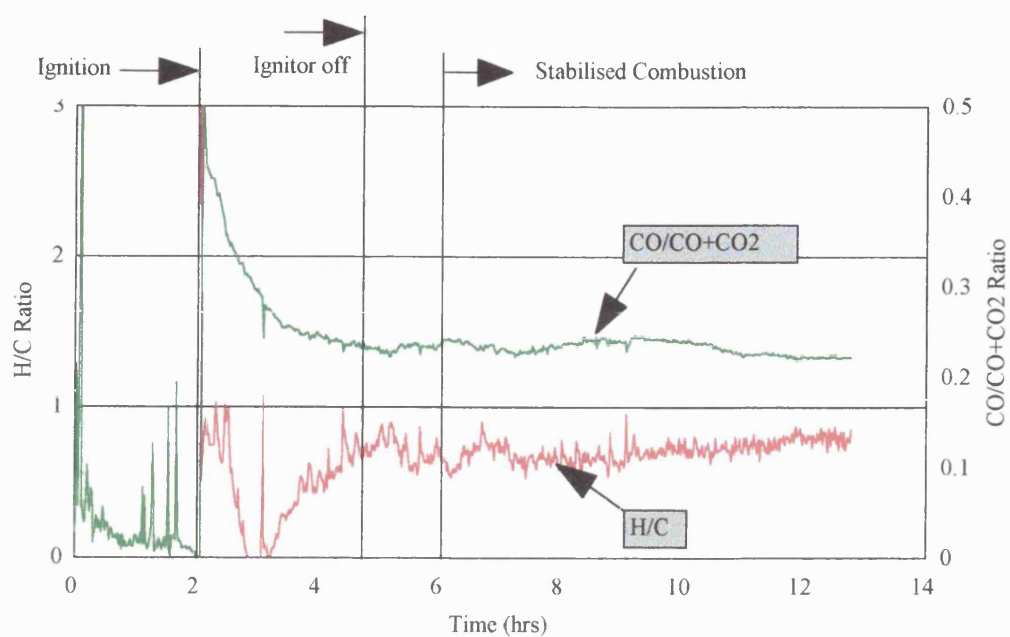


Figure 5.5 H/C and CO/CO+CO₂ ratio for Run 971 (Dry normal, Wolf Lake)

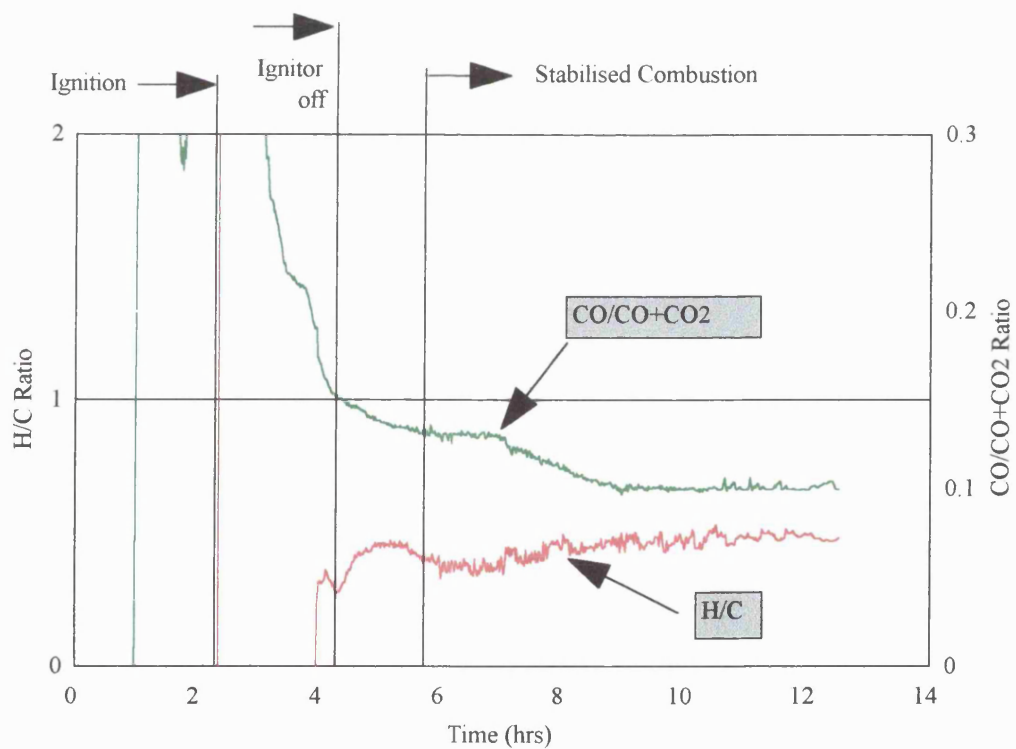


Figure 5.6 H/C and CO/CO+CO₂ ratio for Run 975 (Dry catalytic, Wolf Lake)

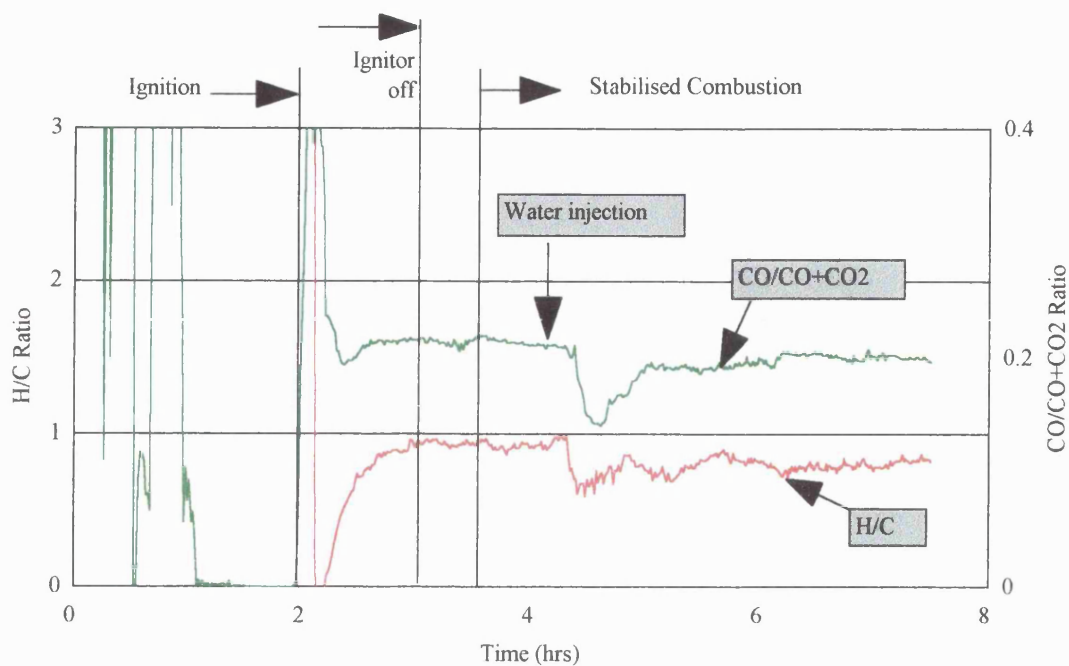


Figure 5.7 H/C and CO/CO+CO₂ ratio for Run 972 (Wet normal, Wolf Lake)

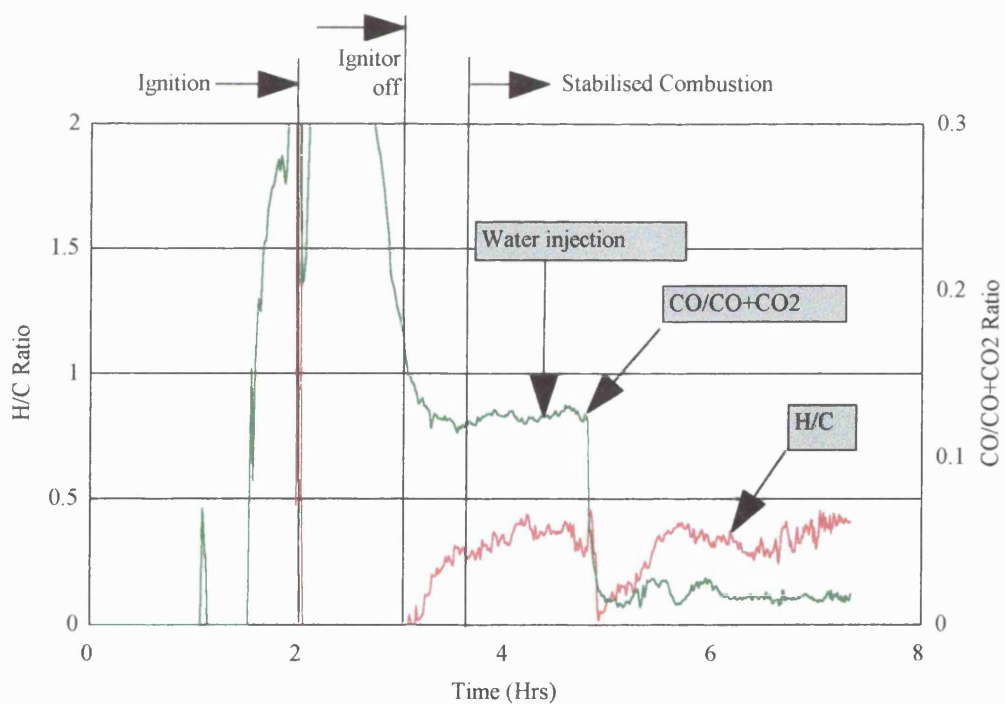


Figure 5.8 H/C and CO/CO+CO₂ ratio for Run 976 (Wet catalytic, Wolf Lake)

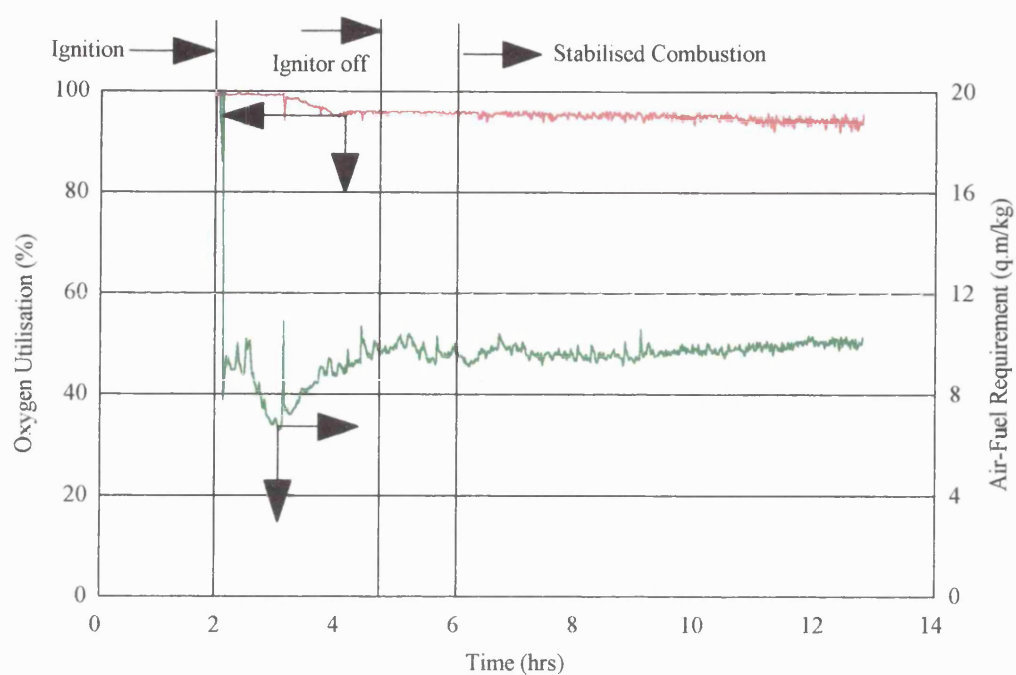


Figure 5.9 Oxygen utilisation and AFR for Run 971 (Dry normal, Wolf Lake)

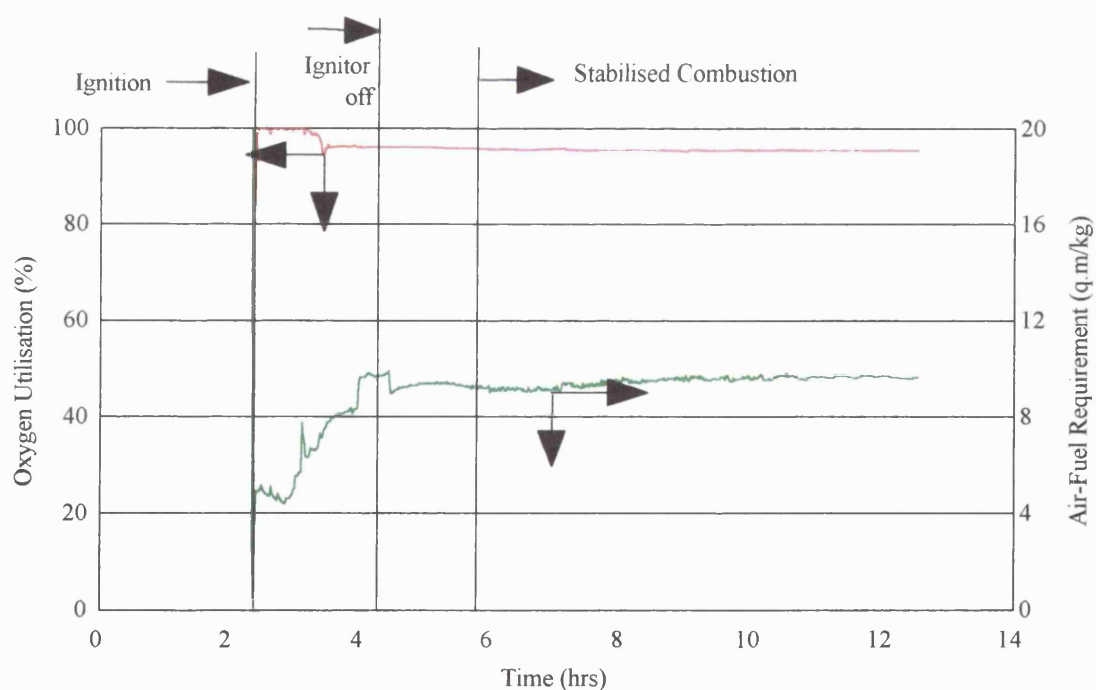


Figure 5.10 Oxygen utilisation and AFR for Run 975 (Dry catalytic, Wolf Lake)

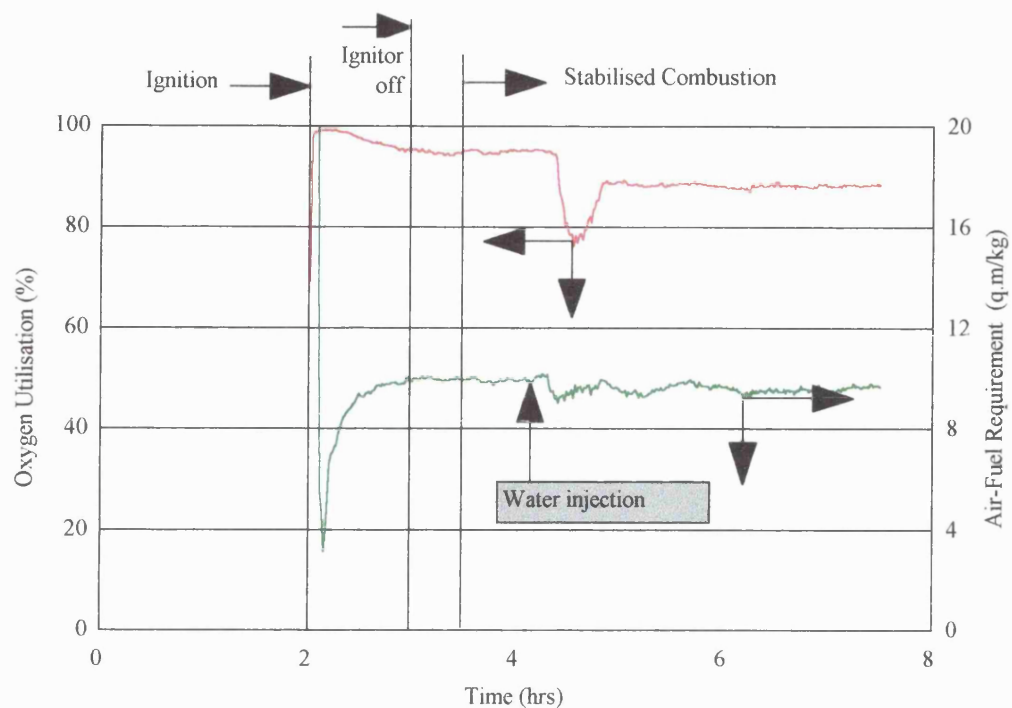


Figure 5.11 Oxygen utilisation and AFR for Run 972 (Wet normal, Wolf Lake)

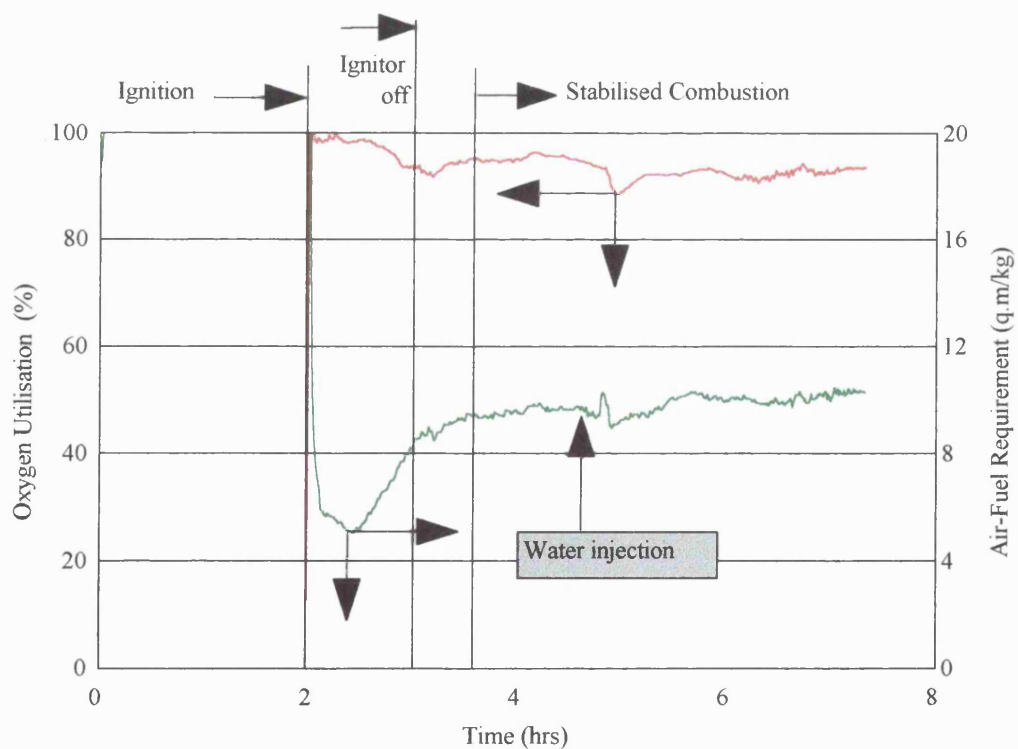


Figure 5.12 Oxygen utilisation and AFR for Run 976 (Wet catalytic, Wolf Lake)

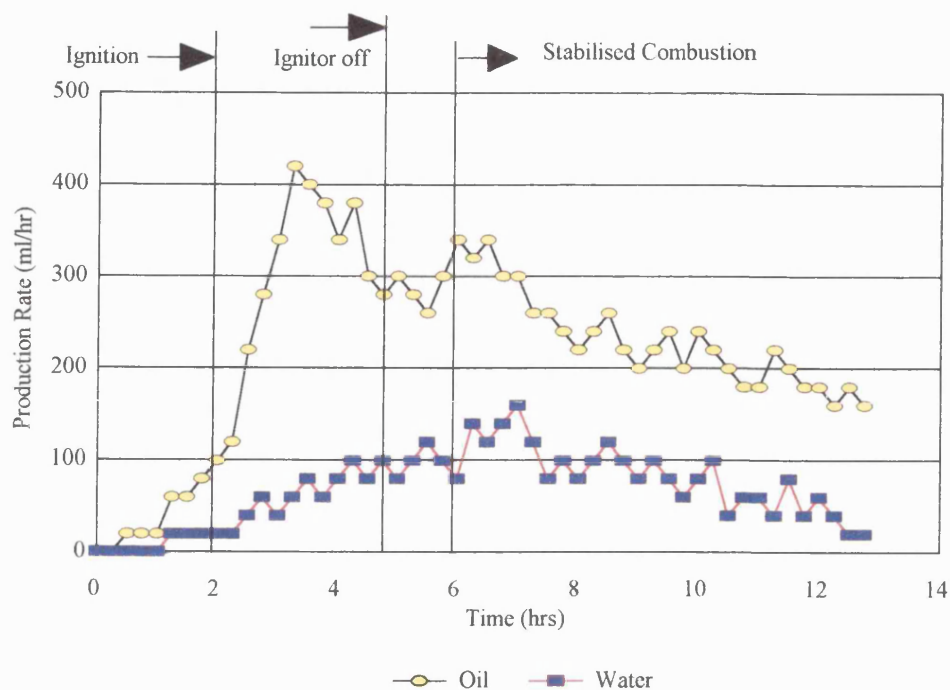


Figure 5.13 Oil and water production rate for Run 971 (Dry normal, Wolf Lake)

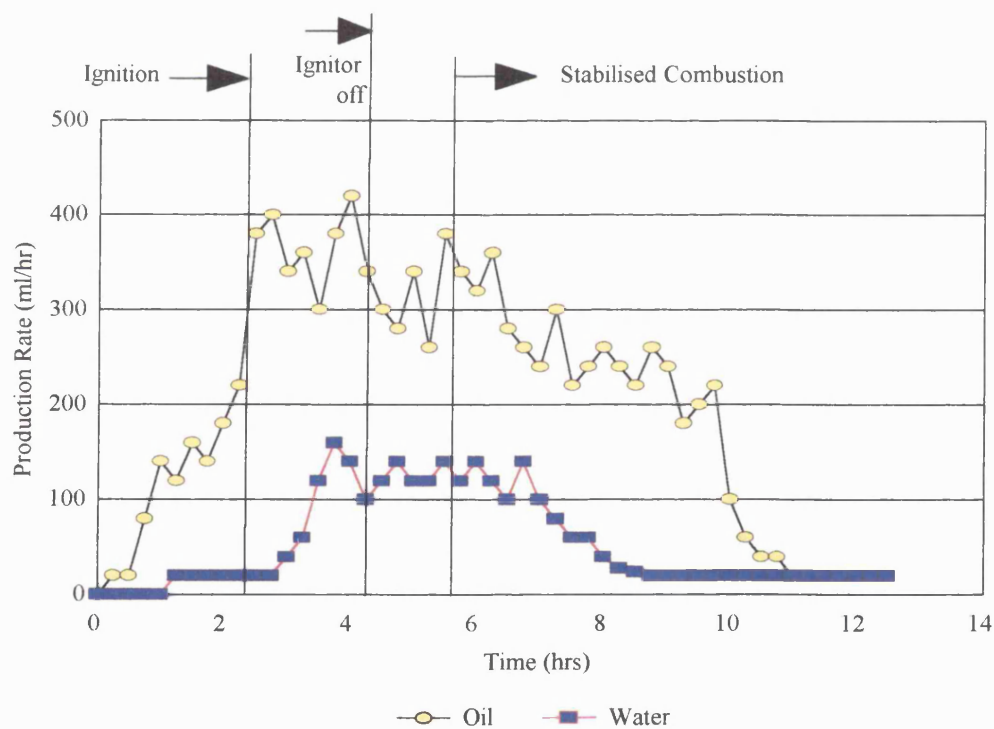


Figure 5.14 Oil and water production rate for Run 975 (Dry catalytic, Wolf Lake)

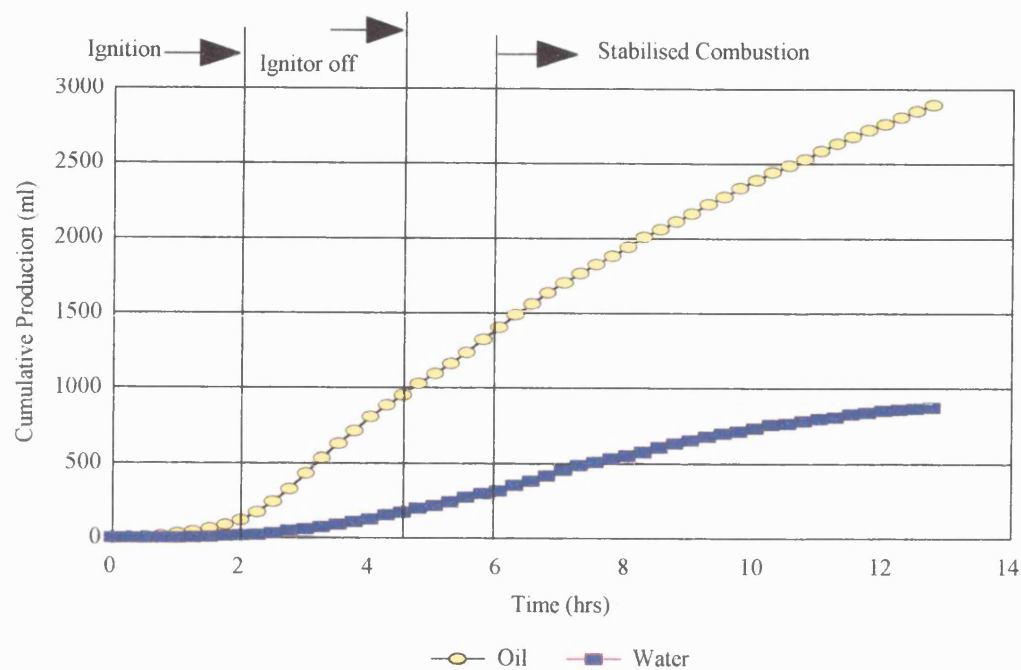


Figure 5.15 Cumulative production for Run 971 (Dry normal, Wolf Lake)

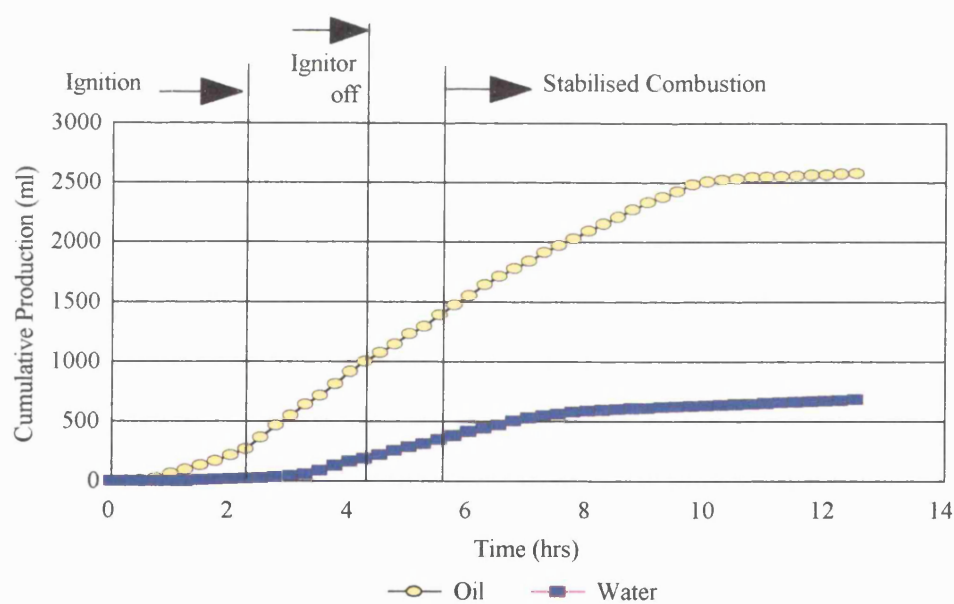


Figure 5.16 Cumulative production for Run 975 (Dry catalytic, Wolf Lake)

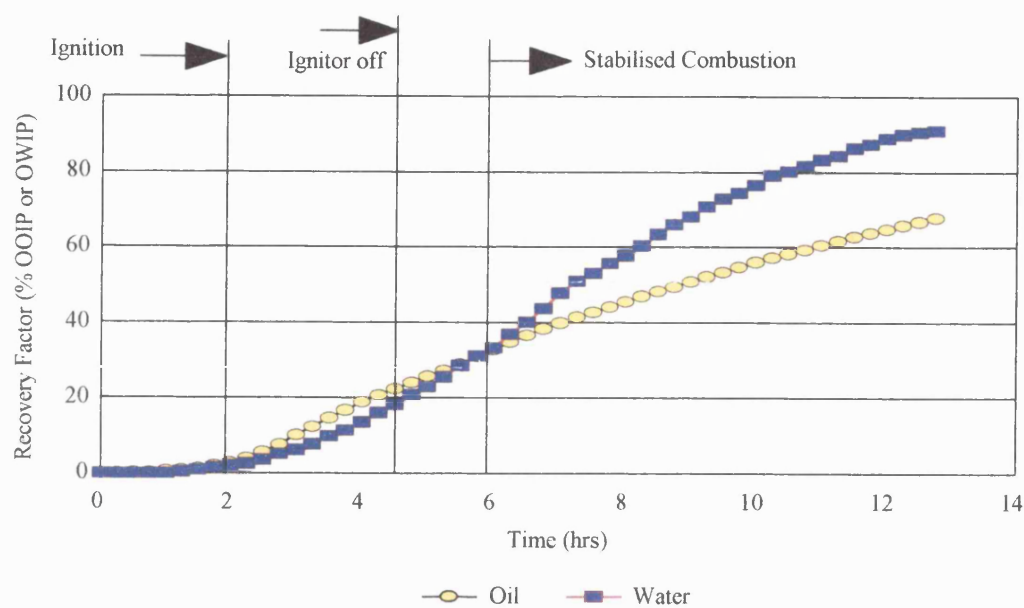


Figure 5.17 Oil and water recover for Run 971 (Dry normal, Wolf Lake)

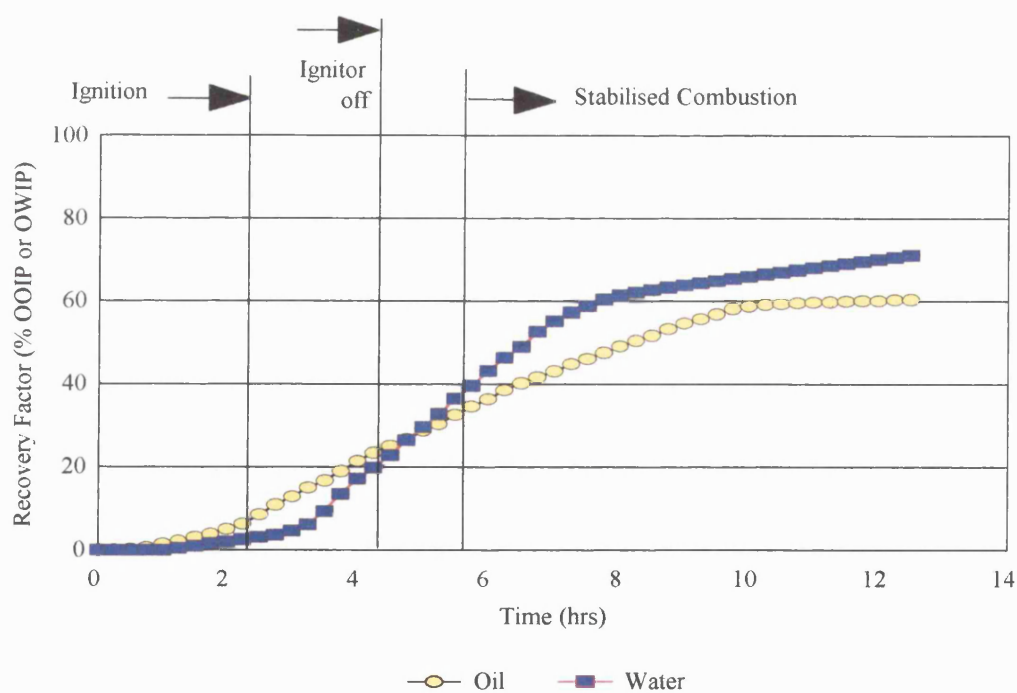


Figure 5.18 Oil and water recovery for Run 975 (Dry catalytic, Wolf Lake)

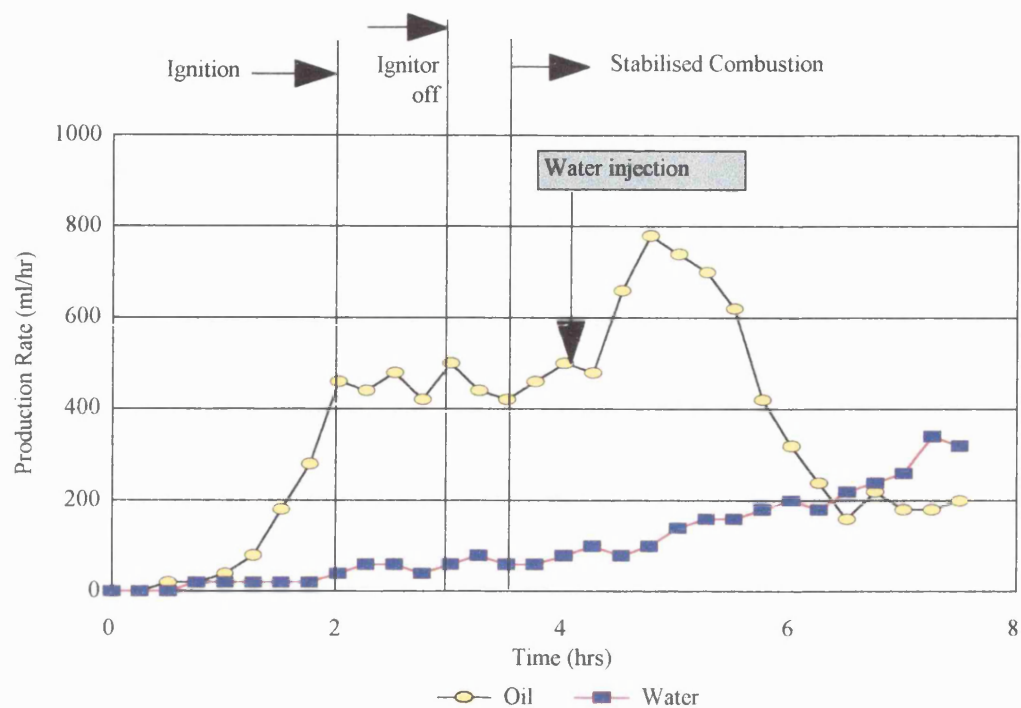


Figure 5.19 Oil and water production rate for Run 972 (Wet normal, Wolf Lake)

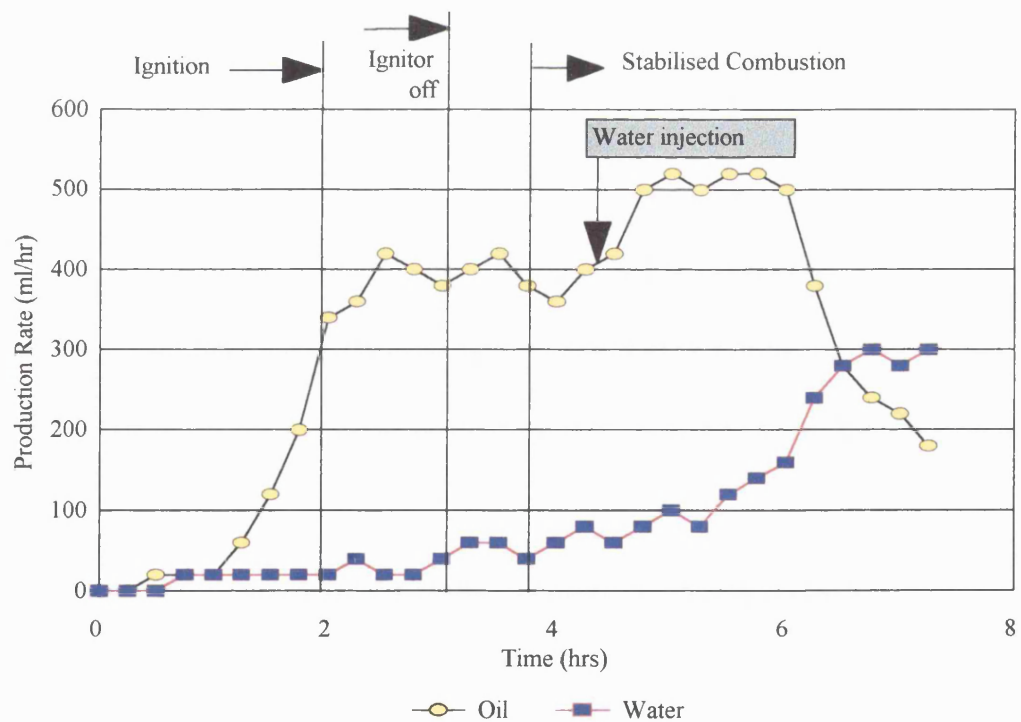


Figure 5.20 Oil and water production rate for Run 976 (Wet catalytic, Wolf Lake)

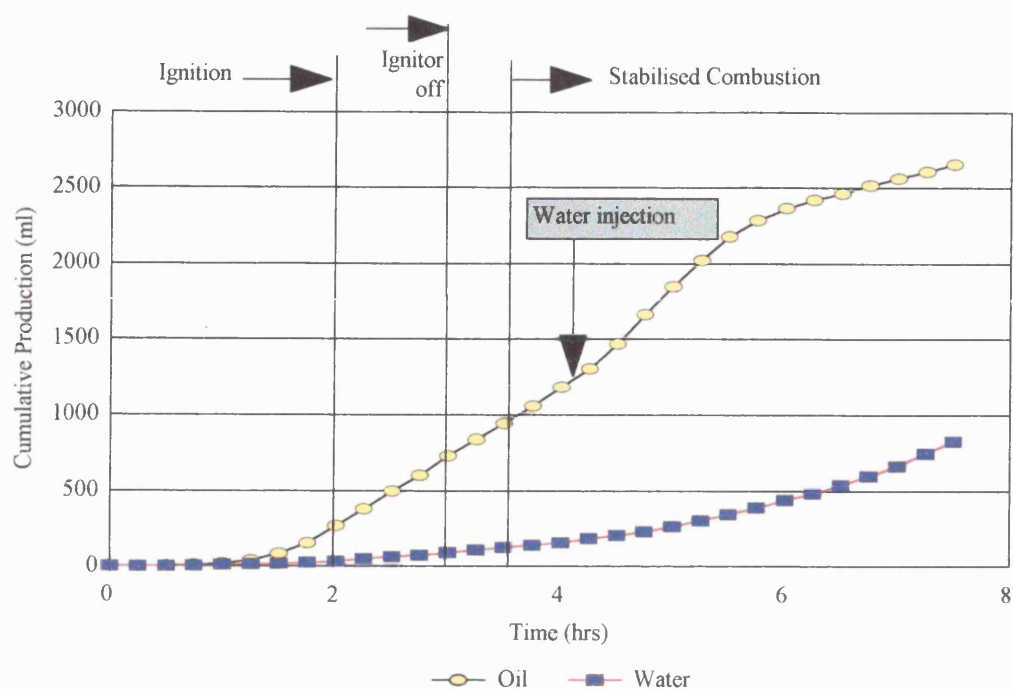


Figure 5.21 Cumulative production for Run 972 (Wet normal, Wolf Lake)

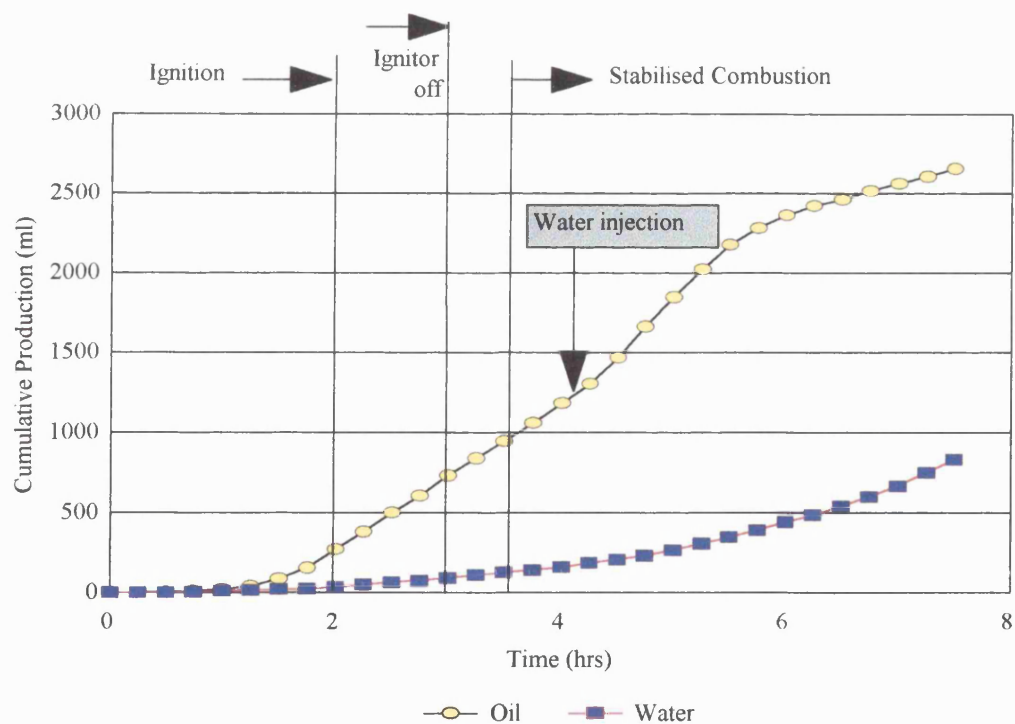


Figure 5.22 Cumulative production for Run 976 (Wet catalytic, Wolf Lake)

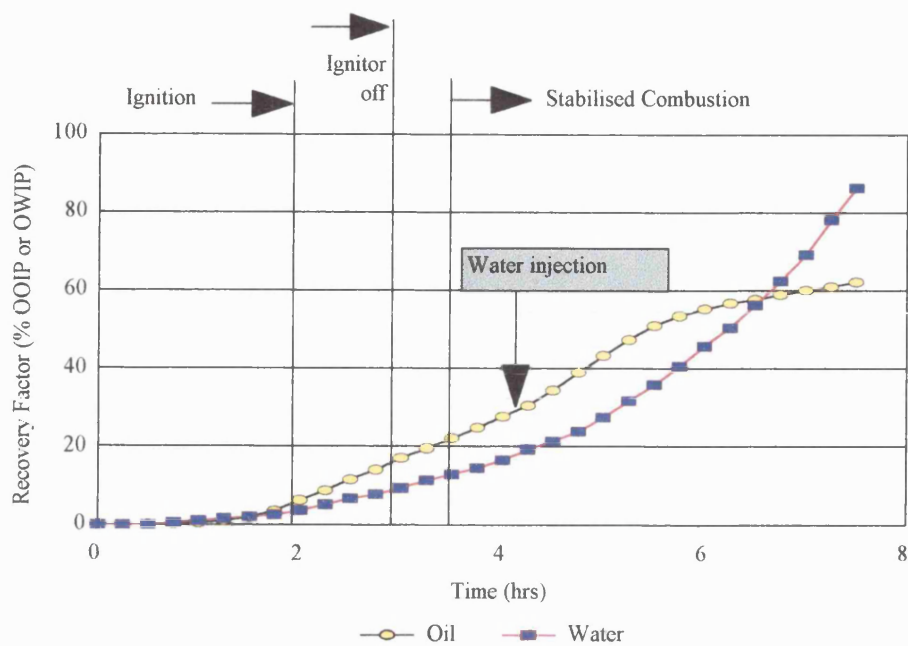


Figure 5.23 Oil and water recovery for Run 972 (Wet normal, Wolf Lake)

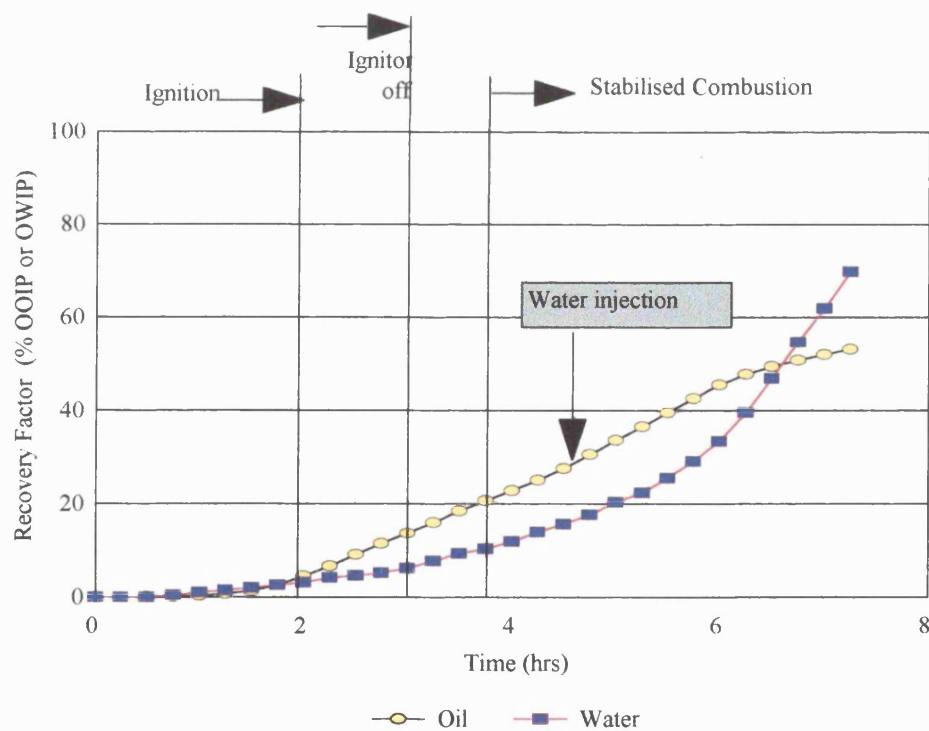


Figure 5.24 Oil and water recovery for Run 976 (Wet catalytic, Wolf Lake)

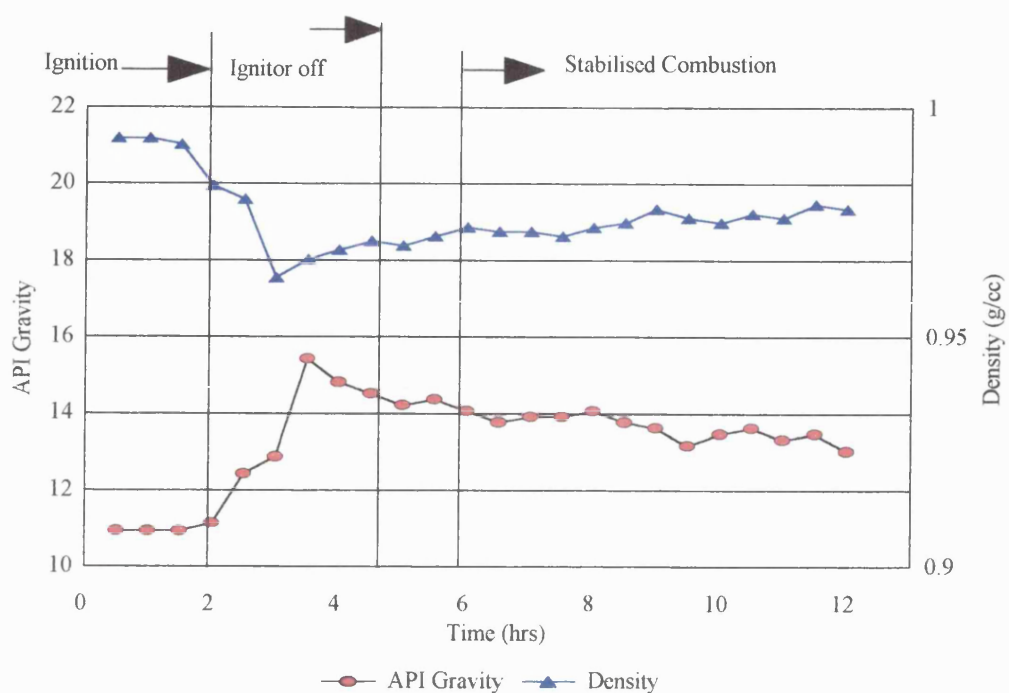


Figure 5.25 Density and API gravity for Run 971 (Dry normal, Wolf Lake)

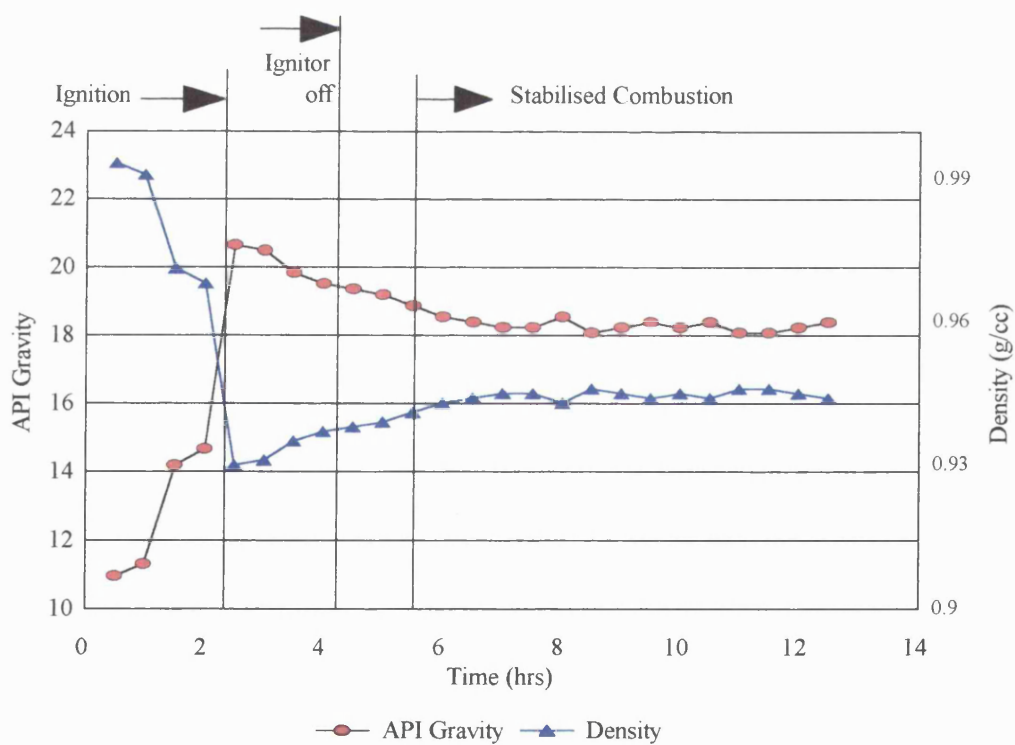


Figure 5.26 Density and API gravity for Run 975 (Dry catalytic, Wolf Lake)

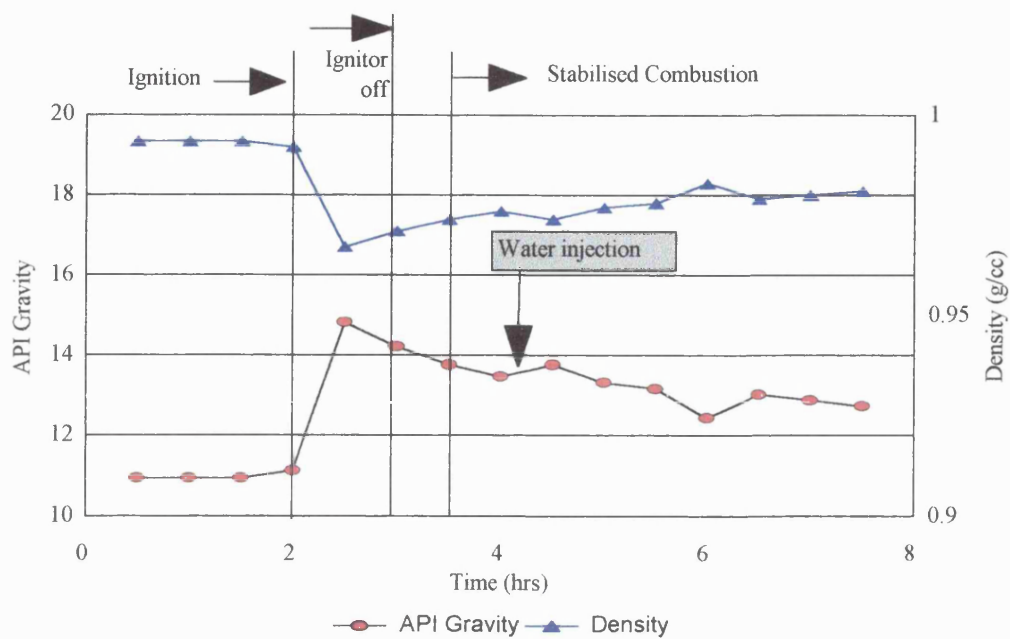


Figure 5.27 Density and API gravity for Run 972 (Wet normal, Wolf Lake)

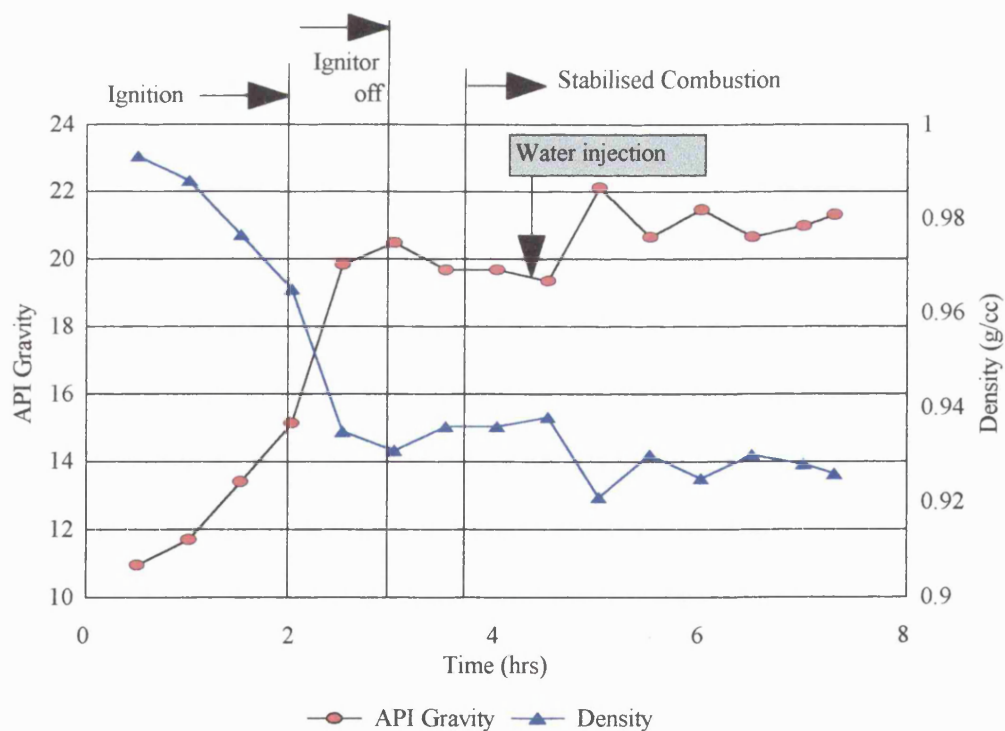


Figure 5.28 Density and API gravity for Run 976 (Wet catalytic, Wolf Lake)

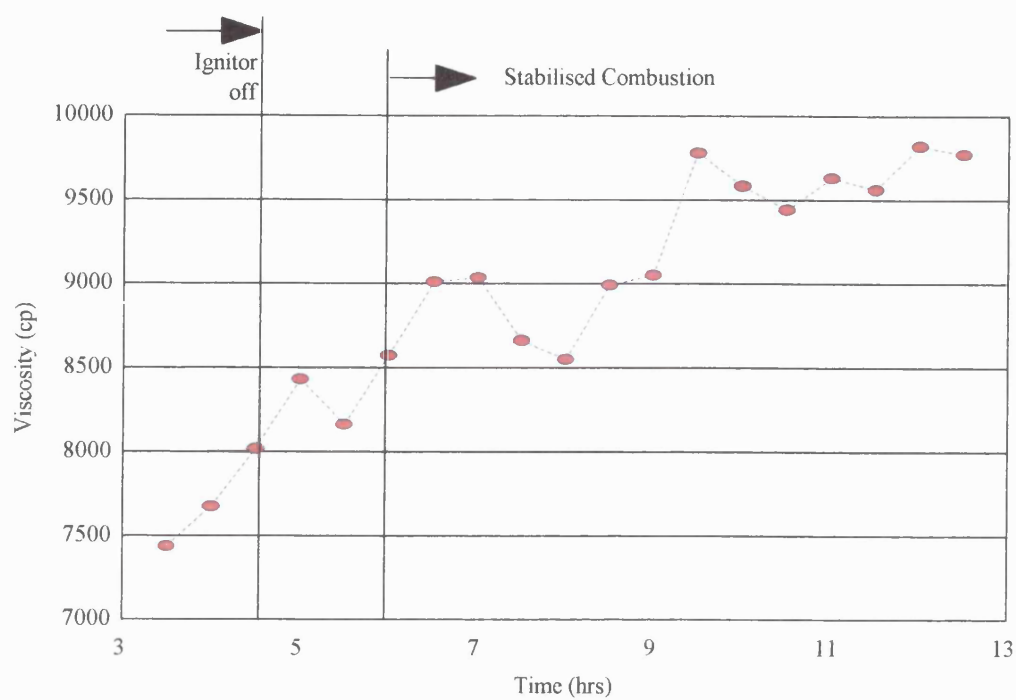


Figure 5.29 Oil viscosity for Run 971 (Dry normal, Wolf Lake)

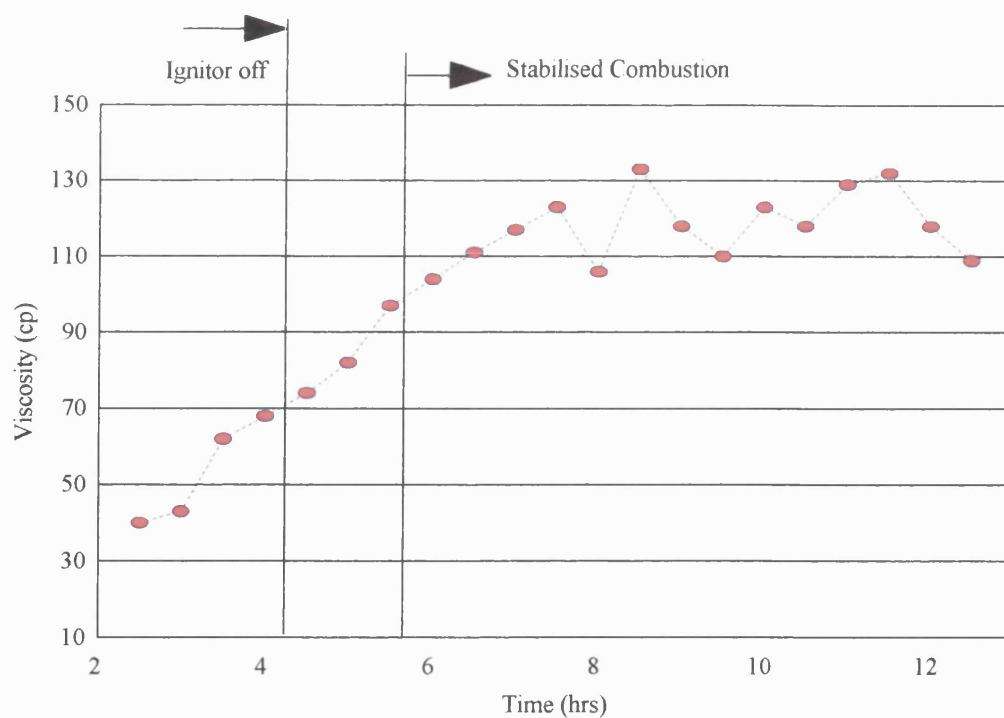


Figure 5.30 Oil viscosity for Run 975 (Dry catalytic, Wolf Lake)

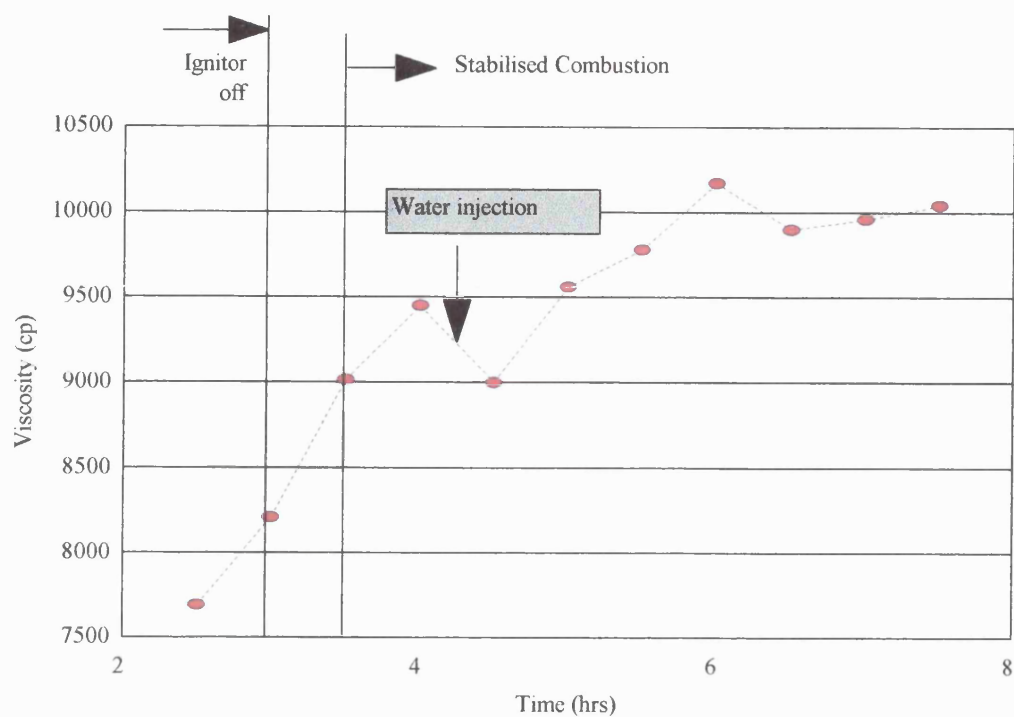


Figure 5.31 Oil viscosity for Run 972 (Wet normal, Wolf Lake)

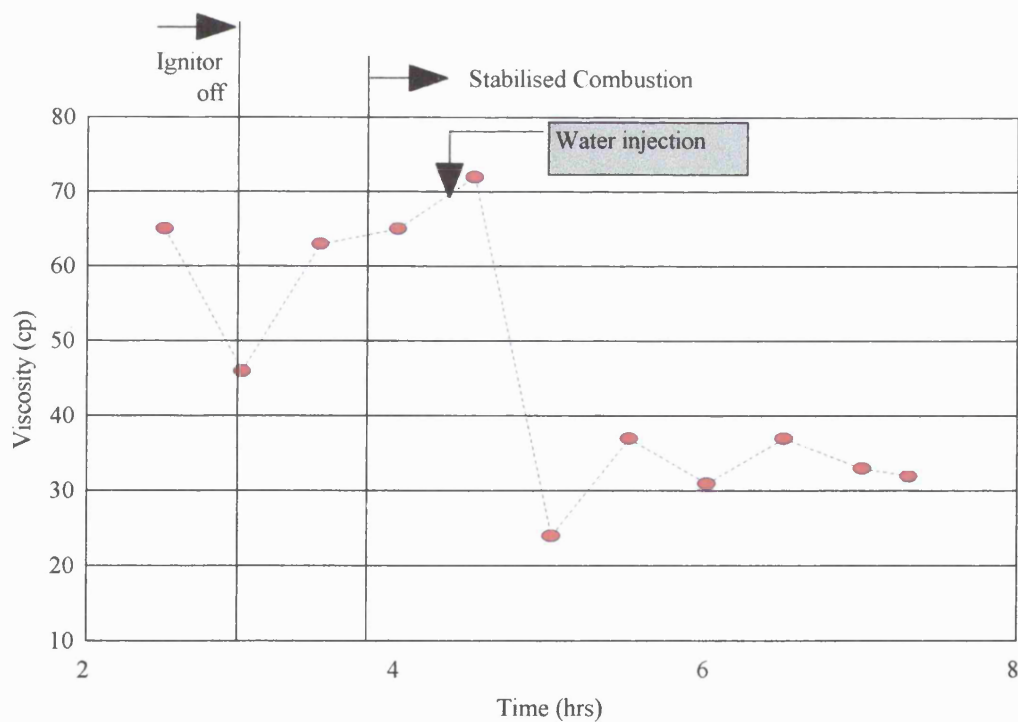


Figure 5.32 Oil viscosity for Run 976 (Wet catalytic, Wolf Lake)

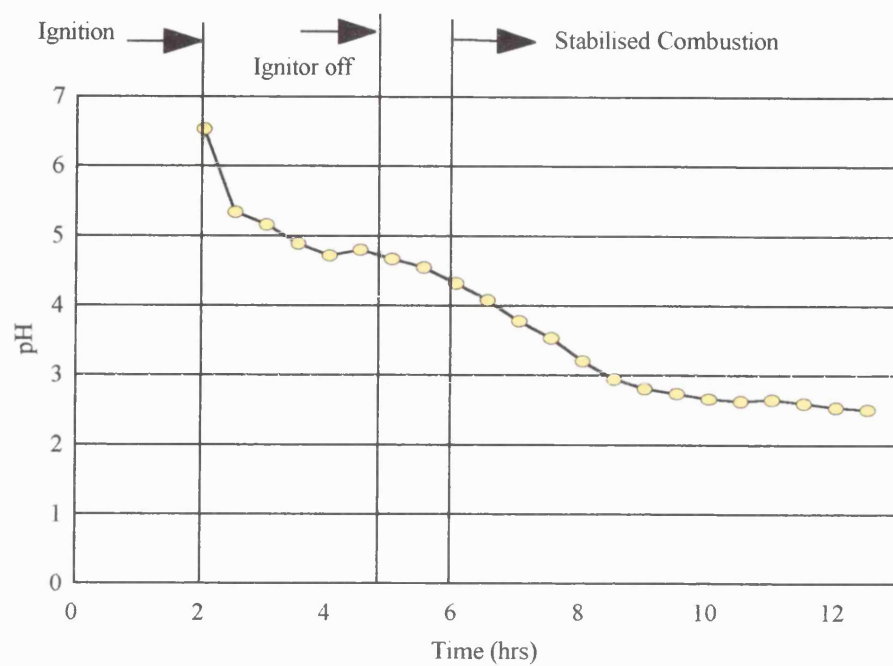


Figure 5.33 pH of produced water for Run 971 (Dry normal, Wolf Lake)

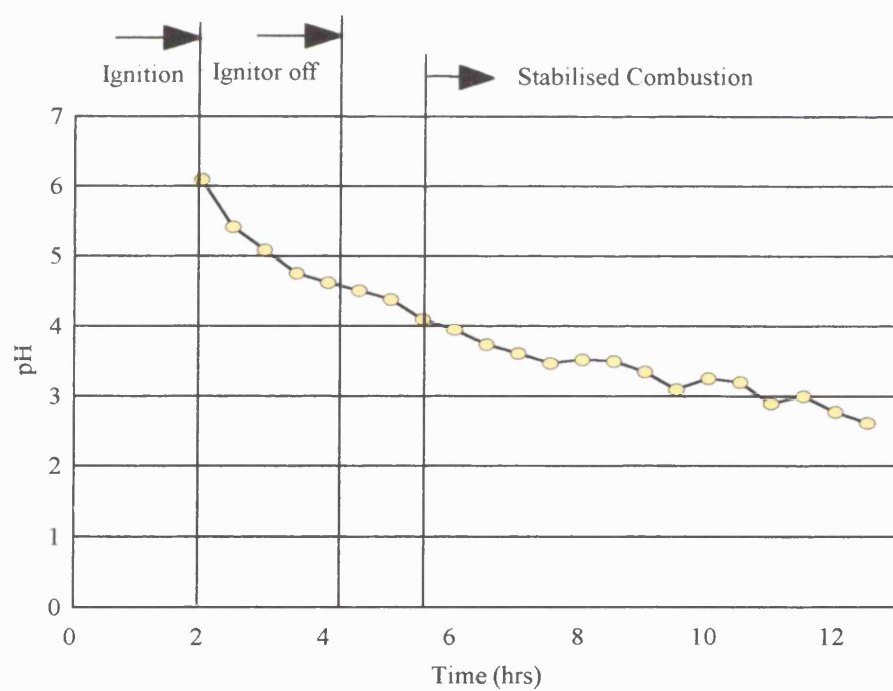


Figure 5.34 pH of produced water for Run 975 (Dry catalytic, Wolf Lake)

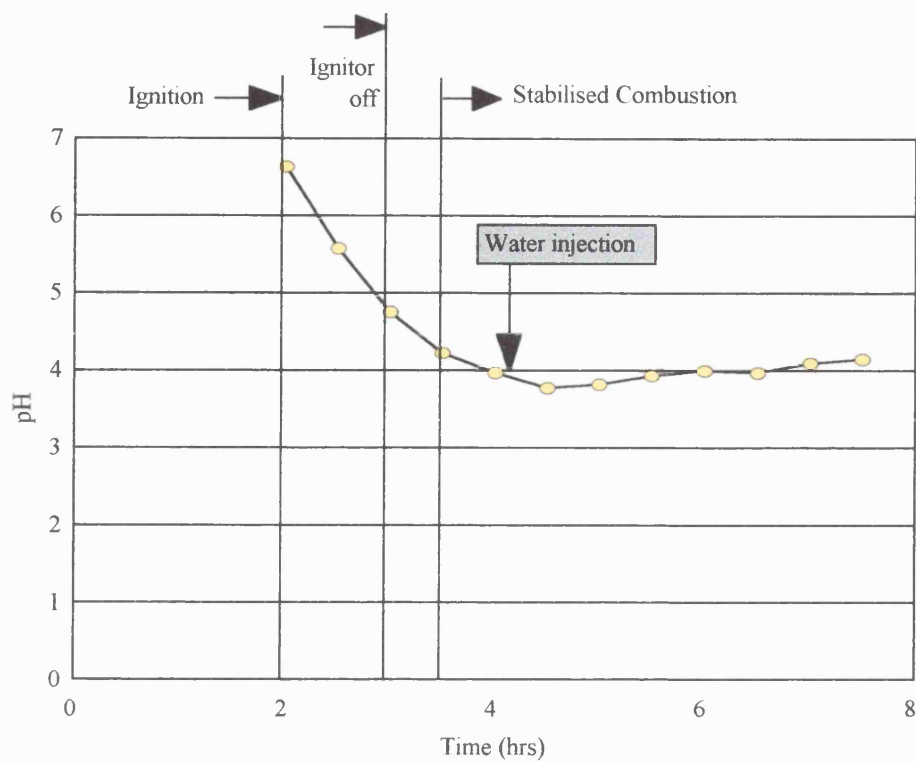


Figure 5.35 pH of produced water for Run 972 (Wet normal, Wolf Lake)

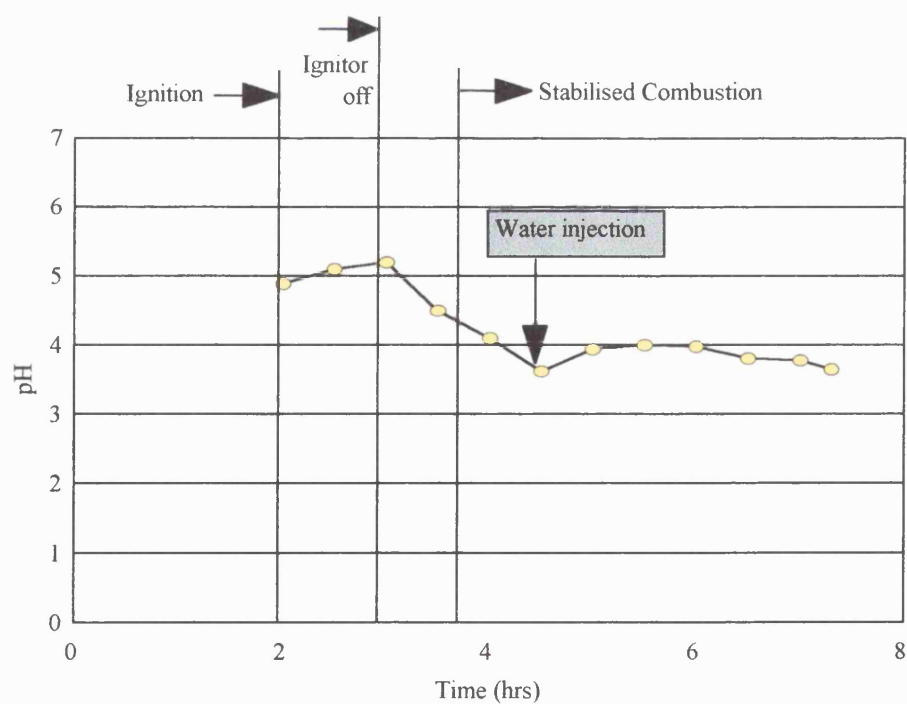


Figure 5.36 pH of produced water for Run 976 (Wet catalytic, Wolf Lake)

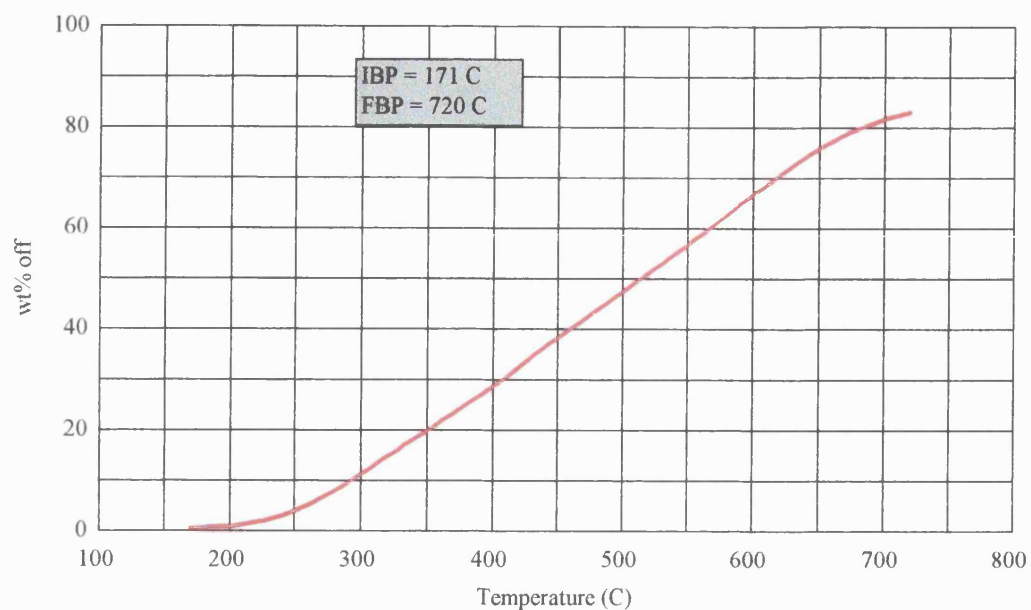


Figure 5.37 Simulated boiling point distribution for Wolf Lake crude oil

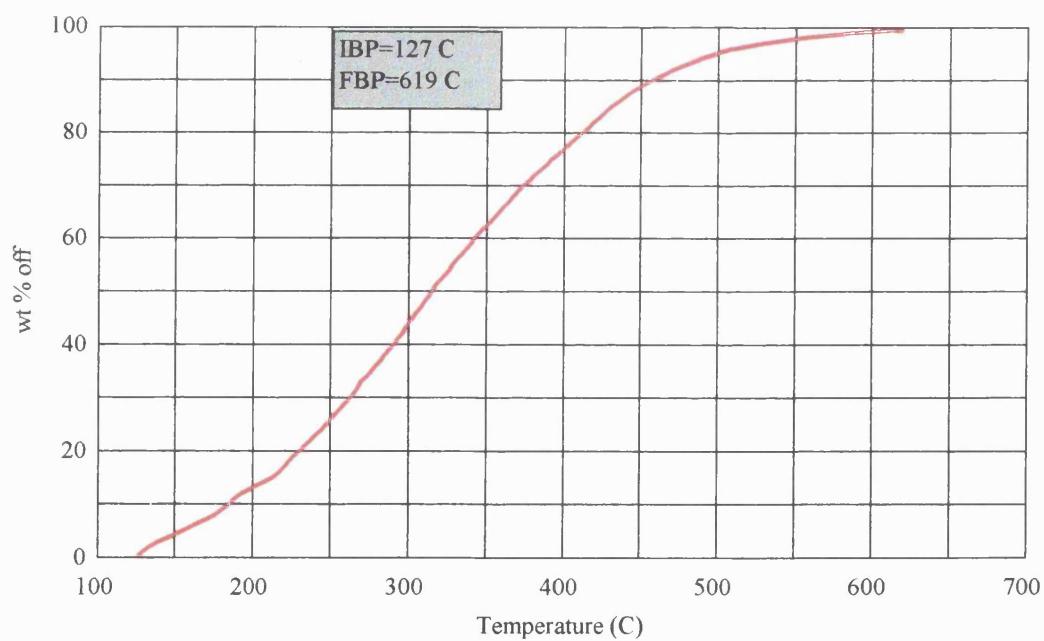


Figure 5.38 Simulated boiling point distribution for produced oil (Run 976, Wet catalytic)

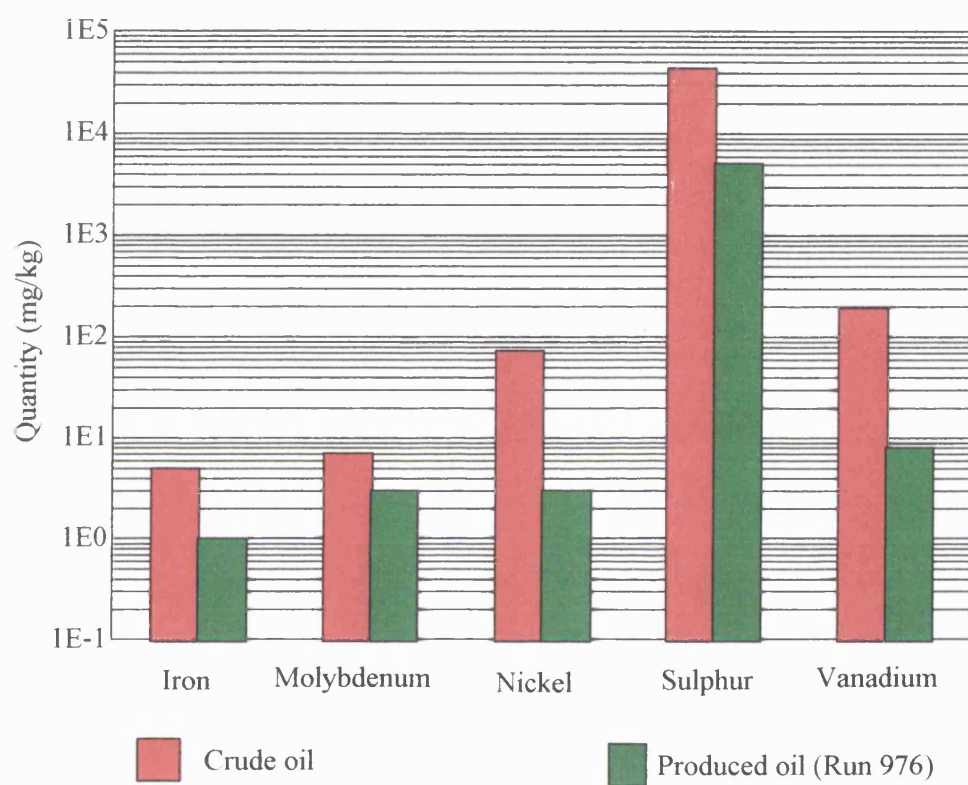


Figure 5.39 Analysis of metal and sulphur content for Wolf Lake crude oil and produced oil from Run 976

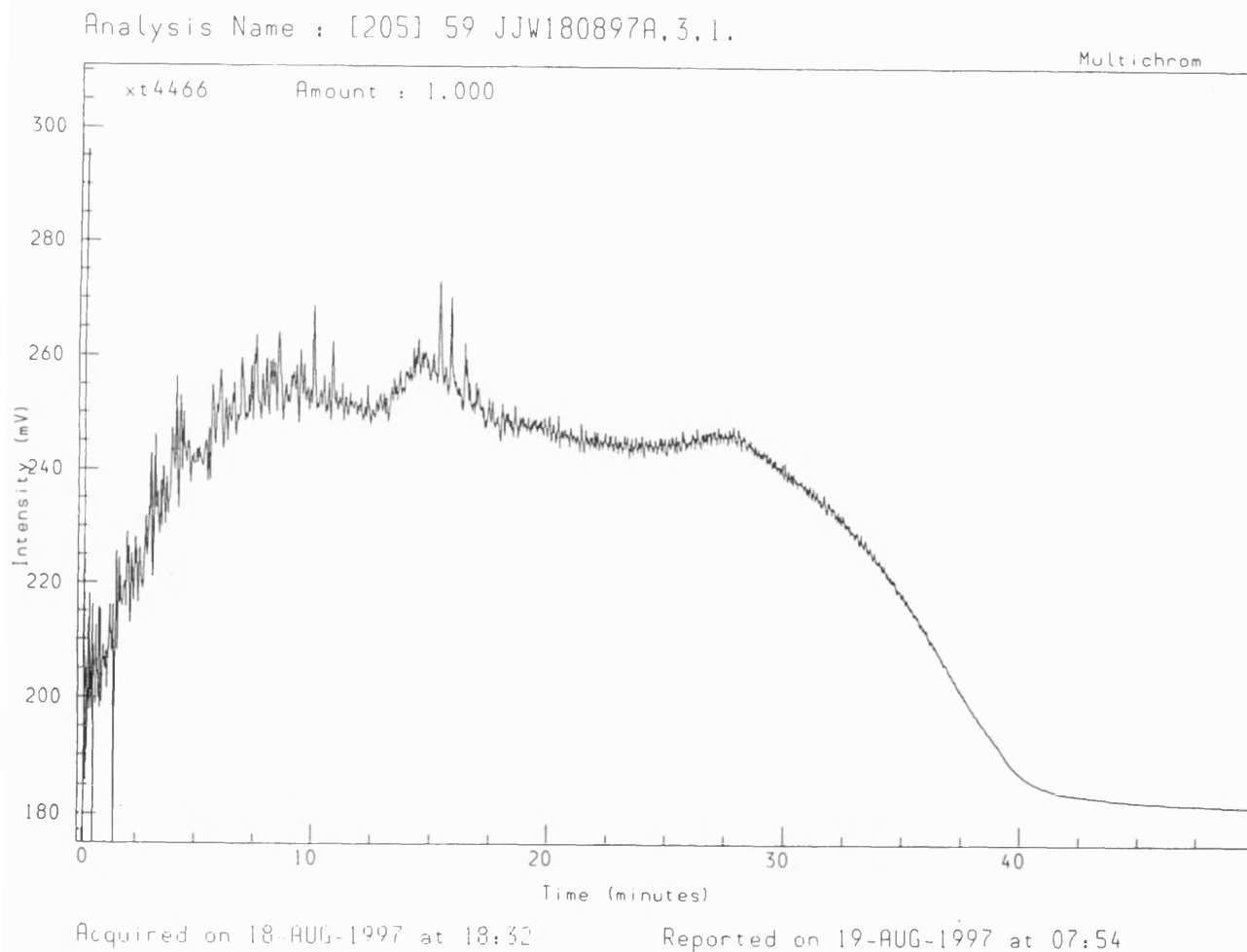
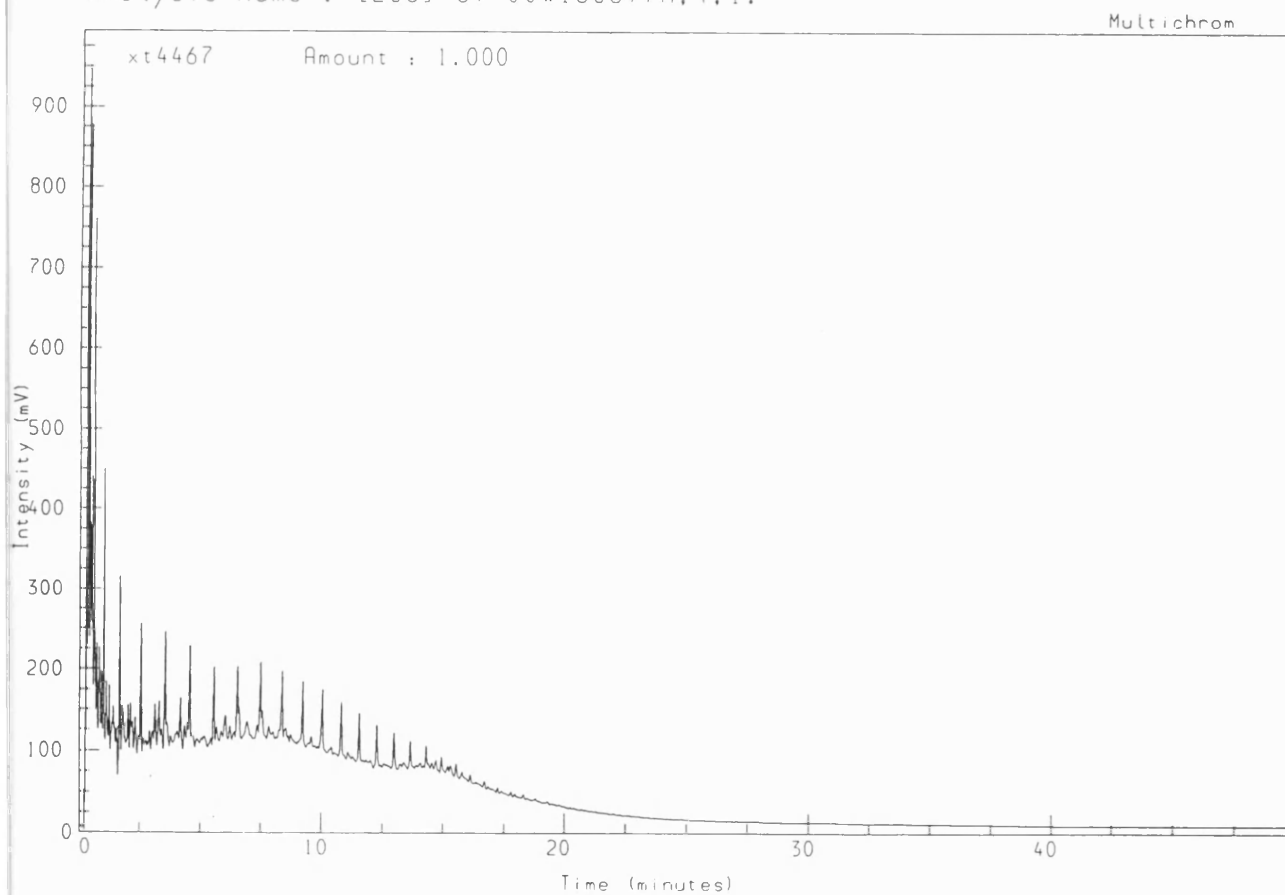


Figure 5.40 GC analysis for Wolf Lake crude oil

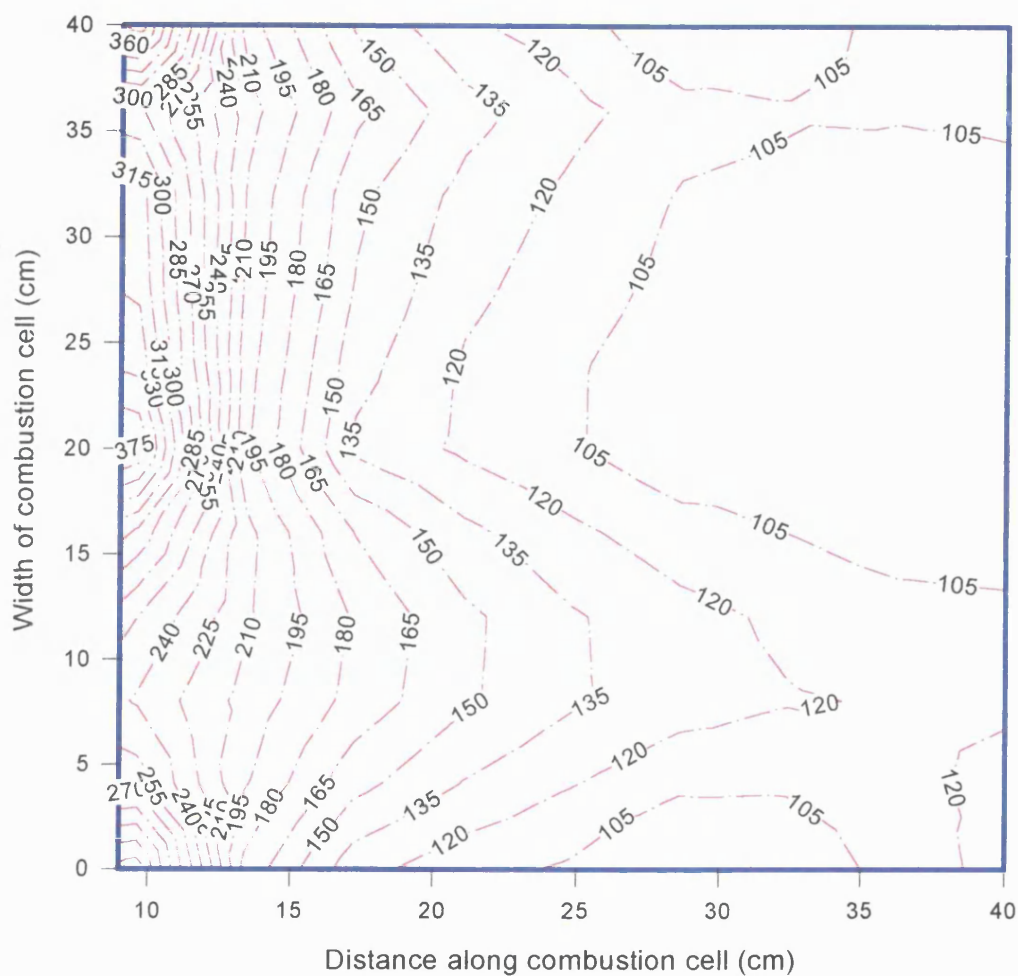
Analysis Name : [205] 59 JJW180897A.4.1.



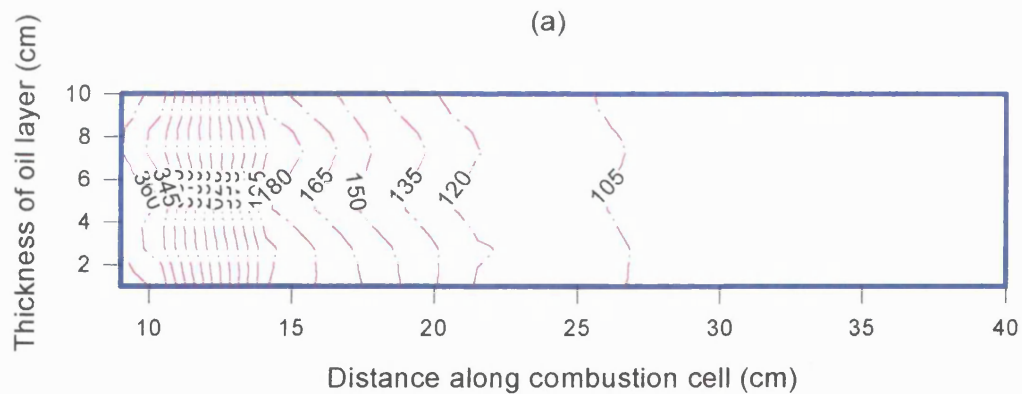
Acquired on 18-AUG-1997 at 20:03

Reported on 19-AUG-1997 at 07:56

Figure 5.41 GC analysis for produced oil from Run 976 (Wet Catalytic)



(a)



(b)

Figure 5.42 Run 971: Temperature profiles in sandpack (a) Horizontal mid-plane, (b) Vertical mid-plane. [Dry normal, Wolf Lake] Combustion Time = at ignition

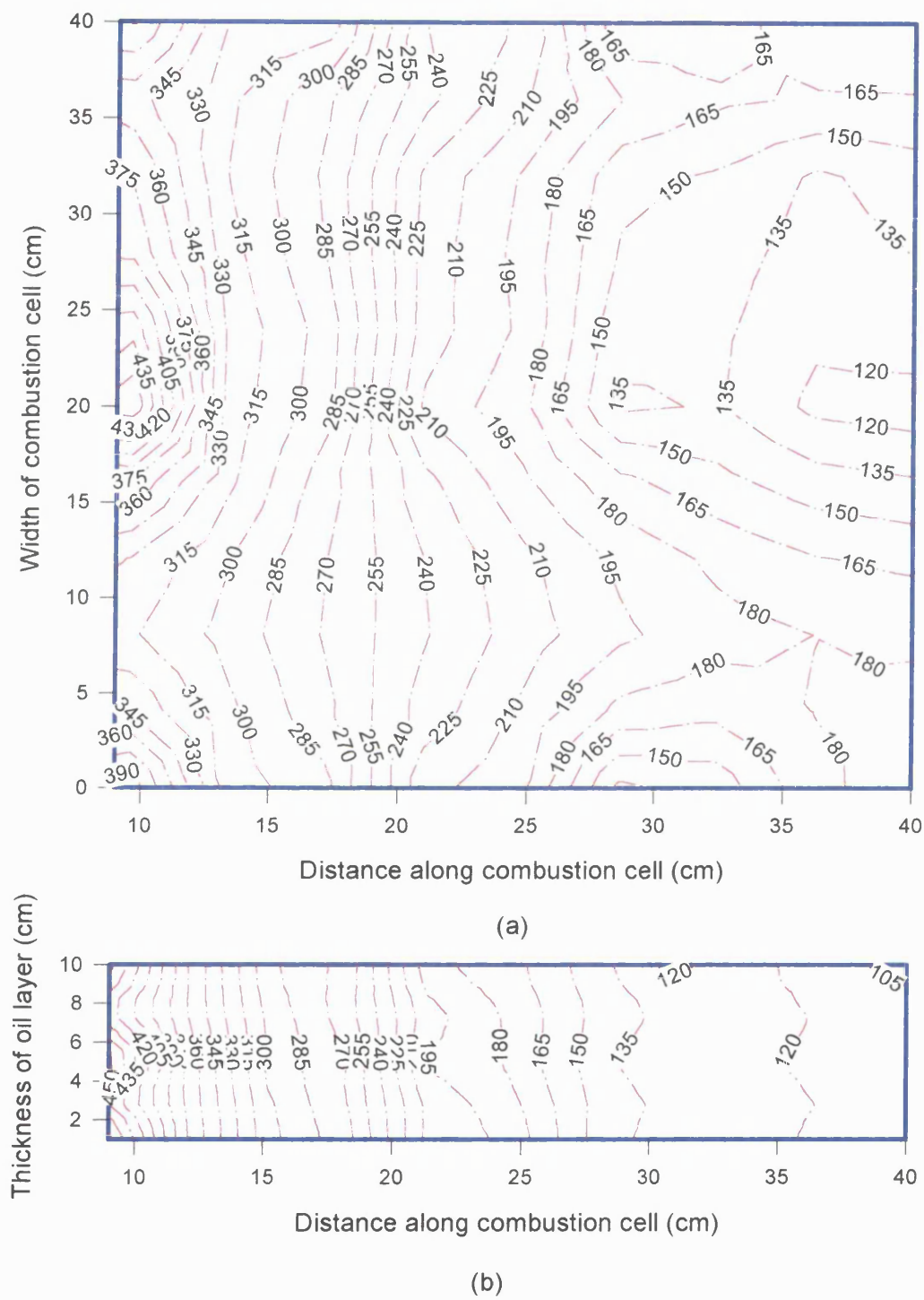
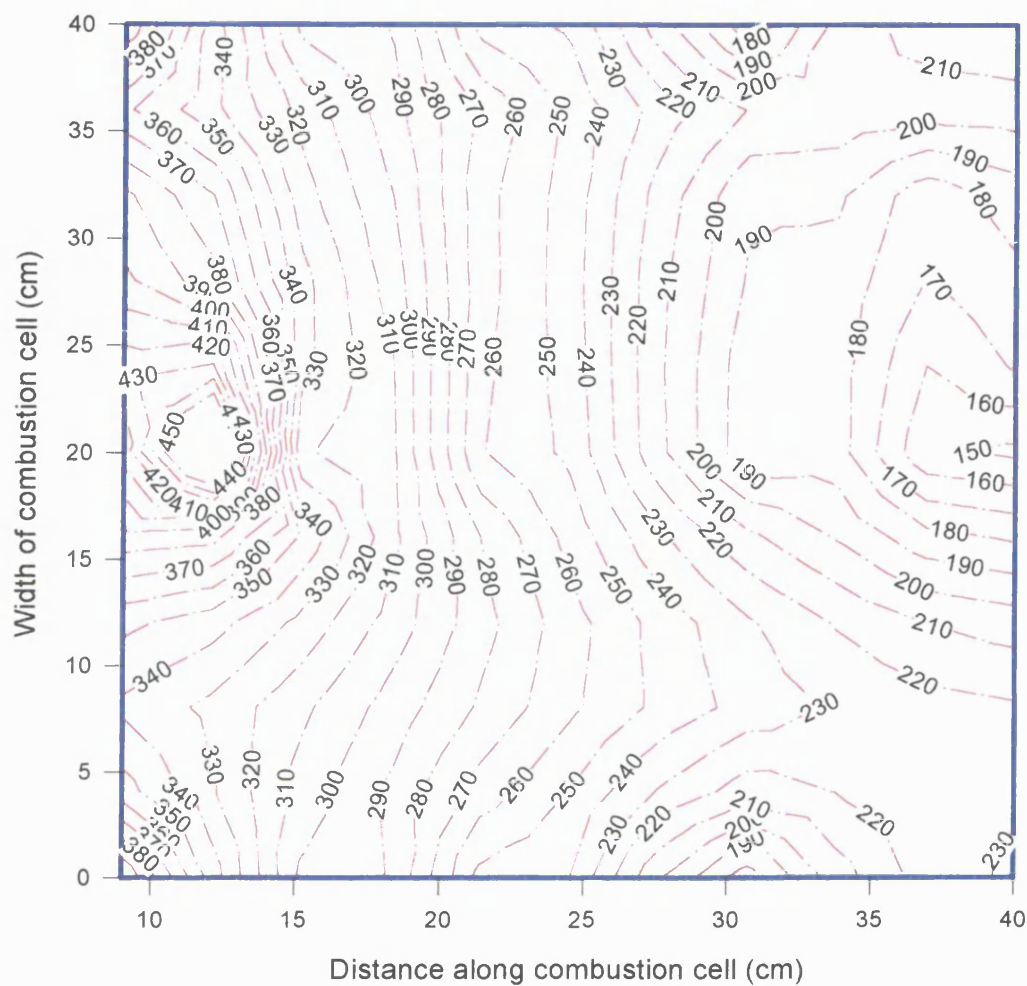
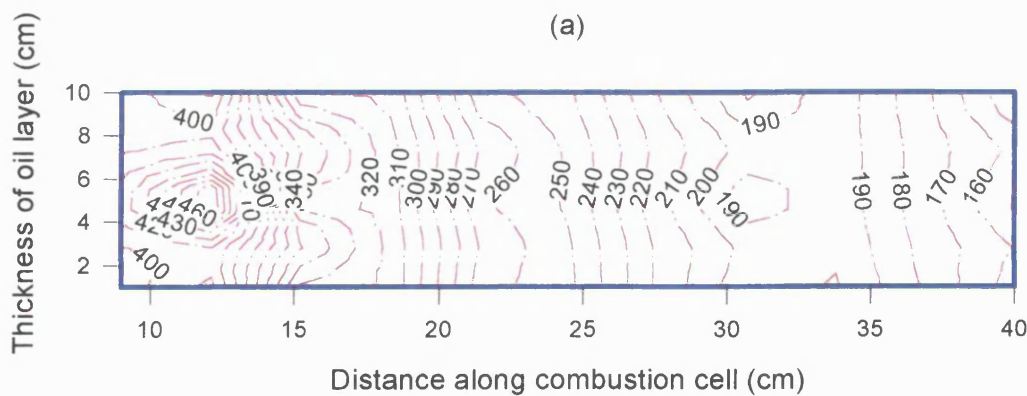


Figure 5.43 Run 971: Temperature profiles in sandpack (a) Horizontal mid-plane, (b) Vertical mid-plane. [Dry normal, Wolf Lake]. Combustion Time = 120 minutes

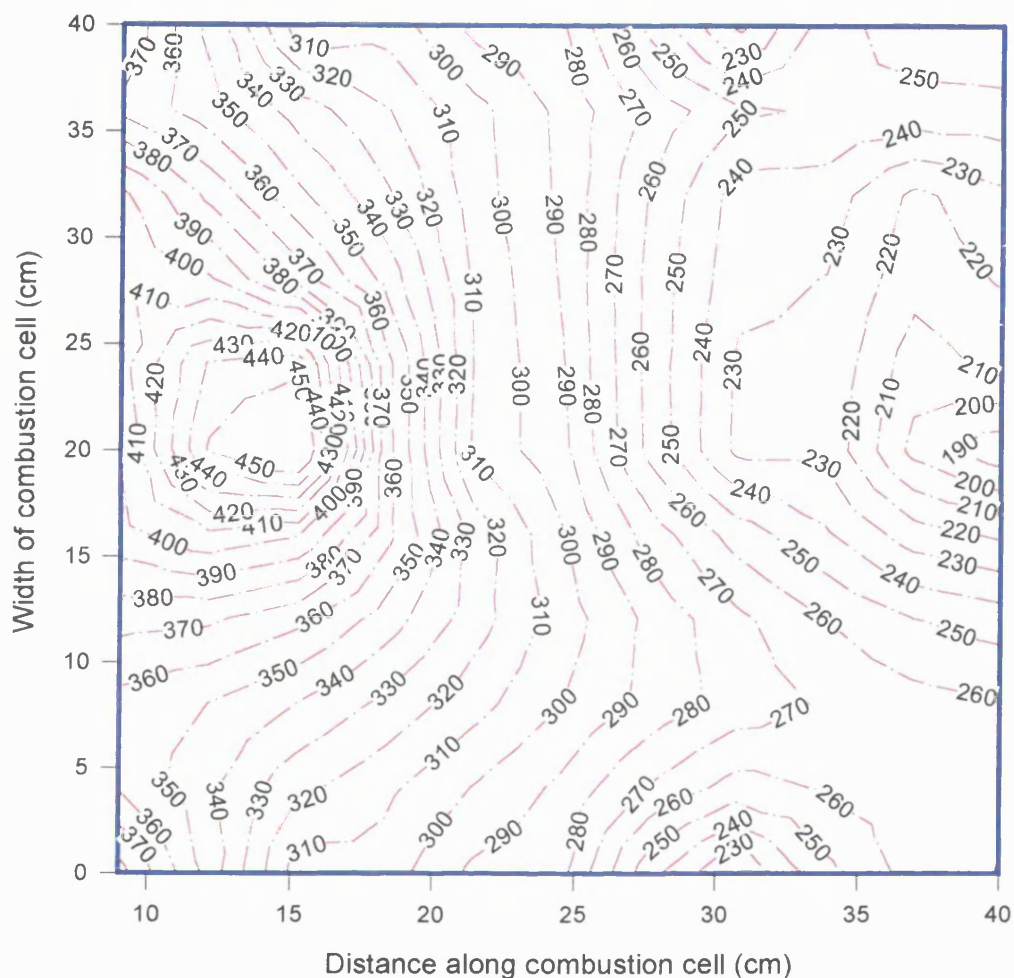


(a)

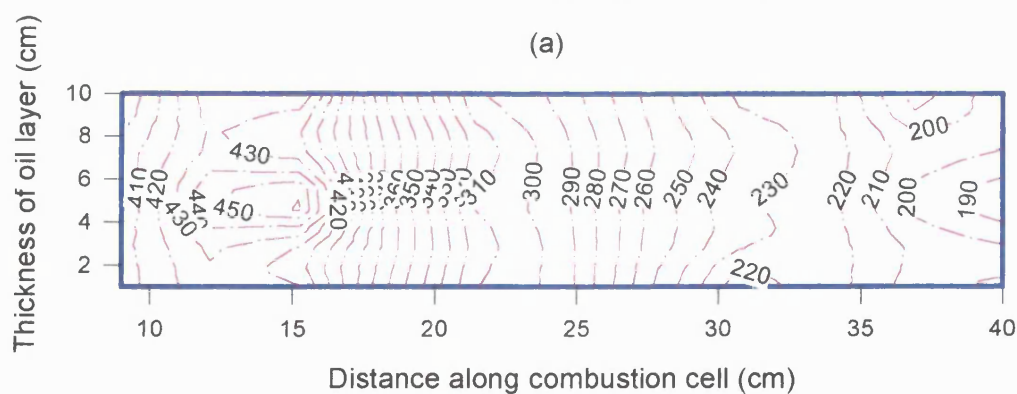


(b)

Figure 5.44 Run 971: Temperature profiles in sandpack (a) Horizontal mid-plane, (b) Vertical mid-plane. [Dry normal, Wolf Lake]. Combustion Time = 240 minutes

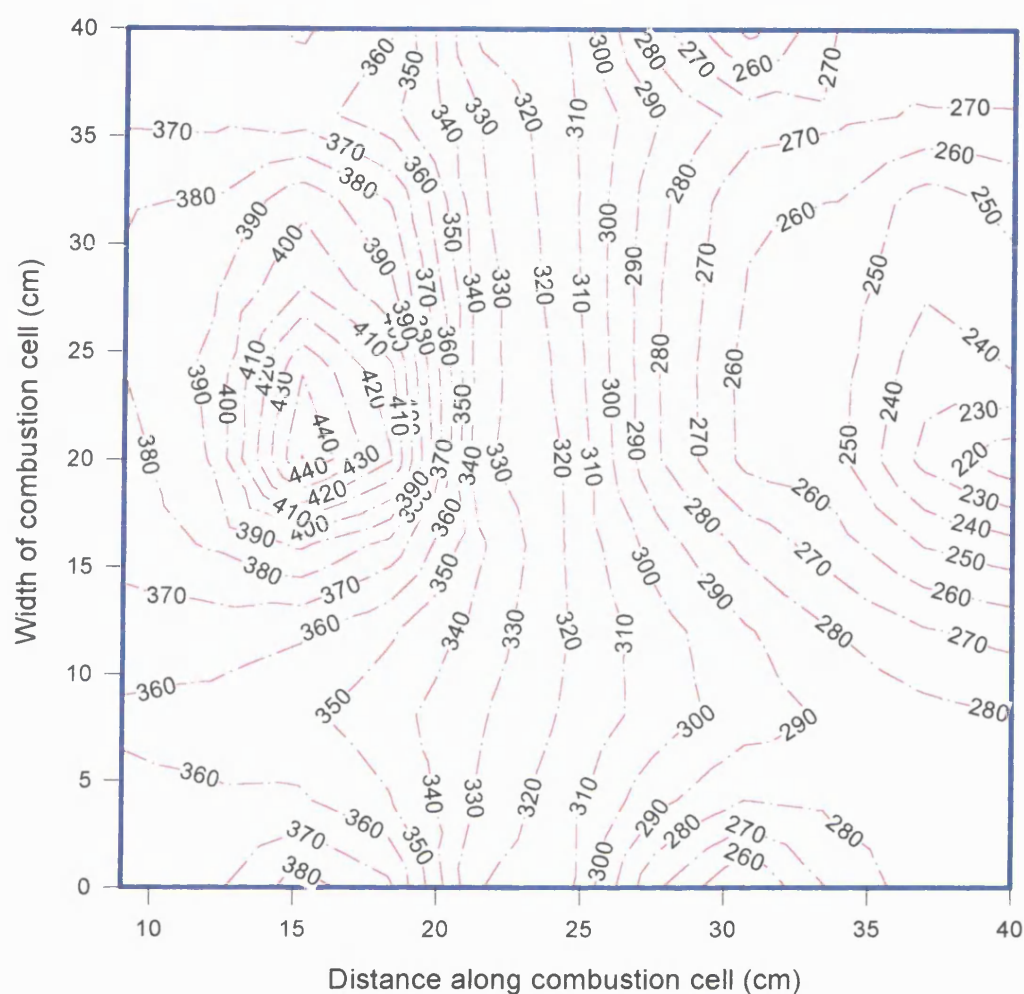


(a)

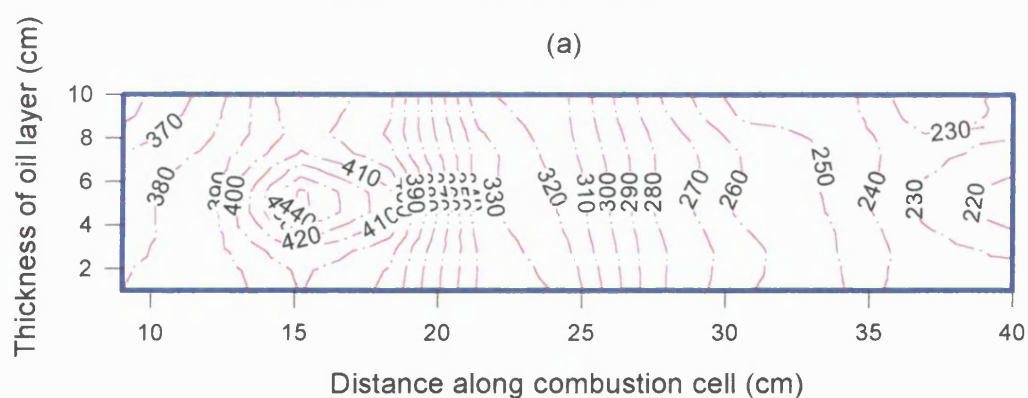


(b)

Figure 5.45 Run 971: Temperature profiles in sandpack (a) Horizontal mid-plane, (b) Vertical mid-plane. [Dry normal, Wolf Lake]. Combustion Time = 360 minutes

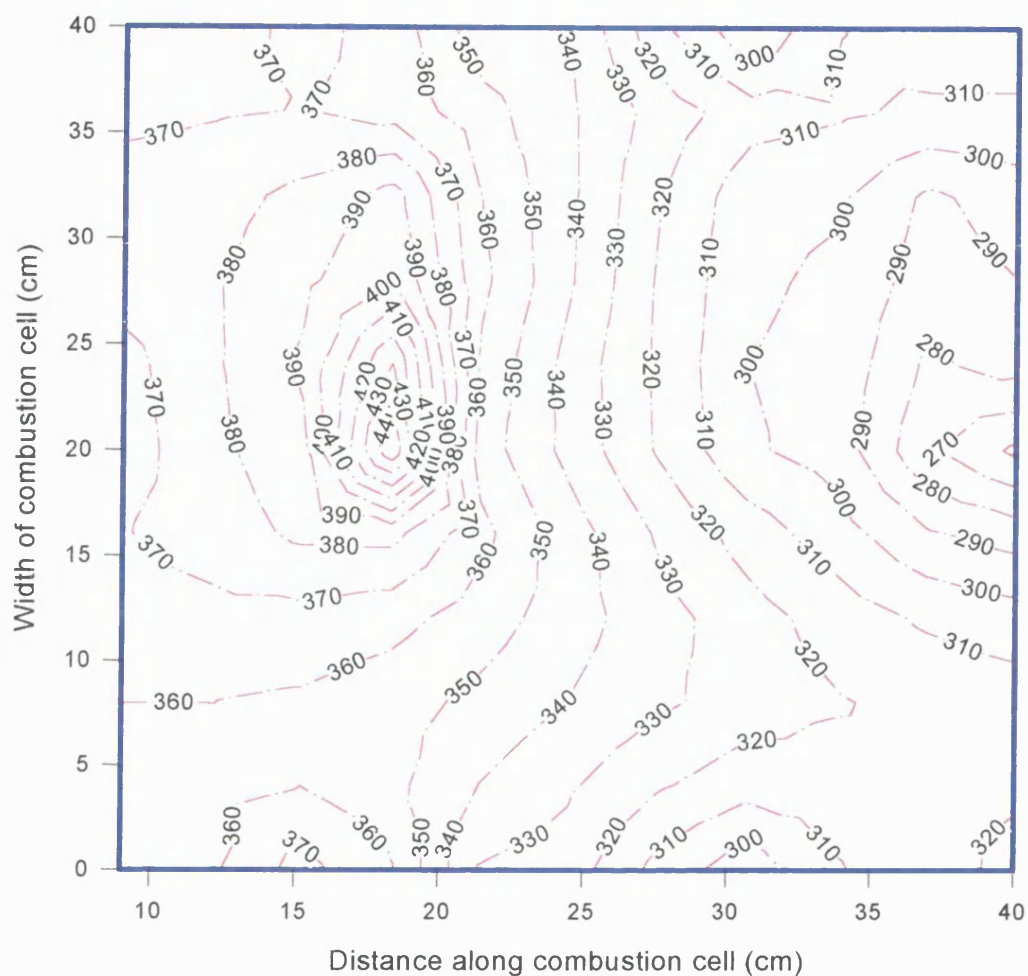


(a)

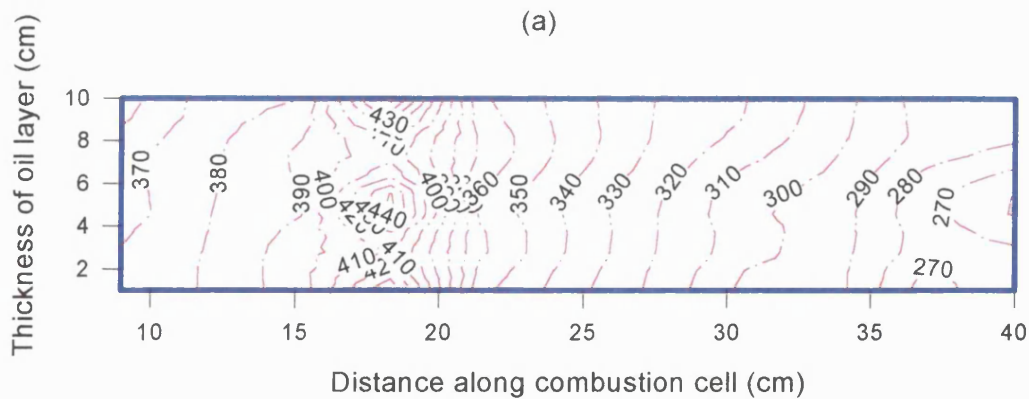


(b)

Figure 5.46 Run 971: Temperature profiles in sandpack (a) Horizontal mid-plane, (b) Vertical mid-plane. [Dry normal, Wolf Lake]. Combustion Time = 480 minutes

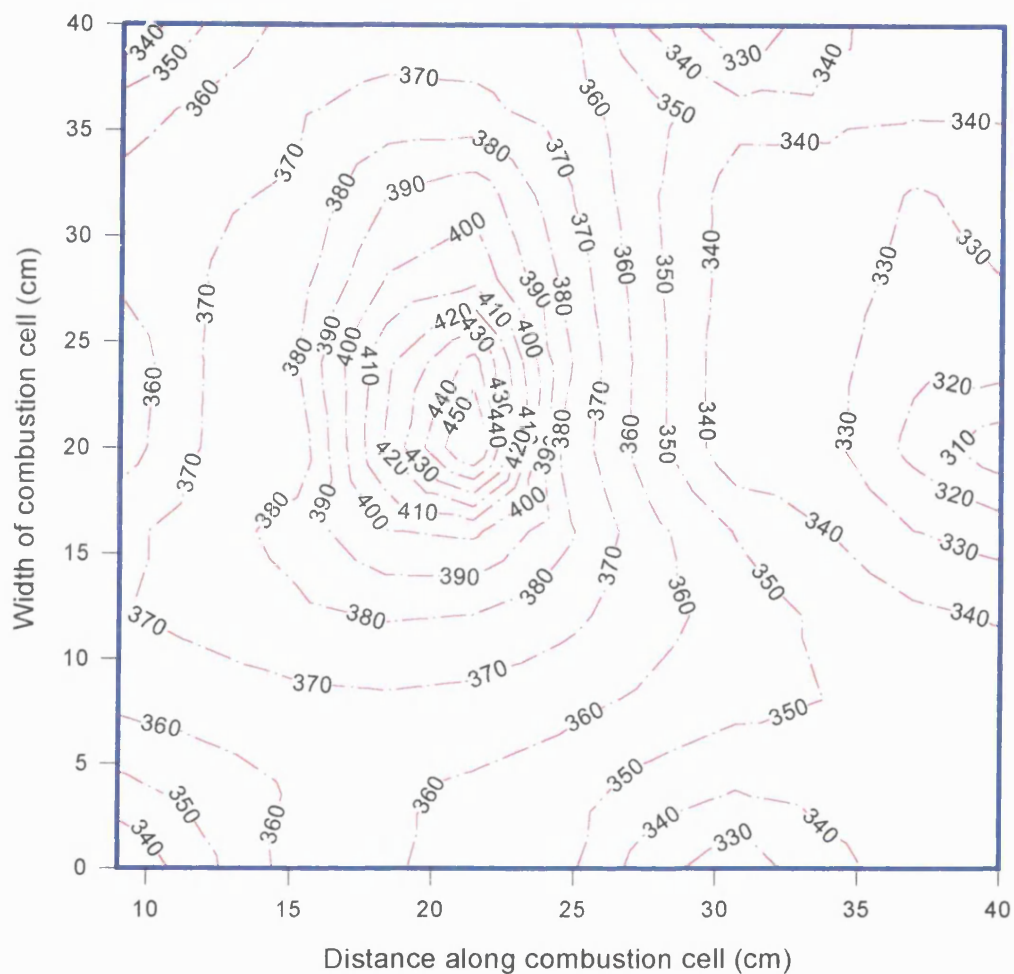


(a)

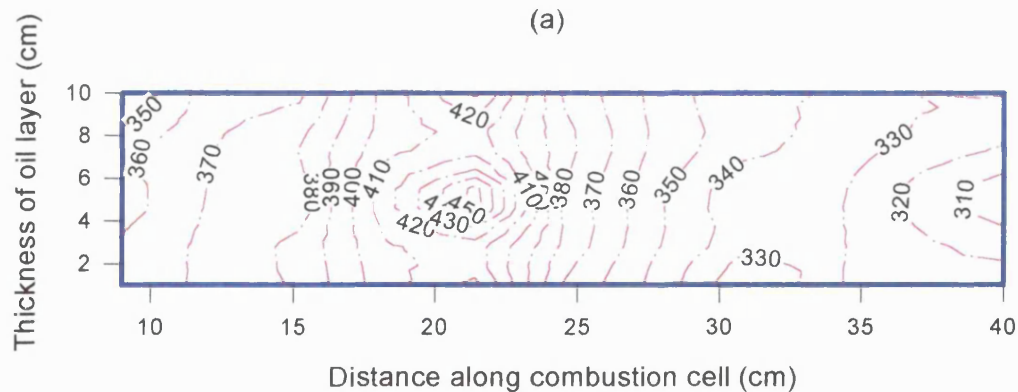


(b)

Figure 5.47 Run 971: Temperature profiles in sandpack (a) Horizontal mid-plane, (b) Vertical mid-plane. [Dry normal, Wolf Lake]. Combustion Time = 600 minutes



(a)



(b)

Figure 5.48 Run 971: Temperature profiles in sandpack (a) Horizontal mid-plane, (b) Vertical mid-plane. [Dry normal, Wolf Lake]. Combustion Time = 720 minutes

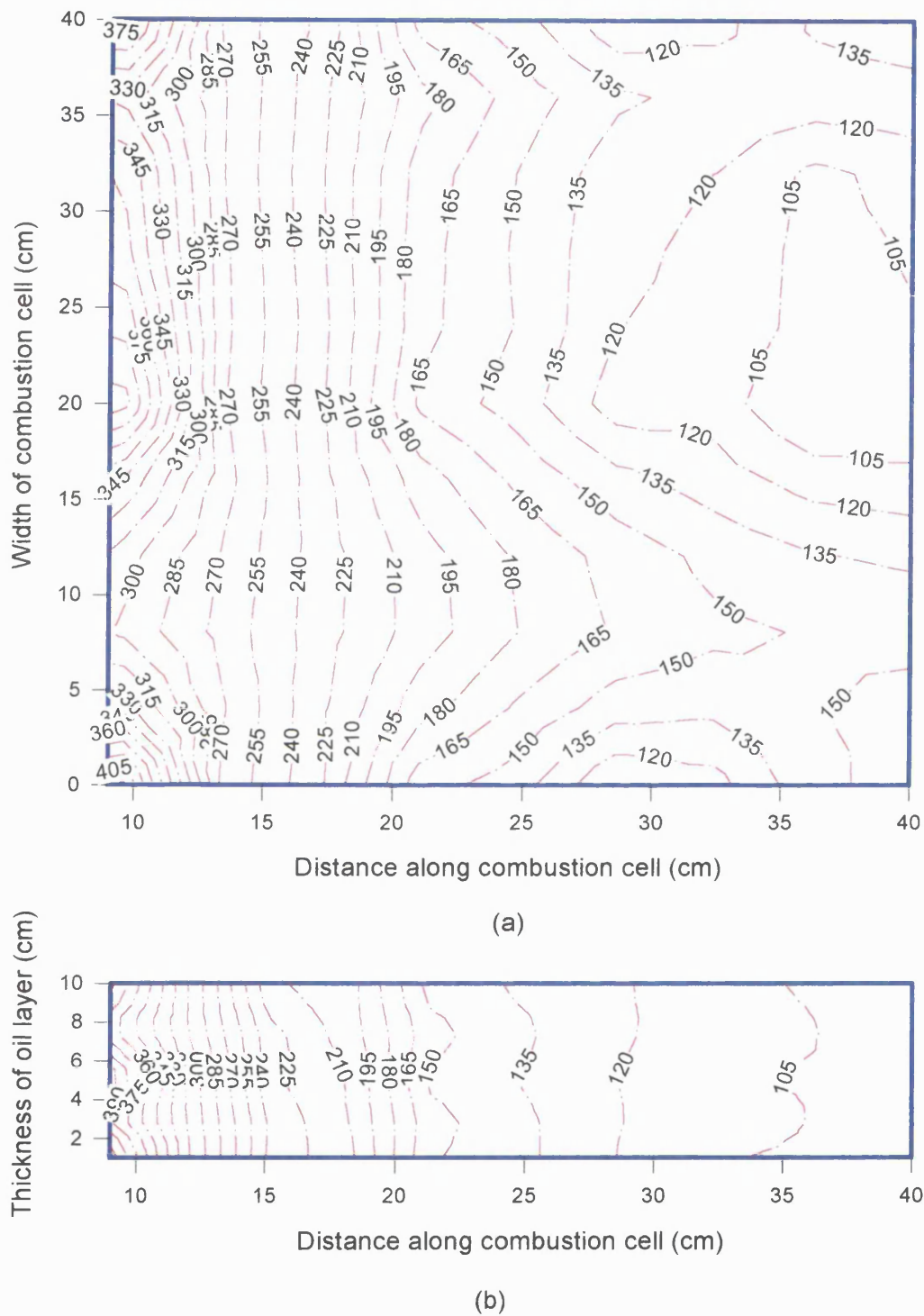
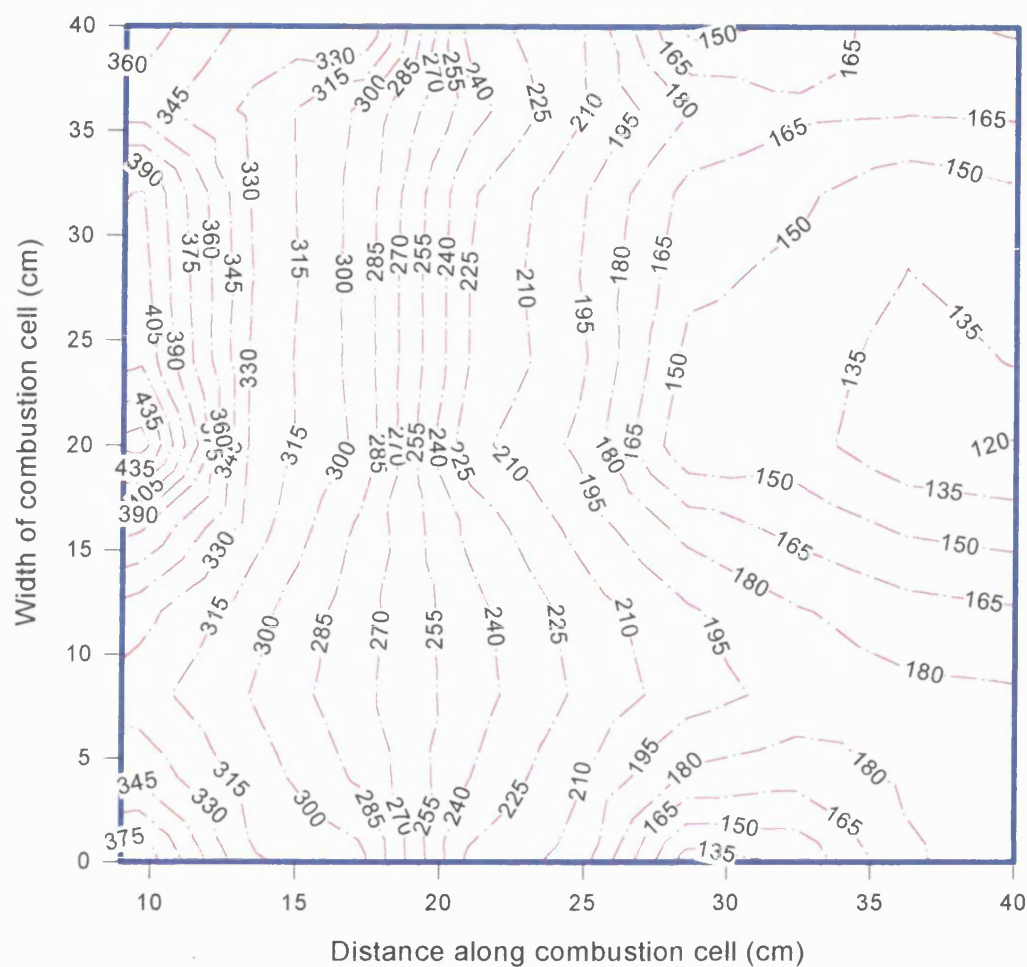
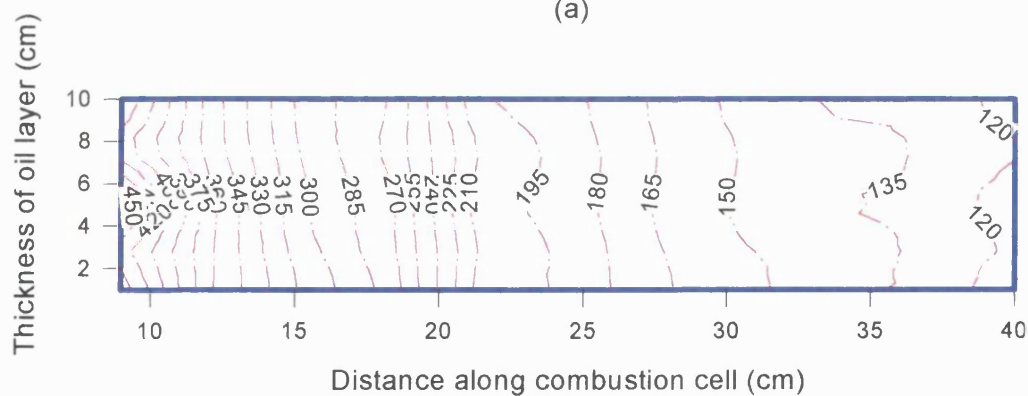


Figure 5.49 Run 975: Temperature profiles in sandpack (a) Horizontal mid-plane, (b) Vertical mid-plane. [Dry catalytic, Wolf Lake]. Combustion Time = at ignition

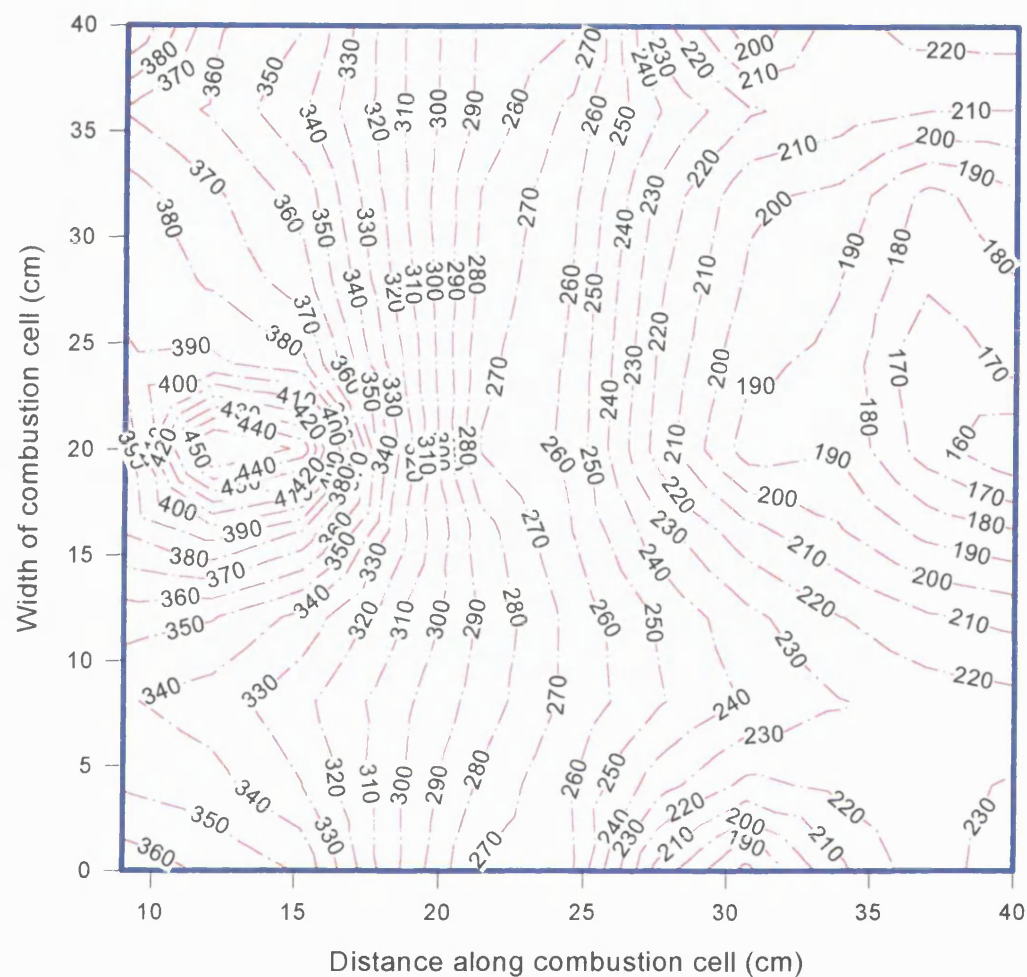


(a)

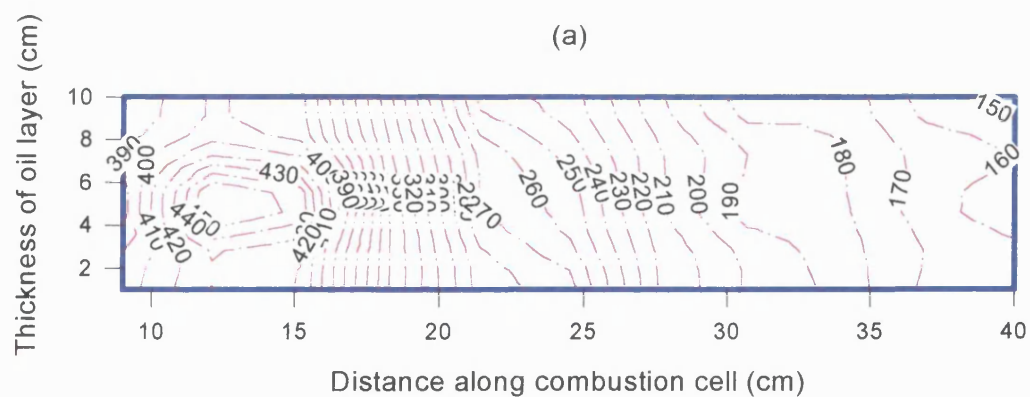


(b)

Figure 5.50 Run 975: Temperature profiles in sandpack (a) Horizontal mid-plane, (b) Vertical mid-plane. [Dry catalytic, Wolf Lake]. Combustion Time = 120 minutes

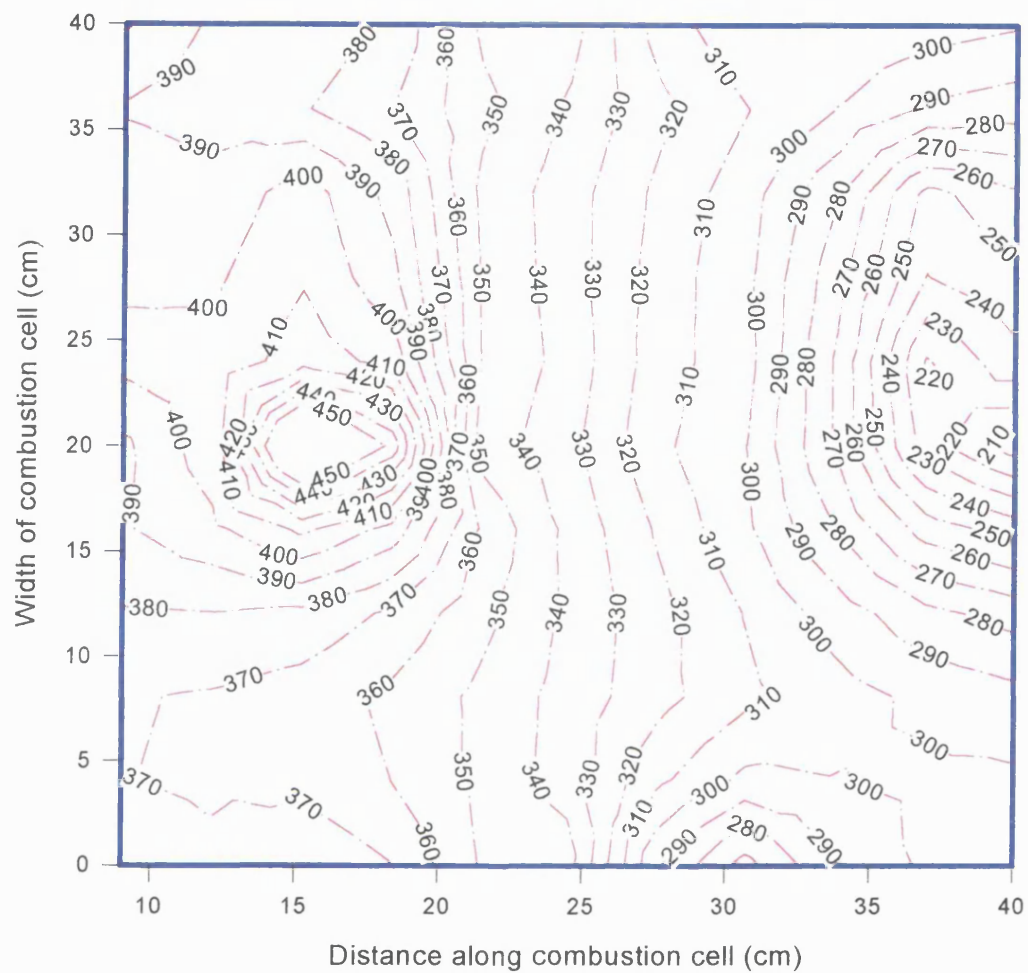


(a)

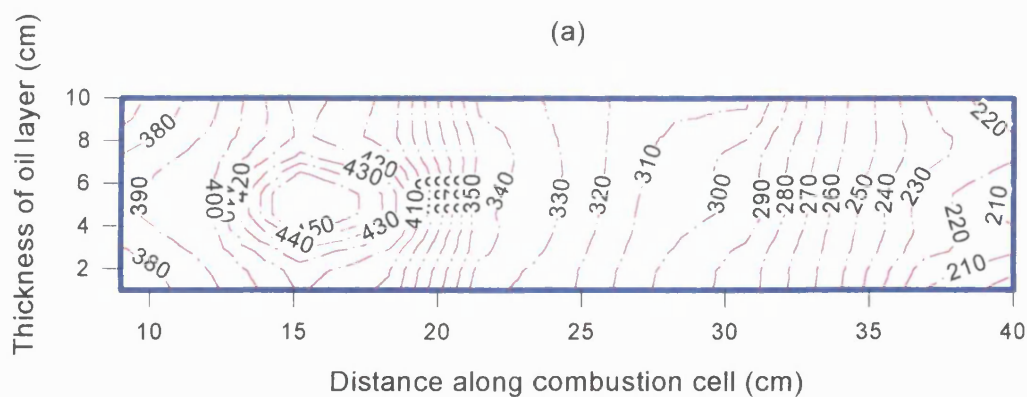


(b)

Figure 5.51 Run 975: Temperature profiles in sandpack (a) Horizontal mid-plane, (b) Vertical mid-plane. [Dry catalytic, Wolf Lake]. Combustion Time = 300 minutes

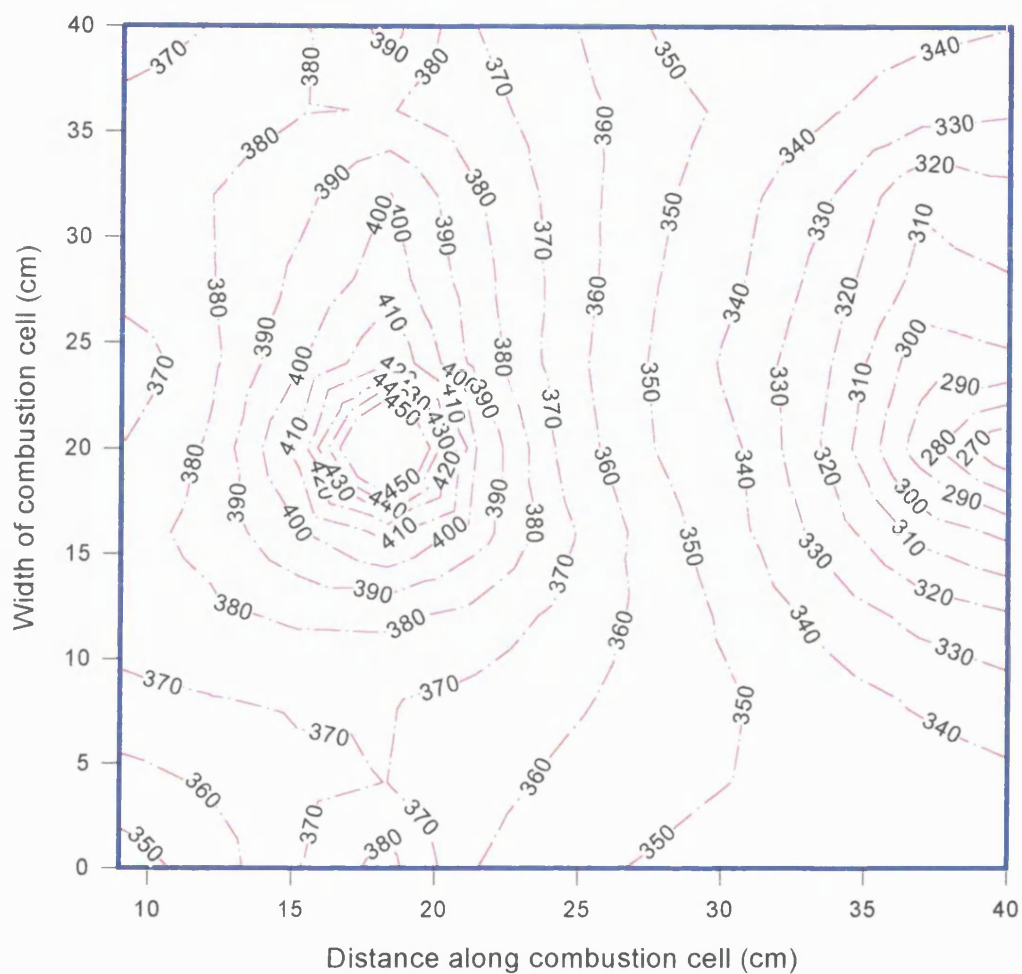


(a)

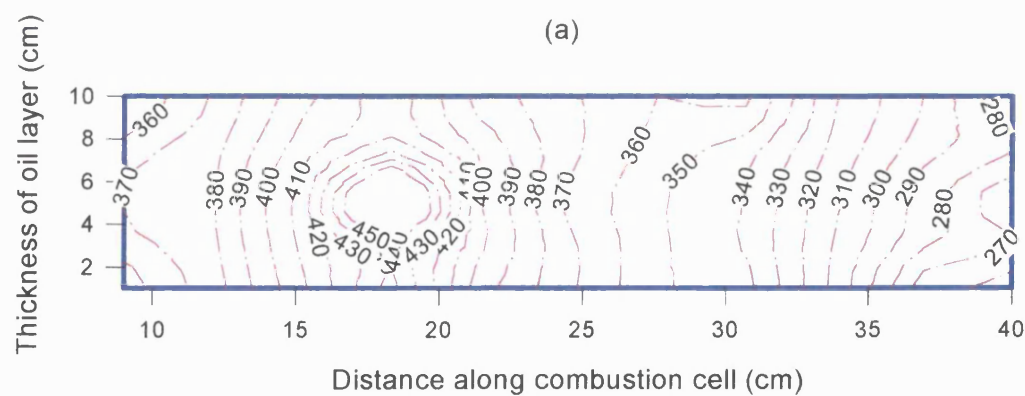


(b)

Figure 5.52 Run 975: Temperature profiles in sandpack (a) Horizontal mid-plane, (b) Vertical mid-plane. [Dry catalytic, Wolf Lake]. Combustion Time = 480 minutes

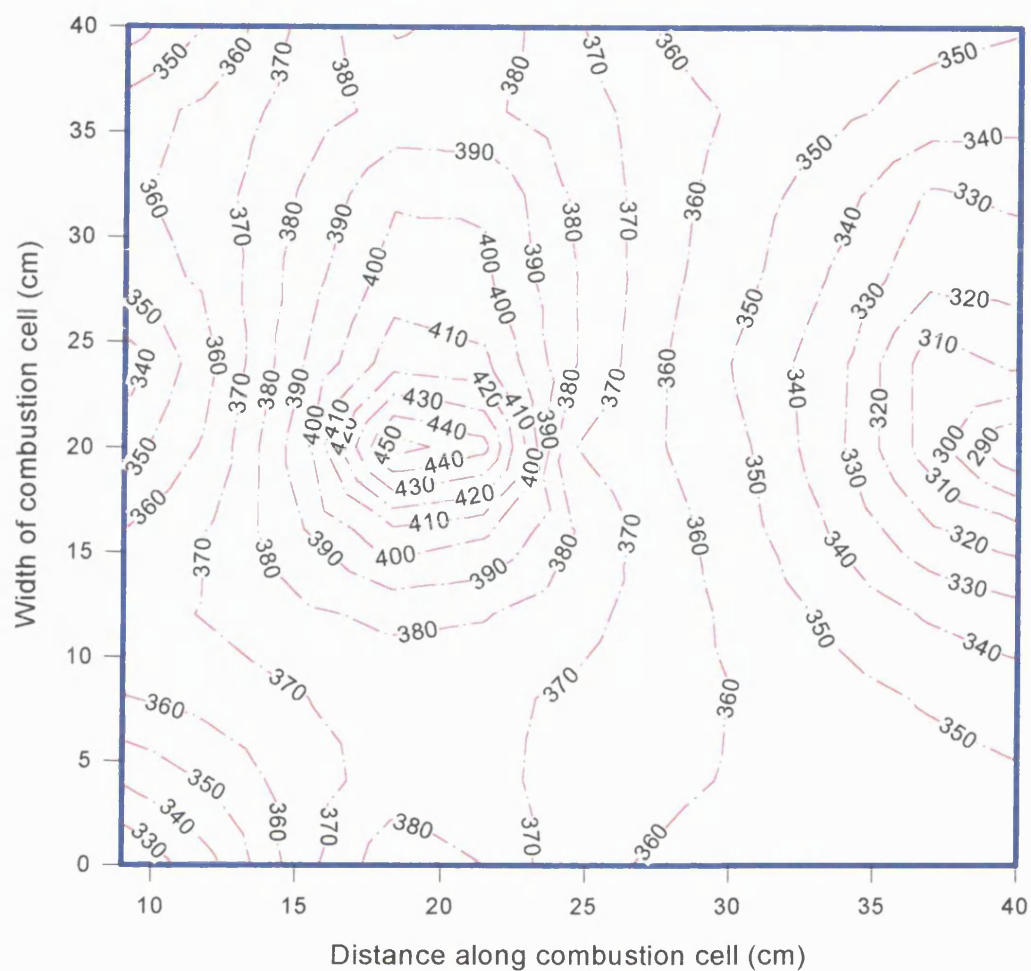


(a)

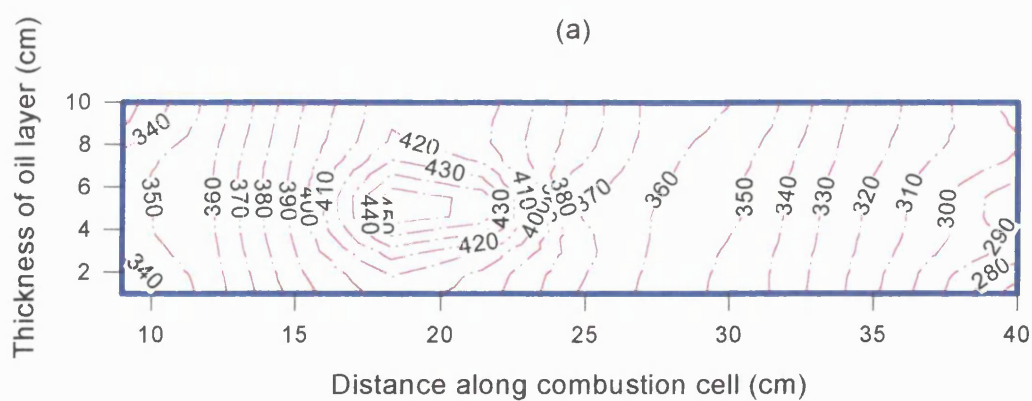


(b)

Figure 5.53 Run 975: Temperature profiles in sandpack (a) Horizontal mid-plane, (b) Vertical mid-plane. [Dry catalytic, Wolf Lake]. Combustion Time = 600 minutes

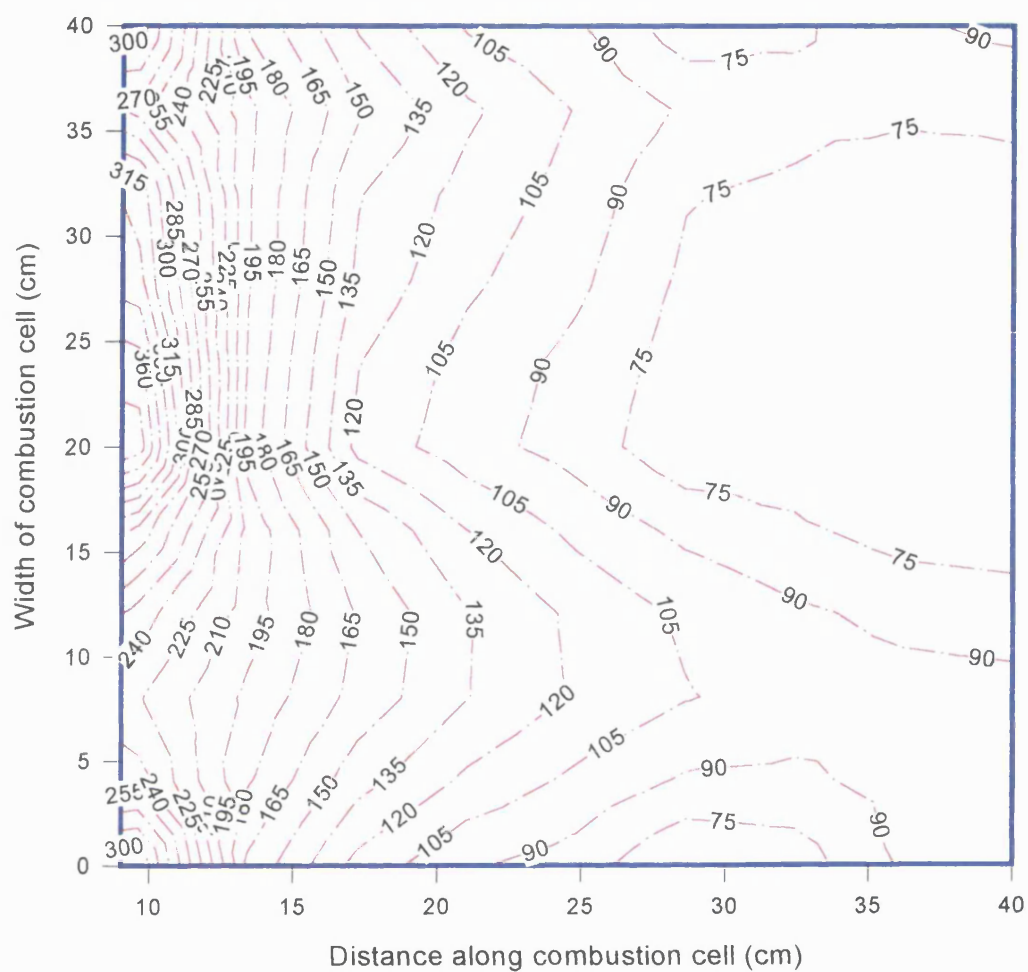


(a)

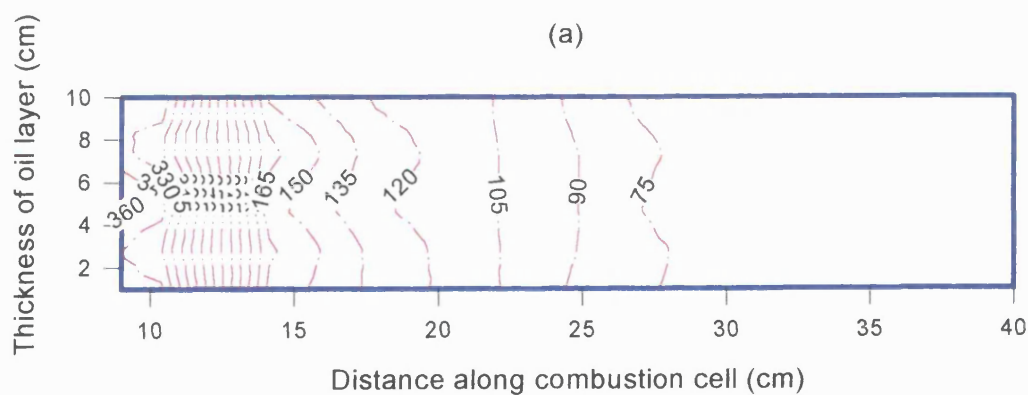


(b)

Figure 5.54 Run 975: Temperature profiles in sandpack (a) Horizontal mid-plane, (b) Vertical mid-plane. [Dry catalytic, Wolf Lake]. Combustion Time = 720 minutes

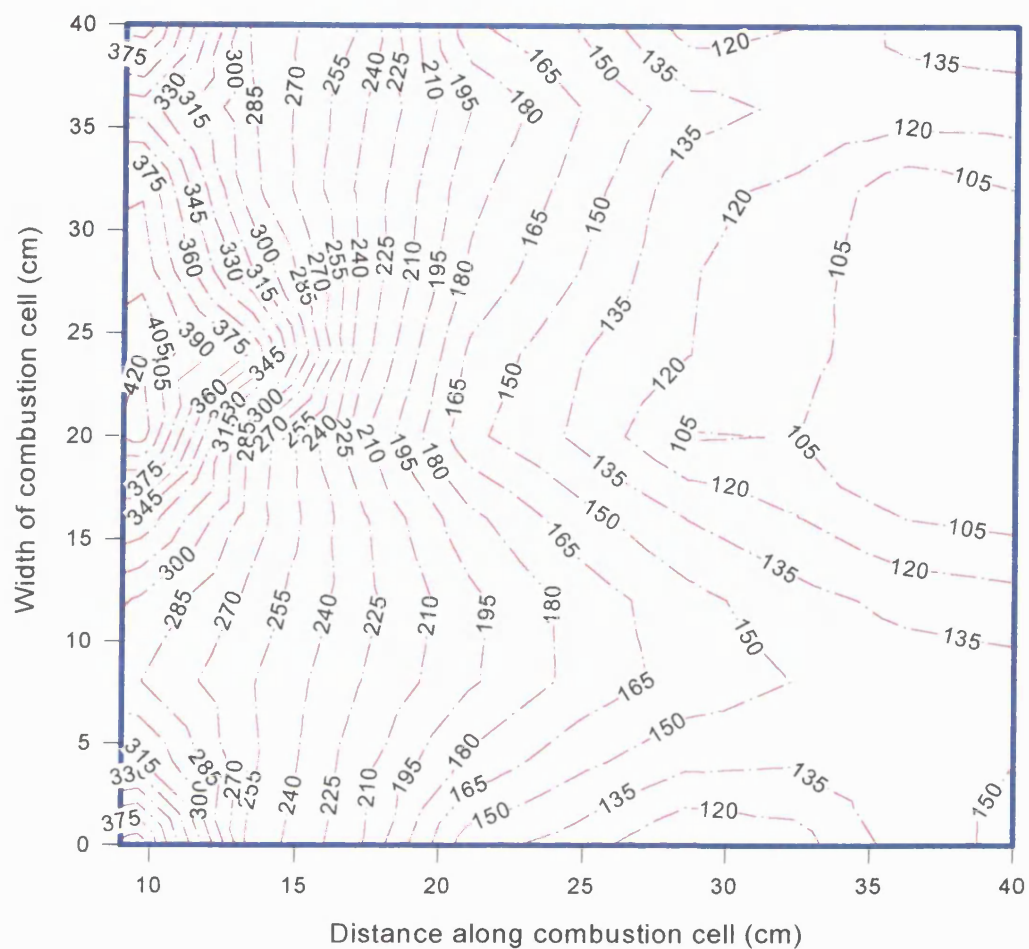


(a)

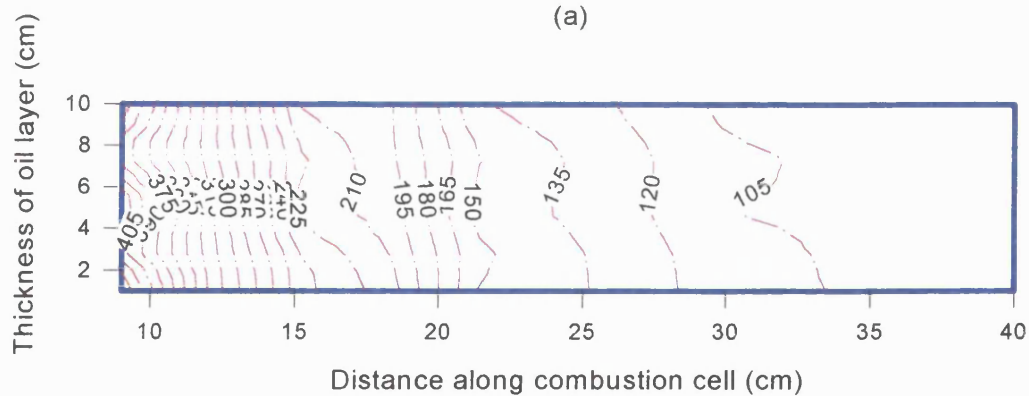


(b)

Figure 5.55 Run 972: Temperature profiles in sandpack (a) Horizontal mid-plane, (b) Vertical mid-plane. [Wet normal, Wolf Lake]. Combustion Time = at ignition

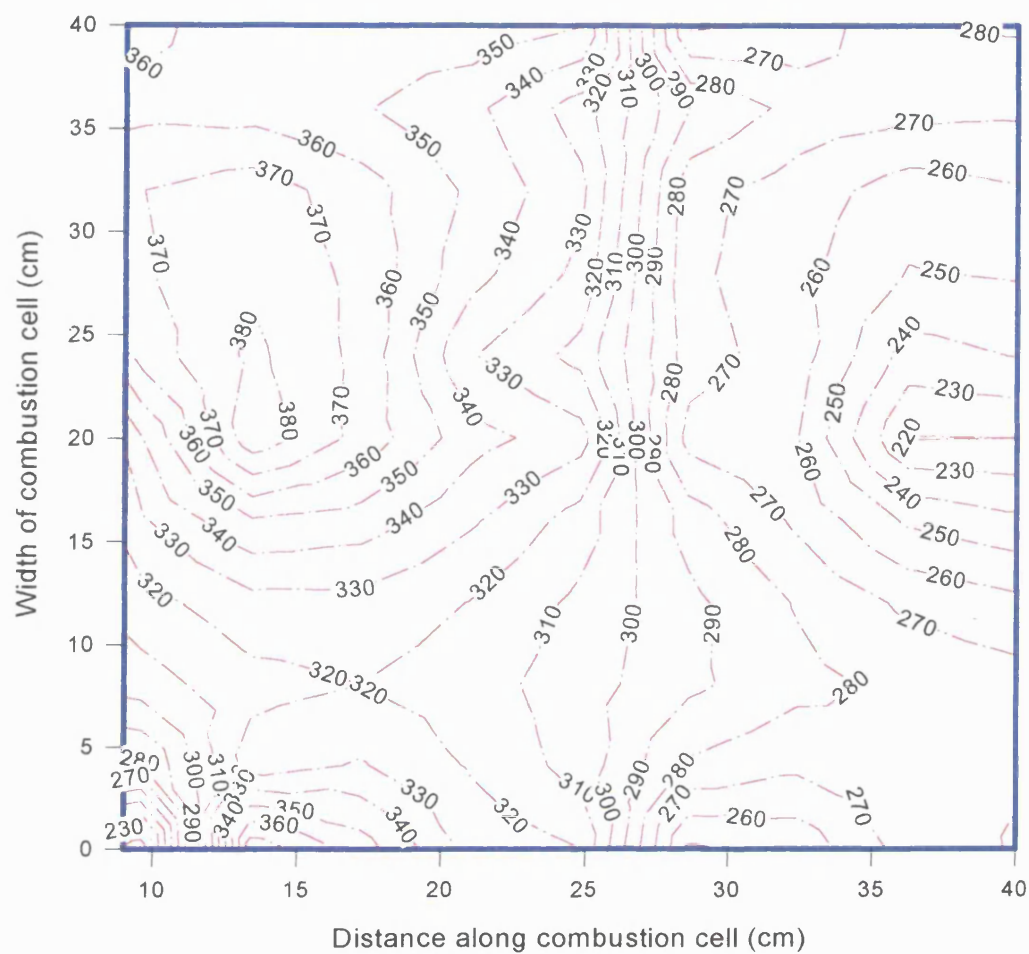


(a)

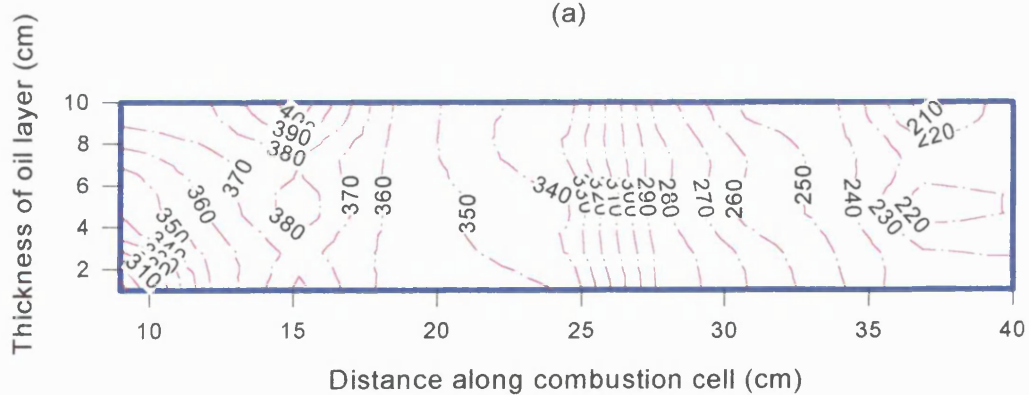


(b)

Figure 5.56 Run 972: Temperature profiles in sandpack (a) Horizontal mid-plane, (b) Vertical mid-plane. [Wet normal, Wolf Lake]. Combustion Time = 120 minutes

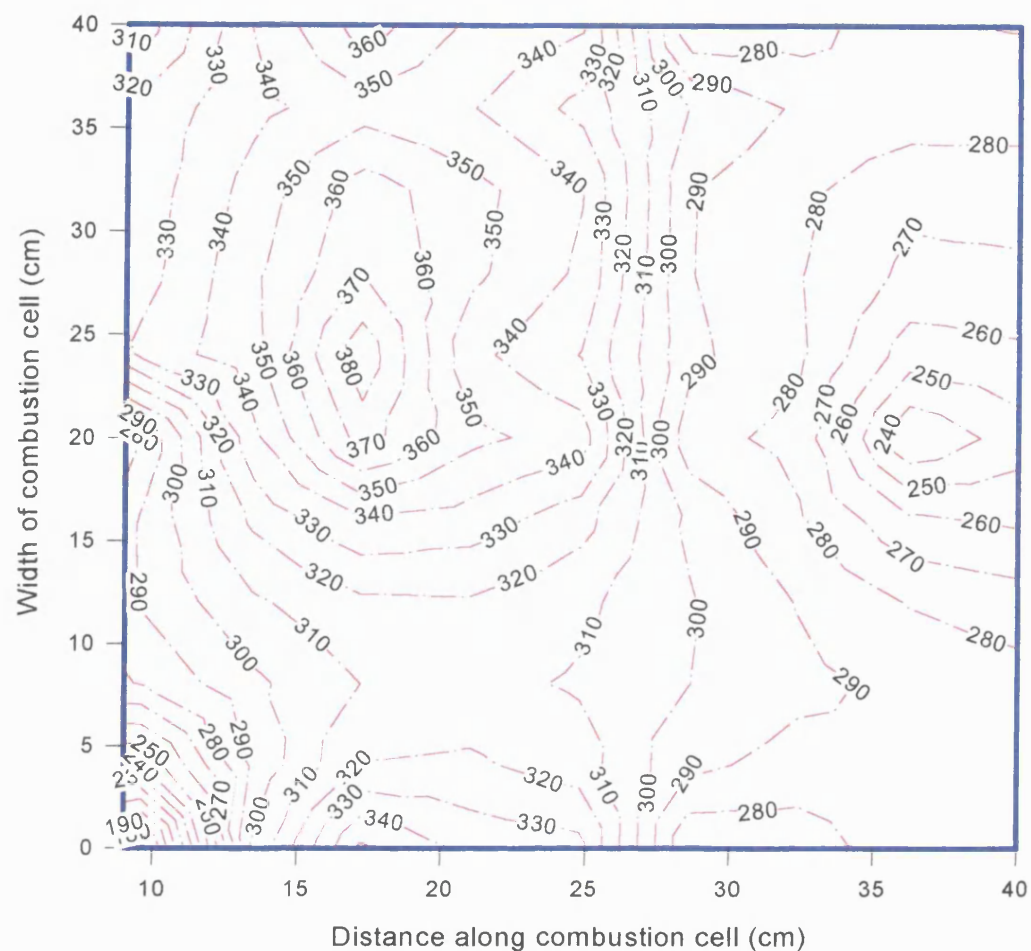


(a)

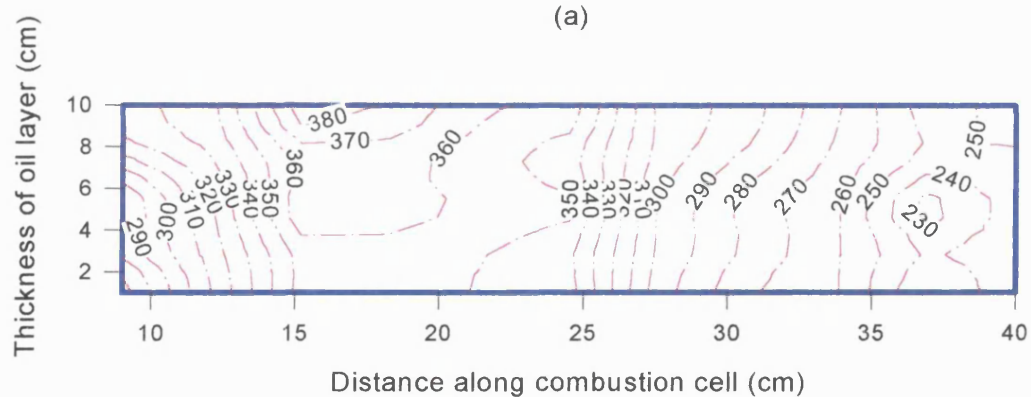


(b)

Figure 5.57 Run 972: Temperature profiles in sandpack (a) Horizontal mid-plane, (b) Vertical mid-plane. [Wet normal, Wolf Lake]. Combustion Time = 180 minutes (35 minutes after water injection)

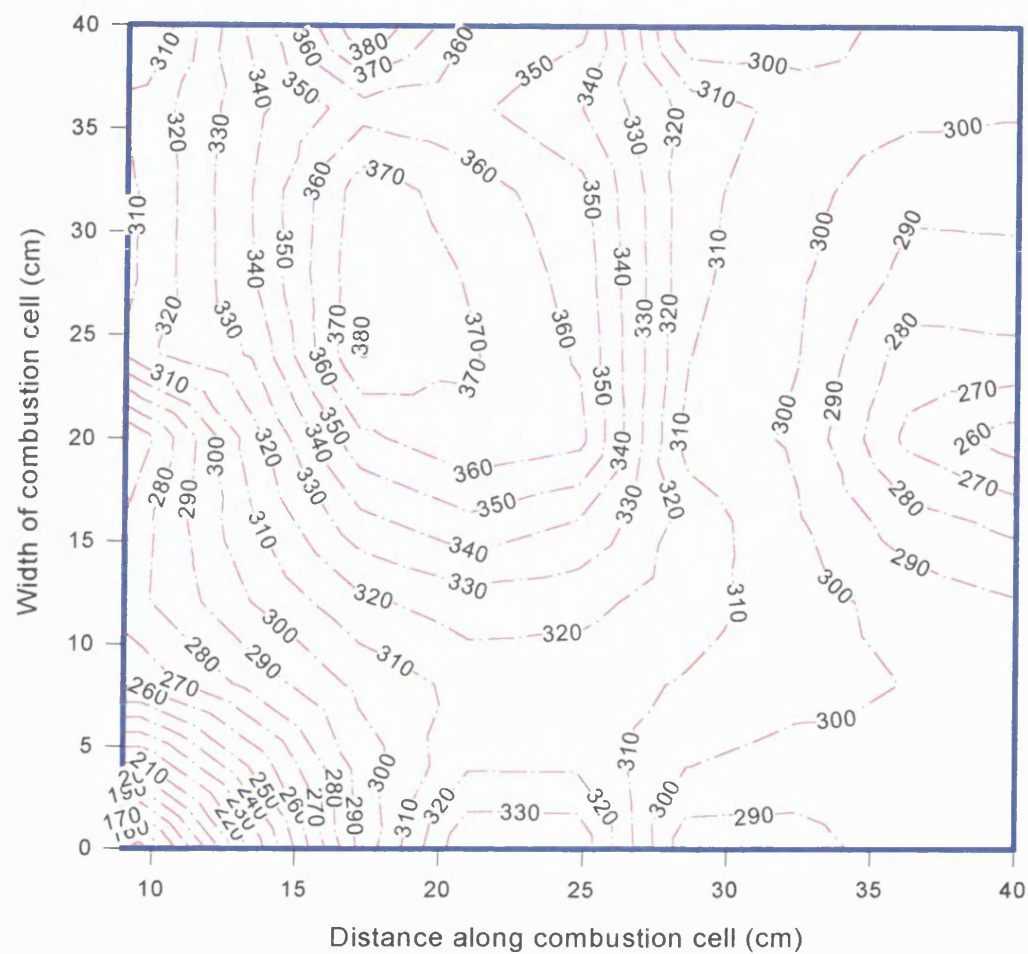


(a)

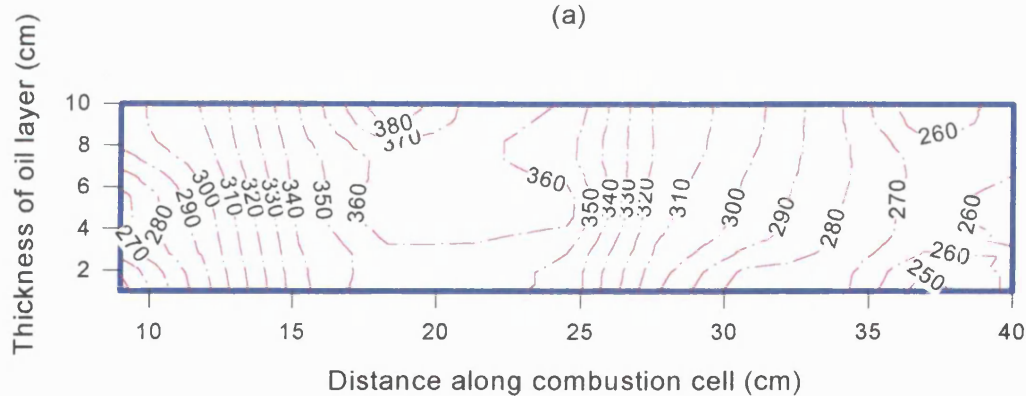


(b)

Figure 5.58 Run 972: Temperature profiles in sandpack (a) Horizontal mid-plane, (b) Vertical mid-plane. [Wet normal, Wolf Lake]. Combustion Time = 240 minutes (94 minutes after water injection)

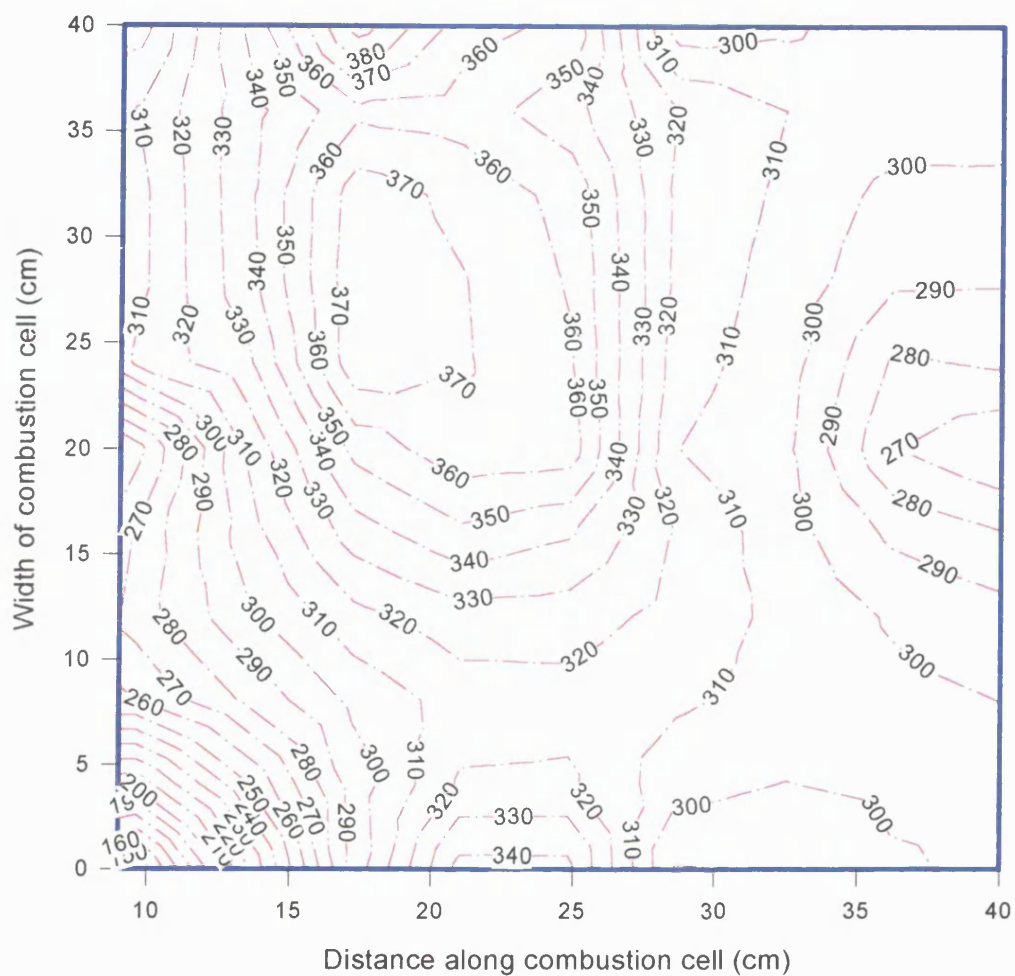


(a)

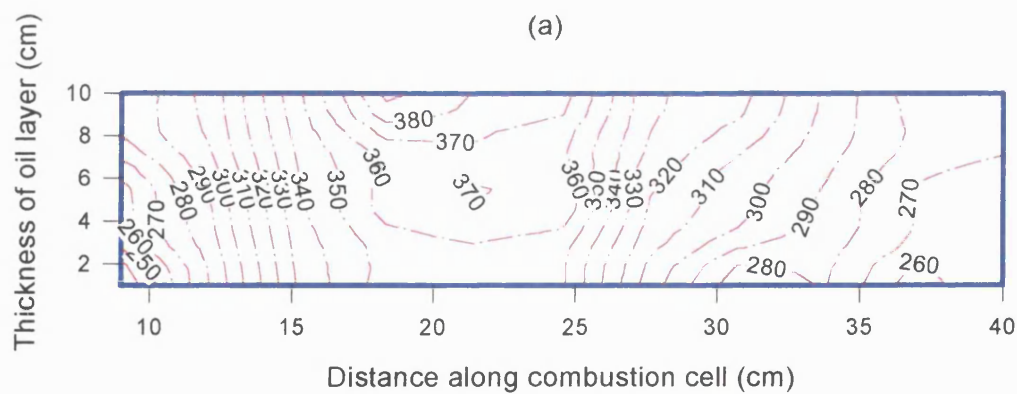


(b)

Figure 5.59 Run 972: Temperature profiles in sandpack (a) Horizontal mid-plane, (b) Vertical mid-plane. [Wet normal, Wolf Lake]. Combustion Time = 300 minutes (154 minutes after water injection)



(a)



(b)

Figure 5.60 Run 972: Temperature profiles in sandpack (a) Horizontal mid-plane, (b) Vertical mid-plane. [Wet normal, Wolf Lake]. Combustion Time = 330 minutes (184 minutes after water injection)

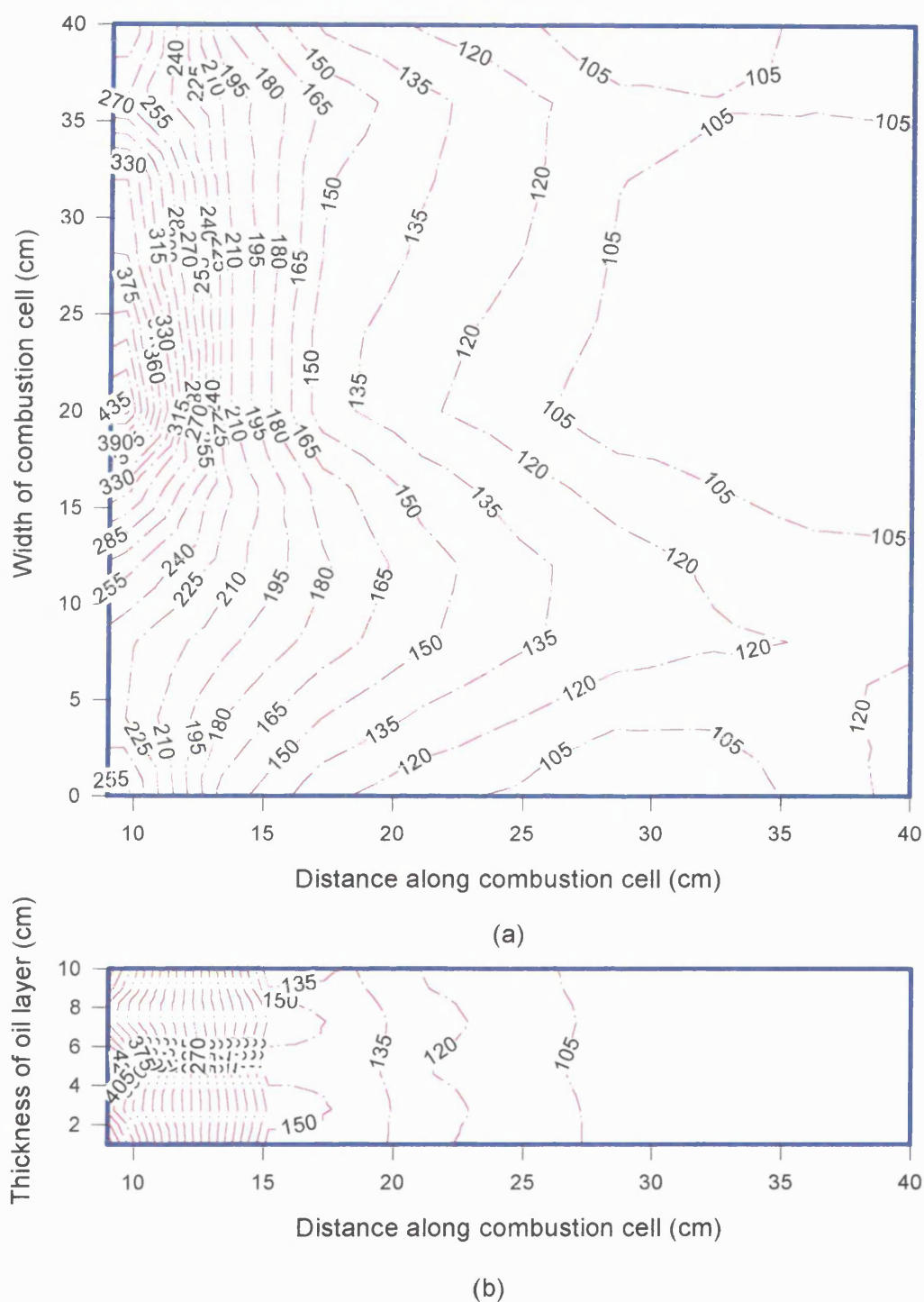
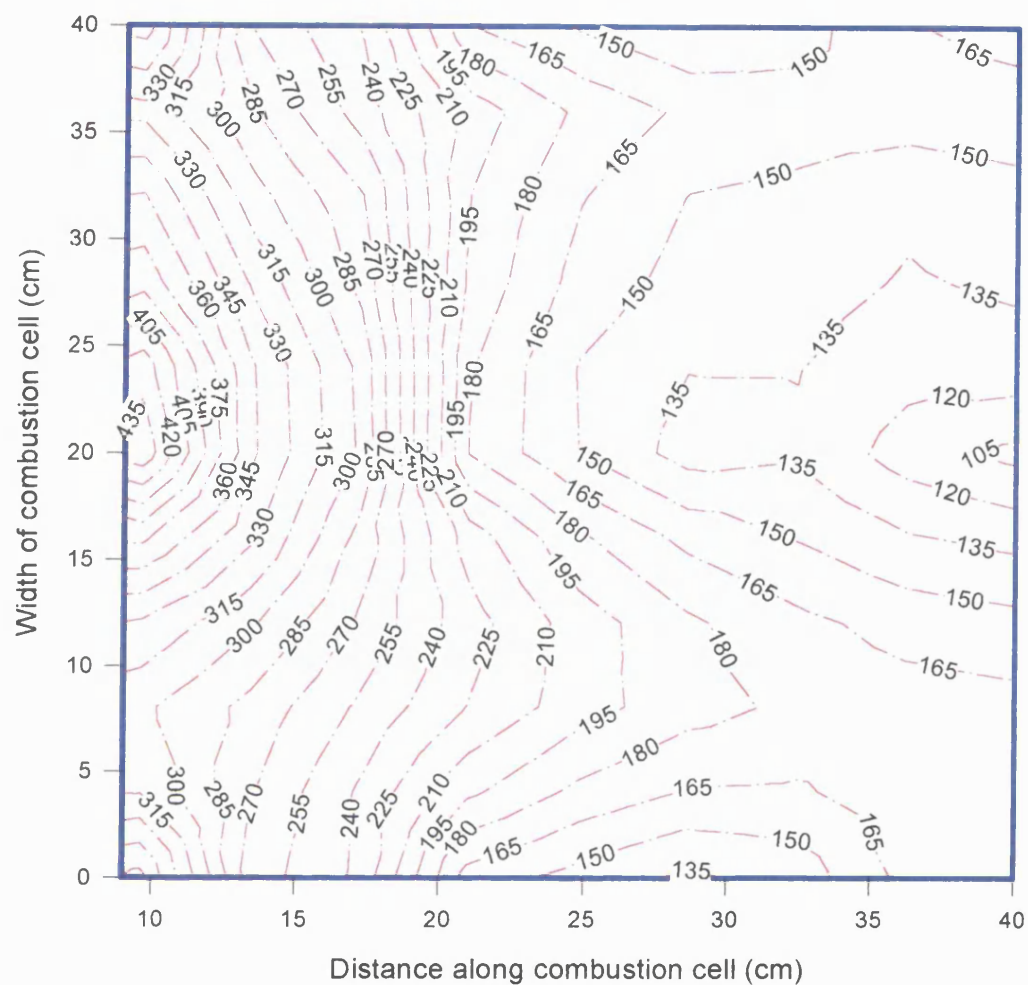
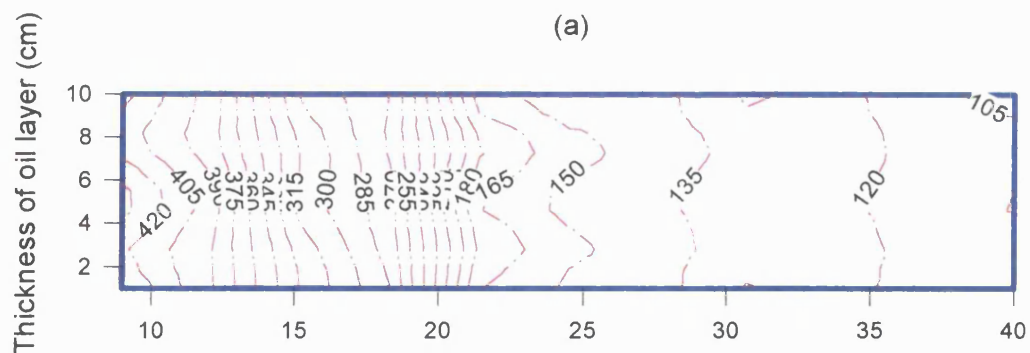


Figure 5.61 Run 976: Temperature profiles in sandpack (a) Horizontal mid-plane, (b) Vertical mid-plane. [Wet catalytic, Wolf Lake]. Combustion Time = at ignition

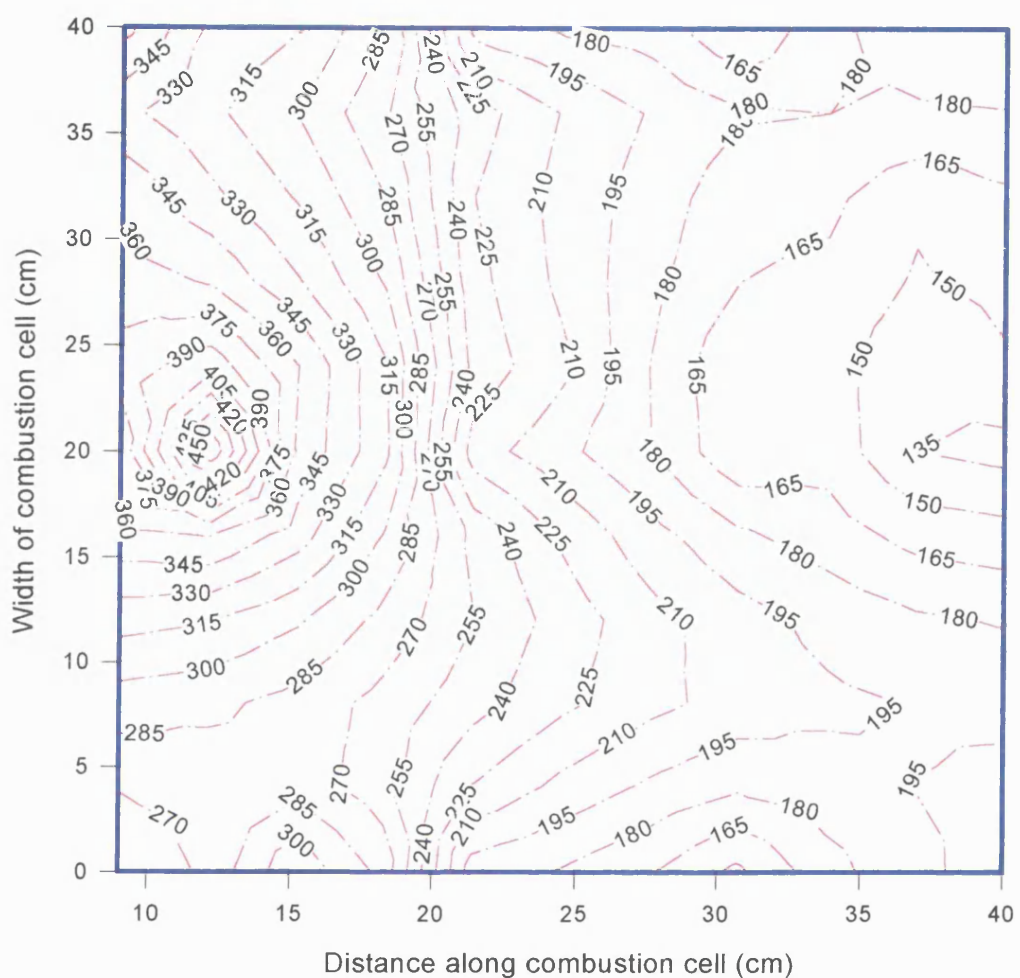


(a)

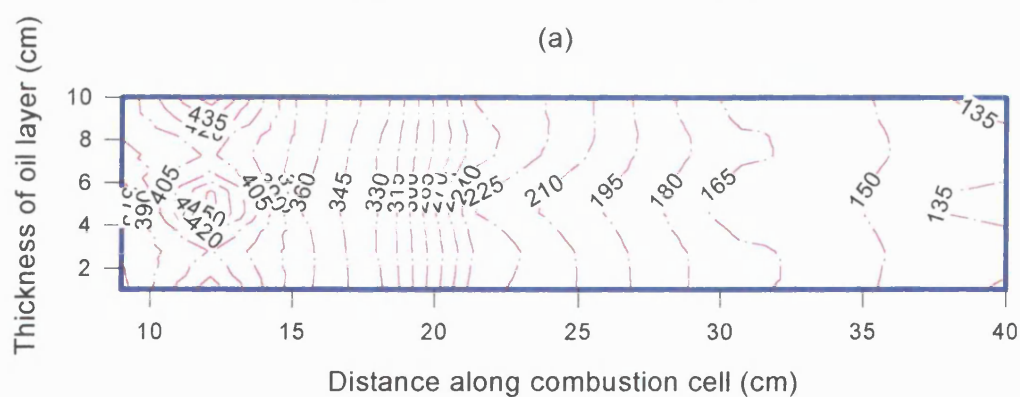


(b)

Figure 5.62 Run 976: Temperature profiles in sandpack (a) Horizontal mid-plane, (b) Vertical mid-plane. [Wet Catalytic, Wolf Lake]. Combustion Time = 120 minutes

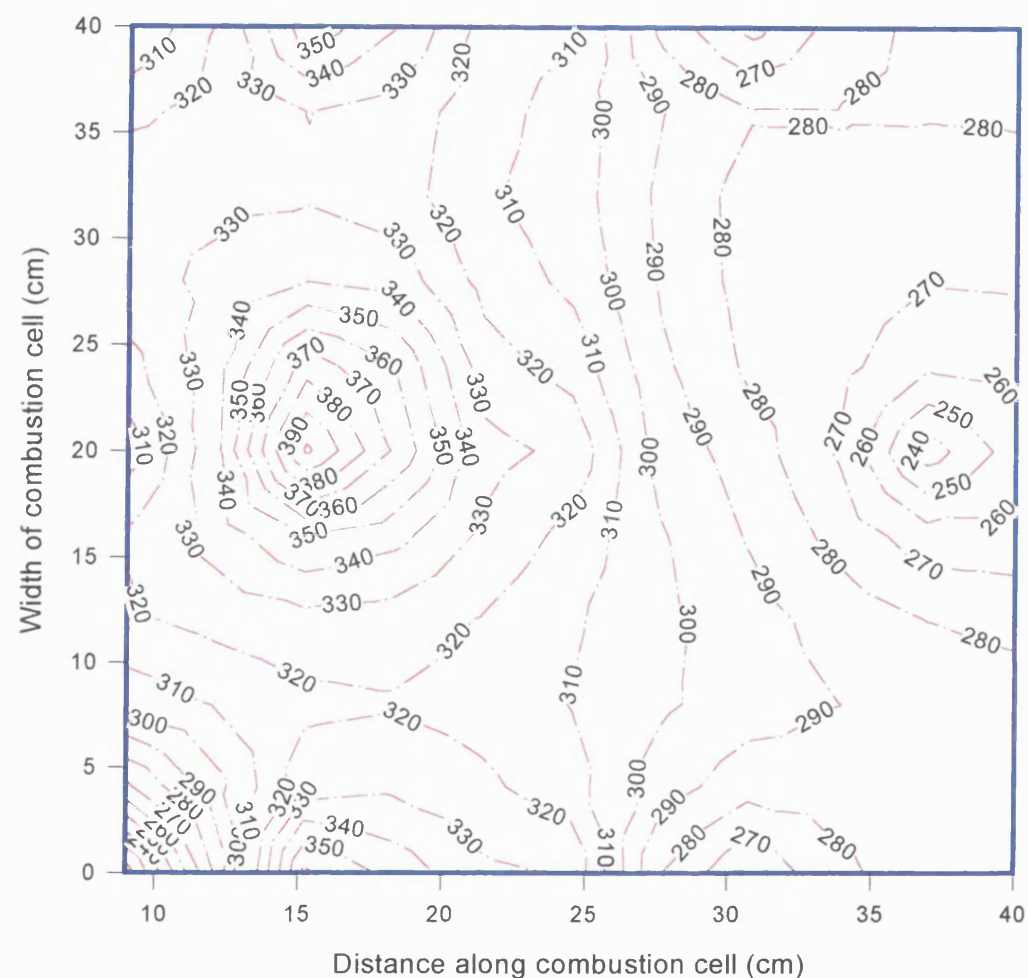


(a)

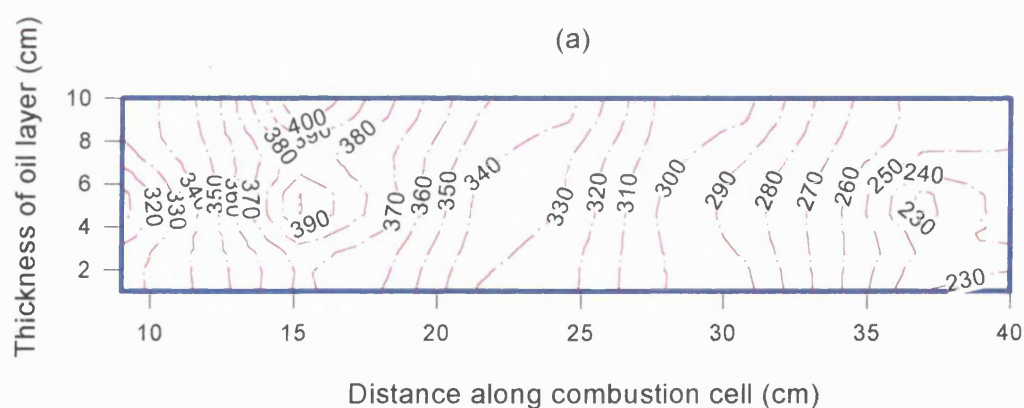


(b)

Figure 5.63 Run 976: Temperature profiles in sandpack (a) Horizontal mid-plane, (b) Vertical mid-lane. [Wet catalytic, Wolf Lake]. Combustion Time = 180 minutes (10 minutes after water injection)



(a)



(b)

Figure 5.64 Run 976: Temperature profiles in sandpack (a) Horizontal mid-plane, (b) Vertical mid-plane. [Wet catalytic, Wolf Lake]. Combustion Time = 240 minutes (70 minutes after water injection)

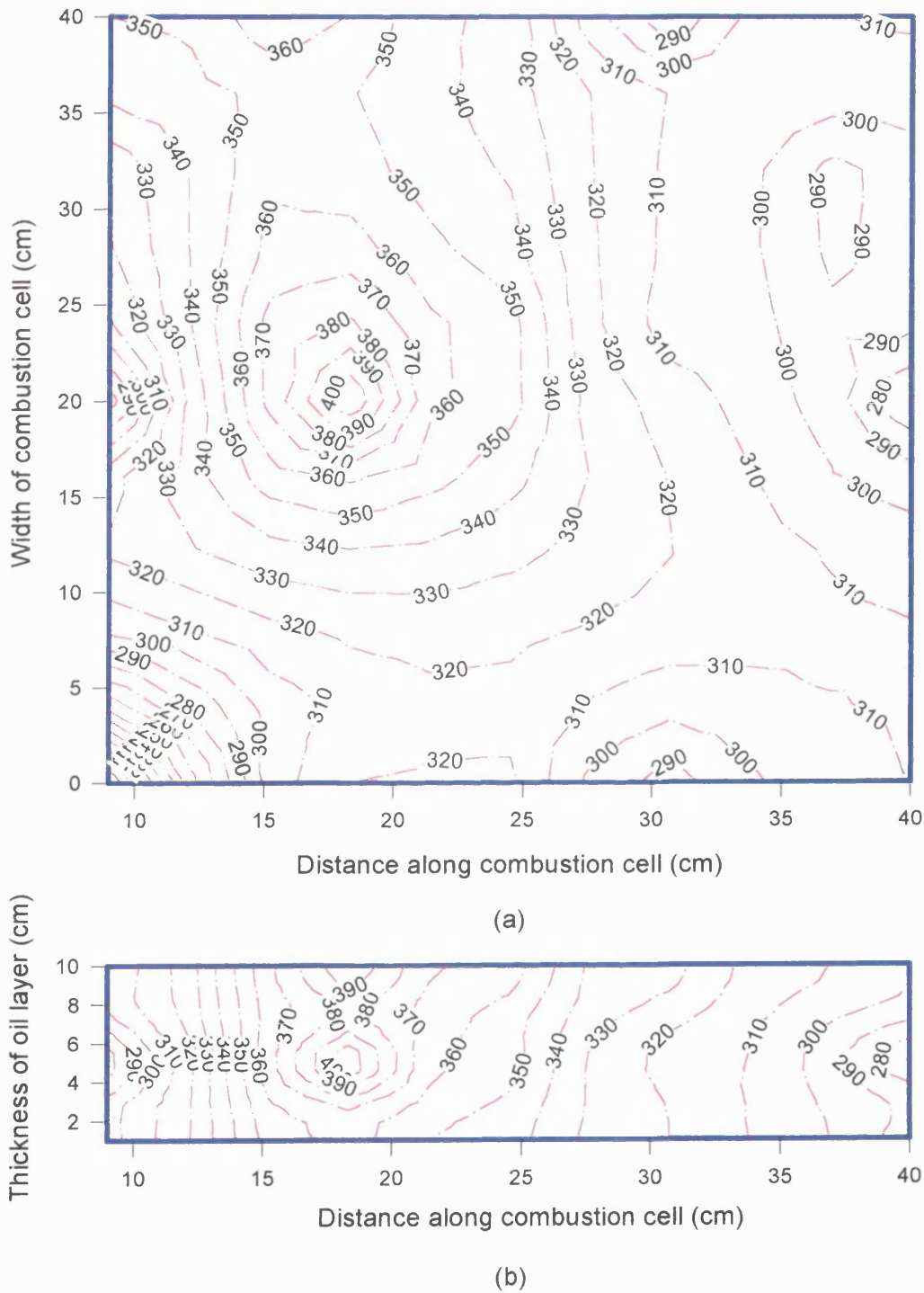
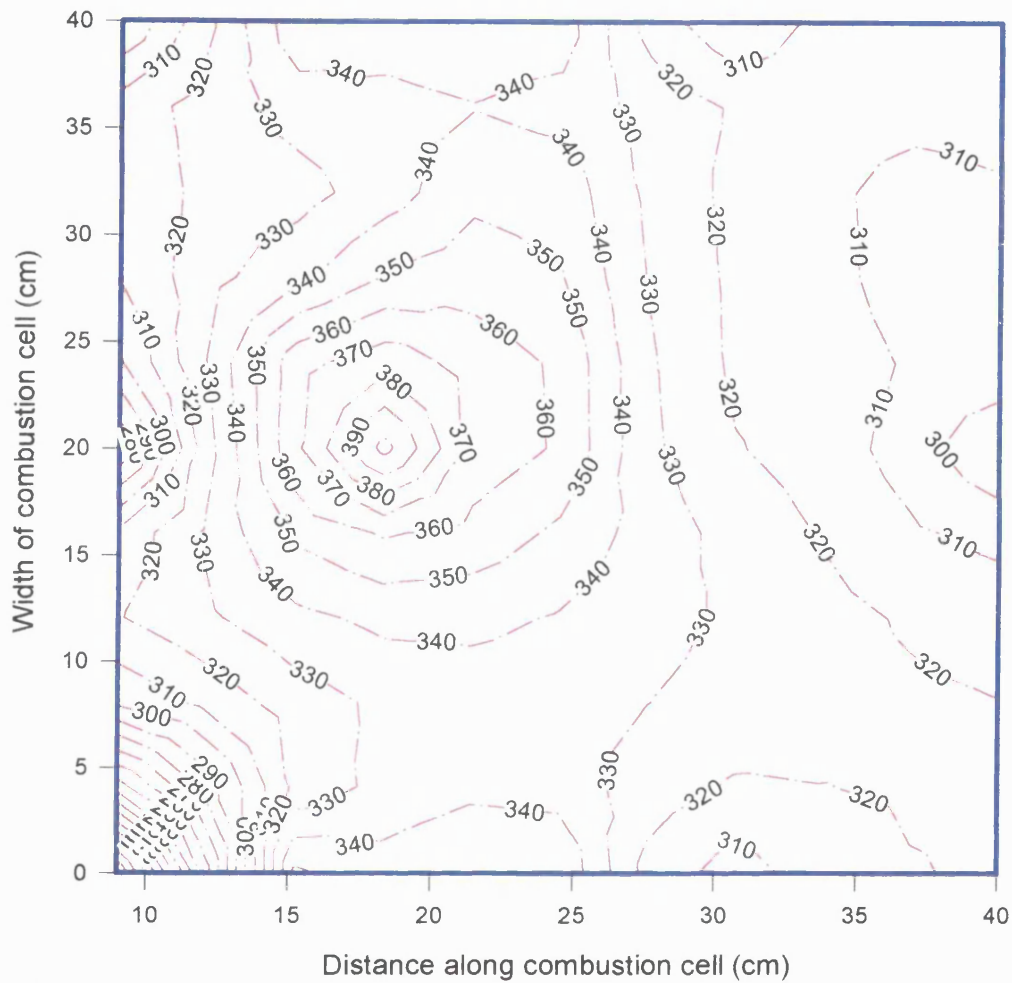
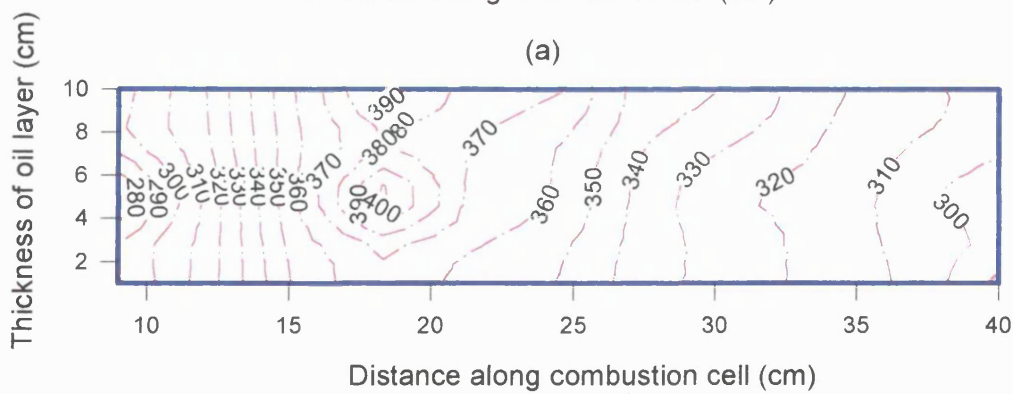


Figure 5.65 Run 976: Temperature profiles in sandpack (a) Horizontal mid-plane, (b) Vertical mid-plane. [Wet catalytic, Wolf Lake]. Combustion Time = 300 minutes (130 minutes after water injection)



(a)



(b)

Figure 5.66 Run 976: Temperature profiles in sandpack (a) Horizontal mid-plane, (b) Vertical mid-plane. [Wet catalytic, Wolf Lake]. Combustion Time = 318 minutes (148 minutes after water injection)

5.4 Post-mortem Analysis

The photographs taken of these experiments were largely of poor quality. Only a few of the ignitor region are given. However, some 'sketches' have been made, which provide a record of the events occurring.

In Figure 5.67 a, b, and c, three photographs taken at the inlet face, at injector and at ignitor for Run 971. They show, to some degree, the vigorous ignition in the right-hand side of the sandpack, which is located opposite to the injection well head. On the other hand, the dark colour is covering most of the left-hand side of the sandpack. This indicates that air supply was not uniformly distributed due to excessive pressure drop along the horizontal injector.

Figure 5.68 a is a sketch of the sandpack condition at 60mm from the inlet face.

There are two dark brown areas, one in the left-hand side covering about 25 % of the sandpack and another dark brown area is restricted on the right-hand side of the sandpack. The variation in size between both areas is most probably related to the amount of air injected into each area. There is a clean dark-grey coloured sand covering about 70 % of the sandpack. This zone is effectively swept by the combustion front and generated gases as evident by coke layers on its edges.

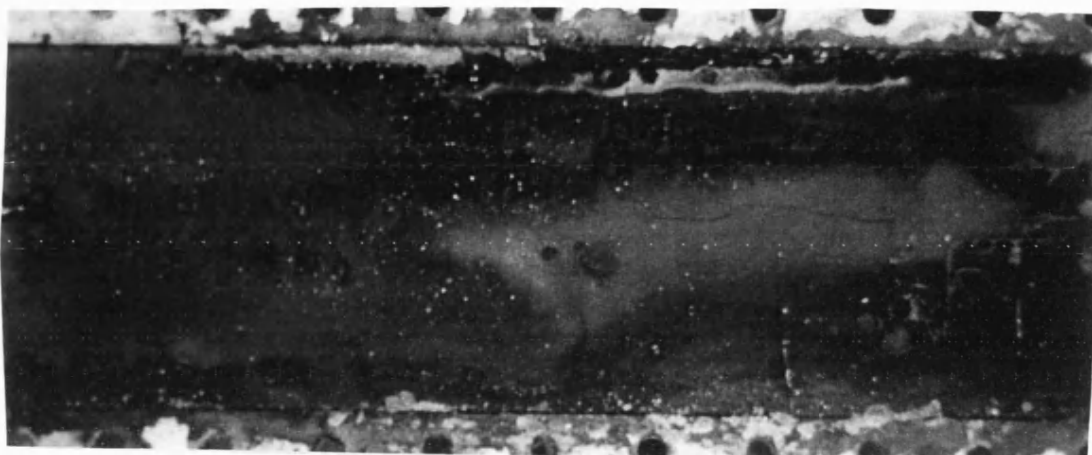
At 170mm, Figure 5.68 c, the clean sand zone is only located in the central region of the sandpack, with almost full cover to the entire thickness of the sandpack and surrounded by a thin coke layer. This suggests that the combustion front was fully controlled with no gas override tendency. At 230mm, Figure 5.68 d, the dark brown coloured sand covers about 75 % of the sandpack, whereas an arch-shaped clean sand zone is restricted in the top section of the sandpack. Clearly, at later stages of the

experiment, gas override occurred as the combustion zone and generated gases approached the lowest pressure point in the sandpack (i.e. production end); therefore, some degree of gas override is expected.

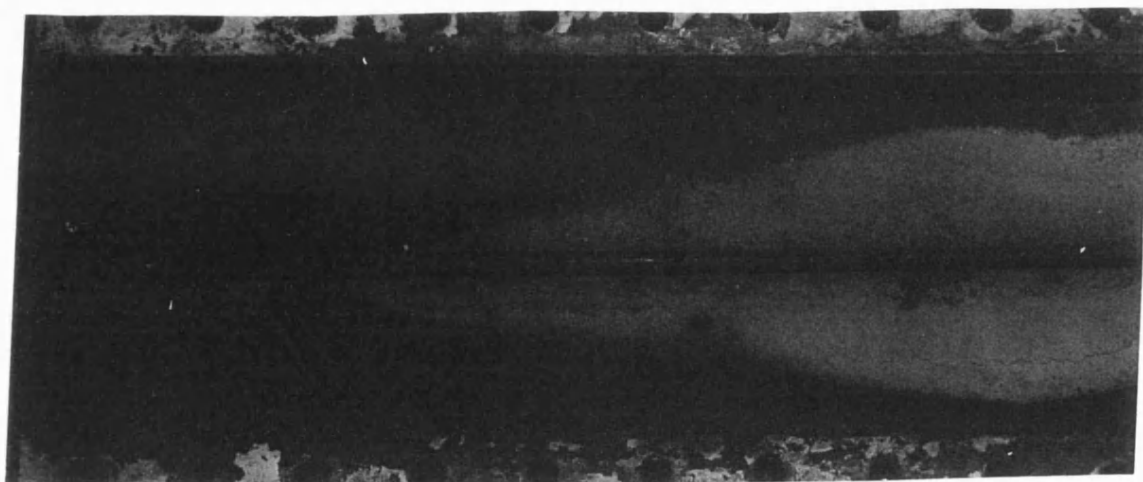
In Run 975, Figure 5.69, the main finding is the presence of a coke layer surrounding the catalyst bed. This was distinguished from the catalyst itself by its semi-solid, very fine texture.

In Run 972, a clean sand zone was only found at about 80mm from the inlet face. At 120mm, a substantial amount of a solid-hydrocarbon residual was found, which covered most of the sand face. This residual probably resulted from incomplete combustion of coke when the injected water quenched the combustion zone.

At 150mm and beyond, the light brown coloured sand was dominant, indicating the effectiveness of wet combustion by the in situ steam generation. At 230mm, Figure 5.70, the swept area is extending along the entire width of the sandpack, and the dark brown area is mainly located near the edges in the middle and bottom of the sandpack. This may explain the high oil recovery achieved in the wet runs although their overall time was about 50 % shorter. For Run 976, a similar trend was also observed, but with the existence of a coke layer around the catalyst bed as shown in Figure 5.71.



(A)



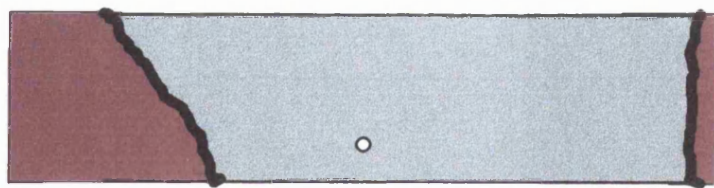
(B)

Figure 5.67 Post-mortem analysis photographs for Run 971 (Dry Normal, Wolf Lake)
(A) at the inlet face, (B) at the injection well

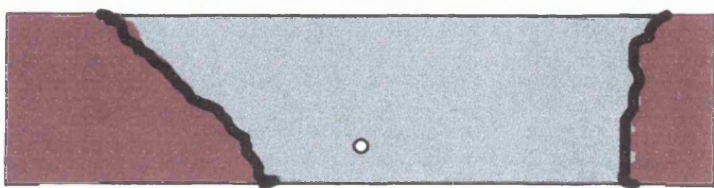


(C)

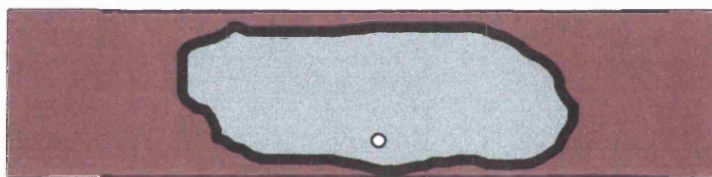
Figure 5.67 Post-mortem analysis photographs for Run 971 (Dry Normal, Wolf Lake)
(C) at the ignitor



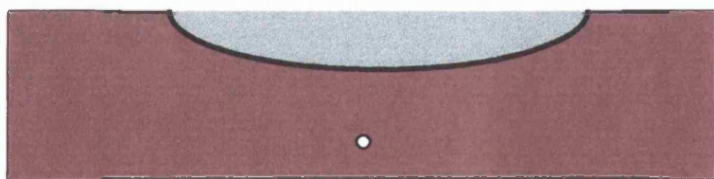
(a)



(b)



(c)



(d)

Figure 5.68 Post-mortem analysis sketches for Run 971 (Dry normal) (a) at 60mm, (b) at 100mm (c) at 170mm, (d) at 230mm from inlet face of the combustion cell.



Figure 5.69 Post-mortem analysis sketch for Run 975 (Dry catalytic) at 150mm from inlet face.

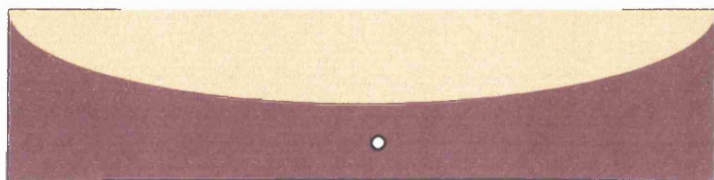


Figure 5.70 Post-mortem analysis sketch for Run 972 (Wet normal) at 230mm from inlet face.

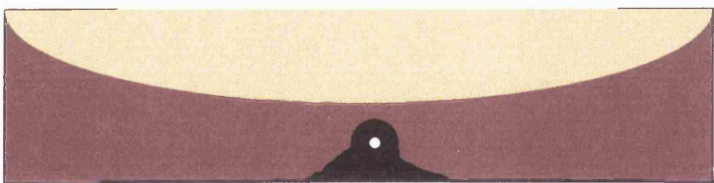


Figure 5.71 Post-mortem analysis sketch for Run 976 (Wet catalytic) at 230mm from inlet face.

CHAPTER SIX

CONCLUSIONS AND RECOMMENDATIONS

CONCLUSIONS

I. In-Situ Combustion Experiments

1. For the lighter Forties Mix 1 crude oil, a high hole perforation density along the horizontal producer (Design 2) was found to increase the desaturation rate of the oil layer in downstream regions (ahead of the combustion front), resulting in a reduced fuel availability ahead of the combustion front, which eventually caused the combustion front to die.

For the medium heavy crude oil (Clair), a high hole perforation density along the horizontal producer well resulted in a higher level of oxygen in the produced gas, but this did not affect combustion front propagation.
2. With medium heavy crude oil, fluid inflow into the horizontal producer well is partially restricted to the narrow mobile zone ahead of the combustion front determined by the 'viscous barrier' downstream in the sandpack. In the case of light Forties Mix 1 crude oil, this does not occur, except in the early stages of the experiment, due to the much higher oil mobility.
3. For the medium heavy crude oil, an oxygen flux of approximately $1.2 \text{ sm}^3/\text{m}^2 \text{ hr}$ was found to be suitable for sustaining a stable high temperature combustion front, whilst for the light Forties Mix 1 crude oil an oxygen flux of $0.95 \text{ sm}^3/\text{m}^2 \text{ hr}$ was satisfactory.
4. A horizontal producer well in direct-line drive is very effective for controlling gas override and maintaining a stable, essentially vertical combustion front when the oil has a sufficiently high viscosity, preventing desaturation of the oil layer

downstream. This is because of the draw-down of combustion gases and mobilised fluids directly into the exposed, or active section, of the well. This effect may also be beneficial for controlling adverse local heterogeneity.

5. For a light crude oil in a watered-out reservoir a limited sweep of only 10 to 20 % of the reservoir length, may still be sufficient to achieve economic oil displacement because of the very effective steam flood created ahead of the combustion front.
6. The new horizontal producer well concept (Design 3), incorporating a continuous 'sleeve-back' principle in the upstream well section was successful in controlling the level of desaturation occurring in the downstream oil layer. This enabled a self-sustained combustion front to be achieved using light 'Forties Mix 1' oil. However, the relatively low combustion front temperature (377 °C) was not sufficient to burn all of the available fuel.

The level of CO₂ in the produced gas was higher than that observed for the conventional horizontal line drive experiments, and the oxygen level was also lower.

7. Restricting gas flow into the downstream region of the sandpack by sleeving-back the well causes a lateral expansion of the gas displacement, greatly improving the overall sweep efficiency. This effect is similar to that created by the 'viscous barrier' with a heavy viscous oil.

II. Downhole Catalytic Upgrading Experiments

1. The recovery of heavy crude under *in-situ* combustion ‘toe-to-heel’ displacement is restricted to a narrow zone ahead of the combustion front, wherein mobilised fluids at high temperature are drained under pressure controlled, gravity-assist flow directly into the horizontal producer well. The exposed section of the horizontal well, corresponding to the longitudinal extent of the mobile oil zone, effectively defines the limits of the active section of the annular catalyst bed, or annular reactor. Placement of the catalyst to create an annular radial inflow reactor in this manner, is very effective for maintaining high catalyst activity. This is because the catalyst only contacts mainly thermally cracked oil and not crude oil. Catalyst activity is further enhanced by the continual exposure of fresh catalyst as the combustion front moves along the horizontal well.
2. Under the experimental conditions used in this study, oil produced by *in-situ* combustion (non-catalytic) is upgraded by 2 to 3 points compared with the original crude oil, whereas the viscosity is reduced from 100,000 to 9246 cp.
3. When a catalyst bed was placed along the horizontal producer well in line drive, higher upgrading was achieved, which ranged from 7 to 10 points for dry and wet ISC/catalytic experiments, respectively. The viscosity of the produced oil was also dramatically reduced to 118 and 34 cp, respectively. The produced oil from the wet-catalytic experiment had a lower IBP and lower residual (0.5 % wt) compared with the original crude oil. GC analysis of the produce oil subjected to

downhole catalytic upgrading, showed that it contained substantially increased amounts of lighter fractions compared to the heavy crude oil.

4. Elemental analysis of produced oil from the wet catalytic experiment showed a very large reduction in the sulphur content of the oil from 43400 to 5100 mg/kg. Also, heavy metals were greatly reduced; Vanadium from 195 to 8 mg/kg and Nickel from 73 to 3 mg/kg, as a result, partly, of HDS and HDM effect of the catalyst along the horizontal producer well.
5. Water injection is beneficial in improved the quality of the produced oil, firstly, by promoting, or increasing, the generation of hydrogen by water-gas shift reaction and, secondly, because of the possible restoration of catalyst activity by the presence of steam.

RECOMMENDATIONS

- 3-D system combustion experiments are valuable for understanding the reservoir dynamics of the ISC/ Horizontal wells process. More sophisticated temperature measurement and control and ability to achieve improved adiabatic temperature conditions would be advantageous. Fibre optics should be investigated.
- An automatic back-pressure control and sampling system would enable improved control of the experiments, leading to increased efficiency and measurement accuracy.
- A new design to the injection well is required to achieve uniform air distribution along the sandpack. The effect of perforation hole diameter and density distribution should be investigated. However, the use of sintered stainless tube may be superior.
- In this study, the effect of hole perforation density was determined at low pressure. Future work should be extended to apply an external pressure on the sandpack by using the pressure shell.
- It is very important to sample the reactant gas produced in the mobile oil zone in order to measure the amount of hydrogen produced by water gas shift reaction. This could be achieved either by using fixed sample probes at specific locations (e.g. at thermocouples ports), or alternatively using a miniaturised version of the sleeve-back well, incorporating a sample probe at the leading toe position. The advantage of the latter is that continuous sampling could be achieved.

- The effectiveness of the narrow mobile zone ahead of the combustion front (created by the ‘viscous barrier’ effect in a heavy oil reservoir, or by artificial means using sleeve-back) for minimising the effect of adverse heterogeneity should be investigated.
- A complete analysis of the produced gas is a very important tool to obtain precise flue gas composition (inerts, hydrocarbons and H_2S), especially for catalytic experiments.
- The base line for the effect of thermal cracking on oil properties and composition must be established. This will require study of a wider range of air flux and WAR.
- Detailed elemental analysis of produced oil is important to determine the precise material balance, especially with respect to sulphur and heavy metals.
- The catalyst used in this study was pre-sulphided and may have provide “extra” reactivity. In the future work, fresh catalyst should be used to evaluate performance when the catalyst is sulphided in situ from the sulphur contained in the heavy crude oil.
- Hydroconversion needs to be studied in terms of the thickness of the annular catalyst layer.
- Analysis of the used catalyst and also sand matrix should be made to determine the extent of HDS and HDM.

- Post-mortem analysis of the sandpack is a very important technique to evaluate the performance of the in situ combustion process. The use of a high resolution digital camera should be considered.

REFERENCES

REFERENCES

- Adegbesan, K. O., Donnelly, J. K., Moore, R. G., and Bennion, D. W.: "Low Temperature Oxidation Kinetic Parameters for In-Situ Combustion Numerical Simulation", SPE 12004, presented at the 58th Annual Technical Conference and Exhibition of SPE-AIME, San Francisco, CA, Oct,5-8,1983.
- Abu-Khamsin, S. A., Brigham, W. E., and Ramey Jr, H. j. : " Reaction Kinetics of Fuel Formation for In Situ Combustion" SPE 15736, presented at the 5th SPE Middle East Oil Show, Manama, Bahrain, March 7-10, 1987.
- Ahner, P. F., Sufi, A. H. , "Physical Model Steam-flood Studies Using Horizontal Wells" SPE/DOE 20247, 7th Symposium on EOR, Tulsa, April 22-25, 1990.
- Alexander, J. D., Martin, W. L., and Dew, J. N.: "Factors Affecting Fuel Availability and Composition During In-Situ Combustion " Journal of Petroleum Technology,Oct.1962, pp1154-64.
- Al Qahtani, A. M., Menouar, H., and Al Majid, A. : "Effect of Length and Distribution of Perforated Intervals on Horizontal Wells Rates" SPE 37112 presented at the 1996 SPE International Conference on Horizontal Well Technology, Calgary, Canada, 18-22 November 1996.
- Alpert, S.B., Chervanak, M.C., Shuman, S. C., and Volk, H. R., AICHE 64th National Mtg., New Orleans, March 16-20, 1969.
- Al Shamali, M.: " In Situ Combustion (ISC) Processes: Compositional Effects and Oil Upgrading", MPhil Thesis, University of Bath, 1993.
- Ames, B. G., Grams, R. E. and Pebdani, F.N. "Improved Sweep Efficiency Through the Application of Horizontal Well Technology in a Mature Combustion EOR Project: Batttrum Field, Saskatchewan, Canada", paper presented at the DOE/NIPER, Tulsa, OK, April 21-22,1994.

REFERENCES

- Babu, D. R., and Cormack, D. E.: “Effect of Low Temperature Oxidation on the Composition of Athabasca Bitumen,” *Fuel*, June 1984, pp 858-61.
- Bae, J. H.:” Characterization of Crude Oil for Fireflooding Using Thermal Analysis Methods” *Soc. Pet. Eng. J.* (June, 1977) pp211-18.
- Bagci, S., Aybak, T., and Shamsul, A.: “The performance of Steam Injection in Heavy Oil Reservoirs with Bottom Water Zone Employing Diverse Well Configurations,” 7th European Symposium on Improved Oil Recovery, Moscow, 27-29 Oct., 1993, Vol.2, pp 185-197.
- Bagci, S., and Gumrah, F.: “An Examination of Steam Injection Processes in Horizontal and Vertical Wells for Heavy-Oil Recovery,” *Journal of Petroleum Science and Engineering*, 8(1992), pp 59-72.
- Bartholomew, C.H., Chemistry Industries, Marcel Dekker, New York, Vol.58, 1994.
- Beckers, H.L. and Harmsen, G.J.:” The Effect of Water Injection on Sustained Combustion in a Porous Medium,” *Soc. Pet. Eng. J.*, June 1970, pp145-163.
- Behar, F., Audibert, A., and Villalba, M “Secondary Cracking of Crude Oils: Experimental Study” *Energy and Fuel*, 1988, pp574-581.
- Binder, G.G., Elzinga, E. R., Tarmy, B. L., and Willman, B. T., ”Scaled-Model Tests of In-Situ Combustion in Massive Unconsolidated Sands” *Proceedings of 7th World Petroleum Congress*, Mexico City, March 1967, pp477-485.
- Bilkar, H., Drevdal, K. E., and Aarestad, T. V. : “Extended Reach, Horizontal and Complex Design Wells: Challenges, Achievements and Cost-Benefits” *SPE 28005*, presented at *SPE Centennial Petroleum Engineering Symposium*, Tulsa, OK, 29-31 Aug. 1994.
- Bousaid, I.S. and Ramey, H. J. ”Oxidation of crude oil in porous media” *Soc. Pet. Eng. J.* June 1968, pp137-148.
- Brekke, K. : “New and Simple Completion Methods for Horizontal Wells Improve the Production Performance in High Permeability, Thin Oil Zones,” *SPE*

REFERENCES

- 24762 presented at the 67th SPE Annual Technical Conference and Exhibition, Washington D.C., USA, October 1992.
- Bulmer, J.T., and Liu, J.K.: “Analytical Technology for Heavy Oil Upgrading” Paper No 48 presented at International Conference on Heavy Oil and Tar Sands, Zhuo Zhuo, China, Oct. 26-30, 1987.
 - Burger, J. G. and Sahuquet, B. C. : “Laboratory Research on Wet Combustion “, Journal of Petroleum Technology, 1973, Vol. 25, pp 1137-1146.
 - Burger, J. G. and Sourieau, P. :” Thermal Recovery Methods”, Institute Francis du Petrol, 1985, pp 146-206.
 - Burger, J. G. and Sahuquet, B. C.: “Chemical Aspects of In Situ Combustion-Heat of Combustion and Kinetics, “ Soc. Pet. Eng. J. Oct 1972, pp 410-422.
 - Butler, R. M. : “ A New Approach to the Modeling of Steam Assisted Gravity Drainage,” Journal of Canadian Petroleum Technology, May-June 1985, pp 24-42.
 - Butler, R. M and Stephens, D. J.:“ The Gravity Drainage of Steam Heated Heavy Oil to Paralleled Horizontal Wells,” Journal of Canadian Petroleum Technology, April-June 1981, pp90-96.
 - Crynes, B.: “Chemical Reactions as a Means of Separation: Sulphur Removal” Marcel Dekker, Inc., New York, Vol.11, 1977, pp2-28.
 - Dabbous, M. K and Fulton, P.F. :” Low Temperature Oxidation Reaction Kinetics and Effects on the In Situ Combustion Process “ Soc. Pet. Eng. J. June 1974, pp 253-262.
 - Dietz, D.N. and Weijdem, J.:” Wet and Partially quenched combustion” Journal of Petroleum Technology , April 1968, pp 411-415
 - Egbogah, E.O., “EOR Target Oil and Techniques of its Estimation,” Journal of Petroleum Science and Engineering, Oct.1994, pp 337-349.
 - Ejioogu, G.C. ,Bennion , D.W. ,Moore , R.G. and Donnelly , J.K, “Wet Combustion: A Tertiary Recovery Process for The Pambina Cardium Reservoir” paper 78-29-32, 29th Annual Technical Meeting of CIM , Calgary, June 13-16, 1978.

REFERENCES

- Farouq Ali, S. M.: "Redeeming of In Situ Combustion" Proceedings DOE /NIPER Symposium on In-Situ Combustion Practices-Past, Present and Future Applications, Tulsa, Oklahoma, 21-22 April 1994, paper No ISI 1.
- Farouq Ali, S. M, Redford, D. A., and Islam, M.R. : "Scaling Laws for Enhanced Oil Recovery Experiments," Zhuo Zhuo, China, 26-30 October 1987.
- Fassihi, M. R., Brigham, W. E., and Ramey, H. J.: "The Reaction Kinetics of In-Situ Combustion, "SPE 9454 paper presented at the 55th Annual Technical Conference and Exhibition, Dallas, Texas, 21-24 Sep.,1980.
- Fassihi, M. R., Brigham, W. E., and Ramey, H. J.: Reaction Kinetics of In Situ Combustion Part 1-Observation, " Soc. Pet. Eng. J. August, 1984, pp 399-407.
- Fassihi, M. R., Meyers, K. O., and Basile, P. F.; "Low-Temperature Oxidation of Viscous Crude Oils," SPE 15648, SPE Reservoir Engineering, Nov. 1990, pp 609-16.
- Fassihi, M. R. and Gillham, T.H.: " The Use of Air Injection to Improve the Double Displacement Processes," Proceedings of DOE/NIPER Symposium on In-Situ Combustion Practices-Past, Present and Future Applications, Tulsa, OK, 21-22 April 1994, pp 105-119.
- Froment, G.F., Delmon, B., and Grange, P.: "Hydrotreatment and Hydrocracking of Oil Fractions" Elsevier Science B.V. 1997, PP13-16.
- Frost, C. M., and Cottingham, P.L.: "Chemical Reactions as a Means of Separation: Sulphur Removal" Marcel Dekker, Inc., New York, Vol.11,1977, pp8.
- Garon, A. M., and Wygal, R. J. : " Laboratory Investigation of Wet Combustion Parameters," Soc. Pet. Eng. J. Dec. 1974, pp 537-544.
- Garon ,A. M., Geisbrecht, R. A., and Lowry jr, W. E.: " Scaled Model Experiments of Fireflooding in Tar Sands," Journal of Petroleum Technology, Sep.1982, pp 2158-2166.
- Garon, A.M., Kumar, M., Lau, K.K., and Sherman, M. D.: "A Laboratory Investigation of Sweep During Oxygen and Air Fireflooding," SPE/DOE 12676 4th Symposium on EOR , Tulsa, OK , April15-18,1984.

REFERENCES

- Greaves, M., and Ben Rahil, M. : "Recovery of Residual Light Oil from Waterflooded Reservoirs Using Horizontal Wells-In Situ Combustion Process" Paper presented at the 8th European IOR Symposium, Vienna, Austria, May 15-17, 1995.
- Greaves, M., Tuwil, A. A , and Field, R. w. : "Horizontal Producers Wells in In Situ Combustion Processes," CIM/AOSTRA Annual Technical Conference, Banff, Canada, 21-24 April 1991.
- Greaves, M., Al Shalabe, M. I. : " In Situ Combustion Studies of North Sea Forties and Maya Crude Oils" Chem.Eng.Res.Des, Vol.65, 1987, pp29-40.
- Greaves, M., and Wang, Y. D. : "3D Physical Modeling of In Situ Combustion (ISC) in Heavy Oil Reservoirs with a Bottom Water Layer", Proceedings of the 7th European Symposium on Improved Oil Recovery, Moscow, 26-29 Oct.1993, pp 198-207.
- Greaves, M., Field, R. W., and Adewusi, V. A.: " In Situ Combustion Kinetics Studies of Medium Heavy Crude Oil," Chem. Eng. Res. Des., Vol. 66,1988, pp 328-333.
- Greaves, M., and Al Shamali , O.: " Wet In Situ Combustion (ISC) Using Horizontal Wells" Proceedings of the 6th UNITAR International Conference on Heavy Crude and Tar Sands, Richard F Meyer (Ed), US DOE, 1995,pp 405-417.
- Greaves, M., Wilson, A., Lockett, A. D., and Al Honi, M.: " Improved Recovery of Light/Medium Heavy Oils In Heterogeneous Reservoirs Using Air Injection/ In Situ Combustion (ISC)," SPE Western Regional Meeting, Anchorage, Alaska, May 1996.
- Greaves, M., and Saghr A.M.: " A New Horizontal Well Concept For IOR from Light Oil Reservoirs Using Air Injection," the 1997 European Symposium on IOR , The Hague, 20-22 Oct. 1997.
- Greaves, M., Ren, S.R., and Rathbone, R.R.: "Air Injection Technique (LTO Process) for IOR from Light Oil Reservoirs: Oxidation Rate and Displacement

REFERENCES

- Studies" SPE 40062, presented at the 1998 SPE/DOE Improved Oil Recovery Symposium, Tulsa, Oklahoma, 19-22 April, 1998.
- Greaves, M., and Xia, T. X.: "Preserving Downhole Thermal Upgrading Using 'Toe-to-Heel' ISC-Horizontal Wells Process," paper to be presented at the 7th UNITAR International Conference on Heavy Crude and Tar Sands, Beijing, Oct.27-30, 1998.
 - Goodman, D. R., and Oxon, B. A.: "Handling and Using of Catalyst on the Plant" in Catalyst Handbook, (Wolfe Scientific Books), 1970, pp161-181.
 - Hajdo, L. E., Hallam, R. J., and Vorndran, L.D.L.: "Hydrogen Generation During In-Situ Combustion" SPE 10204 presented at California Regional Meeting, March 27-29, 1985.
 - Hansel, J. G., Benning, M. A., and Fernbacher, J. M., "Oxygen In Situ Combustion for Oil Recovery Combustion Tube Tests" Journal of Petroleum Technology, Feb.1977,pp111-119.
 - Hardy, W. C., Fletcher, P. B., Shepard, J. C., Dittman, E. W., and Zadow, D. W. : "In Situ Combustion Performance in a Thin Reservoir Containing High Gravity Oil" Journal of Petroleum Technology, Feb. 1972, pp 199-208.
 - Hoffman, E. J., Energy Sources 1989, Vol. (11), pp 263-268.
 - Hughes, R., Kamath, V. M., and Price, D. : " Kinetics of In Situ Combustion for Oil Recovery" Chem. Eng. Res. Des., Jan. 1987, Vol.(65),pp 23-28.
 - Hwessa, M.M.: "Effect of Reservoir Inclination on the In-Situ Combustion-Horizontal Well Process" MPhil Thesis, University of Bath, 1998.
 - Hyne, J.B., and Tyrer, J. D.: "The Use of Hydrogen-Free Carbon Monoxide with Steam in Recovery of Heavy Oil at Low Temperatures", Canadian patent No. 1,170,444. July, 1984.
 - Islam, M. R., Chakma, A., Farouq Ali S.M. : " State of the Art In Situ Combustion Modeling and Operation," SPE 18755, California Regional Meeting, Bakerfield, April 5-7, 1989, pp 105-118.

REFERENCES

- Islam, M.R. and Chakma, A. "A new Recovery Technique for Heavy-Oil Reservoirs with Bottomwater," SPE 20258, SPE Production Engineering, May 1992, pp180-186.
- Johnson, H. S.; Bright. A.: "Upgrading of Heavy Hydrocarbon-aceous Oil Using Carbon Monoxide and Steam" Canadian patent 1,195.639 to Gulf Canada Limited. October 1985.
- Joshi, S. D.: "A laboratory Study of Thermal Oil Recovery Using Horizontal Wells", paper No. SPE 14916 SPE/DOE 5th symp. on EOR, Tulsa. OK, April 20-23 1986.
- Joshi, S. D. : " Augmentation of Well Productivity with Slant and Horizontal Wells," Journal of Petroleum Technology, June 1988, pp 729-739.
- Joshi, S. D. : "Thermal Oil Recovery With Horizontal Wells", paper SPE 21751, Journal of Petroleum Technology, Nov.1991, pp1302-1304.
- Joshi, S. D., and Ding, W. : " Horizontal Well Application: Reservoir Management," SPE 37036, presented at International Conference on Horizontal Well Technology, Calgary, 18-20 Nov.1996.
- Karlsson, H., Cobbley ,R., and Jacques, G. E. : " New Developments in Short-, Medium-, and Long-Radius Lateral Drilling Technology," paper SPE 18708 presented at SPE/IADC Drilling conference, New Orleans, Feb.28-March 3, 1989.
- Kisler, J. P., and Shallcross, D. C.: " The Effect of Metallic Catalysts on Light Crude Oil Oxidation, " In Situ, 20(2),1996, pp137-160.
- Kisman, K. E., and Lau, E. C. : " A New Combustion Process Utilizing Horizontal Wells and Gravity Drainage, " Journal of Canadian Petroleum Technology, 33, No.3,1994, pp39-45.
- Koen, A. D. : "Horizontal Drilling Retains Steady Share of US Activity," Oil and Gas Journal, Aug. 1992, pp 34-41.
- Latil, M.: " Enhanced Oil Recovery," Gulf Publishing Company, Houston,1980.

REFERENCES

- Lin, C. Y., Chen, W. H., Lee, S. T., and Culham, W.E. : “Numerical Simulation of Combustion Tube Experiments and Associated Kinetics of In Situ Combustion Process” *Soe. Pet. Eng. J.* Dec.1984.
- Mahgoub, M.: “ Improved Recovery of Light Oil by Air Injection Using Horizontal Wells” MPhil Thesis, University of Bath, 1995.
- Mamora, D. D., and Brigham , W. E.: “The Effect of Low Temperature Oxidation on Fuel and Produced Oil During In Situ Combustion of a Heavy Oil” *In Situ*, 19 (4),1993, pp341-365.
- McGee, B. C. W., Vermeulen, F. E., and Yu, C. L.: “Electrical Heating with Horizontal and Vertical Wells,” paper 96-98 presented at the 47th Annual Technical Meeting, Calgary, Canada, June 10-12, 1996.
- McIntyre, F., Grenon, J. P., and See, D.: “Horizontal Well Gas-ShutOff-Field Results” paper 96-63 presented at the 47th Annual Technical Meeting of the Petroleum Society, Calgary, Canada,10-12 June 1996.
- Moore, R.G., Bennion, D.W., Millour, J. P., Ursenbach, M. G., and Gie, D.N. , ”Comparison of The Effect of Thermal Cracking and Low-Temperature Oxidation on Fuel Deposition During ISC” *Proc.*,1986 U.S.DOE Tar Sands Symposium, Jackson, WY, July 1986. DOE/METC 87/6073.
- Moore, R.G., Bennion, D.W., Belgrave, J. D.W., Gie, D. N., and Ursenbach, M. G. : “Insights into Enriched Air in In Situ Combustion,” SPE 16740, presented at 62nd Annual Technical Conference and Exhibition, Dallas, Sept. 21-4, 1987, pp 459-471.
- Moore, R.G., Laureshen, C. J., Belgrave, J. D.W., Ursenbach, M. G., Metha, S. A.: “In Situ Combustion: New ideas for an old Process,” 11th Annual Heavy Oil and Sands Technical Symposium of Canadian Heavy Oil Association, Calgary, AB, Canada, March,1994.
- Moore, R.G., Metha, S. A., Belgrave, J. D.W., Ursenbach, M. G., Laureshen, C. J., Weissman, J. G., and Kessler, R.V.: “ Downhole Catalytic Upgrading Process for

REFERENCES

- Heavy Oil Using In Situ Combustion” paper 96-72, presented at the 47th Annual Technical Meeting , Calgary, Canada, June 10-12, 1996.
- Moss, J. T., and Cady, G. V. : “A laboratory Investigation of Oxygen Combustion Process for Heavy Oil Recovery,” SPE 10706, presented at SPE Annual Technical Meeting, San Francisco, March, 1982, pp55-68.
 - Nzekwu, B. I., Hallam, R. .J., and Willimas, G. J. J.: ”Interpretation of Temperature Observations From a Cyclic-Steam/In-Situ Combustion Project” paper SPE 17389, SPE Reservoir Engineering, May.1990,pp163-69.
 - Padamsey, R., Bailey, R.T., and Cyr, T.J.:”(HC)3 Process-An Economical Technology for Upgrading Bitumen and Heavy Oil” paper presented on the 6th UNITAR International Conference on heavy crude and tar sands, Houston, Texas, Feb.12-17,1995.
 - Parrish, D. R. and Craig, F.F. Jr.:” Laboratory Study of a Combination of Forward Combustion and Water Flooding . The COFCAW process,” Journal of Petroleum Technology, June 1969, pp753-761.
 - Parrish, D. R., Pollock, C. B., Ness, N. L. and Craig, F.F. Jr.: ”A Tertiary COFCAW Pilot Test in the Sloss Field, Nebraska” Journal of Petroleum Technology, June 1974,pp667-675.
 - Pearce, R., and Patterson, W.R.: “Catalysis and Chemical Processes” Blackie and Son Ltd., 1981, Glasgow, pp20-21.
 - Petit, H. : “ In Situ Combustion Experiments with Oxygen Enriched Air,” In Situ, 14(1), 1997, pp 49-76.
 - Phillipson, J. J.: “Desulphurisation” in Catalyst Handbook, (Wolfe Scientific Books),1970, pp46-63.
 - Poettmann, F. H.,Schilson, R. E. and Surkalo, H., “Philosophy and Technology of In-Situ Combustion in Light Oil Reservoirs” 7th World Pet. Cong. Mexico City, May 1967, pp487-498.

REFERENCES

- Prasad, R. S. and Slater, J. A., "High Pressure Combustion Tube Tests".
SPE/DOE 14919, 5th Symposium on Enhanced Oil Recovery of The SPE/DOE,
Tulsa, April 1986, pp 503-510.
- Prats, M.: "Thermal Recovery" Monograph series, SPE, Richardson Texas, 1982.
- Pujol, L. and Boberg, T. C.: "Scaling Accuracy of Laboratory Steam Flooding
Models," SPE 4191 presented at the SPE 43rd Annual Californian Regional
Meeting, Bakerfield, Nov. 8-10, 1972.
- Sawhney, G., Eddy, D., and Peters, E.: "Pressure Controlled Gravity Drainage
(PCGD): Method for Effective Utilization of Steam With Horizontal Producers in
Heavy Oil Pools," Paper 97-97, 48th Annual Technical Meeting, Calgary, Canada,
June 8-11 1997.
- Shahani, G. H., and Hansel, J.G.: "Oxygen Fireflooding: Combustion Tube Test
with Light, Medium and Heavy Crude Oils," Soc. Pet. Eng. J. April, 1984, pp 453-
465.
- Shahani, G. H., and Gunardson H. H.: "Oxygen Enriched Fireflooding" paper
presented at the DOE/NIPER, OK, April 21-22, 1994.
- Shallcross, D. C., de los Rios, C. F., Castanier, L. M., and Brigham, W. E.,
"Modifying In-Situ Combustion Performance by the Use of Water-Soluble
Additives," Soc. Pet. Eng. J., Aug 1991, pp 287-294.
- Shihabi, D. S.: "Shape Selective Catalysis in Industrial Applications" Marcel
Dekker, Inc. New York, 1989, pp 254.
- Sibbald, L. R., Moore, R. G., and Bennion, D. W.: "In-Situ Combustion Process
Study With a Combined Experimental / Analytical Approach" paper SPE 18074,
presented at the SPE Annual Technical Conference and Exhibition,
Houston, Oct. 2-5, 1988.
- Simpson, H. D., Stud. Surf. Sci. Catal., 100 (1996) 265.
- Speight, G. J.: "Fuel Science and Technology Handbook" Marcel Dekker, Inc,
New York, 1990.

REFERENCES

- Stapp, P. R. : "In Situ Hydrogenation" National Institute for Petroleum and Energy Research; IIT Research Institute, Bartlesville, OK, 1989; NIPER-434.
- Tadema, H. J.: "Mechanism of Oil Production By Underground Combustion" Proc. 5th World Pet. Cong. New York City, May, 1959. Sec. II paper No. 22, 279-287.
- Takaushi, C, Asaoaka, S, Nakata, S, and Shirito, Y Preprints, ACS Div. Petrol. Chem., 30 (1985) 96.
- Tiffin, P. L. and Yannimaras, D. V "High pressure combustion tube performance of light oils" 8th European IOR symposium ,Vienna, Austria May 16-17, 1995.
- Tiffin, P. L. and Yannimaras, D. V.: " The In Situ Combustion Performance of Light Oils as A function of Pressure (1000 to 6000 psig)," In Situ, 21(1), 1997, pp 47-64.
- Turta, A., and Pantazi, I. G. : "Development of The In Situ Combustion Process on Industrial Scale at Videle Field, Rumania," SPE Res. Eng. Nov. 1986, pp 556-564.
- Turta, A.: "In-Situ Combustion From Pilot to Commercial Application" presented at the DOE/NIPER Symposium on ISC Practices-Past, Present and Future Application, Tulsa, OK, April 21-22, 1994.
- Turta, A., and Singhal, A. K.: "Reservoir Engineering Aspects of Oil Recovery from Low Permeability Reservoirs by Air Injection," SPE 48841, to be presented at 1998 SPE International Conference and Exhibition, Beijing, China, 2-6 Nov. 1998.
- Tuwil, A.: " Horizontal Producer Wells In Situ Combustion Processes," 1991, MPhi Thesis, University of Bath.
- Tzanco, E. T., Moore, R. G., Belgrave, J. D. M, and Ursenbach, M. G.: "Laboratory Combustion Behavior of Countess B Light Oil" paper No CIM/SPE 90-63 presented at the international technical meeting, Calgary, June 10-13, 1990.
- Urban, D. L., and Udell, K. S.: " The Effect of Steam on the Combustion of Oil on Sand," Soe. Pet. Eng. J. May 1990, pp 170-176.

REFERENCES

- Uren, L. C.: “Petroleum Production Engineering” McGraw-Hill Book Company, Inc. Second Edition 1939, pp 433-451.
- Vossoughi, S., Willhite, G. P., Kritikos, W. P., Guvenir, I. M., and El-Shoubary, Y.: “Automation of an In Situ Combustion Tube and Study the Effect of Clay on The In Situ Combustion Process,” Soc. Pet. Eng. J. Aug. 1982, pp 493-502.
- Vossoughi, S., Bartlett, G. W. and Willhite, G. P., “Prediction of in-situ combustion Variables by use of TGA / DSC Techniques and the effect of sand grain specific surface area on the process,” Soc. Pet. Eng. J. Oct 1985, pp 656-664.
- Weijdemans, J.: “Report from Koninklijke, Shell. Explorative En Productie Laboratorium, Rijswijk,” The Netherlands, (1968).
- Weissman, J. G., Kessler, R. V., Sawichi, R. A., Belgrave, J. D. M., Lareshen, C. J., Mehta, S. A., Moore, R. G., and Ursenbach, M. G.: “Down-Hole Catalytic Upgrading of Heavy Crude Oil,” Energy and Fuels 1996, 10, 883-889.
- White, P. D.: “In-Situ Combustion Appraisal and Status” Journal of Petroleum Technology, Nov. 1985, pp 1943-1949.
- Wilson, L. A., Reed, R. L., Reed, D. W., Clay, R. R., and Harrison, N. H.: “Some Effect of Pressure On Forward and Reverse Combustion,” Soc. Pet. Eng. J. Sep. 1963, pp 127-137.
- Wilbur, H. S., and Clayton, J. R.: “Role of Clays in The Enhanced Recovery of Petroleum” SPE 8845, presented at the First Joint SPE/DOE Symposium on EOR, Tulsa, Oklahoma, April 20-23, 1980.
- Wu, C. H., and Fulton, P. F.: “Experimental Simulation of the Zones Preceding the Combustion Front of an In Situ Combustion Process” Soc. Pet. Eng. J. March 1971, pp 38-46
- Yannimaras, D. V., and Tiffin, D. L.: “Screening of Oils from In Situ Combustion at Reservoir Condition by Accelerating Rate Calorimetry,” SPE Res. Eng., Feb. 1995, pp 36-39.

APPENDICES

APPENDIX A

Equipment Specifications and Manufacturers

Equipment Details	Manufacturer
Back pressure regulator Type 44-2300 manual actuator	Tescom Corporation Coatbridge
Ball valves 1/4" Swagelok series 40	Bristol Valves and Fittings Bristol
Check valves 1/4" Swagelok series C	Bristol Valves and Fittings Bristol
Clay Supreme china caly	English China Clays International Ltd St. Austell, Cornwall
CO analyser Type 1400, 0-25%	Servomex Crowborough, Sussex
CO ₂ analyser Type 1400, 0-100%	Servomex Crowborough, Sussex
Combustion cell gasket Unilion, 2mm thick	James Walker & Co. Woking, Surrey
Combustion cell with compression glands	Workshops University of Bath
Combustion cell sealent Type 3145 silicone rubber	Dow Corning Corporation Michigan, USA
Computer software Labview	National Instruments
Crude oil	British Petroleum
Cylinder regulators Inlet 300 bar max, outlet 10 bar max	BOC Bristol
Gas chromatograph Type 8500	Perkin Elmer Ltd. Beaconsfield, Bucks.
Gas cylinders 175 bar	BOC Bristol
Ignitor wire Ø 0.7mm nichrome wire	Kanthal Ltd. Stoke-on-Trent
Jizer cleaning fluid	DEB Ltd. Belper, Derbs.
Mass flow controllers Series 5850 N ₂ 0-20, O ₂ 0-6 l/min, 5 bar inlet pressure	Fisher Rosemount Ltd Stockport
Mesh for wells Stainless steel, 100,250,300 µ gauge	R. Cadish London
Metering pump Type E1A mk.3	MPL Pumps Brixworth, Northants

APPENDICES

PH meter Hand held, ph 0-13, ± 0.01	Whatman Maidstone, Kent
Pressure gauges	Budenburg Altrincham, Cheshire
Sand Washed silica type W50 and W150 Buckland sand	Buckland Sand and Silica Ltd Addington Nr, Wrotham, Kent
Separators	Department of Chemical Engineering Workshops University of Bath
Specific gravity meter Type DMA 35, 0-1.999 g/cc	Paar Scientific Ltd Austria
Tape heaters Type G 400W, 25mm wide, 450°C max, 3m long	Isopad Ltd Weston-super-Mare
Thermocouples \varnothing 1.5mm, type K	BICC Pyrotenax Newcastle
Vermiculite insulation Magnesium aluminium iron sulphate 1300° C max	Dupre Vermiculite Hertford
Viscosity meter Type DV2	Brookfield Stoughton, MA, USA
Wet test meter Type DM3D, 600 l/hr max, 0.1 bar max	Alexander Wright & Co (Westminster) Ltd. Sutton, Surrey
Wells SS 316 stainless steel tubes	Department of Chemical Engineering Workshops University of Bath

APPENDIX B

Technical Information Sheet of Buckland Silica Sand

Product: Wrotham 50 Silica Sand
Location: Addington, Nr. Wrotham, Kent
Geological Type: Lower Greensand of the Cretaceous Period
Grain shape: Sub-Angular

A Typical Chemical Analysis

SiO ₂	99.15%
Al ₂ O ₃	0.163%
Fe ₂ O ₃	0.4000%
Cr ₂ O ₃	0.00045%
Loss on Ignition	0.16%
Clay Fraction	0.09%

Typical Acid Demand

pH3	=	0.60
pH4	=	0.50
pH5	=	0.30

A Typical Grading and Specification:

BS Mesh	Microns	Typical % Retained
22	699	—
30	500	1.0
44	353	8.5
60	251	56.2
72	211	20.8
100	152	10.9
150	104	2.5
200	76	—
PAN	PAN	—
AFS Number		48.1

Bulk Density	Loose	1.49 grms/cm ³
Bulk Density	Compact	1.61 grms/cm ³
Specific Gravity		2.5



BUCKLAND SAND & SILICA CO LTD

A MEMBER OF THE GOLDFIELDS GROUP

REIGATE DIVISION Head Office & Reg. Office: Reigate Heath, Reigate, Surrey RH2 9RG
 Telephone: Reigate 40151 (9 lines) Telex 887718

APPENDIX C

Metal Analysis of Co Mo Catalyst

Maxxam
Analystics Inc.

A Chemical Laboratory for Petrochemical Industries

Client: Petroleum Recovery Institute Sample Ref: PRJ Client ID: PRJ Laboratory Number: **98-24275-04**

City: Calgary State/Prov: Alberta Name of Sample: PRJ Company: PRJ

Sample Description: Catalyst Gauge Pressure MPa: N/A Temperature °C: N/A

Sample Point: PRJ Results: As Received Results: As Received Results: As Received

Date Sampled Start: 1998/08/14 Date Sampled End: 1998/08/20 Date Reported: SS Analyst: SS

Contact Person: PRJ Contact Fax: PRJ

PARAMETER	SYMBOL	DETECTION LIMIT mg/kg	RESULTS mg/kg
Calcium	Ca	8.7	141
Magnesium	Mg	29	2640
Sodium	Na	29	833
Potassium	K	29	ND
Silicon	Si	5.8	3120
Sulphur	S	58	6310
Aluminum	Al	2.9	300000
Barium	Ba	2.9	ND
Beryllium	Be	0.29	ND
Boron	B	2.9	9.6
Cadmium	Cd	0.87	ND
Chromium	Cr	0.58	36.2
Cobalt	Co	0.87	37800
Copper	Cu	0.29	182
Iron	Fe	2.9	686
Lead	Pb	5.8	ND
Lithium	Li	0.29	ND
Manganese	Mn	0.29	0.52
Molybdenum	Mo	0.87	103000
Nickel	Ni	2.9	ND
Phosphorus	P	29	ND
Silver	Ag	2.9	15.7
Strontium	Sr	0.87	6.15
Titanium	Ti	0.87	8.83
Uranium	U	144	ND
Vanadium	V	0.87	ND
Zinc	Zn	0.29	13.5

ND not detected
NA not available
NR not requested

Results relate only to items listed

Remarks:

*No Sample Date

Analysis performed on aqua regia digest.

Solids did not all dissolve during digestion.

weight before ashing (g) = 5.4067

weight after ashing (g) = 3.3967

CALGARY 201 - 41 Avenue NE, Calgary, Canada T2E 0P6 Tel: (403) 291-4977 Fax: (403) 291-4499
EDMONTON 9271 - 49 Street, Edmonton, Canada T6B 2H4 Tel: (403) 488-0540 Fax: (403) 488-2332

GRANDE PRAYE 4105, 600 - 112 Street, Grande Prairie, Canada T6V 0S4 Tel: (800) 385-6227 Fax: (403) 929-8899
STETTIN 407 - 4707 - 42 Street, Stettin, Canada T0C 2L8 Tel: (403) 745-1407 Fax: (403) 742-4970

ARMOUTH (403) 964-6875

APPENDIX D

Properties of Produced Oil and Water for Run 971 (Dry Normal)

Combustion Time (hrs)	Oil Density (g/cc)	API Gravity	Oil Viscosity @ 18° C (cp)	pH
2	0.992	11.14	N.M	6.54
2.5	0.983	12.45	N.M	5.34
3	0.980	12.89	N.M	5.16
3.5	0.963	15.44	7435	4.89
4	0.967	14.83	7675	4.72
4.5	0.969	14.52	8020	4.8
5	0.971	14.22	8430	4.67
5.5	0.970	14.38	8160	4.55
6	0.972	14.08	8570	4.32
6.5	0.974	13.78	9010	4.08
7	0.973	13.92	9035	3.78
7.5	0.973	13.92	8660	3.54
8	0.972	14.08	8550	3.21
8.5	0.974	13.78	8991	2.95
9	0.975	13.62	9050	2.81
9.5	0.978	13.18	9780	2.74
10	0.976	13.47	9580	2.66
10.5	0.975	13.63	9440	2.63
11	0.977	13.33	9630	2.65
11.5	0.976	13.48	9560	2.60
12	0.979	13.04	9820	2.54
12.5	0.978	13.18	9770	2.51

Properties of Produced Oil and Water for Run 975 (Dry Catalytic)

Combustion Time (hrs)	Oil Density (g/cc)	API Gravity	Oil Viscosity @ 18° C (cp)	pH
2	0.968	14.7	7830	6.1
2.5	0.930	20.7	40	5.42
3	0.931	20.5	43	5.09
3.5	0.935	19.84	62	4.75
4	0.937	19.51	68	4.62
4.5	0.938	19.35	74	4.51
5	0.939	19.20	82	4.38
5.5	0.941	18.9	97	4.1
6	0.943	18.55	104	3.95
6.5	0.944	18.4	111	3.74
7	0.945	18.23	117	3.61
7.5	0.945	18.23	123	3.47
8	0.943	18.55	106	3.52
8.5	0.946	18.08	133	3.5
9	0.945	18.23	118	3.35
9.5	0.944	18.40	110	3.1
10	0.945	18.23	123	3.25
10.5	0.944	18.40	118	3.2
11	0.946	18.08	129	2.9
11.5	0.946	18.08	132	3.0
12	0.945	18.23	118	2.78
12.5	0.944	18.40	109	2.62

APPENDICES

Properties of Produced Oil and Water for Run 972 (Wet Normal)

Combustion Time (hrs)	Oil Density (g/cc)	API Gravity	Oil Viscosity @ 18° C (cp)	pH
2	0.992	11.14	N.M	6.64
2.5	0.967	14.83	7690	5.58
3	0.971	14.23	8210	4.76
3.5	0.974	13.78	9015	4.23
4	0.976	13.48	9450	3.98
4.5	0.974	13.78	9000	3.78
5	0.977	13.33	9560	3.83
5.5	0.978	13.18	9780	3.94
6	0.983	12.45	10170	4
6.5	0.979	13.04	9900	3.98
7	0.980	12.89	9960	4.1
7.5	0.981	12.74	10040	4.15

Properties of Produced Oil and Water for Run 976 (Wet Catalytic)

Combustion Time (hrs)	Oil Density (g/cc)	API Gravity	Oil Viscosity @ 18° C (cp)	pH
2	0.965	15.13	6320	4.89
2.5	0.935	19.84	65	5.1
3	0.931	20.49	46	5.2
3.5	0.936	19.67	63	4.5
4	0.936	19.67	65	4.1
4.5	0.938	19.35	72	3.62
5	0.921	22.14	24	3.94
5.5	0.930	20.65	37	4.0
6	0.925	21.47	31	3.98
6.5	0.930	20.65	37	3.81
7	0.928	20.98	33	3.78
7.3	0.926	21.30	32	3.65

APPENDIX E

SIMDIS* Analysis for Wolf Lake Crude Oil

WT %	Temp (°C)	WT %	Temp (°C)
IBP (0.5)	171	44	481
1	204	45	487
2	227	46	492
3	240	47	498
4	251	48	503
5	260	49	508
6	267	50	514
7	274	51	519
8	281	52	524
9	288	53	530
10	293	54	535
11	299	55	540
12	305	56	546
13	311	57	551
14	316	58	556
15	322	59	562
16	328	60	567
17	333	61	572
18	339	62	577
19	345	63	582
20	351	64	587
21	357	65	591
22	362	66	596
23	368	67	601
24	374	68	607
25	379	69	612
26	385	70	617
27	391	71	622
28	396	72	628
29	402	73	633
30	408	74	639
31	413	75	645
32	418	76	651
33	423	77	658
34	428	78	665
35	433	79	673
36	438	80	683
37	443	81	692
38	449	82	703
39	454	83	718
40	459	FBP(83.11)	720
41	465		
42	470		
43	476		

*Performed by BP Sunbury, 20th Aug 1997.

APPENDICES

SIMDIS* Analysis for Produced Oil (Run 976 Wet Catalytic)

WT %	Temp (°C)	WT %	Temp (°C)	WT %	Temp (°C)
IBP (0.5)	127	44	300	88	445
1	129	45	303	89	451
2	134	46	305	90	457
3	141	47	308	91	464
4	149	48	310	92	471
5	156	49	313	93	479
6	162	50	315	94	488
7	169	51	317	95	499
8	176	52	320	96	511
9	180	53	323	97	528
10	185	54	326	98	552
11	188	55	328	99	591
12	193	56	331	FBP (99.5)	619
13	200	57	334		
14	206	58	337		
15	213	59	340		
16	217	60	342		
17	221	61	345		
18	224	62	348		
19	227	63	352		
20	231	64	355		
21	234	65	358		
22	238	66	361		
23	241	67	365		
24	245	68	368		
25	248	69	371		
26	251	70	374		
27	254	71	378		
28	257	72	381		
29	260	73	385		
30	263	74	389		
31	266	75	392		
32	268	76	396		
33	270	77	400		
34	274	78	404		
35	277	79	408		
36	280	80	412		
37	283	81	416		
38	285	82	419		
39	288	83	423		
40	291	84	427		
41	293	85	431		
42	296	86	436		
43	298	87	440		

*Performed by BP Sunbury, 19th Aug 1997.

APPENDIX F

Combustion Parameters Calculation

The following calculation of the combustion parameters based on the results of Run 961 :

Produced Gas Composition:

$$\text{CO}_2 = 11.1 \%$$

$$\text{CO} = 3.4 \%$$

$$\text{O}_2 = 2.9 \%$$

- Apparent atomic H/C ratio (X): (*Burger et al* 1985)

$$X = 4 * [(\text{O}_{2 \text{ cons.}} - \text{CO}_2 \text{ formed} - (\text{CO}_{\text{formed}}/2)] / (\text{CO}_2 \text{ formed} + \text{CO}_{\text{formed}})$$

where

$\text{O}_{2 \text{ cons.}}$ = volume of oxygen used up

$\text{CO}_2 \text{ formed}$ = volume of CO_2 formed

$\text{CO}_{\text{formed}}$ = volume of CO formed

$$= 4 \times [(0.02 - 0.012 - 0.00185)] / (0.012 + 0.0037)$$

$$\text{H/C} = 1.57$$

- Carbon molar ratio (m) = $\text{CO} / (\text{CO} + \text{CO}_2)$

$$= 0.034 / (0.034 + 0.11) = 0.24$$

- Air to fuel requirement

$$= mc. (b/Y_{\text{O}_2}) (2 - \Gamma + (X/2)) / (12 + X) \quad (\text{Burger et al 1985})$$

Where

$$b = 11.82 \text{ sm}^3/\text{kg}$$

$$Y_{\text{O}_2} = 0.21 \text{ (for air injection)}$$

$$mc = \text{mass of fuel burnt (1 kg basis)}$$

$$X = \text{H/C ratio}$$

$$= 1 \times (11.82/0.21) \times (2 - 0.24 + (1.57/2)) / (12 + 1.57)$$

$$= 10.557 \text{ sm}^3/\text{kg of fuel}$$

- Oxygen to fuel requirement

$$= 0.21 \times 10.557 = 2.22 \text{ sm}^3/\text{kg of fuel}$$

- Amount of fuel burnt

$$= O_{2 \text{ cons.}} / O_2 \text{ to fuel requirement}$$

$$= 446.9 / (1000 \times 2.22)$$

$$= 0.20 \text{ kg of fuel}$$

$$= 6.97 \approx 7 \% \text{ OOIP}$$

- Water produced by combustion reactions

$$= [\text{moles of CO}_{\text{produced}} / m] \times (X/2) \quad (Burger \text{ et al } 1985)$$

$$= [0.0037/0.24] \times (1.57/2)$$

$$= 0.012 \text{ kmol of water}$$

$$= 0.012 \times 18 = 0.216 \text{ Kg of water}$$

- Oxygen consumed in combustion reactions

$$= [1-(m/2)+(X/4)] \times (\text{CO}_{\text{produced}} / m) \times 32 \quad (Burger \text{ et al } 1985)$$

$$= [1-(0.24/2)+(1.57/4)] \times (0.0037/0.24) \times 32$$

$$= 0.63 \text{ kg}$$

- Fuel Consumption (kg/m^3) =
$$\frac{\text{Fuel Burned}}{\text{Volume of Burnt Section}}$$

From the post-mortem analysis, volume of the burned section is 0.0083 m^3

$$\text{Therefore, the fuel consumption} = 24 \text{ kg}/\text{m}^3$$

- Air Requirement (m^3/m^3) =
$$\frac{\text{Air Flux}}{\text{Combustion Front Velocity}}$$

$$\text{Air Flux} = 5.7 \text{ m}^3/\text{m}^2 \text{ hr}$$

$$\text{Combustion Front Velocity} = 0.022 \text{ m/hr}$$

$$\text{Air Requirement} = 259 \text{ m}^3/\text{m}^3$$

- Air Oil Ratio (m^3/m^3) =
$$\frac{\text{Volume of air injected}}{\text{Volume of oil produced}}$$

APPENDICES

Volume of air injected = 2.469 m^3

Volume of oil produced = $2.72 \times 10^{-3} \text{ m}^3$

Air Oil Ratio = $908 \text{ m}^3/\text{m}^3$

APPENDIX G**Material Mass Balance**

Sample calculation for Run 961

1. Gas phase

Injected gas composition:

N₂ 79 Vol. %O₂ 21 Vol. %

GAS TYPE	Litre	kg
O ₂ injected	518	0.74
O ₂ produced	71.1	0.102
O ₂ consumed	446.9	0.63
N ₂ injected	1951	2.44
N ₂ produced	2024.6	2.532
CO ₂ produced	272	0.54
CO produced	83.3	0.104

Nitrogen BalanceN₂ Injected = 2.44 kgN₂ Produced = 2.532 kg

Balance = + 3.7 %

The difference is probably caused by light hydrocarbon gases and hydrogen generated during the process.

O₂ BalanceO₂ Injected = 0.74 kgO₂ Produced = 0.102 kgO₂ Consumed = 0.63 kg

Balance = -1.1 %

Overall Gas Balance

Injected Gas:

$N_2 = 2.44 \text{ kg}$

$O_2 = 0.74 \text{ kg}$

Total = 3.18 kg

Produced Gas:

$N_2 = 2.532 \text{ kg}$

$O_2 = 0.102 \text{ kg}$

$CO_2 = 0.54 \text{ kg}$

$CO = 0.104 \text{ kg}$

Total = 3.278 kg

Balance = + 3.1 %

2. Liquid Phase

Oil balance

Initial oil in sandpack = 2.973 kg

Produced oil = 2.494 kg

Consumed oil as fuel = 0.2 kg

Residual oil left = 0.18 kg

Total = 2.874 kg

Balance = - 3.33 %

Water Balance

Initial water in sandpack = 2.120 kg

Water generated by combustion reactions = 0.216 kg

Total water in sandpack = 2.336 kg

Produced water = 1.95 kg

Residual water = 0.32 kg

Balance = - 2.8 %

Overall Liquid Balance

Initial oil in sandpack = 2.973 kg

Initial water in sandpack = 2.120 kg

Water generated by combustion reactions = 0.216 kg

Total = 5.309 kg

Produced oil = 2.494 kg

Consumed oil as fuel = 0.20 kg

Residual oil left = 0.19 kg

Produced water = 1.95 kg

Residual water = 0.32 kg

Total = 5.154 kg

Balance = - 2.92 %

Overall Material Mass Balance

Material in = Material out

8.489 kg 8.432 kg

Balance = - 1 %

APPENDIX H

COSHH

CHEMICAL RISK ASSESSMENT

RESEARCH TITLE : IN-SITU COMBUSTION OF LIGHT OIL USING
HORIZONTAL WELLS

NAME OF SUPERVISOR : DR. M. GREAVES

NAME OF RESEARCH STUDENT : ABDULBASET M. AL-SAGHR

STARTING DATE : 15.3.1996

LOCATION OF WORK : 4 WEST 1.9

Hazardous Substances	Quantity
Crude oil	4000 ml
Silica Sand (Buckland)	25 kg
China Clay	2.5 kg
Oil Degreaser	50 ml
Vermiculite	0.05 m ³

Nature of the hazards

Light oil ,flammable.

Reactive hazards

Crude oil combustible. Reactivity of crude oil increases with increase in oxygen concentration. Moderate degree of hazard.

Experimental procedure

(see Chapter 3 for operating procedure)

Fume cupboard classification

Combustion gases are discharged to atmosphere

Other safeguards/ protective clothing

Only authorised persons are allowed to operate the equipment

During mixing of sand/oil mixture and packing of the combustion cell, protective clothing (mask and gloves) must be worn.

The operator must continually monitor the operation of the system.

Waste Disposal

Crude oil and solvents to be unloaded in waste drums.

Oily sand to be sealed in plastic bags.

Vermiculite powder to be stored in sealed bags.

Action in case of loss of containment / accidental spillage

Cover the crude oil spillage with dry sand, then collect in plastic bags and seal them.

Clean the area with water and detergent.

Action in case of fire /explosion

Isolate the combustion cell by switching off all electrical power.

Switch oxygen/air to nitrogen.

Operate CO₂ fire extinguisher.

Call the fire brigade.

Emergency Shut-Down Procedure

1. In case of equipment malfunction, air injection should be switched to nitrogen by opening BV2 and close BV1.
2. Close BV9 and open BV8 to release the pressure from separators (V2 and V3).
3. Switch off the heating tapes and the ignitor (if still on).
4. Switch off the water pump (wet combustion).
5. Allow combustion cell to cool to room temperature.

Action in case of failure in services

- A. Failure in electricity : operation of combustion cell fails to safe condition and is isolated; nitrogen purge is manually connected to injection line.
- B. Failure in water pump : same as above.
- C. Failure in gas supply : same as above , if nitrogen supply operative other wise combustion cell remains isolated until nitrogen supply is reconnected.
- D. Failure in fume cupboard :shut down experiment, discontinue toluene extraction and close fume cupboard.

Personnel Who Carried Out The Assessment

Name: Dr. M. Greaves

Signature:

A handwritten signature in black ink, appearing to read 'M. Greaves', with a horizontal line preceding it.

Status: Research Supervisor

Date: 19.3.1996

Name: A. Al-Saghr

Signature:

A handwritten signature in black ink, consisting of a large, stylized loop followed by a horizontal line.

Status: Postgraduate student

Date: 19.3.1996